Corso di Dottorato di Ricerca in

Scienze e Biotecnologie Agrarie

Ciclo XXXVIII

Titolo della Tesi

"Ecophysiological responses of maize (*Zea mays* L.) to water stress: remote sensing and upscaling techniques for a more efficient management of water resources in agriculture"

Dottorando

Giacomo Boscarol

Supervisore

Dott.ssa Elisa Petrussa

Co-supervisore

Prof. Enrico Braidot

Anno 2026

Finanziato dall'Unione Europea - Next Generation EU, Missione 4 Componente 1 CUP G23C22001310003

Table of contents

Outline of the Thesis **1**

General Introduction **2**

I. Effects of Climate Change on Agroecosystems 2

II. Strategies and Instruments 3

III. Aim of the Thesis 6

IV. References 6

1. Statistical Models to Predict Mycotoxin Occurrence **11**

1.1. Article Published in Agriculture, Ecosystems and Environment 11

1.2. Supplementary Materials 36

2. Multispectral Imagery as a Tool to Remotely Investigate Maize Health **39**

2.1. Manuscript in Preparation 39

3. Environmental Effects on Maize Associated Rhizobiome **52**

3.1. Manuscript in Preparation 52

3.2. Supplementary Materials 71

4. Bioextracts as Potential Environment-Friendly Anti-Mycotoxin Compounds **81**

4.1. Article Under Review in Scientific Reports 81

4.2. Supplementary Materials 104

5. General Conclusions **106**

6. Future Perspectives **109**

6.1. Multispectral Imagery as a Tool to Remotely Investigate Maize Health – Upscaling to Satellites 109

6.2. Bioextracts as Potential Environment-Friendly Anti-Mycotoxin Compounds – An Open-Field Experiment 111

7. Side Projects and Activities **115**

7.1. Side projects 115

7.2. Conferences – Oral Communications 156

7.3. Conferences – Poster Communications 157

8. Acknowledgments **159**

Outline of the Thesis

Climate change is reshaping agroecosystems by altering temperature and precipitation regimes, increasing the frequency of extreme events, and intensifying plant stress conditions. In maize agroecosystems these shifts not only affect plant morphophysiological traits and yield formation, but also influence plant-microbiome interactions, thereby increasing the risk of grain contamination by mycotoxins (i.e., aflatoxins and fumonisins) and potentially altering the structure and function of the rhizosphere microbiome.

This PhD Thesis adopts an integrated agroecological framework to investigate how environmental drivers operating at different phenological stages shape maize functional traits, modulate grain mycotoxin accumulation, and influence the associated rhizobiome, while simultaneously exploring sustainable mitigation and monitoring strategies.

As described in Chapter 1, statistical models integrating climatic variables, soil properties, and plant functional traits were developed to predict aflatoxin and fumonisin occurrence in maize grain. Results showed that temperature and rainfall patterns exerted stage-dependent effects on mycotoxin accumulation, interacting with plant morphophysiological responses. These findings underscore the importance of considering phenological timing and trait-mediated mechanisms when modelling climate-driven mycotoxin risk.

Chapter 2 investigates how multi-temporal UAV-based multispectral imagery can be employed to monitor maize canopy dynamics throughout the growing season. Multispectral images provided non-destructive proxies of plant physiological status, improving the interpretation of crop-environment interactions and supporting early stress detection.

In Chapter 3 the environmental modulation of the maize-associated rhizobiome was investigated, revealing that climate may directly alter rhizobiome composition rather than acting through climate-driven shifts in plant phenology.

Finally, Chapter 4 evaluates the antifungal potential of bio-based extracts derived from agricultural and marine by-products as an environmentally friendly alternative to synthetic pesticides. *In vitro* assays demonstrated that extracts from the green macroalga *Ulva* sp. markedly inhibited the growth and conidial germination of *Aspergillus flavus*, a major maize pathogen responsible for aflatoxins production. The high efficacy of *Ulva* extract highlights the potential of circular economy-derived bio-extracts as sustainable tools for mycotoxin management.

Overall, this research demonstrates that integrating climate-aware statistical modelling, high-resolution remote sensing, rhizobiome monitoring and sustainable bio-based solutions provides a comprehensive strategy to enhance risk prediction, early stress monitoring, and preventive management of mycotoxin contamination in maize agroecosystems under climate change.

General Introduction

I. Effects of Climate Change on Agroecosystems

Global change is an umbrella term encompassing a wide range of human-driven phenomena that are altering multiple aspects of our planet (Intergovernmental Panel on Climate Change (IPCC), 2014, 2023). Among these, climate change is one of the most relevant and extensively investigated topics in ecology, given its profound impacts on human society (Godfray et al., 2010; Schmidhuber & Tubiello, 2007). In particular, climate change poses one of the major challenges for modern agricultural systems, strongly affecting crop productivity, yield stability, and food safety. Rising mean temperatures, heat waves and shifts in precipitation patterns are progressively reshaping the environmental conditions under which crops grow and develop (Godfray et al., 2010; Mendelsohn, 2009). Moreover, extreme hydrological events such as severe droughts and torrential precipitation events are becoming more frequent (Intergovernmental Panel on Climate Change (IPCC), 2023). In addition, the anthropic activities are accelerating these changes, with human capacity to adapt being inferior to the velocity of this global change (Sánchez-García & Francos, 2022).

This extremely challenging scenario leads to complex impacts on plant morphology and physiology and on plant–pathogen interactions, modulating fundamental physiological processes and developmental trajectories (Cairns et al., 2013; Kang et al., 2009; Lobell et al., 2011; Makowski et al., 2020). Changes in thermal conditions influence plant enzymatic activity, photosynthetic efficiency, respiration rates, and phenological timing, while shifts in water availability affect plant water status, stomatal regulation, and nutrient transport (Seleiman et al., 2021; Toscano et al., 2019). Moreover, the interaction between heat and water stress often leads to coordinated morphological and physiological modifications in plant traits affecting leaf area, canopy architecture, biomass partitioning, and water-use efficiency, which ultimately determine plant performance under variable environmental conditions.

Cereal crops are particularly responsive to these climatic drivers due to their reliance on finely tuned growth and reproductive processes. In cereals, climate-induced morphophysiological responses include (1) increased flowering days, days to maturity and anthesis silk interval, (2) reduced number of leaves, (3) abnormally expressed secondary stress responsive traits, and (4) loss of normal root architecture, leading overall to a reduction in yield per hectare (Sah et al., 2020). Moreover, stress conditions occurring during sensitive phenological stages, such as flowering and grain filling, can disrupt source–sink relationships and reduce allocation to reproductive organs (Tsimba et al., 2013). Moreover, these morphophysiological shifts not only influence yield formation, but also modify the crop microclimate and stress status, potentially increasing susceptibility to biotic pressures, including herbivory-induced damage, fungal infection and mycotoxin production.

Indeed, plant defences against biotic stresses depend not only on climatic conditions but also on plant health status, often mediated by morphological and physiological responses, largely constrained by plant plasticity to environment variations (Barnabás et al., 2008; Jin et al., 2023). For instance, cereal plants with narrower stylar canal are more resistant to infections (Duncan & Howard, 2010), and cultivars with tighter and more complete husks present a physical barrier to insects, reducing in turn their susceptibility to fungal infections (Munkvold, 2003).

Among cereals, maize (*Zea mays* L.) is one of the most widely cultivated crops worldwide and plays a central role in human nutrition, livestock feeding, and industrial applications (FAOSTAT, 2025). Despite being considered an efficient water user, its growth and productivity are highly sensitive to climatic variability across the growing season: both temperature and rainfall influence key developmental processes including vegetative growth, photosynthetic performance, biomass allocation, and grain filling (Mendelsohn, 2009). Deviations from optimal climatic conditions, particularly during critical phenological stages, can induce thermal and water stress, resulting in marked alterations of maize morphophysiological traits and ultimately affecting yield quantity and quality. Moreover, climate-driven unfavourable conditions may promote the development of fungal pathogens and increase the risk of contamination by mycotoxins such as aflatoxins and fumonisins (Battilani et al., 2016; Janić Hajnal et al., 2023; Moretti et al., 2019). The production and accumulation of these fungal secondary metabolites are strongly modulated by environmental factors, and their occurrence is often facilitated by plant stress conditions, highlighting the need for an integrated assessment of climate, plant functional traits, and pathogen dynamics.

II. Strategies and Instruments

Several agronomic strategies have been proposed to mitigate the negative effects of climate variability and biotic stress on maize production. Crop management practices such as optimized irrigation, balanced fertilization, appropriate planting density, and crop rotation can contribute to improving plant vigour and reducing stress conditions that in turn favour pathogen development (Assefa et al., 2016; Zhang et al., 2022). In parallel, the choice of maize hybrids plays a crucial role, as genotypes differ in their phenology, tolerance to thermal and water stress, resistance to insect damage, and susceptibility to fungal infection (Duncan & Howard, 2010; Munkvold, 2003). Breeding efforts have led to the development of hybrids with improved stress resilience and enhanced defensive traits, which can partially reduce yield losses and contamination risks.

In addition, preventive biological control strategies have gained increasing attention as sustainable tools to limit mycotoxin contamination. The usage of non-toxigenic fungal strains, particularly *Aspergillus* spp. and *Penicillium* spp., can reduce the prevalence of toxigenic populations through competitive exclusion, thereby limiting mycotoxin biosynthesis (Llobregat et al., 2024). This approach

represents a promising component of integrated management strategies aimed at reducing contamination risks.

However, the effectiveness of these agronomic and genetic approaches is strongly constrained by the increasing variability and unpredictability of climatic conditions. Extreme weather events, shifting phenological windows, and complex interactions between abiotic and biotic stressors often exceed the adaptive capacity of current management practices and available hybrids. Therefore, traditional agronomic strategies and hybrid selection, although essential components of integrated crop management, are increasingly insufficient on their own to ensure stable yields and food safety under the ongoing climate change. This highlights the need for innovative monitoring and preventive approaches that integrate climate-aware monitoring, early warning systems, and sustainable preventive strategies to effectively manage emerging risks in maize production systems.

In this context, recent advances in remote sensing, particularly the use of multispectral imagery acquired from unmanned aerial vehicles (UAVs) and satellites, offer new opportunities for high-resolution, non-destructive evaluation of crop status. Remote sensing data can indeed capture variations in canopy structure, pigment content, and physiological performance, providing valuable proxies for plant stress and potential disease development (Zhang & Zhu, 2023).

The concept behind multispectral approaches is that different regions of the electromagnetic spectrum provide complementary information on plant status. The visible range (400–700 nm) reflects variations in leaf pigments, particularly chlorophyll, allowing assessment of photosynthetic activity and visible stress symptoms. The near-infrared (NIR, 700–1100 nm) is strongly influenced by leaf internal structure and canopy architecture, providing insights into biomass, leaf area, and overall canopy health. The red-edge region, located at the transition between the red and NIR bands (approximately 700–740 nm), is particularly sensitive to subtle changes in chlorophyll content and stress-related variations, making it a valuable indicator of early physiological alterations before they become visually apparent. Finally, the mid-infrared (MIR, 1100–2600 nm) is primarily sensitive to leaf and canopy water content, as well as to biochemical constituents such as cellulose and lignin, and is therefore closely associated with plant water status, drought stress, and structural changes related to senescence or stress-induced tissue degradation.

By combining reflectance information from these spectral regions, various vegetation indices have been developed to quantify plant status in a standardized way (Zhang & Zhu, 2023). Among the most widely used is the Normalized Difference Vegetation Index (NDVI), which exploits the contrast between red and NIR reflectance to estimate canopy greenness and photosynthetic potential (Carlson & Ripley, 1997). Other indices, such as the Soil-Adjusted Vegetation Index (SAVI) (Huete, 1988), the Normalized Difference Red-Edge Index (NDRE) (Davidson et al., 2022), and the Inverted Red-Edge Chlorophyll Index (IRECI) (Frampton et al., 2013) provide additional sensitivity to chlorophyll content, light-use efficiency, and early stress detection. These indices enable rapid, large-scale

monitoring of plant health, stress response, and potential vulnerability to biotic or abiotic threats, complementing traditional field-based assessments.

Despite the considerable potential offered by UAV-based multispectral sensing in maize research, most studies rely on single or limited time points, which may overlook important temporal dynamics in crop physiology and stress responses (Agüera Vega et al., 2015). However, plant–environment interactions, canopy structure, and spectral signatures change substantially throughout the growing season, influencing both the sensitivity and the interpretation of vegetation indices. Repeated multispectral observations across key phenological stages would therefore provide a more robust and comprehensive assessment of crop status, improving the ability to link spectral traits with environmental drivers, stress conditions, and yield- or disease-related outcomes.

Another widely used technology in the field of remote sensing is Light Detection and Ranging (LiDAR). Unlike multispectral sensors, which are based on the measurement of reflected electromagnetic radiation, LiDAR is an active sensing system that emits laser pulses and measures the time required for the signal to return after interacting with the target. This allows the acquisition of highly accurate three-dimensional information on crop structure, independently of ambient light conditions (Bento et al., 2025).

The integration of LiDAR and multispectral approaches therefore represents a promising framework for comprehensive, multi-dimensional assessment of crop status, supporting improved monitoring of plant stress and associated risks under changing climatic conditions.

Parallel to the development of monitoring tools, another emerging research avenue focuses on the prevention of mycotoxin occurrence through sustainable crop protection strategies. Increasing attention is being directed toward the use of bio-based extracts with antifungal or anti-mycotoxigenic properties derived from agricultural or agro-industrial by-products (Ahmed et al., 2022).

Plant-based extracts are characterized by a high content of phenolic acids and terpenes, widely recognized for their antioxidant and antimicrobial activity, as well as polysaccharides, which contribute to indirect antifungal properties and structural defence (Ahmed et al., 2022; Montibus et al., 2021), representing an environmentally friendly and safe alternative to synthetic pesticides (Giorni et al., 2023; Makhuvele et al., 2020). Moreover, the chemical compounds composing bio-extracts are thought to act synergistically, thereby increasing their efficacy, and to stimulate endogenous plant defence mechanisms, ultimately enhancing crop resilience to biotic stress (Caesar & Cech, 2019). Their use is further supported by the wide availability of raw biomass in natural and agro-industrial systems, as well as by extraction processes that are often less energy-intensive and less polluting than conventional chemical synthesis.

These low-impact solutions, aligned with the principles of circular economy, represent a promising alternative to conventional chemical inputs by reducing environmental burden while contributing to the valorisation of waste streams.

Integrating preventive approaches based on bio-extracts with climate-informed monitoring and multispectral remote sensing techniques may enhance the effectiveness of management strategies under changing climatic conditions.

III. Aim of the Thesis

This PhD Thesis aims to clarify how environmental factors, acting at different phenological stages, shape maize morphophysiological traits in the field and modulate mycotoxin accumulation in the grain, through predictive statistical models integrating plant functional traits and multispectral imagery. Moreover, it explores specific aspects that may influence maize morphophysiological traits such as the associated rhizobiome and the application of sustainable bio-extracts with antifungal properties as preventive tools to mitigate mycotoxin contamination. In particular, this work comparatively investigated four low-impact extracts derived from agricultural and agro-industrial by-products within a circular economy framework evidencing a seaweed extract as the most promising.

IV. References

Agüera Vega, F., Ramírez, F. C., Saiz, M. P., & Rosúa, F. O. (2015). Multi-temporal imaging using an unmanned aerial vehicle for monitoring a sunflower crop. Biosystems Engineering, 132, 19–27. https://doi.org/10.1016/j.biosystemseng.2015.01.008

Ahmed, O., S., Tardif, C., Rouger, C., Atanasova, V., Richard-Forget, F. & Waffo-Téguo, P. Naturally occurring phenolic compounds as promising antimycotoxin agents: Where are we now? Compr. Rev. Food Sci. Food Saf. 21, 1161–1197 (2022).

Assefa, Y., Vara Prasad, P. V., Carter, P., Hinds, M., Bhalla, G., Schon, R., Jeschke, M., Paszkiewicz, S., & Ciampitti, I. A. (2016). Yield Responses to Planting Density for US Modern Corn Hybrids: A Synthesis-Analysis. Crop Science, 56(5), 2802–2817. https://doi.org/10.2135/cropsci2016.04.0215

Barnabás, B., Jäger, K., & Fehér, A. (2008). The effect of drought and heat stress on reproductive processes in cereals. Plant, Cell & Environment, 31(1), 11–38. https://doi.org/10.1111/j.1365-3040.2007.01727.x

Battilani, P., Toscano, P., Van der Fels-Klerx, H. J., Moretti, A., Camardo Leggieri, M., Brera, C., Rortais, A., Goumperis, T., & Robinson, T. (2016). Aflatoxin B1 contamination in maize in Europe increases due to climate change. Scientific Reports, 6(1), 24328. https://doi.org/10.1038/srep24328

Bento, N. L., Ferraz, G. A. e S., Santana, L. S., Faria, R. de O., Rossi, G., & Bambi, G. (2025). Plant Height and Soil Compaction in Coffee Crops Based on LiDAR and RGB Sensors Carried by Remotely Piloted Aircraft. Remote Sensing, 17(8), 1445. https://doi.org/10.3390/rs17081445

Caesar, L. K. & Cech, N. B. Synergy and antagonism in natural product extracts: when 1 + 1 does not equal 2. Nat. Prod. Rep. 36, 869–888 (2019).

Cairns, J. E., Crossa, J., Zaidi, P. H., Grudloyma, P., Sanchez, C., Araus, J. L., Thaitad, S., Makumbi, D., Magorokosho, C., Bänziger, M., Menkir, A., Hearne, S., & Atlin, G. N. (2013). Identification of Drought, Heat, and Combined Drought and Heat Tolerant Donors in Maize. Crop Science, 53(4), 1335–1346. https://doi.org/10.2135/cropsci2012.09.0545

Carlson, T. N., & Ripley, D. A. (1997). On the relation between NDVI, fractional vegetation cover, and leaf area index. Remote Sensing of Environment, 62(3), 241–252. https://doi.org/10.1016/S0034-4257(97)00104-1

Davidson, C., Jaganathan, V., Sivakumar, A. N., Czarnecki, J. M. P., & Chowdhary, G. (2022). NDVI/NDRE prediction from standard RGB aerial imagery using deep learning. Computers and Electronics in Agriculture, 203, 107396. https://doi.org/10.1016/j.compag.2022.107396

Duncan, K. E., & Howard, R. J. (2010). Biology of Maize Kernel Infection by Fusarium verticillioides. Molecular Plant-Microbe Interactions®, 23(1), 6–16. https://doi.org/10.1094/MPMI-23-1-0006

FAOSTAT. (2025, August 29). FAOSTAT. https://www.fao.org/faostat/en/#data/QCL/visualize

Frampton, W. J., Dash, J., Watmough, G., & Milton, E. J. (2013). Evaluating the capabilities of Sentinel-2 for quantitative estimation of biophysical variables in vegetation. ISPRS Journal of Photogrammetry and Remote Sensing, 82, 83–92. https://doi.org/10.1016/j.isprsjprs.2013.04.007

Giorni, P., Bulla, G., Leni, G., Soldano, M., Tacchini, M., Guerrini, A., Sacchetti, G. & Bertuzzi, T. Enhancement of agri-food by-products: green extractions of bioactive molecules with fungicidal action against mycotoxigenic fungi and their mycotoxins. Front. Nutr. 10, (2023).

Godfray, H. C. J., Beddington, J. R., Crute, I. R., Haddad, L., Lawrence, D., Muir, J. F., Pretty, J., Robinson, S., Thomas, S. M., & Toulmin, C. (2010). Food security: The challenge of feeding 9 billion people. Science, 327(5967), 812–818. https://doi.org/10.1126/science.1185383

Huete, A. R. (1988). A soil-adjusted vegetation index (SAVI). Remote Sensing of Environment, 25(3), 295–309. https://doi.org/10.1016/0034-4257(88)90106-X

Intergovernmental Panel on Climate Change (IPCC). (2014). Climate Change 2014: Impacts, Adaptation, and Vulnerability (Contribution to the Fifth Assessment Report of the IPCC No. Working Group II). https://www.ipcc.ch/report/ar5/wg2/

Intergovernmental Panel on Climate Change (IPCC) (Ed.). (2023). Weather and Climate Extreme Events in a Changing Climate. In Climate Change 2021 – The Physical Science Basis: Working Group I Contribution to the Sixth Assessment Report of the Intergovernmental Panel on Climate Change (pp. 1513–1766). Cambridge University Press. https://doi.org/10.1017/9781009157896.013

Janić Hajnal, E., Kos, J., Radić, B., Anić, M., Radović, R., Kudumija, N., Vulić, A., Đekić, S., & Pleadin, J. (2023). Impact of Climate Changes on the Natural Prevalence of Fusarium Mycotoxins in Maize Harvested in Serbia and Croatia. Foods, 12(5). Scopus. https://doi.org/10.3390/foods12051002

Jin, M., Liu, H., Liu, X., Guo, T., Guo, J., Yin, Y., Ji, Y., Li, Z., Zhang, J., Wang, X., Qiao, F., Xiao, Y., Zan, Y., & Yan, J. (2023). Complex genetic architecture underlying the plasticity of maize agronomic traits. Plant Communications, 4(3), 100473. https://doi.org/10.1016/j.xplc.2022.100473

Kang, Y., Khan, S., & Ma, X. (2009). Climate change impacts on crop yield, crop water productivity and food security—A review. Progress in Natural Science, 19(12), 1665–1674. https://doi.org/10.1016/j.pnsc.2009.08.001

Llobregat, B., González-Candelas, L., & Ballester, A.-R. (2024). Exploring the Biocontrol Capability of Non-Mycotoxigenic Strains of *Penicillium expansum*. Toxins, 16(1), 52. https://doi.org/10.3390/toxins16010052

Lobell, D. B., Bänziger, M., Magorokosho, C., & Vivek, B. (2011). Nonlinear heat effects on African maize as evidenced by historical yield trials. Nature Climate Change, 1(1), 42–45. https://doi.org/10.1038/nclimate1043

Makowski, D., Marajo-Petitzon, E., Durand, J.-L., & Ben-Ari, T. (2020). Quantitative synthesis of temperature, CO_2, rainfall, and adaptation effects on global crop yields. European Journal of Agronomy, 115, 126041. https://doi.org/10.1016/j.eja.2020.126041

Makhuvele, R., Naidu, K., Gbashi, S., Thipe, V., C., Adebo, O., A., Njobeh, P., B. The use of plant extracts and their phytochemicals for control of toxigenic fungi and mycotoxins. Heliyon 6, e05291 (2020).

Mendelsohn, R. (2009). The Impact of Climate Change on Agriculture in Developing Countries. Journal of Natural Resources Policy Research, 1(1), 5–19. https://doi.org/10.1080/19390450802495882

Montibus, M., Vitrac, X., Come, V., Loron, A., Pinson-Gadais, L., Ferre, N., Verdal-Bonnin, M., Gabaston, J., Waffo-Téguo, P., Richard-Forget, F., Atanasova, V. Screening of wood/forest and vine by-products as sources of new drugs for sustainable strategies to control *Fusarium graminearum* and the production of mycotoxins. Molecules 26, 405 (2021).

Moretti, A., Pascale, M., & Logrieco, A. F. (2019). Mycotoxin risks under a climate change scenario in Europe. Trends in Food Science & Technology, 84, 38–40. https://doi.org/10.1016/j.tifs.2018.03.008

Munkvold, G. P. (2003). Cultural and Genetic Approaches to Managing Mycotoxins in Maize. Annual Review of Phytopathology, 41(1), 99–116. https://doi.org/10.1146/annurev.phyto.41.052002.095510

Sah, R. P., Chakraborty, M., Prasad, K., Pandit, M., Tudu, V. K., Chakravarty, M. K., Narayan, S. C., Rana, M., & Moharana, D. (2020). Impact of water deficit stress in maize: Phenology and yield components. Scientific Reports, 10(1). https://doi.org/10.1038/s41598-020-59689-7

Sánchez-García, C., & Francos, M. (2022). Human-environmental interaction with extreme hydrological events and climate change scenarios as background. Geography and Sustainability. https://doi.org/10.1016/j.geosus.2022.08.002

Schmidhuber, J., & Tubiello, F. N. (2007). Global food security under climate change. Proceedings of the National Academy of Sciences, 104(50), 19703–19708. https://doi.org/10.1073/pnas.0701976104

Seleiman, M. F., Al-Suhaibani, N., Ali, N., Akmal, M., Alotaibi, M., Refay, Y., Dindaroglu, T., Abdul-Wajid, H. H., & Battaglia, M. L. (2021). Drought Stress Impacts on Plants and Different Approaches to Alleviate Its Adverse Effects. Plants, 10(2), Article 2. https://doi.org/10.3390/plants10020259

Toscano, S., Ferrante, A., & Romano, D. (2019). Response of Mediterranean Ornamental Plants to Drought Stress. Horticulturae, 5(1), Article 1. https://doi.org/10.3390/horticulturae5010006

Tsimba, R., Edmeades, G. O., Millner, J. P., & Kemp, P. D. (2013). The effect of planting date on maize: Phenology, thermal time durations and growth rates in a cool temperate climate. Field Crops Research, 150, 145–155. https://doi.org/10.1016/j.fcr.2013.05.021

Zhang, H., Zhang, C., Sun, P., Jiang, X., Xu, G., & Yang, J. (2022). Optimizing planting density and nitrogen application to enhance profit and nitrogen use of summer maize in Huanghuaihai region of China. Scientific Reports, 12(1), 2704. https://doi.org/10.1038/s41598-022-06059-0

Zhang, Z., & Zhu, L. (2023). A Review on Unmanned Aerial Vehicle Remote Sensing: Platforms, Sensors, Data Processing Methods, and Applications. Drones, 7(6), Article 6. https://doi.org/10.3390/drones7060398

1. Statistical Models to Predict Mycotoxin Occurrence

Understanding the interactions between environmental conditions, plant growth, and mycotoxin accumulation is essential for developing effective mitigation strategies in maize. Environmental stressors such as temperature extremes, drought, or excessive rainfall can influence plant morphology, physiology, and productivity, ultimately affecting the susceptibility of kernels to different mycotoxins. Moreover, the timing of stress during key phenological stages may play a critical role in shaping mycotoxin occurrence, highlighting the need to consider plant development dynamics in predictive and preventive approaches. In this context, we conducted a field experiment to better understand the hidden phenological legacies of environmental stress and plants traits on mycotoxin occurrence in maize.

1.1. Article Published in Agriculture, Ecosystems and Environment

Environmental stress, plant traits, and their phenological legacies determine mycotoxin content in maize

Giacomo Boscarol[1]*, Elisa Petrussa[1], Giacomo Trotta[1,2], Dora Scarpin[1], Enrico Braidot[1], Francesco Boscutti[1,3], Valentino Volpe[4], Stefano Barbieri[4], Valentina Caron[4], Lara Manzoni[4], Linda Stel[4], Michele Fabro[4], Marco Vuerich[1,3]

1 Department of Agricultural, Food, Environmental and Animal Sciences (DI4A), University of Udine, Via delle Scienze 206, 33100 Udine, Italy
2 Biodiversity Research Institute (IMIB), University of Oviedo – CSIC – Principality of Asturias, Mieres, Asturias, Spain
3 National Biodiversity Future Center (NBFC), 90133 Palermo, Italy
4 Servizio fitosanitario e chimico, ricerca, sperimentazione e assistenza tecnica, Regional Agency for Rural Development (ERSA), via Sabbatini 5, 33050 Pozzuolo del Friuli, Italy
* Corresponding Author

DOI: doi.org/10.1016/j.agee.2026.110329

Abstract

Maize (*Zea mays* L.), one of the most important staple crops, is highly vulnerable to fungal infection by *Aspergillus* and *Fusarium* species, which produce aflatoxins and fumonisins respectively. Temperature and precipitation interplay in affecting both plant performance and mycotoxin

dynamics, but their effects might also depend on plant phenology. Timely identification of risk conditions is therefore essential to address preventive strategies.

In 2022 we monitored 20 rainfed maize fields across a pedo-climatic gradient in NE Italy at four phenological stages, namely beginning of stem elongation, end of tassel emergence, milk maturation, dent maturation. At each stage we measured plant functional traits representing maize growth and morpho-physiology; moreover, at harvest, kernel production and mycotoxins accumulation were quantified. All variables were then related to environmental conditions (precipitation, mean temperature, soil texture).

Our results showed that both aflatoxins and fumonisins were strongly related to environmental drivers already at stem elongation. The explained variance decreased afterwards but increased again at harvest. Fumonisins increased when seasonal rainfall was higher, while aflatoxins content was mediated by plant response (plant height and kernel $\delta^{13}C$).

These findings suggest a strong interplay between crop phenology, stress responses, and the occurrence of mycotoxins, shedding new light on the stress-induced vulnerability of plants to mycotoxin production. Stress timing is crucial, as it also affects final harvest conditions and points out possible underlying plant response legacies. We hence stress the importance of early-season monitoring of crops and tailored predictive models to anticipate mycotoxin risk in maize under variable climate scenarios.

Keywords

Maize • fungal pathogens • mycotoxins • plant stress • crop production • climate change • prediction models

Introduction

Maize (*Zea mays* L.) is one of the most important crops worldwide both in terms of yield and cultivated area, with more than 1.2 billion tons produced and 200 million hectares cultivated in 2023 (FAOSTAT, 2025). Driven by the growing human population, the demand for maize is expected to increase in the coming years, along with the natural resources required for its cultivation. Among these resources, water demand is of great concern: the usage of water in agriculture is a global issue, and water shortage has become the main constraint on food security worldwide (Hanjra & Qureshi, 2010). Agriculture is the largest water-user sector worldwide, accounting for 70% (2 710 km^3) of total freshwater withdrawals on average (The United Nations, 2013) with cereals consumption showing 26% of the total water footprint in 2000 (Ercin & Hoekstra, 2014). Therefore, agriculture is one of the most vulnerable human activities to climate change, with particular concern to weather variability, extreme events and droughts (Mendelsohn, 2009). Optimal maize production requires between 500

and 800 mm of water (FAOSTAT, 2025), highlighting its critical role in global agricultural water management. Moreover, heat waves and extreme meteorological conditions are rapidly increasing in terms of duration, intensity, and frequency (Intergovernmental Panel on Climate Change (IPCC), 2023), and the combination of heat and drought stresses negatively impacts the yield of major crop plants, including cereals such as maize (Cairns et al., 2013; Lobell et al., 2011).

As a consequence, in the last decades both maize quality and quantity are being threatened, inducing a marked increase of mycotoxins (mainly aflatoxins and fumonisins), which are highly toxic for humans (Kamle et al., 2019; Kumar et al., 2017; Marasas, 1995; Payne & Brown, 1998). Mycotoxins occurrence in maize is closely related to climatic conditions (Battilani et al., 2016; Janić Hajnal et al., 2023; Moretti et al., 2019), particularly in temperate areas bordering arid Mediterranean climates, such as those in the Southern Europe (e.g. Po Valley) (Giorgi, 2006; Giorgi & Lionello, 2008). Janić Hajnal et al., (2023) observed that in Serbia and Croatia some of these mycotoxins (i.e., deoxynivalenol and zearalenone) seem to depend on extreme level of precipitations, while others (i.e., fumonisins) are the result of dry and hot weather followed by warm and wet conditions. Moreover, it has been demonstrated that aflatoxin B1 contamination risk in European wheat is expected to increase according to temperature raise projected by models (Battilani et al., 2016).

Plant infection by mycotoxigenic fungi depends not only on climatic conditions but also on plant health status, often mediated by morphological and physiological responses, largely constrained by the plant plasticity to environment variations (Barnabás et al., 2008; Jin et al., 2023; Lanubile et al., 2017). For instance, maize plants with narrower stylar canal are more resistant to infections (Duncan & Howard, 2010), and maize cultivars with tighter and more complete husks present a physical barrier to insects, reducing in turn their susceptibility to fungal infections (Munkvold, 2003). While most studies on pathogen occurrence focused on climate-pathogen relationships (Blacutt et al., 2018), less attention has been paid to the complex interplay between abiotic factors, plant functional response and mycotoxin occurrence.

Plants respond to drought stress by altering their functional traits (e.g., by reducing leaf area and stomatal conductance), resulting in stunted growth and canopy thinning, with negative consequences for photosynthesis and productivity (Seleiman et al., 2021; Toscano et al., 2019). Maize has been proved to respond to drought and heat stress mainly by (1) increasing flowering days, days to maturity and anthesis silk interval, (2) reducing the number of leaves, (3) abnormally expressing secondary stress responsive traits, and (4) losing normal root architecture, leading overall to a reduction in yield per hectare (Sah et al., 2020). Moreover, soil texture also influences maize growth and productivity by modifying N mobilization and water availability (Ziadi et al., 2013). Finally, all these environmental factors can interact among each other resulting in complex growth and functional response patterns by the plant (Chukwudi et al., 2021).

These effects of environmental stress on plants can greatly vary according to the timing and duration of stress. In fact, it is already well known that plants at certain phenological stages might be more sensitive than others to environmental stresses (García-Tejero et al., 2010; Soares et al., 2021; Yavuz et al., 2021). In this light, plant phenology is another important aspect to be considered in climate-plant-pathogen interactions. In maize, the shift between vegetative and reproductive stages (anthesis) and the grain-filling stage are considered the most critical ones, where drought and heat lead to significant yield penalty, ranging from 34.3 to 66.2% (López-Galiano et al., 2019; Tsimba et al., 2013). To get better insights into the relationships between environmental stress, maize growth, productivity, and mycotoxin occurrence we conducted a field observational study along a climate and soil gradient in North-Eastern Italy. In particular, we investigated the relationships between environment (i.e., temperature, precipitation and soil structure), plant functional response (i.e., plant morphological and physiological traits together with productivity data) and grain mycotoxin content at different phenological stages. We hypothesized that the environment-plant relationships leading to mycotoxin occurrence in the kernels were shaped by the phenological stage of the plant: stress experienced by plants during a critical phenological stage may promote mycotoxin proliferation at the harvest. In particular, we expected these relationships to be different between aflatoxins and fumonisins, the former being favoured by drought and heat stress while the latter by rainy conditions. We also expected mycotoxin accumulation to be higher in stressed plants, i.e. the smaller ones. Moreover, we expected drought and heat stresses to influence both plant morpho-physiology (e.g., by reducing plant height and leaf chlorophyll content) and productivity (e.g., by reducing kernel dry weight and increasing kernel $\delta^{13}C$).

Material and methods

Experimental design

The study was conducted during summer 2022 in the Friuli Venezia Giulia region in the North-Eastern part of Italy, corresponding to the plain sector of the region (45°44'56"N, 12°59'56"E to 46°11'52"N, 13°29'56"E; Figure 1A). The climate is characterized by a mean annual temperature of 13 °C and an average annual precipitation ranging from 1100 to 1600 mm. The main crops grown in the area include maize, soybean, winter cereals (primarily barley and wheat), and grapevine. In this area 20 not irrigated (rainfed) maize fields were selected along a climatic and soil gradient (Figure 1A, Table S1). In each sample site maize hybrids belonging to FAO 500 maturity class were sown in between the 10th of April and the 3rd of May 2022, and a sampling area of 225 m^2 (15 x 15 m) was selected. Plant traits were measured four times along the growing season, corresponding to phenological stages 30 (T1, beginning of stem elongation), 59 (T2, end of tassel emergence), 73 (T3, milk maturation) and 89 (T4, dent maturation) of BBCH scale for cereals (Lancashire et al., 1991;

Meier, 2018). The sampling for the quantification of maize production and mycotoxin content was performed right before the harvest (stage 99, harvested product, T5) (Figure 1A).

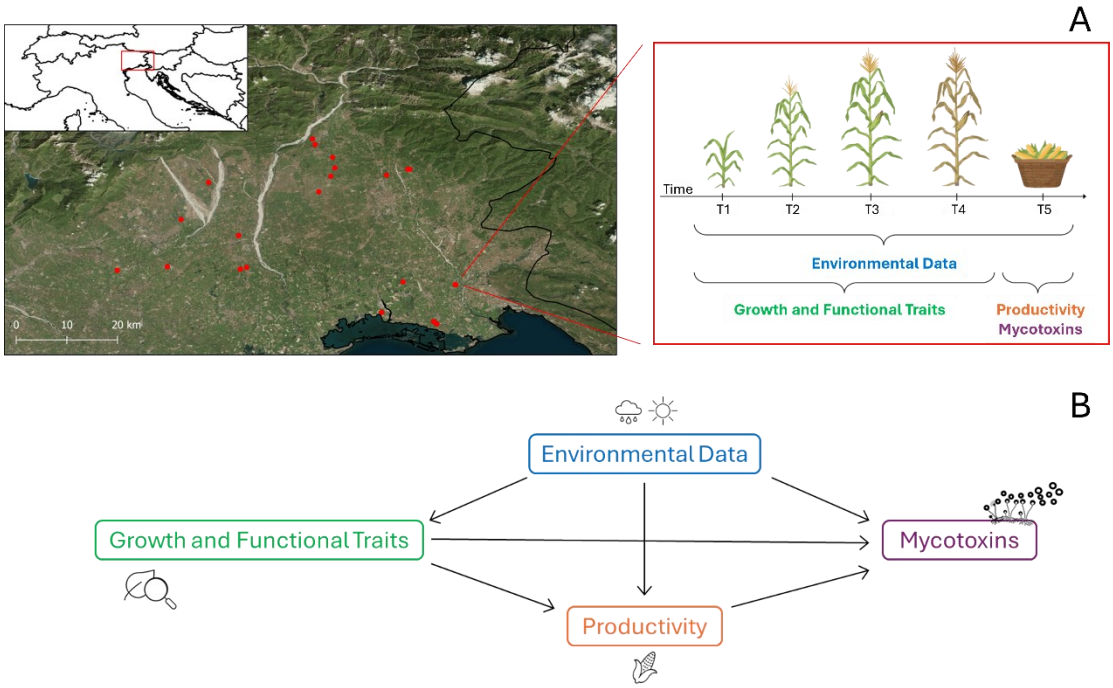


Figure 1 Experimental area and design. (A) Each dot represents a sampling site of 225 m² within a maize field. Environmental data were collected along the whole season; plant traits were measured four times (T1–T4); quantification of maize production and mycotoxin content was performed at the harvest (T5). T1: beginning of stem elongation; T2: end of tassel emergence; T3: milk maturation; T4: dent maturation; T5: harvest. (B) Hypothesised causal relationships.

Data collection

Soil and Climate

A sample of the first 35 cm of soil, corresponding to the ploughed layer, was collected at the centre of each plot using a soil core sampler and transported to laboratory (Regional Agency for Rural Development, ERSA) for soil texture analyses. The analyses covered the percentage of sand, silt and clay, the total limestone, the organic carbon content and the quantity of phosphorus (mg kg^{-1}). All analyses were performed in accordance with the Italian official protocol for soil chemical analysis (Metodi ufficiali di analisi chimica del suolo, 1999).

Climate data were provided by the Regional Environment Protection Agency (ARPA, Friuli Venezia Giulia) as GeoTIFF raster format with a spatial resolution of 500 × 500 m $pixel^{-1}$, derived from a network of >60 permanent monitoring stations. The dataset provided daily records of precipitation and mean temperature. For each sampling area, when more than one pixel was included inside the sampling plot, the mean value across pixels was used. For each phenological stage, cumulative

precipitation (sum of daily values, mm) and mean temperature (average of daily temperatures, °C) were then calculated for the period between sowing and the corresponding sampling date.

Maize growth and functional traits

In each sampling area and at each sampling time the growth of maize was assessed by measuring the height of five random plants, not including the male inflorescence when present. Moreover, the last fully expanded leaf was randomly collected from 10 different individuals (10 leaves in total), sealed in moistened plastic bags, stored in portable refrigerators and transported to the laboratory. Pictures of five leaves were acquired with digital camera, and the size of each leaf (cm^2) was determined with the software ImageJ (Schindelin et al., 2012). The same leaves were further weighed to determine fresh mass (FW), dried at 70 °C for 72 h and weighed again to quantify dry mass (DW). Specific leaf area (SLA, $cm^2\ g^{-1}$) and dry matter content were calculated from the dry mass, leaf area and fresh mass according to Pérez-Harguindeguy et al., (2013). Two one-centimetre radius disks were collected from the middle part of the lamina of each of the remaining five leaves, avoiding the midrib, and processed to quantify chlorophyll, carotenoids, and flavonoid content. The disks were ground into fine powder under liquid nitrogen. Chlorophyll *a* and *b* and carotenoid concentration analyses were performed following Marchiol et al., (2019) protocol and expressed as micrograms per gram of fresh weight ($\mu g\ g_{FW}^{-1}$). For the calculation methods see Wellburn (1994). Flavonoid content was quantified according to the method described by Filippi et al. (2021), with minor changes and expressed as quercetin-equivalent content per gram of fresh weight (μg quercetin-eq g^{-1}).

Maize production

At the harvest, ten ears per plot were randomly collected from different individuals, sealed in moistened plastic bags, stored in portable refrigerators, and transported to the laboratory. After removing the bracts and the cob, kernels were dried at 70 °C for 72 h and weighed to obtain their dry mass. The dry biomass of kernels was then used to measure carbon (C) and nitrogen (N) content and their isotopic signature ($\delta^{13}C$). Each dry sample was homogenized using a grinding mill. Then, a subsample was ball-milled and used for the analysis. The C and N content and the isotopic signature analyses were performed using a CHNS Elemental Analyser (Vario Microcube, © Elementar) coupled to a stable isotope ratio mass spectrometer (IRMS; Isoprime 100, © Elementar).

Mycotoxin quantification

The remaining part of the milled kernels was used for mycotoxin quantification at the ERSA laboratory. Samples were hydrated with a 0.1% v/v formic acid solution and then extracted with acetonitrile. The aqueous and organic phases were separated by adding a mixture of salts: magnesium sulphate to promote the passage of analytes in the organic phase, sodium chloride to decrease the residual water content in the organic phase, and a mixture of citrates (i.e., trisodium citrate dihydrate and disodium hydrogen citrate sesquihydrate) to maintain a slightly acidic pH. The organic phase was then removed and placed at -18°C overnight to remove fatty substances by precipitation. After

filtration, instrumental analysis was performed using LC-HRMS spectrometer, using the labelled isotopes for each toxin as analytical standards.

The concentration (ppb) of the following mycotoxins was obtained: aflatoxin B1, aflatoxin B2, aflatoxin G1, aflatoxin G2, deoxynivalenol, fumonisin B1, fumonisin B2, fumonisin B3, HT-2 and zearalenone. Because of the low content of other mycotoxins, we focused our analyses on the total amount of aflatoxins (calculated as the sum of aflatoxin B1 and B2) and the total amount of fumonisins (calculated as the sum of fumonisin B1 and B2).

Data analysis

Initially, individual measurements of plant traits were pooled for each plot to calculate the mean value. Data were subdivided into four categories: environmental data, plant growth and functional traits, plant productivity data and mycotoxin occurrence data. We assumed the following causal framework: plant growth and functional traits are only affected by the environment; both environment and plant growth and functional traits affect plant productivity; all the previous categories affect mycotoxin occurrence (Figure 1B).

In order to check for multicollinearity among explanatory variables, we computed a correlation matrix (Pearson's r) of the explanatory variables considered in the models using in the "corrplot" R package (Taiyun & Viliam, 2021). To avoid collinearity in the models, variables were excluded from the full models when correlations were higher than $|0.65|$ in at least one paired combination and at least one sampling time (Dormann et al., 2013). As a result, we considered the following variables: daily mean temperature, cumulative daily precipitation, and soil clay content as environmental predictors; plant height as a measure of plant growth; total chlorophyll content and SLA regarding leaf functional traits; kernel $\delta^{13}C$ and kernel DW as indicators of plant productivity; and the total amounts of aflatoxins and fumonisins.

We then tested separate linear models to assess (1) the effects of environmental predictors on plant growth and functional traits, (2) the effects of environmental predictors, plant growth, and functional traits on plant productivity, and (3) the effects of all selected predictors on aflatoxins and fumonisins separately for each phenological stage (Table S2). The assumptions of the full models were verified using diagnostic plots of the residuals. If model assumptions were not satisfied, standard transformations (i.e., logarithmic, square root, and exponential) were applied (Table S2).

Subsequently, to identify the most relevant explanatory variables for each model, we employed a manual backward selection procedure starting from each full linear model: variables were iteratively removed based on their lack of statistical significance (p-value > 0.05).

In order to represent the actual contribution of environmental, plant growth and functional predictors, while accounting for the variance explained by the final plant productive effort, all environmental predictors and plant traits were referred to each phenological stage from T1 to T4,

with plant productivity additionally included at each stage. This approach allowed us to identify which of the phenological stages analysed contributed most to the final occurrence of mycotoxins, while accounting for the plants' final productivity. To quantify that, for all the models of aflatoxins and fumonisins, we calculated the relative importance of each predictor, which represents the percentage of variance explained by each independent variable, using the "relaimpo" R package (Groemping, 2006).

All the graphs of the linear models were created with the "visreg" R package (Breheny & Burchett, 2017). All statistical analyses were performed with R v4.5.0 and RStudio v2025.09.0-387 (R Core Team, 2023).

Results

Effects of environmental conditions on maize growth and functional traits across phenological stages

	Phenology	Predictor	Df	F-value	p-value		R^2
Chlorophyll	**T1**	-	-	-	-		-
	T2	-	-	-	-		-
	T3	-	-	-	-		-
	T4	-	-	-	-		-
Plant Height	**T1**	(Intercept)	1,17	13.7408	**0.002**	**	0.29
		Temperature	1,17	6.4465	**0.021**	*	
		Clay	1,17	4.0897	0.059	.	
	T2	-	-	-	-		-
	T3	-	-	-	-		-
	T4	(Intercept)	1,15	54.121	**<0.001**	***	0.63
		Precipitation	1,15	27.834	**<0.001**	***	
log(SLA)	**T1**	-	-	-	-		-
	T2	(Intercept)	1,16	9.0933	**0.008**	**	0.66
		Temperature	1,16	7.9643	**0.012**	*	
		Clay	1,16	26.3443	**<0.001**	***	
	T3	(Intercept)	1,18	149.9188	**<0.001**	***	0.28
		Precipitation	1,18	8.3954	**0.009**	**	
	T4	-	-	-	-		-

Table 1 ANOVA outcomes for reduced models explaining the variance of leaf chlorophyll content, plant height and SLA across phenological stages. T1: beginning of stem elongation; T2: end of tassel emergence; T3: milk maturation; T4: dent maturation.

Among the maize growth traits, leaf chlorophyll content did not show any significant relationship with the environmental predictors considered at any of the phenological stages tested (see Table 1). Leaf chlorophyll content values varied between 0.34 and 2.74 μg g_{FW}^{-1}, with a mean of 1.61±0.55 μg g_{FW}^{-1}.

Plant height varied from an average of 150.5±50.0 cm at T1 to 251.8±36.3 cm at T4, the minimum being 75.4 cm at T1 and the maximum being 312.2 cm at T4. Plant height at T1 was significantly affected by environmental conditions (Table1), explaining 29 % of the total variation in maize height. In particular, plant height was negatively related to daily mean temperature and clay content (Figure 2A-B; R^2 = 0.29). There were no significant effects of environmental predictors at T2 and T3, while at T4 plant height was strongly positively related to the total amount of rain throughout the whole growing season (Figure 2C; R^2 = 0.63).

SLA values varied from 16.2 $cm^2\ g^{-1}$ to 55.3 $cm^2\ g^{-1}$, with a mean of 32.5±7.4 $cm^2\ g^{-1}$. No statistically significant relationship was found at T1 (see Table 1). At T2 SLA was strongly positively related to both clay content and mean temperature experienced by plants from the sowing up to the sampling date (Figure 2D-E; R^2 = 0.66). We also found a positive relationship at T3 between SLA and the total precipitation occurred from the beginning of the season (Figure 2F; R^2 = 0.28). No statistically significant relationship was found at T4 (see Table 1).

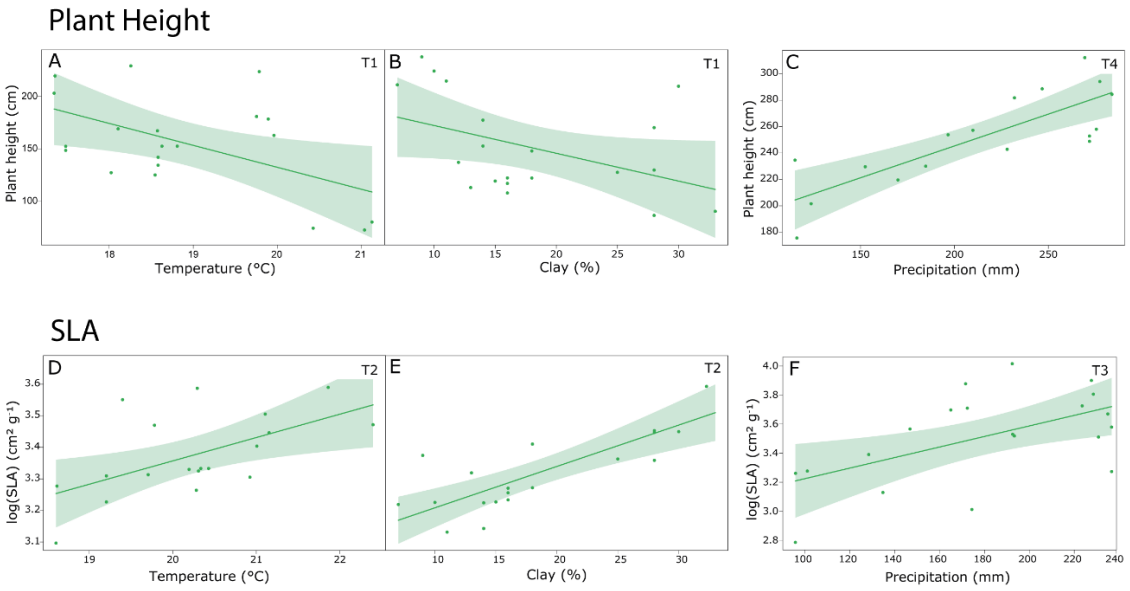


Figure 2 Reduced linear models explaining the variance of plant height and SLA over phenological stages. T1: beginning of stem elongation; T2: end of tassel emergence; T3: milk maturation; T4: dent maturation.

Effects of environmental conditions and plant functional response on maize production and kernel physiological traits over phenological stages

	Phenology	Predictor	Df	F-value	*p*-value		R^2
$\delta^{13}C$	**T1**	(Intercept)	1,17	226.3401	**<0.001**	***	0.25
		SLA	1,17	6.8894	**0.018**	*	
	T2	-	-	-	-		-
	T3	-	-	-	-		-
	T4	-	-	-	-		-
	T5	(Intercept)	1,17	3206.141	**<0.001**	***	0.25
		Precipitation	1,17	7.0601	**0.017**	*	
DW kernel	**T1**	(Intercept)	1,17	2.016	0.174		0.21
		SLA	1,17	5.6894	**0.029**	*	
	T2	-	-	-	-		-
	T3	(Intercept)	1,17	0.0314	0.861		0.18
		Plant height	1,17	4.9145	**0.041**	*	
	T4	-	-	-	-		-
	T5	-	-	-	-		-

Table 2 ANOVA outcomes for reduced models explaining the variance of kernel $\delta^{13}C$ and kernel DW over phenological stages. T1: beginning of stem elongation; T2: end of tassel emergence; T3: milk maturation; T4: dent maturation; T5: harvest.

Kernel $\delta^{13}C$ varied between -13.6 ‰ and -12.1 ‰ with an average of -12.8±0.4 ‰. Kernel $\delta^{13}C$ was positively related to SLA at T1 (Figure 3A; $R^2 = 0.25$). No statistically significant relationship was found between T2 and T4 (Table 2). Kernel $\delta^{13}C$ was positively related to the total precipitation throughout the entire growing season at T5 (Figure 3B; $R^2 = 0.25$).

Kernel dry weight varied from 18.7 g to 202.3 g, with a mean of 116.8±47.9 g. Kernel DW was positively related to SLA at T1 (Figure 3C; $R^2 = 0.21$) and to plant height at T3 (Figure 3D; $R^2 = 0.18$). No statistically significant relationship was found at T2, T4 and T5 (Table 2).

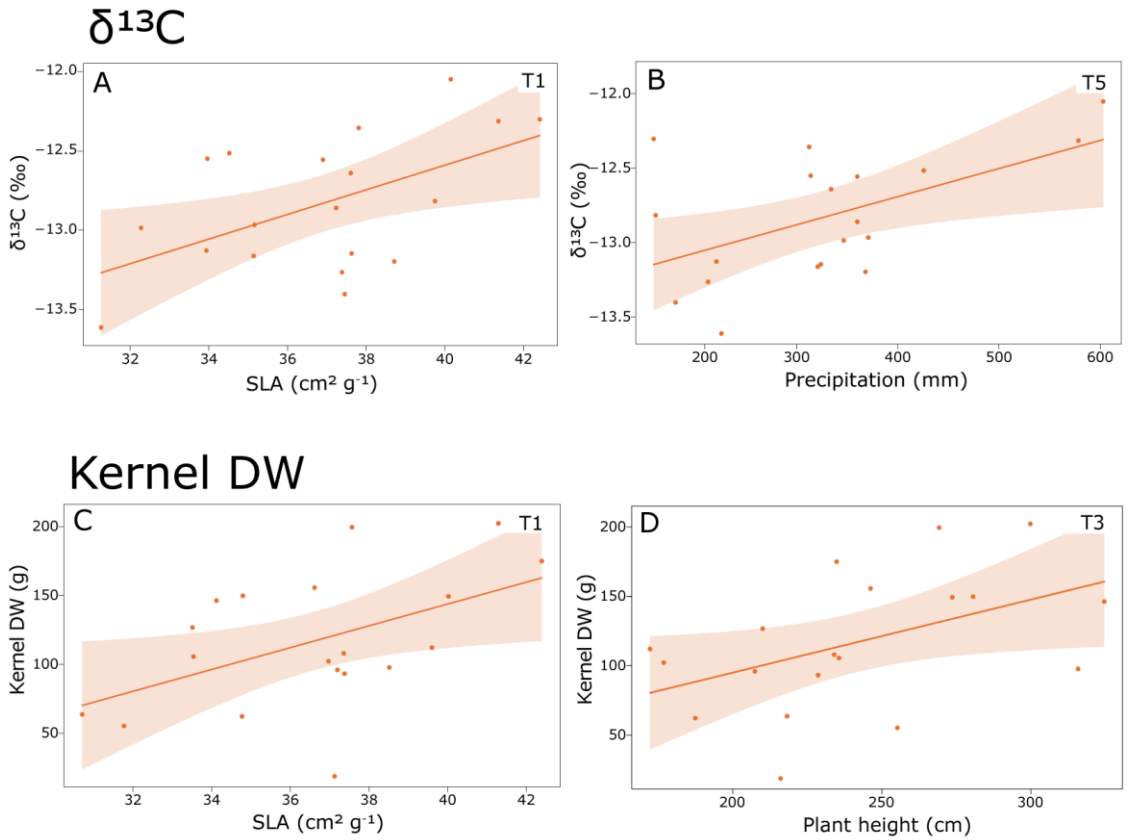


Figure 3 Reduced linear models explaining the variance of kernel $\delta^{13}C$ and kernel DW over phenological stages. T1: beginning of stem elongation; T2: end of tassel emergence; T3: milk maturation; T4: dent maturation; T5: harvest.

Relationship between kernel aflatoxins and fumonisins, environmental variable and plant functional response over phenological stages

	Phenology	Predictor	Df	F-value	*p*-value		R^2
log(Aflatoxins)	T1	(Intercept)	1,16	6.6887	**0.019**	*	0.54
		Plant height	1,16	19.9997	**<0.001**	***	
		$\delta^{13}C$	1,16	8.7648	**<0.001**	**	
	T2	-	-	-	-		-
	T3	-	-	-	-		-
	T4	-	-	-	-		-
	T5	(Intercept)	1,15	6.4	**0.023**	*	0.24
		Precipitation	1,15	5.9354	**0.028**	*	
		$\delta^{13}C$	1,15	5.2304	**0.037**	*	
		Clay	1,15	3.9039	0.068	.	

Fumonisins	**T1**	(Intercept)	1,17	35.537	**<0.001**	***	0.56
		Clay	1,17	12.374	**0.003**	**	
		Plant height	1,17	22.119	**<0.001**	***	
	T2	(Intercept)	1,18	10.248	**0.005**	**	0.36
		Temperature	1,18	11.725	**0.003**	**	
	T3	(Intercept)	1,18	9.7121	**0.006**	**	0.34
		Temperature	1,18	10.9696	**0.004**	**	
	T4	(Intercept)	1,14	23.144	**<0.001**	***	0.62
		Temperature	1,14	18.608	**<0.001**	***	
		Plant height	1,14	14.281	**0.002**	**	
	T5	(Intercept)	1,18	11.786	**0.003**	**	0.63
		Precipitation	1,18	32.571	**<0.001**	***	

Table 3 ANOVA outcomes for reduced models explaining the variance of aflatoxins and fumonisins over phenological stages. T1: beginning of stem elongation; T2: end of tassel emergence; T3: milk maturation; T4: dent maturation; T5: harvest.

As shown in Supplemental Figure S1, the importance of environment, plant growth and functional traits and plant productivity in shaping the final mycotoxin contamination varied over time and between aflatoxins and fumonisins. Aflatoxin variance was initially mostly explained by plant growth and functional traits and productivity (T1), with productivity remaining a relevant—though not statistically significant—factor throughout the season, mainly due to kernel $\delta^{13}C$. At T3 (early milk maturation) both precipitation and SLA became important, even if not statistically significant. At the end of the season (T5) the total seasonal precipitation and kernel $\delta^{13}C$ were the most important predictors in explaining aflatoxins variance.

The variance of fumonisin models had a very different pattern: plant growth and functional traits and productivity declined in importance in favour of environmental drivers. Throughout the vegetative phases (T1-T4), temperature played a leading role, while at T5 total seasonal rainfall emerged as the primary explanatory variable.

Overall, fumonisins resulted to be strictly related to the environment (both temperature and precipitation), while aflatoxins – although strongly influenced by environmental factors – were also mediated by the plant growth and functional response to the environmental conditions.

Aflatoxins varied between 0.0 ppb and 250.0 ppb, with a mean of 27.7±61.8 ppb. The model selection highlighted that aflatoxins concentration at T1 was strongly negatively related to plant height and final kernel $\delta^{13}C$ (Figure 4A-B; $R^2 = 0.54$). No statistically significant relationship was found between T2 and T4 (Table 3). At T5 aflatoxins concentration decreased with kernel $\delta^{13}C$ and increased with both total precipitation and clay content (Figure 4C-E; $R^2 = 0.24$).

Fumonisins varied between 0.0 ppb and 25244.0 ppb, with a mean of 5474.3±7466.2 ppb. Fumonisins concentration at T1 was negatively related to both clay content and plant height (Figure 4F-G; R^2 = 0.56). At T2 and T3 fumonisins increased with increasing temperatures (Figure 4H-I; R^2 = 0.36 and 0.34 respectively), while at T4 it increased with both temperature and plant height (Figure 4J-K; R^2 = 0.62). At T5 the total precipitation strongly positively influenced the final presence of fumonisins (Figure 4L; R^2 = 0.63).

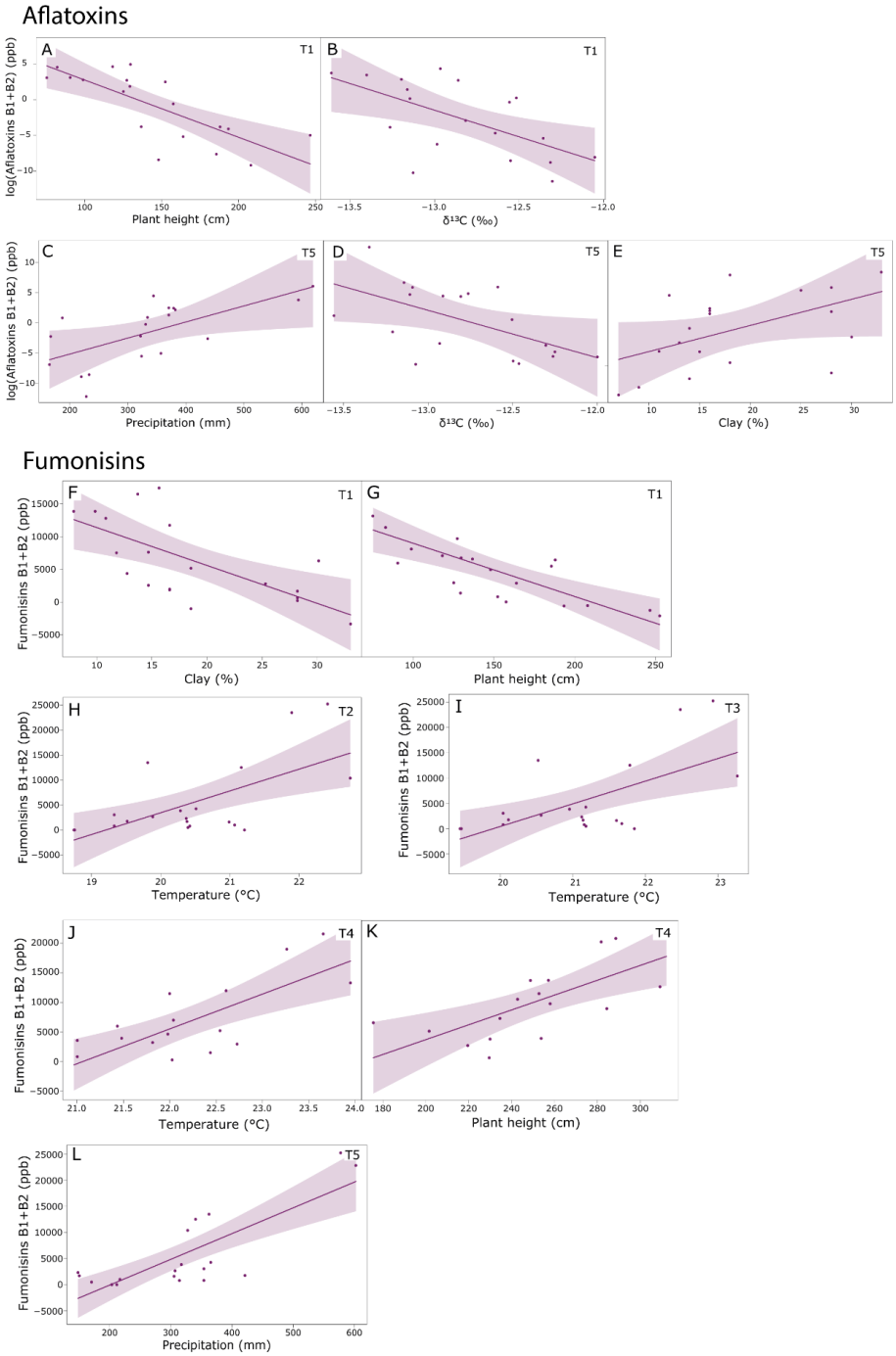


Figure 4 Reduced linear models explaining the variance of mycotoxins over phenological stages. T1: beginning of stem elongation; T2: end of tassel emergence; T3: milk maturation; T4: dent maturation; T5: harvest.

Discussion

This study aimed to investigate the temporal dynamics of environmental and plant-related predictors influencing mycotoxin contamination in the field (i.e., aflatoxins and fumonisins) at different stages of plant phenology. The results highlighted both mycotoxin-specific and phenological stage-specific sensitivities to the drivers. In particular, we demonstrated that environmental conditions at the early stages of phenology can exert a legacy effect on the final accumulation of mycotoxins in the kernels. This pattern was especially evident for fumonisins, which were strongly related to temperature trends during plant growth. In contrast, aflatoxin contamination appeared to be more strongly associated with the plants' responses to stress over time.

Effects of environmental condition on maize growth and functional response over phenological stages

Contrary to expectations, chlorophyll content showed no significant dependence on the tested environmental variables. Our results suggest a strong capacity of maize to acclimate the pigment contents even at very different phenological stages and environmental conditions (Ciganda et al., 2008; Drozak & Romanowska, 2006).

The plant height during the considered phenological stages was consistent to what indicated in the BBCH scale for cereals (Lancashire et al., 1991; Meier, 2018), reaching its maximum already at T2 (end of tassel emergence). Also values of SLA were in line with other studies conducted on maize (L. L. Xu et al., 2017).

Plant height and specific leaf area (SLA) responded to environmental drivers in a time-dependent manner. At the beginning of stem elongation (T1), height decreased with increasing temperature and clay content, pointing to potential early heat stress when high temperatures were combined with high water storage capability. This decrease in plant elongation might be related to a necessary investment by the plant in developing a more structured root system (S. Yan et al., 2022). Plant height increased at T4 when high seasonal precipitation was observed, indicating the importance of water availability during the whole growing season. The dependence of maize height on water availability and temperature is commonly observed as a plant response to climate stresses (Laskari et al., 2022; Ma et al., 2008; Sunoj et al., 2016). SLA at T2 increased with temperature and clay content, reflecting a rapid growth in warmer and finer-textured soils, probably due to a generalized non-limiting water condition (Rosbakh et al., 2015; Zhou et al., 2020). At T3, SLA was positively related to precipitation, suggesting a plastic response to increased water availability, possibly enhancing light interception and hence photosynthetic efficiency under more favorable conditions.

Taken together, all these conditions support the hypothesis that favorable plant growing conditions are necessary for toxins development, except for the initial stage (T1) where both aflatoxins and fumonisins took advantage from a low plant height.

Effects of environmental condition and plant growth and leaf functional traits on maize production and kernel physiological traits over phenological stages

$\delta^{13}C$ is a widely used proxy for assessing physiological response related to drought stress and stomatal dynamics in plants. In C3 plants' leaves it typically tends to increase (become less negative) under water-limited conditions, while C4 plants are less sensitive to environmental factors, as a lower correlation with water shortage has been reported (Dercon et al., 2006; Murphy & Bowman, 2009). Moreover, literature provides rare yet clear evidence of a variable trend in various C4 plant species, ranging from negative to positive correlations with water availability (Weiguo et al., 2005). In addition, some studies found that both leaf and kernel $\Delta^{13}C$ (which is the isotopic discrimination and is inversely related to $\delta^{13}C$) increases in drought conditions in both sorghum (Williams et al., 2001) and maize (Cabrera-Bosquet et al., 2009) (C4 plants). Moreover, some authors recently found that $\delta^{13}C$ values are positively correlated with water availability in pearl millet and others C4 plants (Flohr et al., 2019; Murphy & Bowman, 2009; Sanborn et al., 2021). Although a comprehensive explanation for $\delta^{13}C$ trend in C4 plants is still lacking, the most frequently cited hypothesis is that C4 discrimination power against ^{13}C is partially influenced by CO_2 leakage from the bundle sheath cells to the mesophyll cells, which can result in higher rather than lower $\Delta^{13}C$ when the internal CO_2 concentration decreases (Farquhar, 1983; Henderson et al., 1992).

In addition, nitrogen fertilization is often cited as a further confounding factor, as it is closely linked to water uptake, photosynthesis and stomatal conductance and can consequently affect the $\delta^{13}C$ pattern (Xing et al., 2021; Yang et al., 2021). In this perspective, although not in line with the majority of studies, our findings are nonetheless supported by years of similar results.

Finally, in our study, kernel dry weight (DW) was positively associated with SLA at the beginning of stem elongation (T1) and with plant height at the end of tassel emergence (T3), indicating that early vigor and vegetative growth during critical periods contribute to final yield (Golam et al., 2011; L. Zhang et al., 2022).

At the beginning of stem elongation (T1), SLA proved to be a better indicator of early stress conditions that may leave a legacy affecting the final grain production (Golam et al., 2011). Plants exhibiting a higher SLA at this stage, typically associated with thinner leaves and lower structural investment per unit leaf area, appeared to experience lower physiological stress (Liu et al., 2023; Scheepens et al., 2010), which was later reflected in greater kernel dry weight (DW) (L. Zhang et al., 2022). This suggests that an early acclimation strategy based on maintaining high SLA may allow plants to optimize resource use efficiency and preserve photosynthetic potential during the

reproductive phase. Later in season (T3), kernel DW became more closely related to plant height, indicating that once the canopy is fully developed, structural vigor and biomass accumulation play a greater role in determining yield. Together, these results suggest a temporal shift in the traits linked to productivity: during early development, physiological traits such as SLA capture the plant's capacity to cope with environmental stress, while at later stages, morphological traits like plant height better reflect the plant's ability to sustain grain filling and final yield.

These results underline the importance of early physiological traits and mid-season biomass accumulation for yield determination.

Relationships between kernel aflatoxin and fumonisin, environmental variables and plant functional response over phenological stages

Our results highlight both mycotoxin-specific and phenological stage-specific sensitivities to the drivers.

Regarding aflatoxins, the best model in terms of explained variance was the one at the beginning of stem elongation (T1): aflatoxin concentration decreased with plant height and $\delta^{13}C$ ($R^2 = 0.54$). At the same phenological stage, plant height decreased with temperature and clay content in the soil, while $\delta^{13}C$ increased with SLA. Overall, higher temperatures before maize stem elongation resulted in shorter plants at T1, which at the harvest had higher concentrations of aflatoxins. This is consistent with previous studies on aflatoxin contamination in maize (Kos et al., 2018; Pleadin et al., 2023). This result indicates that early (T1) morphological plant responses to the environment may leave a legacy affecting the aflatoxins accumulation at the harvest (T5).

Flowering is often highlighted as a highly sensitive stage, as described by Bailly et al., (2025), but high temperatures and low rainfall during the early maturation stage resulted in higher risk of aflatoxin contamination in the study of Temba et al., (2021). In our study, aflatoxin contamination increased with seasonal precipitation, probably meaning that low-precipitation fields presented too low humidity for *A. flavus* to properly grow and produce mycotoxins. Indeed, some studies indicate that *A. flavus* does not grow properly nor produce aflatoxins in low relative humidity conditions *in vitro* (Choi et al., 2015; Pratiwi et al., 2015).

Aflatoxin concentration was higher in plants whose kernel $\delta^{13}C$ values were lower. This pattern may reflect a reduced ability of these plants to fully exploit the photosynthetic efficiency typical of C4 plants. Such an interpretation may be plausible given that these plants also received more rainfall, likely under more cloudy conditions, which could have limited their C4 photosynthetic efficiency and in turn favored the high ^{13}C discrimination of Rubisco.

An interesting hypothesis regarding the functional role of aflatoxins was formulated by Reverberi et al., (2021): aflatoxins produced by *Aspergillus flavus* during stable growth may act as strong antioxidants enhancing its tolerance to oxidative stress. This is consistent with active resistance against the

pathogen by the plant host and a consequent fungal functional response. Although fungal growth may be enhanced in stressed plants, the peak of mycotoxin accumulation appears to be associated with a high level of resistance in maize and the consequent oxidative conditions that are critical for the pathogen survival. These observations could explain that vigorous and well-watered plants produced strong oxidative defenses and induced the fungus to synthesize aflatoxins as response (Reverberi et al., 2022). On the other hand, the higher susceptibility to mycotoxins in stressed plants could be explained considering that $\delta^{13}C$ values refer to the kernel reserves, and not to carbohydrates invested in vegetative metabolism.

Regarding fumonisins, the best model in terms of explained variance was the one at T5: fumonisin concentration increases with seasonal precipitation ($R^2 = 0.63$). We also found positive relationships with temperature at T2, T3 and T4. This is consistent with the results of many previous studies (Picot et al., 2010; Santiago et al., 2015). Nevertheless, Santiago R. et al., (2015) concluded that climatic conditions cannot satisfactorily explain differences in fumonisin contamination among different environments. Although greater fumonisin contaminations were often associated with warmer or drier years, some studies have pointed out the lack of a clear association between drought and fumonisin contamination because seasons with combined conditions of warm weather and high precipitation before harvest resulted in higher fumonisin accumulation (Santiago et al., 2015). This would confirm our results, in which fumonisin concentration is mainly related to pre-harvest precipitation and to high temperature during intermediate phenological stages.

Fumonisins in our study were also strongly negatively related at T1 to plant height and clay content ($R^2 = 0.56$), suggesting that more vigorous and well hydrated plants were probably more able to reduce fumonisin accumulation.

Overall, our findings highlight the potential of this approach to identify early plant–environment interactions and physiological legacies of stress across phenological stages, providing new insights into how transient conditions during vegetative growth can shape the final outcome of aflatoxin contamination at harvest.

Conclusions

This study provides evidence that both aflatoxin and fumonisin contamination in maize are shaped by dynamic interactions between environmental conditions and plant growth and leaf functional traits responses across phenological stages. While some plant traits, such as chlorophyll content, appeared to be genetically determined and environmentally insensitive, others (e.g., plant height and SLA) responded variably to environmental drivers depending on timing and specific stress factors.

Grain yield components, including kernel $\delta^{13}C$ and dry weight, were also influenced by early functional traits, confirming the importance of early vigour and mid-season biomass accumulation for productivity.

Interestingly, aflatoxins and fumonisins showed distinct temporal sensitivities: aflatoxins were influenced not only by environmental conditions (such as high temperatures and low rainfall early in the season) but also by plant responses like height and kernel $\delta^{13}C$, particularly at the beginning of stem elongation (T1). This suggests that aflatoxin risk is partially mediated by the plant's physiological ability to cope with stress. Conversely, fumonisin contamination was more consistently and directly linked to environmental conditions, especially temperature during vegetative growth and rainfall prior to harvest. The strong positive relationship with total seasonal precipitation at the harvest (T5) suggests that warm and wet conditions in the later phenological stages are critical for fumonisin production.

These findings reinforce the need for a multi-stage, integrative approach in mycotoxin risk assessment. Studying the crop-environment-pathogen system across phenological stages allows for the identification of critical windows of vulnerability and highlights the potential for early-stage intervention. Moreover, the dent stage also emerges as a strategic phase for mitigation, where practices such as avoiding excessive irrigation may reduce fungal growth and toxins accumulation.

Overall, this temporal perspective opens new avenues for sustainable, targeted management of mycotoxin risks in maize under changing climatic scenarios.

References

Bailly S, El Mahgubi A, Puel O, et al (2025) Implantation of Aspergillus Section Flavi in French Maize and Consequences on Aflatoxin Contamination of Maize at Harvest: Three-Year Survey. Toxins 17:155. https://doi.org/10.3390/toxins17040155

Barnabás B, Jäger K, Fehér A (2008) The effect of drought and heat stress on reproductive processes in cereals. Plant, Cell & Environment 31:11–38. https://doi.org/10.1111/j.1365-3040.2007.01727.x

Battilani P, Toscano P, Van der Fels-Klerx HJ, et al (2016) Aflatoxin B1 contamination in maize in Europe increases due to climate change. Sci Rep 6:24328. https://doi.org/10.1038/srep24328

Blacutt AA, Gold SE, Voss KA, et al (2018) Fusarium verticillioides: Advancements in Understanding the Toxicity, Virulence, and Niche Adaptations of a Model Mycotoxigenic Pathogen of Maize. Phytopathology® 108:312–326. https://doi.org/10.1094/PHYTO-06-17-0203-RVW

Breheny P, Burchett W (2017) Visualization of Regression Models Using visreg

Cabrera-Bosquet L, Sánchez C, Araus JL (2009) How yield relates to ash content, Δ13C and Δ18O in maize grown under different water regimes. Ann Bot 104:1207–1216. https://doi.org/10.1093/aob/mcp229

Cairns JE, Crossa J, Zaidi PH, et al (2013) Identification of Drought, Heat, and Combined Drought and Heat Tolerant Donors in Maize. Crop Science 53:1335–1346. https://doi.org/10.2135/cropsci2012.09.0545

Choi S, Jun H, Bang J, et al (2015) Behaviour of *Aspergillus flavus* and *Fusarium graminearum* on rice as affected by degree of milling, temperature, and relative humidity during storage. Food Microbiology 46:307–313. https://doi.org/10.1016/j.fm.2014.08.019

Chukwudi UP, Kutu FR, Mavengahama S (2021) Maize response to combined heat and water stresses under varying growth conditions. Agron J 113:4672–4689. https://doi.org/10.1002/agj2.20820

Ciganda V, Gitelson A, Schepers J (2008) Vertical Profile and Temporal Variation of Chlorophyll in Maize Canopy: Quantitative "Crop Vigor" Indicator by Means of Reflectance-Based Techniques. Agronomy Journal 100:1409–1417. https://doi.org/10.2134/agronj2007.0322

Dercon G, Clymans E, Diels J, et al (2006) Differential 13C Isotopic Discrimination in Maize at Varying Water Stress and at Low to High Nitrogen Availability. Plant Soil 282:313–326. https://doi.org/10.1007/s11104-006-0001-8

Dormann CF, Elith J, Bacher S, et al (2013) Collinearity: a review of methods to deal with it and a simulation study evaluating their performance. Ecography 36:27–46. https://doi.org/10.1111/j.1600-0587.2012.07348.x

Drozak A, Romanowska E (2006) Acclimation of mesophyll and bundle sheath chloroplasts of maize to different irradiances during growth. Biochim Biophys Acta Bioenerg 1757:1539–1546. https://doi.org/10.1016/j.bbabio.2006.09.001

Duncan KE, Howard RJ (2010) Biology of Maize Kernel Infection by *Fusarium verticillioides*. MPMI 23:6–16. https://doi.org/10.1094/MPMI-23-1-0006

Ercin AE, Hoekstra AY (2014) Water footprint scenarios for 2050: A global analysis. Environment International 64:71–82. https://doi.org/10.1016/j.envint.2013.11.019

FAOSTAT (2025) FAOSTAT. https://www.fao.org/faostat/en/#data/QCL/visualize. Accessed 9 Sept 2025

Farquhar GD (1983) On the Nature of Carbon Isotope Discrimination in C4 Species. Functional Plant Biol 10:205–226. https://doi.org/10.1071/pp9830205

Filippi A, Braidot E, Petrussa E, et al (2021) Plant growth shapes the effects of elevation on the content and variability of flavonoids in subalpine bilberry stands. Plant Biology 23:241–249. https://doi.org/10.1111/plb.13194

Flohr P, Jenkins E, Williams HRS, et al (2019) What can crop stable isotopes ever do for us? An experimental perspective on using cereal carbon stable isotope values for reconstructing water availability in semi-arid and arid environments. Veget Hist Archaeobot 28:497–512. https://doi.org/10.1007/s00334-018-0708-5

García-Tejero I, Romero-Vicente R, Jiménez-Bocanegra JA, et al (2010) Response of citrus trees to deficit irrigation during different phenological periods in relation to yield, fruit quality, and water productivity. Agricultural Water Management 97:689–699. https://doi.org/10.1016/j.agwat.2009.12.012

Giorgi F (2006) Climate change hot-spots. Geophysical Research Letters 33:. https://doi.org/10.1029/2006GL025734

Giorgi F, Lionello P (2008) Climate change projections for the Mediterranean region. Global and Planetary Change 63:90–104. https://doi.org/10.1016/j.gloplacha.2007.09.005

Golam F, Farhana N, Zain MF, et al (2011) Grain yield and associated traits of maize (*Zea mays* L.) genotypes in malaysian tropical environment. Afr J Agr Res 6:6147–6154. https://doi.org/10.5897/AJAR11.1331

Groemping U (2006) Relative Importance for Linear Regression in R: The Package relaimpo

Hanjra MA, Qureshi ME (2010) Global water crisis and future food security in an era of climate change. Food Policy 35:365–377. https://doi.org/10.1016/j.foodpol.2010.05.006

Henderson SA, Caemmerer SV, Farquhar GD (1992) Short-Term Measurements of Carbon Isotope Discrimination in Several C4 Species. Functional Plant Biol 19:263–285. https://doi.org/10.1071/pp9920263

Intergovernmental Panel on Climate Change (IPCC) (ed) (2023) Weather and Climate Extreme Events in a Changing Climate. In: Climate Change 2021 – The Physical Science Basis: Working Group I Contribution to the Sixth Assessment Report of the Intergovernmental Panel on Climate Change. Cambridge University Press, Cambridge, pp 1513–1766

Janić Hajnal E, Kos J, Radić B, et al (2023) Impact of Climate Changes on the Natural Prevalence of *Fusarium* Mycotoxins in Maize Harvested in Serbia and Croatia. Foods 12:. https://doi.org/10.3390/foods12051002

Jin M, Liu H, Liu X, et al (2023) Complex genetic architecture underlying the plasticity of maize agronomic traits. Plant Communications 4:100473. https://doi.org/10.1016/j.xplc.2022.100473

Kamle M, Mahato DK, Devi S, et al (2019) Fumonisins: Impact on Agriculture, Food, and Human Health and their Management Strategies. Toxins 11:328. https://doi.org/10.3390/toxins11060328

Kos J, Janić Hajnal E, Šarić B, et al (2018) Aflatoxins in maize harvested in the Republic of Serbia over the period 2012–2016. Food Additives & Contaminants: Part B 11:246–255. https://doi.org/10.1080/19393210.2018.1499675

Kumar P, Mahato DK, Kamle M, et al (2017) Aflatoxins: A Global Concern for Food Safety, Human Health and Their Management. Frontiers in Microbiology 7:

Lancashire PD, Bleiholder H, Boom TVD, et al (1991) A uniform decimal code for growth stages of crops and weeds. Annals of Applied Biology 119:561–601. https://doi.org/10.1111/j.1744-7348.1991.tb04895.x

Lanubile A, Maschietto V, Borrelli VM, et al (2017) Molecular basis of resistance to *Fusarium* ear rot in maize. Frontiers in Plant Science 8:. https://doi.org/10.3389/fpls.2017.01774

Laskari M, Menexes G, Kalfas I, et al (2022) Water Stress Effects on the Morphological, Physiological Characteristics of Maize (*Zea mays* L.), and on Environmental Cost. Agronomy 12:. https://doi.org/10.3390/agronomy12102386

Liu Z, Zhao M, Zhang H, et al (2023) Divergent response and adaptation of specific leaf area to environmental change at different spatio-temporal scales jointly improve plant survival. Global Change Biol 29:1144–1159. https://doi.org/10.1111/gcb.16518

Lobell DB, Bänziger M, Magorokosho C, Vivek B (2011) Nonlinear heat effects on African maize as evidenced by historical yield trials. Nature Clim Change 1:42–45. https://doi.org/10.1038/nclimate1043

López-Galiano MJ, García-Robles I, González-Hernández AI, et al (2019) Expression of miR159 Is Altered in Tomato Plants Undergoing Drought Stress. Plants 8:201. https://doi.org/10.3390/plants8070201

Ma S-Q, Wang Q, Luo X-L (2008) Effect of climate change on maize (*Zea mays*) growth and yield based on stage sowing. Shengtai Xuebao/ Acta Ecologica Sinica 28:2131–2139

Marasas WFO (1995) Fumonisins: Their implications for human and animal health. Natural Toxins 3:193–198. https://doi.org/10.1002/nt.2620030405

Marchiol L, Filippi A, Adamiano A, et al (2019) Influence of Hydroxyapatite Nanoparticles on Germination and Plant Metabolism of Tomato (*Solanum lycopersicum* L.): Preliminary Evidence. Agronomy 9:161. https://doi.org/10.3390/agronomy9040161

Meier U (2018) Growth stages of mono- and dicotyledonous plants: BBCH Monograph. Open Agrar Repositorium

Mendelsohn R (2009) The Impact of Climate Change on Agriculture in Developing Countries. Journal of Natural Resources Policy Research 1:5–19. https://doi.org/10.1080/19390450802495882

Metodi ufficiali di analisi chimica del suolo, Pub. L. No. 248, Gazzetta Ufficiale della Repubblica Italiana n.248 del 21/10/1999 (1999). https://www.gazzettaufficiale.it/eli/id/1999/10/21/099A8497/sg

Moretti A, Pascale M, Logrieco AF (2019) Mycotoxin risks under a climate change scenario in Europe. Trends in Food Science & Technology 84:38–40. https://doi.org/10.1016/j.tifs.2018.03.008

Munkvold GP (2003) Cultural and Genetic Approaches to Managing Mycotoxins in Maize. Annual Review of Phytopathology 41:99–116. https://doi.org/10.1146/annurev.phyto.41.052002.095510

Murphy BP, Bowman DMJS (2009) The carbon and nitrogen isotope composition of Australian grasses in relation to climate. Functional Ecology 23:1040–1049. https://doi.org/10.1111/j.1365-2435.2009.01576.x

Payne GA, Brown MP (1998) GENETICS AND PHYSIOLOGY OF AFLATOXIN BIOSYNTHESIS. Annu Rev Phytopathol 36:329–362. https://doi.org/10.1146/annurev.phyto.36.1.329

Pérez-Harguindeguy N, Diaz S, Garnier E, et al (2013) New handbook for standardised measurement of plant functional traits worldwide. Australian Journal of Botany 61:167–234. https://doi.org/10.1071/BT12225

Picot A, Barreau C, Pinson-Gadais L, et al (2010) Factors of the *Fusarium verticillioides*-maize environment modulating fumonisin production. Crit Rev Microbiol 36:221–231. https://doi.org/10.3109/10408411003720209

Pleadin J, Kos J, Radić B, et al (2023) Aflatoxins in Maize from Serbia and Croatia: Implications of Climate Change. Foods 12:548. https://doi.org/10.3390/foods12030548

Pratiwi C, Rahayu W, Lioe H, et al (2015) The effect of temperature and relative humidity for *Aspergillus flavus* BIO 2237 growth and aflatoxin production on soybeans. International Food Research Journal 22:82–87

R Core Team (2023) R: A Language and Environment for Statistical Computing

Reverberi M, Beccaccioli M, Zaccaria M (2021) The Role of Aflatoxins in *Aspergillus flavus* Resistance to Stress. The Genus *Aspergillus* - Pathogenicity, Mycotoxin Production and Industrial Applications

Reverberi M, Beccaccioli M, Zaccaria M (2022) The role of aflatoxins in *Aspergillus flavus* resistance to stress. In: Razzaghi-Abyaneh M, Rai M (eds) The genus *Aspergillus* - pathogenicity, mycotoxin production and industrial applications. IntechOpen

Rosbakh S, Römermann C, Poschlod P (2015) Specific leaf area correlates with temperature: new evidence of trait variation at the population, species and community levels. Alpine Bot 125:79–86. https://doi.org/10.1007/s00035-015-0150-6

Sah RP, Chakraborty M, Prasad K, et al (2020) Impact of water deficit stress in maize: Phenology and yield components. Sci Rep 10:2944. https://doi.org/10.1038/s41598-020-59689-7

Sanborn LH, Reid REB, Bradley AS, Liu X (2021) The effect of water availability on the carbon and nitrogen isotope composition of a C4 plant (pearl millet, *Pennisetum glaucum*). Journal of Archaeological Science: Reports 38:103047. https://doi.org/10.1016/j.jasrep.2021.103047

Santiago R, Cao A, Butrón A (2015) Genetic Factors Involved in Fumonisin Accumulation in Maize Kernels and Their Implications in Maize Agronomic Management and Breeding. Toxins 7:3267–3296. https://doi.org/10.3390/toxins7083267

Scheepens JF, Frei ES, Stöcklin J (2010) Genotypic and environmental variation in specific leaf area in a widespread Alpine plant after transplantation to different altitudes. Oecologia 164:141–150. https://doi.org/10.1007/s00442-010-1650-0

Schindelin J, Arganda-Carreras I, Frise E, et al (2012) Fiji: an open-source platform for biological-image analysis. Nat Methods 9:676–682. https://doi.org/10.1038/nmeth.2019

Seleiman MF, Al-Suhaibani N, Ali N, et al (2021) Drought Stress Impacts on Plants and Different Approaches to Alleviate Its Adverse Effects. Plants 10:259. https://doi.org/10.3390/plants10020259

Soares LA dos A, Fernandes PD, Lima GS de, et al (2021) Phytomass and production components of colored cotton under salt stress in different phenological stages. Rev bras eng agríc ambient 25:132–138. https://doi.org/10.1590/1807-1929/agriambi.v25n2p132-138

Sunoj VSJ, Shroyer KJ, Jagadish SVK, Prasad PVV (2016) Diurnal temperature amplitude alters physiological and growth response of maize (*Zea mays* L.) during the vegetative stage. Environ Exp Bot 130:113–121. https://doi.org/10.1016/j.envexpbot.2016.04.007

Taiyun W, Viliam S (2021) R package "corrplot": Visualization of a Correlation Matrix

Temba BA, Darnell RE, Gichangi A, et al (2021) The Influence of Weather on the Occurrence of Aflatoxin B1 in Harvested Maize from Kenya and Tanzania. Foods 10:216. https://doi.org/10.3390/foods10020216

The United Nations FAAO (2013) The State of the World's Land and Water Resources for Food and Agriculture, 0 edn. Routledge

Toscano S, Ferrante A, Romano D (2019) Response of Mediterranean Ornamental Plants to Drought Stress. Horticulturae 5:6. https://doi.org/10.3390/horticulturae5010006

Tsimba R, Edmeades GO, Millner JP, Kemp PD (2013) The effect of planting date on maize: Phenology, thermal time durations and growth rates in a cool temperate climate. Field Crops Research 150:145–155. https://doi.org/10.1016/j.fcr.2013.05.021

Weiguo L, Xiahong F, Youfeng N, et al (2005) δ13C variation of C3 and C4 plants across an Asian monsoon rainfall gradient in arid Northwestern China. Global Change Biology 11:1094–1100. https://doi.org/10.1111/j.1365-2486.2005.00969.x

Wellburn AR (1994) The Spectral Determination of Chlorophylls a and b, as well as Total Carotenoids, Using Various Solvents with Spectrophotometers of Different Resolution. Journal of Plant Physiology 144:307–313. https://doi.org/10.1016/S0176-1617(11)81192-2

Williams DG, Gempko V, Fravolini A, et al (2001) Carbon isotope discrimination by *Sorghum bicolor* under CO_2 enrichment and drought. New Phytologist 150:285–293. https://doi.org/10.1046/j.1469-8137.2001.00093.x

Xing H, Zhou W, Wang C, et al (2021) Excessive nitrogen application under moderate soil water deficit decreases photosynthesis, respiration, carbon gain and water use efficiency of maize. Plant Physiology and Biochemistry 166:1065–1075. https://doi.org/10.1016/j.plaphy.2021.07.014

Xu LL, Li H, Wang JL, Wang ZW (2017) Response of specific leaf area of summer maize to water gradient in Hebei Gucheng. Shengtai Xuebao 37:8101–8106. https://doi.org/10.5846/stxb201701130104

Yan S, Weng B, Jing L, et al (2022) Adaptive pathway of summer maize under drought stress: Transformation of root morphology and water absorption law. Front Earth Sci 10:. https://doi.org/10.3389/feart.2022.1020553

Yang M, Ma S, Mei F, et al (2021) Adjusting Nitrogen Application in Accordance with Soil Water Availability Enhances Yield and Water Use by Regulating Physiological Traits of Maize under Drip Fertigation. PHYTON 90:417–435. https://doi.org/10.32604/phyton.2021.013175

Yavuz D, Seymen M, Yavuz N, et al (2021) Effects of water stress applied at various phenological stages on yield, quality, and water use efficiency of melon. Agricultural Water Management 246:106673. https://doi.org/10.1016/j.agwat.2020.106673

Zhang L, Yu P, Liu J, et al (2022) Spatial variability of maize leaf area and relationship with yield. Agron J 114:461–470. https://doi.org/10.1002/agj2.20963

Zhou H, Zhou G, He Q, et al (2020) Environmental explanation of maize specific leaf area under varying water stress regimes. Environ Exp Bot 171:. https://doi.org/10.1016/j.envexpbot.2019.103932

Ziadi N, Cambouris AN, Nyiraneza J, Nolin MC (2013) Across a landscape, soil texture controls the optimum rate of N fertilizer for maize production. Field Crops Res 148:78–85. https://doi.org/10.1016/j.fcr.2013.03.023

1.2. Supplementary Materials

Locality	*Coordinates*	*Altitude (m)*	*Soil (%)*			*Mean Temperature (°C)*	*Precipitation (mm)*
			Sand	*Silt*	*Clay*		
Adegliacco	46° 7' 34.7" N, 13° 14' 10.66" E	148	51	31	18	21.7	307
Aquileia	45° 45' 17.46" N, 13° 21' 19.43" E	1	15	52	33	22.3	150
Aquileia	45° 44' 54.07" N, 13° 21' 52.04" E	0	39	33	28	22.3	148
Campolongo	45° 50' 52.31" N, 13° 24' 43.41" E	15	42	46	12	23.7	328
Caporiacco	46° 8' 39.37" N, 13° 6' 20.13" E	184	41	43	16	22.0	318
Casarsa	45° 58' 22.97" N, 12° 51' 42.65" E	50	38	51	11	22.6	305
Fagagna	46° 7' 24.1" N, 13° 5' 43.69" E	188	42	42	16	21.7	362
Majano	46° 12' 13.31" N, 13° 3' 19.68" E	158	41	44	15	22.0	577
Mels	46° 10' 16.15" N, 13° 5' 58.59" E	161	15	60	25	22.3	365
Povoletto	46° 8' 27.85" N, 13° 17' 24.89" E	145	19	53	28	21.3	354
Povoletto	46° 8' 27.81" N, 13° 17' 42.8" E	143	40	44	16	21.3	354
Puja	45° 53' 5.27" N, 12° 33' 15.83" E	14	9	61	30	22.8	217
Rivoli	46° 13' 5.63" N, 13° 2' 56.23" E	159	40	47	13	21.8	602
San Giorgio di Nogaro	45° 46' 41.41" N, 13° 13' 26.24" E	0	36	46	18	22.3	170
San Quirino	46° 0' 49.57" N, 12° 42' 57.59" E	70	15	75	10	22.4	340
San Vito di Fagagna	46° 5' 2.27" N, 13° 3' 52.97" E	124	47	39	14	22.3	314
San Vito al Tagliamento	45° 53' 29.82" N, 12° 52' 53.72" E	23	17	69	14	20.0	203
San Vito al Tagliamento	45° 53' 15.41" N, 12° 51' 54.98" E	22	17	69	14	20.1	204
Tiezzo	45° 53' 38.46" N, 12° 40' 52.66" E	14	17	55	28	23.0	212
Vivaro	46° 6' 26.57" N, 12° 47' 9.23" E	163	33	58	9	21.3	421

Table S1 List of the sampling sites. Coordinates of the central point of each 225 m^2 (15 x 15 m) sampling area are reported in geographic coordinate system (latitude/longitude, WGS84 datum), in degrees–minutes–seconds (DMS) format. Temperatures and precipitation are referred to 2022 growing season (sowing to harvest).

Y Variable	*Phenology*	*Full model*
Plant height	T1	Y ~ Temperature + Precipitation + Clay
	T2	Y ~ Temperature + Precipitation + Clay
	T3	Y ~ Temperature + Precipitation + Clay
	T4	Y ~ Temperature + Precipitation + Clay
	T5	Y ~ Temperature + Precipitation + Clay
Chlorophyll	T1	Y ~ Temperature + Precipitation + Clay
	T2	Y ~ Temperature + Precipitation + Clay
	T3	Y ~ Temperature + Precipitation + Clay
	T4	Y ~ Temperature + Precipitation + Clay
	T5	Y ~ Temperature + Precipitation + Clay
SLA	T1	Y ~ Temperature + Precipitation + Clay
	T2	log(Y) ~ Temperature + Precipitation + Clay
	T3	log(Y) ~ Temperature + Precipitation + Clay
	T4	Y ~ Temperature + Precipitation + Clay
	T5	Y ~ Temperature + Precipitation + Clay
Kernel DW	T1	Y ~ Temperature + Precipitation + Clay + Plant height + SLA + Chlorophyll
	T2	Y ~ Temperature + Precipitation + Clay + Plant height + SLA + Chlorophyll
	T3	Y ~ Temperature + Precipitation + Clay + Plant height + SLA + Chlorophyll
	T4	Y ~ Temperature + Precipitation + Clay + Plant height + SLA
	T5	Y ~ Temperature + Precipitation + Clay + Plant height
Kernel $\delta^{13}C$	T1	Y ~ Temperature + Precipitation + Clay + Plant height + SLA + Chlorophyll
	T2	Y ~ Temperature + Precipitation + Clay + Plant height + SLA + Chlorophyll
	T3	Y ~ Temperature + Precipitation + Clay + Plant height + SLA + Chlorophyll
	T4	Y ~ Temperature + Precipitation + Clay + Plant height + SLA
	T5	Y ~ Temperature + Precipitation + Clay + Plant height
Aflatoxins B1+B2	T1	log(Y) ~ Temperature + Precipitation + Clay + Plant height + SLA + Chlorophyll + Kernel $\delta^{13}C$ + Kernel DW
	T2	Y ~ Temperature + Precipitation + Clay + Plant height + SLA + Chlorophyll + Kernel $\delta^{13}C$ + Kernel DW
	T3	log(Y) ~ Temperature + Precipitation + Clay + Plant height + SLA + Chlorophyll + Kernel $\delta^{13}C$ + Kernel DW
	T4	Y ~ Temperature + Precipitation + Clay + Plant height + SLA + Kernel $\delta^{13}C$ + Kernel DW
	T5	log(Y) ~ Temperature + Precipitation + Clay + Plant height + Kernel $\delta^{13}C$ + Kernel DW
Fumonisins B1+B2	T1	Y ~ Temperature + Precipitation + Clay + Plant height + SLA + Chlorophyll + Kernel $\delta^{13}C$ + Kernel DW
	T2	Y ~ Temperature + Precipitation + Clay + Plant height + SLA + Chlorophyll + Kernel $\delta^{13}C$ + Kernel DW
	T3	Y ~ Temperature + Precipitation + Clay + Plant height + SLA + Chlorophyll + Kernel $\delta^{13}C$ + Kernel DW
	T4	Y ~ Temperature + Precipitation + Clay + Plant height + SLA + Kernel $\delta^{13}C$ + Kernel DW
	T5	Y ~ Temperature + Precipitation + Clay + Plant height + Kernel $\delta^{13}C$ + Kernel DW

Table S2 Full linear models. To meet normality, SLA was log- transformed at T2 and T3, and Aflatoxins was log-transformed at T1, T3 and T5. SLA = specific leaf area; kernel DW = kernel dry weight. T1: beginning of stem elongation; T2: end of tassel emergence; T3: milk maturation; T4: dent maturation; T5: harvest.

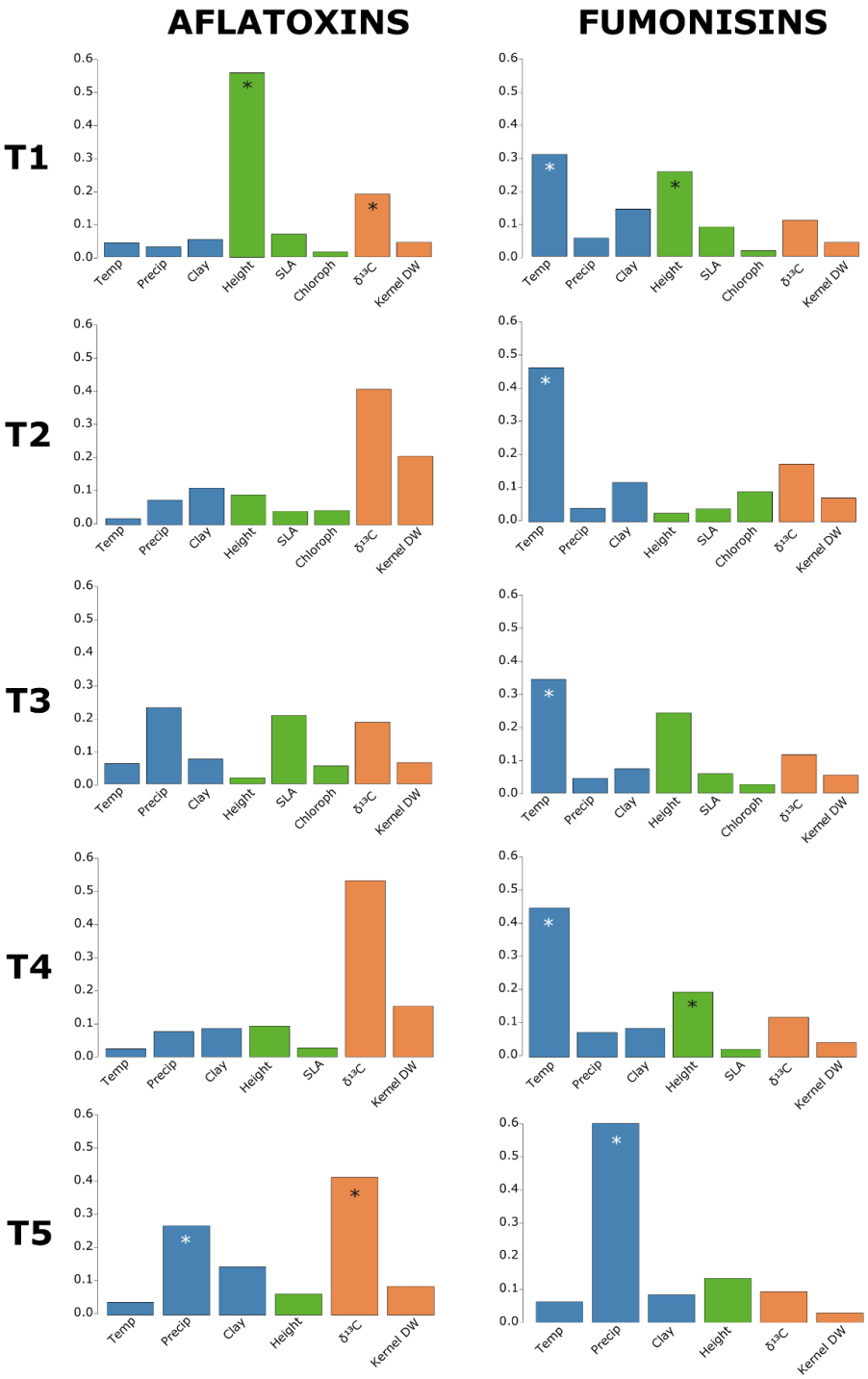


Figure S1 Relative importance of models' predictors. Y-axes represent the percentage of variance explained (R^2). Each bar chart corresponds to a specific model at a given time point and shows the proportion of variance explained (R^2) by each predictor. Predictors are color-coded by group (i.e., blue for environmental variables, green for plant growth and functional traits, orange for plant productivity variables), and their individual contributions are displayed as vertical bars. SLA = specific leaf area; kernel DW = kernel dry weight. T1: beginning of stem elongation; T2: end of tassel emergence; T3: milk maturation; T4: dent maturation; T5: harvest. Asterisks (*) indicate predictors that are statistically significant after model reduction and therefore are part of the minimal adequate models.

2. Multispectral Imagery as a Tool to Remotely Investigate Maize Health

Climate change is increasingly affecting maize production by altering environmental conditions and plant morphophysiological responses across the growing season. Recent advances in multispectral remote sensing and machine-learning approaches, such as random forest models, offer new opportunities for non-destructive, high-resolution assessment of crop status across space and time. In this context, this study investigates the potential of multispectral remote sensing combined with random forest models to capture crop responses to environmental stress and to support scalable monitoring of maize health under field conditions.

2.1. Manuscript in Preparation

Predicting maize functional traits using random forest models and multitemporal UAV multispectral imagery

Giacomo Boscarol[1], Giacomo Trotta[1,2], Elisa Petrussa[1], Enrico Braidot[1], Valentino Volpe[3], Stefano Barbieri[3], Michele Fabro[3], Francesco Boscutti[1], Marco Vuerich[1]

1 Department of Agricultural, Food, Environmental and Animal Sciences, University of Udine, via delle Scienze 91, 33100 Udine, Italy
2 Biodiversity Research Institute (IMIB), University of Oviedo – CSIC – Principality of Asturias, Mieres, Asturias, Spain
3 Servizio fitosanitario e chimico, ricerca, sperimentazione e assistenza tecnica, Regional Agency for Rural Development (ERSA), via Sabbatini 5, 33050 Pozzuolo del Friuli, Italy

Abstract

Maize (*Zea mays* L.) production is increasingly threatened by climate change, with rising temperatures, altered precipitation regimes, and more frequent extreme events affecting crop performance and food security, particularly in climate-vulnerable regions such as the Mediterranean basin. Plant responses to environmental stress are strongly modulated by phenology, as morphophysiological traits vary dynamically throughout the growing season. In this context, multispectral remote sensing combined with machine-learning approaches offers a promising, non-destructive perspective for monitoring crop functional traits under field conditions.

In this study, we evaluated the ability of UAV-based multispectral imagery combined with random forest (RF) models to predict key maize morphophysiological traits across multiple phenological stages. Field experiments were conducted during the 2022 and 2023 growing seasons in 70 maize fields in northeastern Italy. Plant functional traits related to leaf pigments (chlorophylls, carotenoids,

flavonoids), leaf morphology (specific leaf area, dry matter content), and plant height were measured at four phenological stages, from early stem elongation to dent maturation. Multispectral images were acquired concurrently using a five-band sensor (visible, red-edge, and near-infrared) mounted on a drone, and RF models were calibrated and validated separately for each trait and time point.

Model performance varied markedly across traits and phenological stages. Overall, these results highlight the strong temporal dependency of trait–spectral relationships and underscore the importance of phenology-aware modelling approaches. Our findings demonstrate that integrating multispectral remote sensing with machine-learning models provides a scalable framework for monitoring maize functional traits and supports improved assessment of crop stress responses under changing environmental conditions.

Introduction

Maize (*Zea mays* L.) is one of the most extensively cultivated staple crops worldwide, with global production exceeding 1.2 billion tons over more than 200 million hectares in 2024 (FAOSTAT, 2025). However, the rapid intensification of climate change (Intergovernmental Panel on Climate Change (IPCC), 2023) is threatening agricultural activities, including maize production. Droughts, floods, irregular rainfall distribution, and pest outbreaks are among the main factors affecting crop performance and food security (Bita & Gerats, 2013; Liaqat et al., 2022; Makowski et al., 2020), and the Mediterranean basin, which is recognized as a climate change hotspot, is particularly vulnerable to such impacts (Giorgi & Lionello, 2008).

Drought and heat stresses induce physiological adjustments in plants (e.g., reduced leaf area, lower stomatal conductance, and altered biomass allocation) that compromise photosynthesis and yield (Seleiman et al., 2021; Toscano et al., 2019). In particular, maize typically responds to water and heat stress by (1) extending the anthesis–silking interval, (2) reducing leaf number and canopy thickness, (3) modifying root architecture, and (4) expressing secondary stress-related traits, all contributing to yield losses (Sah et al., 2020).

Moreover, the effects of environmental stress on plants can greatly vary according to the timing and duration of stress, as plant sensitivity varies across phenological stages (García-Tejero et al., 2010; Soares et al., 2021; Yavuz et al., 2021). In maize, the transition from vegetative to reproductive phase (anthesis) and the grain-filling stage are known to be the most critical for yield, with drought and heat causing penalties of 34–66% (López-Galiano et al., 2019; Tsimba et al., 2013). Nevertheless, recent evidence suggests that morphophysiological changes linked to reduced yield quality may arise even earlier, before stem elongation. Thus, plant phenology plays a pivotal role in climate–plant interactions, and temporal variations in functional traits can provide valuable insights into plant health and stress responses.

To address these challenges, the complex and multivariate agricultural ecosystems need to be better understood by constantly monitoring environmental conditions and plant functional traits. Many are the functional traits that can be measured, ranging from individual- to ecosystem-level (Violle et al., 2007). For an exhaustive list of the most used plant functional traits and how to properly measure them, see Pérez-Harguindeguy et al. (2016).

Many studies rely on these classical manual-collected morphophysiological traits to ensure plant health and foresee productivity (Greef, 1994; Wiethorn et al., 2021; Yasin et al., 2024; Zhao et al., 2014). Despite being extremely informative, widely used in literature, and strongly reliable, the assessment of many functional traits is time-consuming and labour-intensive, often requiring extensive fieldwork, specific technical expertise, and careful experimental protocols. In many cases, trait quantification involves destructive sampling, the use of specific solvents or reagents, strict storage conditions (e.g., −80 °C), and complex physical or chemical analytical procedures. Moreover, these traits are calculated on single individuals, therefore should be replicated many times to obtain a representative sample at larger scales. These constraints limit the scalability and temporal resolution of trait-based approaches, particularly in field conditions and large-scale studies.

In this context, recent advances in remote sensing, particularly the use of multispectral imagery acquired from unmanned aerial vehicles (UAVs) and satellites, combined with random forest (RF) models, offer new opportunities for high-resolution, non-destructive evaluation of crop status. Multispectral data can indeed capture variations in canopy structure, pigment content, and physiological performance, providing valuable proxies for plant stress and potential disease development (Zhang & Zhu, 2023). The great potential of multispectral remote sensing is the possibility to remotely obtain high-resolution, precise and non-invasive information on a huge number of individuals at the same time, without the necessity to destroy plant's organs or entire individuals. Moreover, this powerful technique allows measurements to be easily repeated on the same area at different phenological stages. This is particularly valuable in agriculture, where fields are typically considered relatively homogeneous and most of the time monospecific. On the other hand, RF can effectively handle high-dimensional, non-linear, and multicollinear data, while capturing complex relationships between multispectral features without requiring strong parametric assumptions (Belgiu & Drăgu, 2016; Breiman, 2001).

The concept behind multispectral approaches is that different regions of the electromagnetic spectrum provide complementary information on plant status. The visible range (400–700 nm) reflects variations in leaf pigments, particularly chlorophyll, allowing assessment of photosynthetic activity and visible stress symptoms. The near-infrared (NIR, 700–1100 nm) is strongly influenced by leaf internal structure and canopy architecture, providing insights into biomass, leaf area, and overall canopy health. The red-edge region, located at the transition between the red and NIR bands (approximately 700–740 nm), is particularly sensitive to subtle changes in chlorophyll content and

stress-related variations, making it a valuable indicator of early physiological alterations before they become visually apparent. Finally, the mid-infrared (MIR, 1100–2600 nm) is primarily sensitive to leaf and canopy water content, as well as to biochemical constituents such as cellulose and lignin, and is therefore closely associated with plant water status, drought stress, and structural changes related to senescence or stress-induced tissue degradation.

By combining reflectance information from these spectral regions, various vegetation indices have been developed to quantify plant status in a standardized way (Zhang & Zhu, 2023). Among the most widely used is the Normalized Difference Vegetation Index (NDVI), which exploits the contrast between red and NIR reflectance to estimate canopy greenness and photosynthetic potential (Carlson & Ripley, 1997). Other indices, such as the Soil-Adjusted Vegetation Index (SAVI) (Huete, 1988), the Normalized Difference Red-Edge Index (NDRE) (Davidson et al., 2022), and the Inverted Red-Edge Chlorophyll Index (IRECI) (Frampton et al., 2013) provide additional sensitivity to chlorophyll content, light-use efficiency, and early stress detection. These indices enable rapid, large-scale monitoring of plant health, stress response, and potential vulnerability to biotic or abiotic threats, complementing traditional field-based assessments.

By combining multispectral remote sensing data with random forest models, it would be possible to exploit the high information content of spectral features while effectively capturing complex, non-linear relationships between canopy reflectance and plant morphophysiological traits, resulting in robust predictions and improved assessment of crop stress under field conditions.

In this context, the aim of this study was to evaluate whether UAV-derived multispectral imagery can detect field-level morphophysiological responses of maize to environmental stresses, and to explore relationships between commonly used multispectral bands and plant functional traits across different phenological stages. Understanding these links could support early stress detection and improve strategies for climate-resilient crop management. The next step would be to upscale the information obtained with drone multispectral images, and to classify all maize fields of the Friuli Venezia Giulia Region with Sentinel-2 satellite multispectral images.

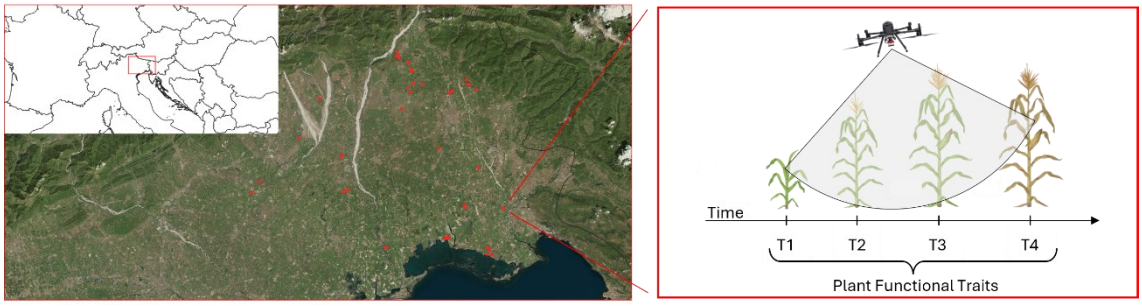


Figure 1 Experimental area and design. Each dot represents a sampling site of 225 m^2 within a maize field. Four times during the season (T1-T4) we measured Plant Functional Traits and performed flyovers to collect multispectral images. T1: beginning of stem elongation; T2: end of tassel emergence; T3: milk maturation; T4: dent maturation; T5: harvest.

Material and methods

Experimental design

The study was conducted during summer 2022 and 2023 in the Friuli Venezia Giulia region in the North-Eastern part of Italy, corresponding to the plain sector of the region (45°44'56"N, 12°59'56"E to 46°11'52"N, 13°29'56"E; Figure 1A). In 2022 the area was characterized by a cumulate annual precipitation of ~1000 mm and a mean annual temperature of 15 °C, with the highest temperature (39 °C) reached between July and August (OSMER, 2025). In 2023 the cumulate annual precipitation was ~1600 mm and the mean annual temperature was 14.5 °C with a peak at 37 °C at the end of August (OSMER, 2025). The main crops grown in the area include maize, soybean, winter cereals (primarily barley and wheat), and grapevine. In this area the Regional Agency for Rural Development (ERSA) selected a total of 70 maize fields ensuring comparable management practices across sites. FAO 500 maturity class was chosen to reduce phenological variability. The experimental sites were selected as 225 m^2 (15 x 15 m) plots within each maize field. Plant traits were measured four times along the growing season, corresponding to phenological stages 30 (T1, beginning of stem elongation), 59 (T2, end of tassel emergence), 73 (T3, milk maturation) and 89 (T4, dent maturation) of BBCH scale for cereals (Lancashire et al., 1991; Meier, 2018). At the same four phenological stages, drone flyovers were also performed to acquire multispectral images.

Data collection

At each sampling time, maize growth was assessed by measuring the height of five random plants per plot, not including the male inflorescence when present. In each plot the last fully expanded leaf was randomly collected from 10 different individuals (10 leaves per plot), sealed in moistened plastic bags, stored in portable refrigerators and transported to the laboratory. Pictures of five leaves were acquired with digital camera, and the size of each leaf (cm^2) was determined with the software ImageJ (Schindelin et al., 2012). The same leaves were further weighed to determine fresh mass (FW), dried at 70 °C for 72 h and weighed again to quantify dry mass (DW). Specific leaf area (SLA, $cm^2\ g^{-1}$) and dry matter content (DMC) were calculated from the dry mass, leaf area and fresh mass according to Pérez-Harguindeguy et al. (2013). Two one-centimetre radius disks were collected from the middle part of the lamina of each of the remaining five leaves, avoiding the midrib, and processed to quantify chlorophyll, carotenoids, and flavonoid content. The disks were ground into fine powder under liquid nitrogen. Chlorophyll *a* and *b* and carotenoid concentration analyses were performed following Marchiol et al., (2019) protocol and expressed as micrograms per gram of fresh weight ($\mu g\ g_{FW}^{-1}$). For the calculation methods see Wellburn (1994). Flavonoid content was quantified according to the method described by Filippi et al. (2021), with minor changes and expressed as quercetin-equivalent content per gram of fresh weight (μg quercetin-eq g^{-1}).

In 2023, due to heavy hailstorms occurred between T2 and T3, some maize fields were destroyed. The collected T1 and T2 data were retained in the models.

At each sampling date, multispectral images were acquired with DJI Matrice 200 drone coupled with Micasense RedEdge-P camera. This setup provided 5 spectral bands covering the visible part of the spectrum, the red edge and the near infrared (Table 1). Flyovers were performed at 20 m above ground level, with 75 % frontal and side overlap between images. The average ground resolution obtained was 1.5 cm pixel^{-1}. To ensure radiometric consistency across different acquisitions, incident light conditions were recorded by the onboard Downwelling Light Sensor (DLS), and absolute reflectance calibration was performed using reference panels with certified reflectance values, imaged before each flight.

Band name	***Wavelength (nm)***	***Band width (nm)***
Blue	475	32
Green	560	27
Red	668	14
Red Edge	717	12
Near-Infrared	845	57

Table 1 Central wavelength (nm) and band width (nm) of the five bands of Micasense RedEdge-P camera.

Data analyses

Multispectral images radiometric calibration was performed in Agisoft Metashape v2.2.2 (Agisoft, 2025) using pre-flight images of the reflectance calibration panel, following the manufacturer's workflow to convert raw digital numbers to surface reflectance (Use of Calibrated Reflectance Panels For MicaSense Data, 2023). Subsequently, multispectral images were aligned, and orthomosaics were created for each plot. For each plot, mean pixel values were computed for each of the five radiometric bands using all pixels contained within the plot boundaries.

Random forest (RF) models were implemented in R to assess the relationships between multispectral bands and plant morphophysiological traits. For each time point (T1–T4), the 5 multispectral bands were used as predictor variables and, in separate models, flavonoids, chlorophyll, carotenoids, leaf DMC, plant height, and SLA were used as response variables. RF models were implemented using the "randomForest" R package (Liaw et al., 2002). Missing values in the predictor variables were imputed prior to model fitting using the "missForest" R package, a non-parametric random forest-based imputation method that can handle mixed data types and complex interactions (Stekhoven & Bühlmann, 2012; Stekhoven, 2025).

For each model, the original dataset was randomly split into a training set (70% of the original data) and a test set (30% of the original data), which were used for model calibration and independent

validation, respectively. The number of variables randomly sampled at each split (mtry) was tuned by testing multiple values based on the total number of predictors (p), including p/4, p/2, and 0.6p.
RF models were trained using the "caret" R package (Kuhn, 2008). Model performance was optimized by tuning the mtry parameter through repeated 10-fold cross-validation with 10 repetitions. For each model, 500 trees were grown, and the optimal model was selected by minimizing the root mean square error (RMSE). To compare RF models between different time points (T1-T4), RMSE values were normalized (NRMSE) by dividing them by the mean of the response variable.
Each RF model was evaluated using the R^2 and the NRMSE calculated for both the training and the test datasets. Models were considered to perform well when R^2 values for training and test sets were both relatively high and comparable (>0.60), while NRMSE values for training and test sets were consistently low (<0.30), indicating good predictive accuracy and limited overfitting.
All the graphs of the linear models were created with the "visreg" R package (Breheny & Burchett, 2017). All statistical analyses were performed with R v4.5.0 and RStudio v2025.09.0-387 (R Core Team, 2023).

Preliminary results

A total of 24 random forest models were developed, corresponding to six morphophysiological traits (chlorophylls, flavonoids, carotenoids, leaf DMC, SLA and plant height) evaluated at four phenological stages (T1-T4). Model performance varied across time and response variables, as indicated by changes in normalized root mean square error (NRMSE) and coefficient of determination (R^2). Traits related to leaf pigments and morphology, such as chlorophyll content, carotenoids, and SLA, were more accurately predicted at early phenological stages, whereas leaf DMC and flavonoid concentration were better described at later stages of the growing season. Plant height was consistently well predicted across all time points, with the highest performance observed at T3. The best-performing model for flavonoids was obtained at T3, where prediction accuracy was mainly driven by reflectance in the red-edge band. Chlorophyll content at T1 was primarily explained by green and near-infrared (NIR) bands, while carotenoids were associated with green and NIR bands at T1 and with NIR and red-edge bands at T3. Leaf DMC was best explained by green and NIR reflectance at T1 and by red and NIR bands at T3. Plant height showed a strong dependence on NIR reflectance throughout the season, particularly at T3, whereas SLA at T1 was mainly driven by reflectance in the green band.

Discussion

In this study, multispectral remote sensing combined with random forest models proved effective in capturing temporal variations in key maize morphophysiological traits under field conditions,

highlighting the strong dependence of trait–spectral relationships on phenological stage. Overall, model performance varied markedly across time and response variables, supporting the idea that plant phenology plays a central role in modulating how physiological and structural traits are expressed at the canopy level and, consequently, how they are detected by multispectral signals.

Traits related to leaf pigments and leaf morphology, such as chlorophyll content, carotenoids, and specific leaf area (SLA), were best predicted early in the growing season, probably because at early phenological stages maize canopies are less structurally complex and leaf-level signals are less confounded by canopy closure, self-shading, and biomass accumulation. Under these conditions, reflectance in the visible and near-infrared regions is more directly linked to pigment concentration and leaf structural properties, explaining the strong contribution of the green and NIR bands to the prediction of chlorophyll, carotenoids, and SLA at T1.

In contrast, traits associated with biomass allocation and secondary metabolism, such as dry matter content (DMC) and flavonoid concentration, were more accurately described later in the season. As maize plants progress toward reproductive stages, changes in tissue composition, senescence processes, and carbon allocation become more pronounced, leading to stronger spectral signatures related to leaf density, water content, and internal structure. The improved performance of DMC models at later stages, and the shift in key explanatory bands toward red and NIR reflectance, likely reflect these structural and compositional changes at the canopy level. Similarly, the highest predictive accuracy for flavonoids at T3, driven primarily by the red-edge band, supports the role of this spectral region in capturing subtle physiological and stress-related alterations that emerge during critical developmental phases. The sensitivity of the red-edge to changes in pigment composition and cellular structure makes it particularly well suited for detecting secondary metabolites and stress-related responses that are not necessarily reflected in visible-range indices alone.

Plant height was consistently well predicted across all phenological stages, confirming the robustness of multispectral approaches for estimating structural traits. The dominant contribution of the NIR band, especially at T3, underscores the strong relationship between NIR reflectance and canopy architecture, biomass accumulation, and leaf internal structure. The peak performance observed at mid-season likely corresponds to maximum canopy development, when height differences are fully expressed and less affected by early growth variability or late-season senescence.

The temporal shifts observed in model performance and in the relative importance of spectral bands emphasize that trait–reflectance relationships are not static but dynamically evolve throughout the growing season. This temporal dependency has important implications for trait-based remote sensing applications, suggesting that models calibrated at a single phenological stage may not be transferable across the season. Instead, phenology-specific models or temporally explicit approaches may be required to accurately capture plant functional traits under variable environmental conditions.

From an applied perspective, the ability to accurately predict different classes of traits at different times of the season is particularly relevant in the context of climate change and increasing environmental stress. Early-season prediction of pigment-related and morphological traits could support timely identification of stress signals and guide adaptive management practices. Meanwhile, late-season monitoring of biomass-related and secondary metabolic traits may provide insights into stress legacy effects, impacting yield quantity and quality projections and potential mycotoxin mitigation. The consistent performance of height models further highlights the potential of multispectral data to support large-scale structural monitoring of crops.

Overall, our preliminary results demonstrate that multispectral remote sensing combined with machine-learning models can provide a flexible and scalable framework for monitoring maize functional traits across phenological stages. By explicitly accounting for temporal dynamics, this approach enhances our capacity to assess crop responses to environmental stress and supports the development of climate-resilient crop monitoring and management strategies.

References

Agisoft. (2025). Agisoft Metashape (Version 2.2.2) [Computer software]. https://www.agisoft.com/downloads/installer/

Belgiu, M., & Drăgu, L. (2016). Random forest in remote sensing: A review of applications and future directions. ISPRS Journal of Photogrammetry and Remote Sensing, 114, 24–31. https://doi.org/10.1016/j.isprsjprs.2016.01.011

Bita, C. E., & Gerats, T. (2013). Plant tolerance to high temperature in a changing environment: Scientific fundamentals and production of heat stress-tolerant crops. Frontiers in Plant Science, 4(JUL). https://doi.org/10.3389/fpls.2013.00273

Breheny, P., & Burchett, W. (2017). Visualization of Regression Models Using visreg [Computer software]. 9: 56-71.

Breiman, L. (2001). Random Forests. Machine Learning, 45(1), 5–32. https://doi.org/10.1023/A:1010933404324

FAOSTAT. (2025, August 29). FAOSTAT. https://www.fao.org/faostat/en/#data/QCL/visualize

Filippi, A., Braidot, E., Petrussa, E., Fabro, M., Vuerich, M., & Boscutti, F. (2021). Plant growth shapes the effects of elevation on the content and variability of flavonoids in subalpine bilberry stands. Plant Biology, 23(2), 241–249. https://doi.org/10.1111/plb.13194

García-Tejero, I., Romero-Vicente, R., Jiménez-Bocanegra, J. A., Martínez-García, G., Durán-Zuazo, V. H., & Muriel-Fernández, J. L. (2010). Response of citrus trees to deficit irrigation during different phenological periods in relation to yield, fruit quality, and water productivity. Agricultural Water Management, 97(5), 689–699. https://doi.org/10.1016/j.agwat.2009.12.012

Giorgi, F., & Lionello, P. (2008). Climate change projections for the Mediterranean region. Global and Planetary Change, 63(2), 90–104. https://doi.org/10.1016/j.gloplacha.2007.09.005

Greef, J. M. (1994). Productivity of Maize (Zea mays L.) in Relation to Morphological and Physiological Characteristics under Varying Amounts of Nitrogen Supply. Journal of Agronomy and Crop Science, 172(5), 317–326. https://doi.org/10.1111/j.1439-037X.1994.tb00182.x

Intergovernmental Panel on Climate Change (IPCC) (Ed.). (2023). Weather and Climate Extreme Events in a Changing Climate. In Climate Change 2021 – The Physical Science Basis: Working Group I Contribution to the Sixth Assessment Report of the Intergovernmental Panel on Climate Change (pp. 1513–1766). Cambridge University Press. https://doi.org/10.1017/9781009157896.013

Kuhn, M. (2008). Building Predictive Models in R Using the caret Package. *Journal of Statistical Software*, **28**(5), 1-26. doi:10.18637/jss.v028.i05, https://www.jstatsoft.org/index.php/jss/article/view/v028i05

Liaqat, W., Barutçular, C., Farooq, M. U., Ahmad, H., Jan, M. F., Ahmad, Z., Nawaz, H., & Li, M. (2022). Climate change in relation to agriculture: A review. Spanish Journal of Agricultural Research, 20(2), e03R01-e03R01. https://doi.org/10.5424/sjar/2022202-17742

Liaw A, Wiener M (2002). Classification and Regression by randomForest. *R News*, **2**(3), 18-22. https://CRAN.R-project.org/doc/Rnews/

López-Galiano, M. J., García-Robles, I., González-Hernández, A. I., Camañes, G., Vicedo, B., Real, M. D., & Rausell, C. (2019). Expression of miR159 Is Altered in Tomato Plants Undergoing Drought Stress. Plants, 8(7), Article 7. https://doi.org/10.3390/plants8070201

Makowski, D., Marajo-Petitzon, E., Durand, J.-L., & Ben-Ari, T. (2020). Quantitative synthesis of temperature, CO_2, rainfall, and adaptation effects on global crop yields. European Journal of Agronomy, 115, 126041. https://doi.org/10.1016/j.eja.2020.126041

Marchiol, L., Filippi, A., Adamiano, A., Degli Esposti, L., Iafisco, M., Mattiello, A., Petrussa, E., & Braidot, E. (2019). Influence of Hydroxyapatite Nanoparticles on Germination and Plant Metabolism of Tomato (*Solanum lycopersicum* L.): Preliminary Evidence. Agronomy, 9(4), 161. https://doi.org/10.3390/agronomy9040161

OSMER, meteo fvg. (2025). ARPA FVG - OSMER. www.meteo.fvg.it/clima.php. Retrieved October 28, 2025, from https://www.meteo.fvg.it/clima.php

Pérez-Harguindeguy, N., Diaz, S., Garnier, E., Lavorel, S., Poorter, H., Jaureguiberry, P., Bret-Harte, M., Cornwell, W., Craine, J., Gurvich, D., Urcelay, C., Veneklaas, E., Reich, P., Poorter, L., Wright, I., Ray, P., Enrico, L., Pausas, J., Vos, A., & Cornelissen, J. (2013). New handbook for standardised measurement of plant functional traits worldwide. Australian Journal of Botany, 61, 167–234. https://doi.org/10.1071/BT12225

Pérez-Harguindeguy, N., Díaz, S., Garnier, E., Lavorel, S., Poorter, H., Jaureguiberry, P., Bret-Harte, M. S., Cornwell, W. K., Craine, J. M., Gurvich, D. E., Urcelay, C., Veneklaas, E. J., Reich, P. B., Poorter, L., Wright, I. J., Ray, P., Enrico, L., Pausas, J. G., de Vos, A. C., … Cornelissen, J. H. C. (2016). Corrigendum to: New handbook for standardised measurement of plant functional traits worldwide. Australian Journal of Botany, 64(8), 715–716. https://doi.org/10.1071/BT12225_CO

R Core Team. (2023). R: A Language and Environment for Statistical Computing [Computer software]. R Foundation for Statistical Computing. https://www.R-project.org/

Sah, R. P., Chakraborty, M., Prasad, K., Pandit, M., Tudu, V. K., Chakravarty, M. K., Narayan, S. C., Rana, M., & Moharana, D. (2020). Impact of water deficit stress in maize: Phenology and yield components. Scientific Reports, 10(1), Article 1. https://doi.org/10.1038/s41598-020-59689-7

Schindelin, J., Arganda-Carreras, I., Frise, E., Kaynig, V., Longair, M., Pietzsch, T., Preibisch, S., Rueden, C., Saalfeld, S., Schmid, B., Tinevez, J.-Y., White, D. J., Hartenstein, V., Eliceiri, K., Tomancak, P., & Cardona, A. (2012). Fiji: An open-source platform for biological-image analysis. Nature Methods, 9(7), 676–682. https://doi.org/10.1038/nmeth.2019

Seleiman, M. F., Al-Suhaibani, N., Ali, N., Akmal, M., Alotaibi, M., Refay, Y., Dindaroglu, T., Abdul-Wajid, H. H., & Battaglia, M. L. (2021). Drought Stress Impacts on Plants and Different Approaches to Alleviate Its Adverse Effects. Plants, 10(2), Article 2. https://doi.org/10.3390/plants10020259

Soares, L. A. dos A., Fernandes, P. D., Lima, G. S. de, Silva, S. S. da, Moreira, R. C. L., & Medeiros, T. L. F. (2021). Phytomass and production components of colored cotton under salt stress in different phenological stages. Revista Brasileira de Engenharia Agrícola e Ambiental, 25, 132–138. https://doi.org/10.1590/1807-1929/agriambi.v25n2p132-138

Stekhoven DJ (2025). *missForest: Nonparametric Missing Value Imputation using Random Forest*. R package version 1.6.1.

Stekhoven DJ, Bühlmann P (2012). MissForest: nonparametric missing value imputation for mixed-type data. *Bioinformatics*, **28**(1), 112–118. doi:10.1093/bioinformatics/btr597

Toscano, S., Ferrante, A., & Romano, D. (2019). Response of Mediterranean Ornamental Plants to Drought Stress. Horticulturae, 5(1), Article 1. https://doi.org/10.3390/horticulturae5010006

Tsimba, R., Edmeades, G. O., Millner, J. P., & Kemp, P. D. (2013). The effect of planting date on maize: Phenology, thermal time durations and growth rates in a cool temperate climate. Field Crops Research, 150, 145–155. https://doi.org/10.1016/j.fcr.2013.05.021

Use of Calibrated Reflectance Panels For MicaSense Data. (2023, August 30). MicaSense Knowledge Base. https://support.micasense.com/hc/en-us/articles/115000765514-Use-of-Calibrated-Reflectance-Panels-For-MicaSense-Data

Violle, C., Navas, M.-L., Vile, D., Kazakou, E., Fortunel, C., Hummel, I., & Garnier, E. (2007). Let the concept of trait be functional! Oikos, 116(5), 882–892. https://doi.org/10.1111/j.0030-1299.2007.15559.x

Wellburn, A. R. (1994). The Spectral Determination of Chlorophylls a and b, as well as Total Carotenoids, Using Various Solvents with Spectrophotometers of Different Resolution. Journal of Plant Physiology, 144(3), 307–313. https://doi.org/10.1016/S0176-1617(11)81192-2

Wiethorn, M., Penn, C., & Camberato, J. (2021). A Research Method for Semi-Automated Large-Scale Cultivation of Maize to Full Maturity in an Artificial Environment. Agronomy, 11(10), 1898. https://doi.org/10.3390/agronomy11101898

Yasin, S., Zavala-García, F., Niño-Medina, G., Rodríguez-Salinas, P. A., Gutiérrez-Diez, A., Sinagawa-García, S. R., & Lugo-Cruz, E. (2024). Morphological and Physiological Response of Maize (*Zea mays* L.) to Drought Stress during Reproductive Stage. Agronomy, 14(8), 1718. https://doi.org/10.3390/agronomy14081718

Yavuz, D., Seymen, M., Yavuz, N., Çoklar, H., & Ercan, M. (2021). Effects of water stress applied at various phenological stages on yield, quality, and water use efficiency of melon. Agricultural Water Management, 246, 106673. https://doi.org/10.1016/j.agwat.2020.106673

Zhang, Z., & Zhu, L. (2023). A Review on Unmanned Aerial Vehicle Remote Sensing: Platforms, Sensors, Data Processing Methods, and Applications. Drones, 7(6), Article 6. https://doi.org/10.3390/drones7060398

Zhao, W., Sun, Y., Kjelgren, R., & Liu, X. (2014). Response of stomatal density and bound gas exchange in leaves of maize to soil water deficit. Acta Physiologiae Plantarum, 37(1), 1704. https://doi.org/10.1007/s11738-014-1704-8

3. Environmental Effects on Maize Associated Rhizobiome

A further promising direction for future research builds on the activities carried out during the period abroad at the Institut Diversité, Écologie et Évolution du Vivant (IDEEV) of Gif-sur-Yvette, France. This experience highlighted the potential of integrating complementary methodological approaches and analytical frameworks to better capture the complexity of crop–environment interactions. In particular, the rhizosphere represents a key interface in plant–environment interactions, where complex exchanges between roots and soil microbial communities influence plant nutrition, development, and stress tolerance. In crop species such as maize, rhizobiome composition is shaped by multiple interacting factors, including plant genotype, developmental stage, and environmental conditions. At the same time, climate-driven shifts in plant phenology are altering the timing of plant–soil interactions, raising questions about how developmental transitions affect rhizosphere microbial dynamics. In this study, carried out in collaboration with the Institut Diversité, Écologie et Évolution du Vivant (IDEEV) of Gif-sur-Yvette in France, we aimed to disentangle the effects of plant phenology from genetic and environmental variability by monitoring rhizosphere bacterial communities throughout development in maize populations with contrasting flowering times but a shared genetic background.

3.1. Manuscript in Preparation

Modest impact of phenology shifts on maize rhizobiome

Giacomo Boscarol[1]*, Philippe Deschamps[2], Purificación López-García[2], Maud Tenaillon[3], Judith Legrand[4]

1 Department of Agricultural, Food, Environmental and Animal Sciences (DI4A), University of Udine, Via delle Scienze 206, 33100 Udine, Italy
2 Laboratoire Écologie, Société et Évolution, Université Paris-Saclay, CNRS, AgroParisTech, 91400, Orsay, France
3 Université Paris-Saclay, INRAE, CNRS, AgroParisTech, GQE - Le Moulon, EMR 9005, 91190, Gif-sur-Yvette, France
4 Université Paris-Saclay, INRAE, AgroParisTech, GQE - Le Moulon, 91190, Gif-sur-Yvette, France
* Corresponding author

Abstract

Climate change is altering plant phenology, shifting developmental cycles by days to weeks under continued warming. However, the consequences of these phenological shifts for root-associated bacterial communities remain largely unknown. Here we tested the effect of phenology on the rhizobiome while minimizing genetic variability. We monitored the rhizobiome dynamics throughout

the growing season in the offspring derived from the selfing of three maize genotypes: a commercial inbred line (MBS847, the ancestor) and two genotypes (early- and late-flowering) derived from the commercial line after 18 years of divergent selection for flowering time, and differing by 10 degree days. Plants were sown in a randomized design with three blocks and three sowing dates, each one week apart, except for the ancestor, which was sown at a single date. Starting 41 days after sowing and continuing for seven weeks, three samples of bare soil and rhizospheric soil (from three different plants) within each block were collected once a week at the same soil horizon, pooled, and analyzed using 16S metabarcoding. In total, the Amplicon Sequences Variants (ASVs) from 210 samples were analyzed, yielding 26,052 ASVs. Only a small fraction of ASVs constituted the core microbiome in both bare (5%) and rhizospheric (2%) soil, with no consistent change in core size across developmental stages. Plant genotypes did not significantly affect bacterial alpha diversity. Instead, alpha diversity differed primarily between bare soil and rhizospheric soil and also varied over time. We found that time expressed as calendar date best explained the observed alpha diversity temporal pattern. In contrast, plant phenology expressed as days after sowing had limited explanatory power, and sowing date and its interaction with days after sowing significantly improved model performance. Overall, environmental variation was the primary driver of rhizosphere alpha diversity dynamics, whereas phenological divergence exerted a modest and sowing-dependent influence. These findings indicate that phenology shifts alone are insufficient to consistently reshape rhizosphere bacterial diversity, emphasizing the dominant role of environmental fluctuations in structuring plant-microbiome interactions.

Introduction

The rhizosphere, defined as the narrow zone of soil influenced by plant roots, represents a critical interface for plant–environment interactions (Larsen et al., 2014; Saleem et al., 2019). The microbial communities inhabiting this compartment, collectively referred to as the rhizosphere microbiome or rhizobiome, play fundamental roles in plant nutrition, growth, and development (Ali et al., 2009; Larsen et al., 2014), protection against root-colonizing pathogens (Innerebner et al., 2011; Lugtenberg & Kamilova, 2009; Van der Ent et al., 2009), and tolerance to abiotic stresses such as drought or nutrient limitation (Berendsen et al., 2012; Castiglioni et al., 2008). In return, plants actively shape their rhizobiome by releasing a wide array of organic compounds through root exudation, including sugars, amino acids, organic acids, and secondary metabolites, which provide both carbon sources and selective cues for microbial colonization (Morgan et al., 2005).

The composition and structure of the rhizobiome are influenced by multiple plant-related factors, including plant phenology, root system architecture and the qualitative and quantitative composition of root exudates (Aira et al., 2010; Bais et al., 2006; Grayston et al., 1997). These traits vary across plant species and genotypes and can strongly affect microbial activity and community assembly. In

this context, plant genotype has repeatedly been identified as a determinant of rhizobiome composition (Bulgarelli et al., 2012; Wagner et al., 2016), acting through genetically controlled differences in root morphology (Ao et al., 2010; Wagner et al., 2016) and exudation patterns (Aminurrasyid et al., 2025; Rodriguez et al., 2025).

It is already well known that plants can selectively recruit microbial taxa from the immense diversity present in bare (not vegetated) soil. Although bare soil harbours a highly diverse pool of microorganisms, only a subset of this pool is consistently found in close association with roots, indicating a selective filtering process driven by root traits and exudation patterns. For example, several studies have shown that microbial alpha diversity is often higher in bare soil than in the rhizosphere (Essel et al., 2019; Ling et al., 2022), implying that the rhizosphere represents a narrower ecological niche within the broader soil microbiome (Moretti et al., 2024). Work comparing bacterial communities from rhizosphere and adjacent bare soils has demonstrated clear compositional differences attributable to plant influence, with distinct taxa enriched around roots, further supporting the notion of plant-mediated selection rather than passive coexistence, recruiting beneficial or functionally compatible taxa while excluding others (Essel et al., 2019; Ling et al., 2022).

Among crop species, maize (*Zea mays* L.) represents a particularly well-studied model for investigating plant–rhizobiome interactions, owing to its global agronomic importance and extensive genetic and genomic resources (FAO, 2025). Early studies demonstrated that maize genotype can significantly modify the structure and growth of rhizosphere microbial communities. For example, Aira et al. (2010) reported strong genotype-dependent effects on rhizosphere microbial assemblages. Subsequently, a large-scale field experiment involving 27 maize lines grown across five environments revealed that a significant proportion of the variation in bacterial diversity, measured 12 weeks after sowing, was heritable (Peiffer et al., 2013), a result later confirmed under controlled greenhouse conditions (Bouffaud et al., 2016). However, more recent work has suggested a more nuanced picture: plant age emerged as the primary driver of rhizosphere microbial diversity, followed by environmental factors such as soil physicochemical properties and climate, whereas plant genotype explained only a small fraction of the observed variation, despite significant genotype-by-environment interactions (Walters et al., 2018).

It is important to note here that plant age (i.e., days or weeks since sowing) should not be conflated with plant developmental stage, as the two may diverge under different environmental conditions.

Collectively, these findings highlight maize as a robust and informative system for disentangling the relative contributions of host genetics, development, and environment in shaping rhizobiome.

Plant–microbiome interactions are bidirectional and dynamic. In addition to being shaped by the host plant, soil microbial communities can influence key plant traits, including the timing of phenological events. For instance, distinct soil microbiomes have been shown to alter flowering time in *Boechera stricta* (Wagner et al., 2014) and to affect spring foliar phenology and biomass accumulation in *Populus*

angustifolia (Van Nuland et al., 2021), suggesting that microbial communities can contribute to phenotypic plasticity and potentially modulate plant responses to local environmental conditions.

In parallel, plant phenology has undergone profound changes over recent decades because of global climate change (Bernier, 1988; Cleland et al., 2007). Rising temperatures have generally led to earlier leaf emergence, earlier onset of the growing season, and advanced flowering dates across a wide range of ecosystems (Gordo & Sanz, 2010; Piao et al., 2019). For instance, Parent et al. (2018) showed that climate change is projected to advance optimal flowering time and alter crop cycle duration in European maize. Other simulations indicate that crops may require earlier sowing and modified phenological development to maximize yield under future climatic conditions (Zimmermann et al., 2017). However, recent evidence suggests that phenological adaptation alone may fail to maintain optimal reproductive timing, highlighting the limits of phenological plasticity under contemporary climate change scenarios (Kusmec & Schnable, 2024).

These climate-driven phenological shifts raise important questions about their potential consequences for rhizobiome dynamics and, more broadly, for plant–soil feedbacks. Because plant developmental stage is a major determinant of rhizosphere microbial composition, even subtle changes in phenological timing may alter the temporal trajectory of microbiome assembly and function.

While previous studies have extensively investigated the effects of plant genotype, environmental conditions, and developmental stage on rhizobiome composition, comparatively little attention has been paid to the role of phenological variation *per se*, particularly when genetic variability is minimized. In this study, we aimed to isolate the effect of phenological differences on rhizosphere bacterial communities while controlling for genetic background. Microenvironmental heterogeneity was accounted for through a randomized block design. The implementation of three staggered sowing dates allowed developmental stages to occur at different calendar times, separating the relative contribution of environmental drivers from plant phenology in shaping rhizosphere communities.

Specifically, we monitored the rhizobiome dynamics throughout the growing season in the offspring derived from the selfing of three maize genotypes: a commercial inbred line (MBS847, the ancestor) and two derived genotypes (early- and late-flowering), obtained from the inbred line through 18 years of divergent selection for flowering time, and differing by 10 degree days.

Our study addresses the following questions: (i) is there a consistent temporal trend in rhizosphere microbial community composition over the maize growing season? (ii) To what extent is this temporal pattern influenced by plant phenology, specifically differences between early- and late-flowering genotypes? (iii) Are observed temporal dynamics primarily driven by plant developmental stage, or are they predominantly shaped by environmental fluctuations across the experimental setting? Figure 1 summarizes alternative hypotheses tested in the above questions 2 and 3.

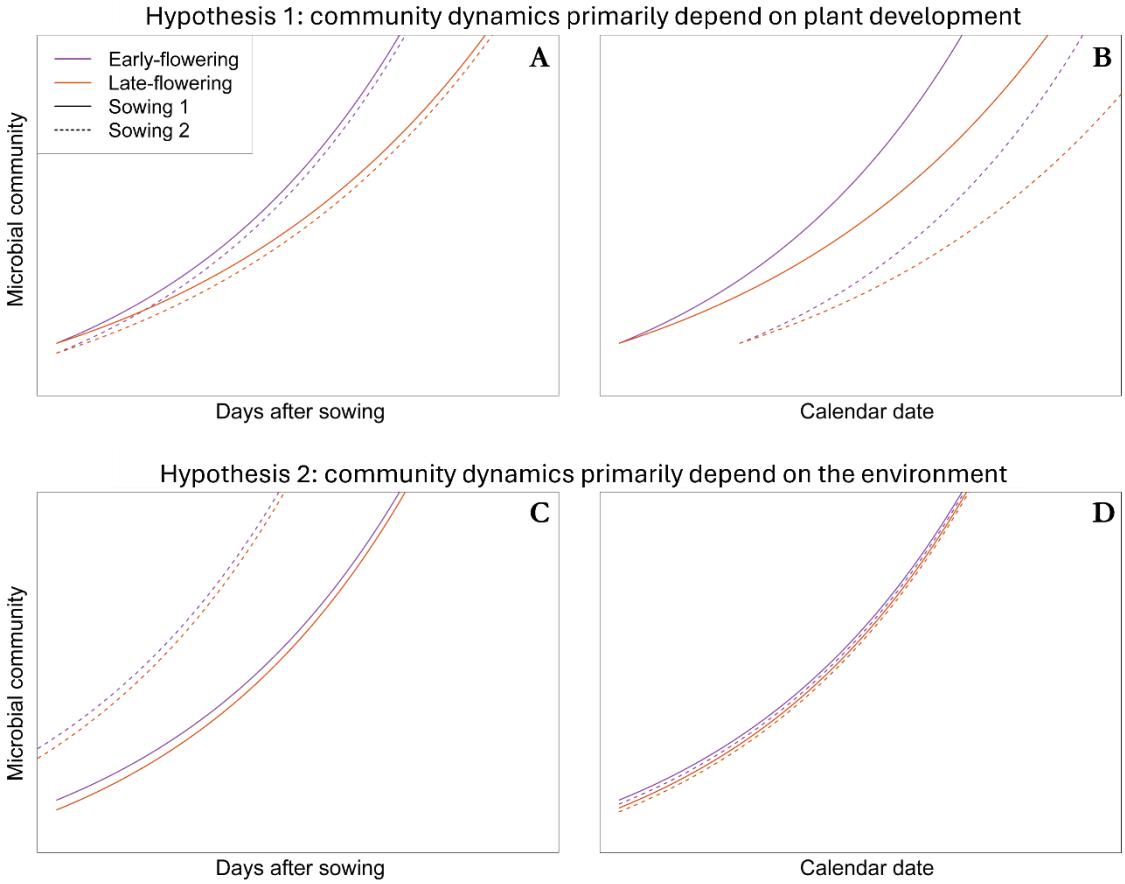


Figure 1 Conceptual framework illustrating two alternative hypotheses tested in this study that are whether the observed temporal dynamics are primarily driven by plant developmental stage, or by environmental fluctuations. For simplicity, we considered that there was a temporal trend in the rhizobiome composition. Upper panels (A, B) represent the plant development-driven hypothesis. (A) when plotted against days since sowing, bacterial community trajectories from different sowing dates converge, indicating that community dynamics are primarily structured by plant developmental stage. (B) when plotted against calendar date (day of year), trajectories diverge because identical phenological stages occur at different times. Lower panels (C, D) represent the environment-driven hypothesis. (C) when plotted against days since sowing, trajectories diverge across sowing dates, reflecting differing environmental conditions experienced during development. (D) when plotted against calendar date, trajectories converge, indicating that community dynamics are primarily structured by temporal environmental variation rather than plant phenology.

Material and methods

Maize populations

Two maize populations were developed through an 18-year Divergent Selection Experiment (DSE) targeting flowering time (Desbiez-Piat et al., 2023; Durand et al., 2015). Starting from the maize commercial inbred MBS847 (referred to as the ancestor, A), the most contrasted genotypes for

flowering time were selected and self-fertilized: the 10 latest-flowering individuals from the late population and the 10 earliest-flowering individuals from the early population. Genotypes from the ancestral population (A), the early (sdpM325, ME2 family) and the late (sdpM326, ML1 family) populations were evaluated in the field in 2019 in a randomized-block design, revealing contrasted Best Linear Unbiased Estimates (BLUES) for flowering time after correcting for fixed spatial and year effects and their interaction: 81.72, 79.76, 86.24 for the A, the early and the late populations, respectively (Desbiez-Piat et al., 2023). Note that flowering time is here expressed in days to flowering equivalent to a growth at 20 °C (DTF). In addition to 6.5 DTF difference, early and late genotypes also exhibited distinct developmental patterns, with the late flowering lines showing a delayed floral transition. Previously published data suggested that these differences are due to shifts in the timing of developmental transitions (i.e., the onset of flowering) rather than differences in the overall rate of development (Plancade et al., 2023). Progenies obtained from self-fertilization of a single early (E) and a single late (L) genotype at generation 18 were used for a field trial held on the Saclay plateau (Île-de-France, France) in 2019 (Desbiez-Piat et al., 2023).

Experimental design

Individuals from the ancestral (A), early-flowering (E), and late-flowering (L) genotypes were sown in a randomized field trial. Seeds of E and L were sown at three time points: April 23rd (first sowing, S1), April 30th (second sowing, S2) and May 7th (third sowing, S3), while the ancestral genotype (A) was only sown at S1 (Figure 2). Four 10-plants rows were randomized for each sowing date. The entire design was repeated three times (Blocks 1-3) (Figure 2). Soil sampling began on June 3rd, 10th and 17th for plants sown at S1, S2 and S3 respectively (6 weeks after sowing), and continued once a week for 7 weeks, ending on July 15th, 22nd and 29th respectively (Figure 3). Each sample consisted of a pool of rhizospheric soil taken with a single-use scalpel from three randomly selected plants per block. The roots from which the soil was taken were located within the top 20 cm layer of soil. Three gatherings per block of "bare" (non-rhizospheric) soil were also collected and pooled into a single sample for the 9 sampling dates in each block (Figure 3). Sampling occurred in the morning, between 8:00 AM and 12:00 AM. The final dataset consisted of 210 samples: 63 samples from E genotype, 63 from L genotype, 63 from bare soil (BS), and 21 from A genotype.

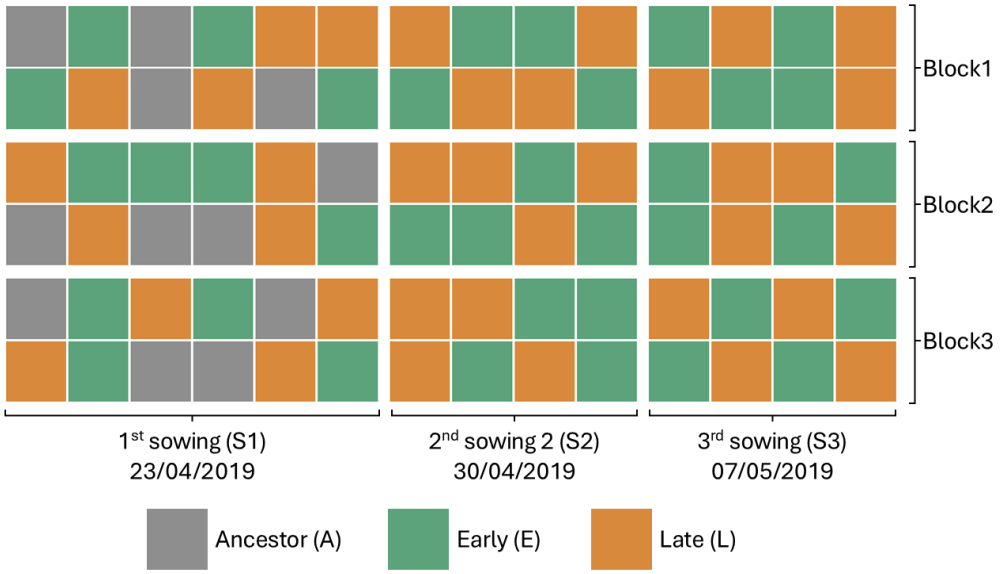


Figure 2 Experimental site. Each square represents a randomly distributed 10-plants row. Colours indicate the genotype of the plants. At the 1st sowing date (S1) 40 maize plants of each genotype were sown; at the 2nd and 3rd sowing dates (S2, S3) 40 plants of E (early flowering) and L (late flowering) plants were sown. The experimental design was replicated 3 times (Block1, Block2, Block3).
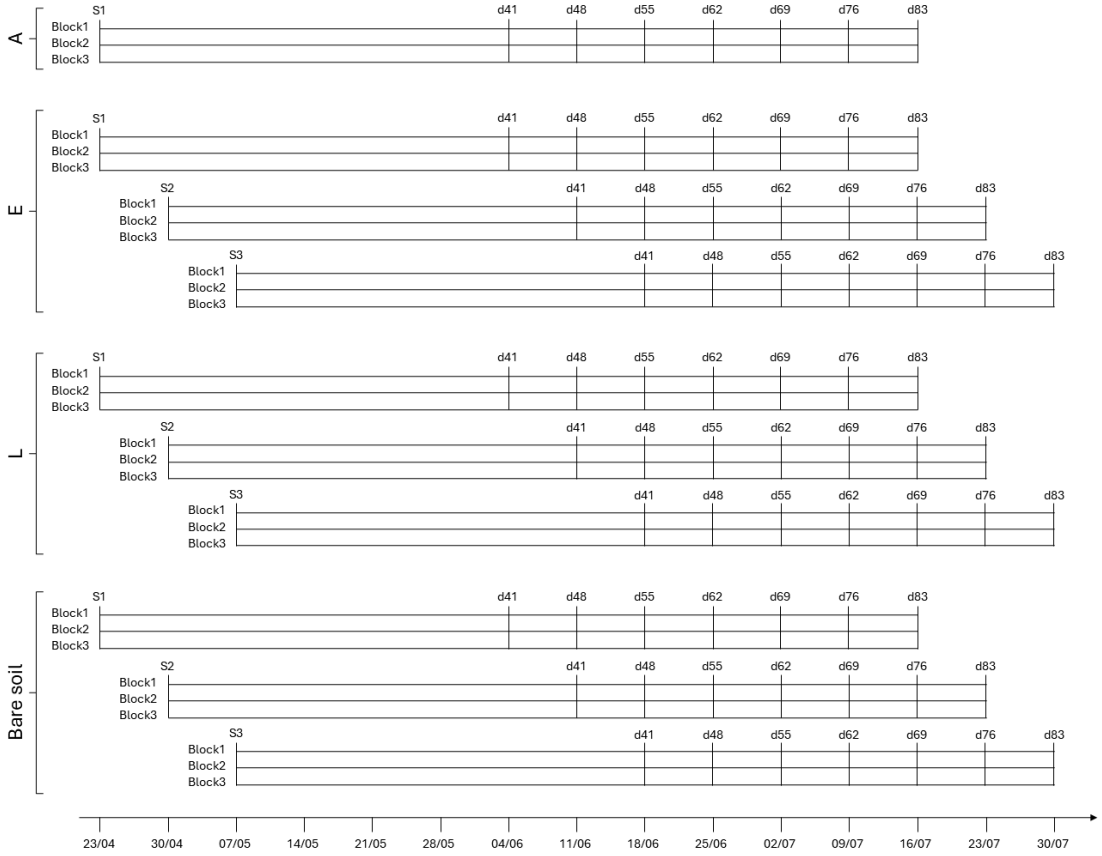


Figure 3 Sampling design. The X axis represents the calendar date. A: Ancestor genotype; E: early flowering genotype; L: late flowering genotype. d41-d48: days between sowing and soil samples collection.

DNA extraction, PCR amplification, and sequencing

Genomic DNA was extracted using the PowerSoil DNA Isolation Kit (MoBio/Quiagen). DNA was used as a template for the amplification of the V4-V5 region (~290 bp fragments) of the prokaryotic 16S rRNA with the primer set U515F (5'-GTGCCAGCMGCCGCGGTAA-3') and U806R (5'-GGACTACVSGGGTATCTAAT-3'). Forward and reverse primers were tagged with 10 bp molecular identifiers (MIDs) before PCR to allow pooling and identification of amplicons from different samples, bringing the total amplification length to ~310 bp. MID to sample assignment was randomized. PCR-amplification reactions were performed in 25 μL volume reaction and contained 0.5–3 μL of eluted sample DNA, 1.5 mM of $MgCl_2$, 0.2 mM of deoxynucleotide (dNTP) mix, 0.3 μM of each primer, and 0.5 U of the hot-start Platinum Taq DNA Polymerase (Invitrogen, Carlsbad, CA). PCR reactions were carried out for 35 cycles (94 °C for 30 s, 55–58 °C for 30–45 s, and 72 °C for 90 s) preceded by 2 min denaturation at 94 °C and followed by five additional minutes of polymerization at 72 °C. Amplification efficiency was checked using electrophoresis; amplicons were purified using the QIAquick PCR purification kit (Qiagen, Hilden, Germany), assayed for DNA concentration using a NanoDrop© Microvolume Spectrophotometer (Thermo Fisher) and pooled at equimolarity according to the randomized MID scheme. Sequencing was done using Illumina Hiseq Paired End (2 × 250 bp, paired-end) at Eurofins Genomics (Konstanz, Germany), the 210 samples were spread over three Illumina runs.

Amplicon data processing

A total of 22,100,084 raw sequences (reads) of 16S amplicons were obtained from the three Illumina sequencing runs. Raw reads were analysed using QIIME2-amplicon v2023.9 (Bolyen et al., 2019). Reads were demultiplexed and MIDs removed using the "cutadapt demux-paired" function of QIIME2. The DADA2 plugin was used to determine amplicon sequence variants (ASVs) following three steps: dereplication, denoising and merging (Callahan et al., 2016). Trimming/clipping/max-exp-errors parameters were of 20/200/4 and 20/110/8 for forward and reverse reads respectively. Denoised sequences with one or more mismatches in the overlap region were removed during the merging phase. ASV statistics are provided in Supplementary Table S1. Direct MID tagging on primers leads to ASVs oriented both in coding and non-coding directions. Consequently, ASVs were reoriented using a custom QIIME2 plugin (https://gitlab.com/DeemTeam/q2_readorient). Potential chimera sequences were removed using the "uchime-denovo" function of QIIME2. Finally, 100% identical ASVs of different lengths were clustered together using vsearch v2.26.0 (Rognes et al., 2016), leading to a total of 88,190 sequences. ASVs were then assigned to archaeal and bacterial taxa with the "feature-classifier" function of QIIME2 using a pretrained dataset derived from the SILVA database release 138 (Quast et al., 2013). All ASVs attributed to plastids or mitochondria were removed from our analysis. To further control the quality of our ASVs, we placed them in a

phylogenetic tree. Each ASV was used as query for similarity search against SILVA reference sequences using BlastN (Altschul et al., 1990); ASVs and hit sequences were aligned together using mafft v7.508 (Katoh & Standley, 2013); gaps were removed from the alignment using trimAl v1.4.1 automated mode (Capella-Gutiérrez et al., 2009), and the final alignment was submitted to fasttree v2.1.8 (Price et al., 2010) with model GTR+G. We excluded from our analysis all ASVs that formed a spurious outgroup in the tree. Given the complexity of the ASV set, we removed from statistical analysis all singletons (ASVs represented by only one read across all samples) and uni-sample ASVs (represented by more than one read but restricted to one sample), leading to a total of 26,052 sequences.

Statistical analysis

Our aim was to describe the diversity within and across samples and study the variations of alpha diversity depending on several factors: rhizospheric or bare soil, maize genotype, plant development, sampling date.

Some samples had a low sequencing depth which did not allow to estimate correctly alpha diversity indices and had to be excluded from downstream analyses (Figure S1). To select a sequencing threshold below which samples were discarded, rarefaction curves were produced for several alpha diversity indices (i.e., ASV richness, Shannon and Simpson diversity indices, inverse Simpson diversity index, and the effective number of ASV (ENA) calculated as the exponential of Shannon diversity index). Each rarefaction curve was produced using 100 rarefied count tables sampled without replacement as suggested in Cameron et al. (2021). A threshold of 14,000 reads was selected as a reasonable compromise between the quality of estimated indices and the number of samples retained for the statistical analysis. As a result, 8 out of 210 samples (3.8%) were removed from the downstream analyses. From these samples, rarefied tables were produced by sampling without replacement.

For a given set of samples, the core microbiome was described as the fraction of ASVs shared by the samples using one rarefied count table. The core microbiome of all samples, of rhizospheric samples only, and of replicates were computed.

We determined alpha diversity indices as the mean over 500 estimates of the index produced from 500 rarefied count tables (Figure S2-S5).

To investigate how alpha diversity was shaped by plant earliness (early or late genotype) and temporal dynamics (plant development or sampling date), we analyzed the variations of the effective number of ASVs calculated as the exponential of the Shannon diversity index. This index provides an easily interpretable measure of biological diversity and was estimated with accuracy at the rarefaction depth we used.

To disentangle environmental fluctuations from crop development effects on the alpha diversity variations, two different gaussian linear models were built. Both models explained the variations of ENA and included the soil compartment from which samples were collected (bare soil, early-flowering or late-flowering plants) and the sowing (S1, S2, S3) as explaining factors. In addition, each model included one parameter related to temporal variations, either the development stage of the plant expressed as the number of days after sowing (model 1) or the sampling date expressed as calendar date (model 2). As we had no prior assumption about the shape of the relationship between ENA and these variables, they were treated as factors rather than quantitative variables. Each model included additive effects of each of the three factors (soil compartment, sowing, temporal factor) as well as the three paired interactions and the triple interaction. Using this model, we estimated the mean of ENA in each condition and computed the variance components. Given the staggered experimental design, model 2 had to be estimated with a subset of the dataset excluding sampling dates for which data were collected for only one or two sowings (see Figure 3).

To test for the effect of plant earliness, we compared model 1 to a nested model were the early and late genotype modalities were both replaced by the modality "rhizospheric soil". To test the effect of each factor, nested models were compared. Type III ANOVA was used to compute the variance components and test for factors effects.

All statistical analyses were conducted in R (v4.3.1) and RStudio (v2023.06.0) using the libraries vegan, car and ggplot2.

Preliminary results

Core microbiome

Overall, the root-associated microbiome exhibited high compositional heterogeneity across samples, including among biological replicates (blocks). Community composition varied markedly even among samples collected at the same phenological stage, indicating substantial within-stage variability (Figure 4).

Only a limited number of ASVs were consistently detected across all samples, reflecting the high diversity characterizing the dataset. No clear trend in either the size or the composition of the core microbiome was observed across maize developmental stages. Specifically, the number of core ASVs did not show a consistent increase or decrease along plant phenology (days after sowing) or over chronological time (calendar date), indicating that neither developmental nor temporal progression resulted in an enrichment or depletion of shared taxa.

When comparing bare soil and rhizospheric soil, the bare soil core microbiome comprised 206 ASVs out of 3884 detected ASVs (5% of all ASVs identified in bare soil), whereas the rhizosphere core included 78 ASVs out of 3964 total ASVs (2%). Although the bare soil core was numerically larger,

the difference between bare and rhizospheric soil was relatively modest, indicating that both environments were characterized by a limited proportion of shared ASVs. Thus, despite the selective influence exerted by plant roots, the overall number of shared ASVs remained comparable between compartments, with only a slight reduction in the rhizosphere.

Alpha diversity

Alpha diversity was assessed using the effective number of ASVs (ENA), which showed stable rarefaction plateau and met model assumptions. In both model 1 and model 2 plant earliness had no significant effect (p-value = 0.995 and p-value = 0.203, respectively). In contrast, alpha diversity differed between soil compartments, with bare soil and rhizosphere showing different ENA values (p-value < 0.001 for model 1 and p-value = 0.005 for model 2), and overall variation was influenced by temporal progression (p-value < 0.001 for both models) (Figure 5).

In model 1 (time expressed as days after sowing), time and sowing accounted for 20% of the variance, and their interaction accounted for 30%, indicating that alpha diversity differed among sowing times (Figure 6). In contrast, in model 2 (time expressed as calendar date), the sowing effect was negligible, and the interaction between sowing and time accounted for less than 10% of the variance, while time accounted for more than 30%, indicating that seasonal variation accounted for part of the observed alpha diversity dynamics independently of sowing date (Figure 6).

Overall, these results seem to suggest that alpha diversity dynamics were primarily driven by environmental fluctuations, while plant phenology exerted a context-dependent effect that became evident only in interaction with sowing time.

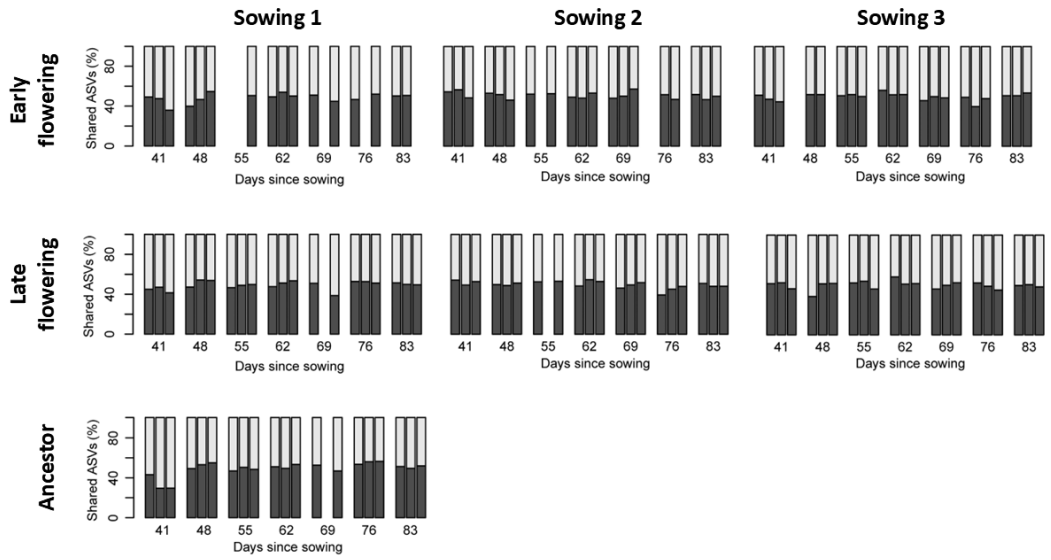


Figure 4 Core microbiome. Each bar represents the percentage of shared ASVs between one sample from the bare soil and its counterpart coming from the rhizosphere. Biological replicates are displayed as three adjacent bars. Missing bars are due to the exclusion of low sequencing depth-samples from the analyses.

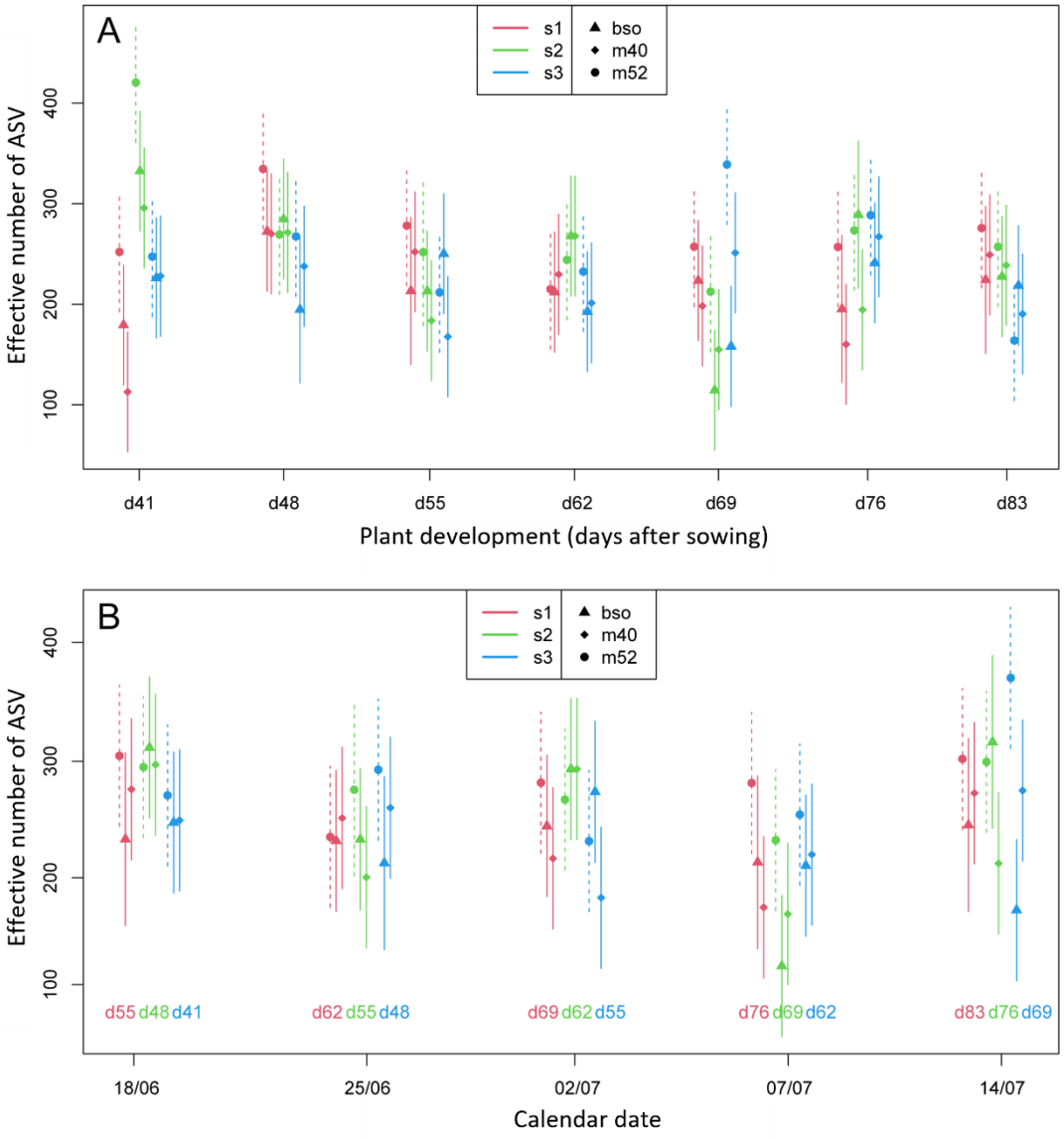


Figure 5 Estimated effective number of ASVs (ENA) from model 1 and model 2. In model 1 (A) time was represented as plant development expressed as the number of days after sowing; in model 2 (B) time was represented as the sampling date expressed as calendar date.

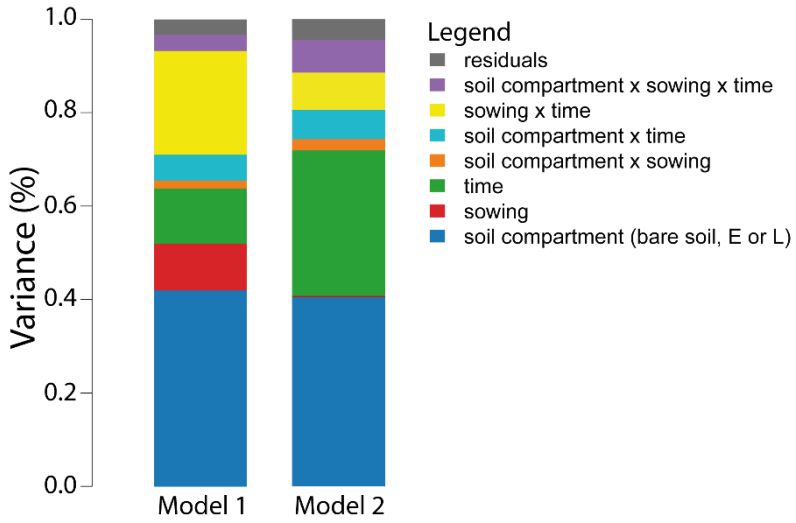


Figure 6 Percentage of variance explained by model 1 and model 2 for the effective number of ASVs (ENA) partitioned into the contributions of fixed effects (soil type, sowing, time, and their interactions) and residual variance. Soil type represents the soil compartment from which samples were collected: bare soil, rhizosphere of early-flowering plants, or rhizosphere of late-flowering plants. In model 1, time was expressed as days after sowing; in model 2, time was expressed as calendar date. Bars represent the proportion (%) of total variance attributable to each model term.

Discussion

Our preliminary results reveal a highly heterogeneous rhizosphere bacterial community, with substantial compositional variation even among biological replicates sampled at the same phenological stage. This within-stage variability highlights the fine-scale spatial heterogeneity that characterizes soil microbial communities and suggests that drivers such as plant development influence the microbiome within a system that is inherently highly variable.

The stringent criterion adopted to define the core microbiome revealed a remarkably small set of shared ASVs both in the rhizosphere and in bare soil. The rhizosphere core microbiome (2% of total ASVs) was only slightly smaller than the bare soil core microbiome (5%), indicating that, despite selective recruitment by roots, persistent taxa represent only a minor fraction of total diversity. This finding reinforces the view that the rhizosphere microbiome is largely dynamic and context-dependent, rather than dominated by a stable and extensive core. The absence of a consistent trend in the size of core microbiome across developmental stages further suggests that maize phenological progression does not lead to a progressive enrichment or depletion of shared taxa.

Alpha diversity patterns provided additional insight into the relative importance of host and environmental drivers. Plant earliness did not significantly affect bacterial alpha diversity, consistent with previous reports showing that host genetic background often explains a limited fraction of total microbiome variation compared with environmental influences (Bouffaud et al., 2016; Peiffer et al.,

2013; Walters et al., 2018). In contrast, soil compartment (bare soil vs. rhizosphere) and temporal progression significantly influenced alpha diversity. The consistent differences between bare soil and rhizosphere confirm that root presence alters overall diversity patterns, even if it does not dramatically expand or contract the shared core.

Importantly, the effect of time progression on alpha diversity depended on how time was parameterized. When time was expressed as days after sowing, representing plant phenology, its significant interaction with sowing indicated that alpha diversity trajectories differed depending on sowing date. This interaction suggests that phenological effects are not absolute but are modulated by the environmental context in which development unfolds. By contrast, when time was expressed as calendar date, sowing date and its interaction were no longer significant, and only temporal progression explained variation in alpha diversity. This pattern indicates that seasonal environmental conditions (e.g., temperature, moisture, and other unmeasured abiotic factors) were the primary drivers of alpha diversity dynamics, overriding differences attributable solely to flowering-time divergence.

Together, these results suggest that phenological divergence, when decoupled from broader genetic variation, is not sufficient to impose strong, consistent shifts in rhizosphere bacterial diversity. Instead, environmental seasonality emerges as the dominant structuring force, with phenology influencing microbiome dynamics in a sowing-dependent manner. In practical terms, this implies that climate-driven shifts in flowering time may alter rhizobiome assembly primarily through their interaction with seasonal environmental conditions rather than through plant developmental timing alone. Consequently, predictions about plant-microbiome responses to climate change must consider not only host phenological shifts but also the environmental conditions within which these shifts occur.

By disentangling phenology from the genetic background in two divergently selected maize populations derived from the same inbred line (MBS847), our study provided a focused test of the role of phenology variation in rhizobiome assembly. The limited and sowing-dependent phenological effects observed here indicate that host developmental timing alone exerts a comparatively modest influence relative to seasonal environmental drivers.

References

Aira, M., Gómez-Brandón, M., Lazcano, C., Bååth, E., & Domínguez, J. (2010). Plant genotype strongly modifies the structure and growth of maize rhizosphere microbial communities. Soil Biology and Biochemistry, 42(12), 2276–2281. https://doi.org/10.1016/j.soilbio.2010.08.029

Ali, B., Sabri, A. N., Ljung, K., & Hasnain, S. (2009). Auxin production by plant associated bacteria: Impact on endogenous IAA content and growth of Triticum aestivum L. Letters in Applied Microbiology, 48(5), 542–547. https://doi.org/10.1111/j.1472-765X.2009.02565.x

Altschul, S. F., Gish, W., Miller, W., Myers, E. W., & Lipman, D. J. (1990). Basic local alignment search tool. Journal of Molecular Biology, 215(3), 403–410. https://doi.org/10.1016/S0022-2836(05)80360-2

Aminurrasyid, A. H. B., Mohd Ikmal, A., & Nadarajah, K. K. (2025). The Rice-Microbe Nexus: Unlocking Productivity Through Soil Science. Rice, 18(1), 56. https://doi.org/10.1186/s12284-025-00809-0

Ao, J., Fu, J., Tian, J., Yan, X., & Liao, H. (2010). Genetic variability for root morph-architecture traits and root growth dynamics as related to phosphorus efficiency in soybean. Functional Plant Biology, 37(4), 304–312. https://doi.org/10.1071/FP09215

Bais, H. P., Weir, T. L., Perry, L. G., Gilroy, S., & Vivanco, J. M. (2006). THE ROLE OF ROOT EXUDATES IN RHIZOSPHERE INTERACTIONS WITH PLANTS AND OTHER ORGANISMS. Annual Review of Plant Biology, 57(Volume 57, 2006), 233–266. https://doi.org/10.1146/annurev.arplant.57.032905.105159

Berendsen, R. L., Pieterse, C. M. J., & Bakker, P. A. H. M. (2012). The rhizosphere microbiome and plant health. Trends in Plant Science, 17(8), 478–486. https://doi.org/10.1016/j.tplants.2012.04.001

Bernier, G. (1988). The Control of Floral Evocation and Morphogenesis. Annual Review of Plant Biology, 39(Volume 39, 1988), 175–219. https://doi.org/10.1146/annurev.pp.39.060188.001135

Bolyen, E., Rideout, J. R., Dillon, M. R., Bokulich, N. A., Abnet, C. C., Al-Ghalith, G. A., Alexander, H., Alm, E. J., Arumugam, M., Asnicar, F., Bai, Y., Bisanz, J. E., Bittinger, K., Brejnrod, A., Brislawn, C. J., Brown, C. T., Callahan, B. J., Caraballo-Rodríguez, A. M., Chase, J., … Caporaso, J. G. (2019). Reproducible, interactive, scalable and extensible microbiome data science using QIIME 2. Nature Biotechnology, 37(8), 852–857. https://doi.org/10.1038/s41587-019-0209-9

Bouffaud, M.-L., Renoud, S., Moënne-Loccoz, Y., & Muller, D. (2016). Is plant evolutionary history impacting recruitment of diazotrophs and nifH expression in the rhizosphere? Scientific Reports, 6(1), 21690. https://doi.org/10.1038/srep21690

Bulgarelli, D., Rott, M., Schlaeppi, K., Ver Loren van Themaat, E., Ahmadinejad, N., Assenza, F., Rauf, P., Huettel, B., Reinhardt, R., Schmelzer, E., Peplies, J., Gloeckner, F. O., Amann, R., Eickhorst, T., & Schulze-Lefert, P. (2012). Revealing structure and assembly cues for Arabidopsis root-inhabiting bacterial microbiota. Nature, 488(7409), 91–95. https://doi.org/10.1038/nature11336

Callahan, B. J., McMurdie, P. J., Rosen, M. J., Han, A. W., Johnson, A. J. A., & Holmes, S. P. (2016). DADA2: High-resolution sample inference from Illumina amplicon data. Nature Methods, 13(7), 581–583. https://doi.org/10.1038/nmeth.3869

Cameron, E. S., Schmidt, P. J., Tremblay, B. J.-M., Emelko, M. B., & Müller, K. M. (2021). Enhancing diversity analysis by repeatedly rarefying next generation sequencing data describing microbial communities. Scientific Reports, 11(1), 22302. https://doi.org/10.1038/s41598-021-01636-1

Capella-Gutiérrez, S., Silla-Martínez, J. M., & Gabaldón, T. (2009). trimAl: A tool for automated alignment trimming in large-scale phylogenetic analyses. Bioinformatics, 25(15), 1972–1973. https://doi.org/10.1093/bioinformatics/btp348

Castiglioni, P., Warner, D., Bensen, R. J., Anstrom, D. C., Harrison, J., Stoecker, M., Abad, M., Kumar, G., Salvador, S., D'Ordine, R., Navarro, S., Back, S., Fernandes, M., Targolli, J., Dasgupta, S., Bonin, C., Luethy, M. H., & Heard, J. E. (2008). Bacterial RNA Chaperones Confer Abiotic Stress Tolerance in Plants and Improved Grain Yield in Maize under Water-Limited Conditions. Plant Physiology, 147(2), 446–455. https://doi.org/10.1104/pp.108.118828

Cleland, E. E., Chuine, I., Menzel, A., Mooney, H. A., & Schwartz, M. D. (2007). Shifting plant phenology in response to global change. Trends in Ecology & Evolution, 22(7), 357–365. https://doi.org/10.1016/j.tree.2007.04.003

Desbiez-Piat, A., Ressayre, A., Marchadier, E., Noly, A., Remoué, C., Vitte, C., Belcram, H., Bourgais, A., Galic, N., Le Guilloux, M., Tenaillon, M. I., & Dillmann, C. (2023). Pervasive G × E interactions shape adaptive trajectories and the exploration of the phenotypic space in artificial selection experiments | Genetics | Oxford Academic. https://academic.oup.com/genetics/article/225/4/iyad186/7310833

Durand, E., Tenaillon, M. I., Raffoux, X., Thépot, S., Falque, M., Jamin, P., Bourgais, A., Ressayre, A., & Dillmann, C. (2015). Dearth of polymorphism associated with a sustained response to selection for flowering time in maize. BMC Evolutionary Biology, 15(1), 103. https://doi.org/10.1186/s12862-015-0382-5

Essel, E., Xie, J., Deng, C., Peng, Z., Wang, J., Shen, J., Xie, J., Coulter, J. A., & Li, L. (2019). Bacterial and fungal diversity in rhizosphere and bulk soil under different long-term tillage and cereal/legume rotation. Soil and Tillage Research, 194, 104302. https://doi.org/10.1016/j.still.2019.104302

FAO. (2025). Agricultural production statistics. FAO. https://doi.org/10.4060/cd8035en

Gordo, O., & Sanz, J. J. (2010). Impact of climate change on plant phenology in Mediterranean ecosystems. Global Change Biology, 16(3), 1082–1106. https://doi.org/10.1111/j.1365-2486.2009.02084.x

Grayston, S. J., Vaughan, D., & Jones, D. (1997). Rhizosphere carbon flow in trees, in comparison with annual plants: The importance of root exudation and its impact on microbial activity and nutrient availability. Applied Soil Ecology, 5(1), 29–56. https://doi.org/10.1016/S0929-1393(96)00126-6

Innerebner, G., Knief, & Vorholt, J. A. (2011). Protection of Arabidopsis thaliana against Leaf-Pathogenic Pseudomonas syringae by Sphingomonas Strains in a Controlled Model System. Applied and Environmental Microbiology. https://journals.asm.org/doi/10.1128/AEM.00133-11

Katoh, K., & Standley, D. M. (2013). MAFFT Multiple Sequence Alignment Software Version 7: Improvements in Performance and Usability. Molecular Biology and Evolution, 30(4), 772–780. https://doi.org/10.1093/molbev/mst010

Kusmec, A., & Schnable, P. S. (2024). Phenological Adaptation Is Insufficient to Offset Climate Change-Induced Yield Losses in US Hybrid Maize. Global Change Biology, 30(10), e17539. https://doi.org/10.1111/gcb.17539

Larsen, J., Jaramillo-López, P., Najera, M., & González-Esquivel, C. (2014). Biotic interactions in the rhizosphere in relation to plant and soil nutrient dynamics. Journal of Soil Science and Plant Nutrition, 15. https://doi.org/10.4067/S0718-95162015005000039

Ling, N., Wang, T., & Kuzyakov, Y. (2022). Rhizosphere bacteriome structure and functions. Nature Communications, 13(1), 836. https://doi.org/10.1038/s41467-022-28448-9

Lugtenberg, B., & Kamilova, F. (2009). Plant-Growth-Promoting Rhizobacteria. Annual Review of Microbiology, 63(Volume 63, 2009), 541–556. https://doi.org/10.1146/annurev.micro.62.081307.162918

Moretti, L. G., Crusciol, C. A. C., Leite, M. F. A., Momesso, L., Bossolani, J. W., Costa, O. Y. A., Hungria, M., & Kuramae, E. E. (2024). Diverse bacterial consortia: Key drivers of rhizosoil

fertility modulating microbiome functions, plant physiology, nutrition, and soybean grain yield. Environmental Microbiome, 19(1), 50. https://doi.org/10.1186/s40793-024-00595-0

Morgan, J. a. W., Bending, G. D., & White, P. J. (2005). Biological costs and benefits to plant-microbe interactions in the rhizosphere. Journal of Experimental Botany, 56(417), 1729–1739. https://doi.org/10.1093/jxb/eri205

Parent, B., Leclere, M., Lacube, S., Semenov, M. A., Welcker, C., Martre, P., & Tardieu, F. (2018). Maize yields over Europe may increase in spite of climate change, with an appropriate use of the genetic variability of flowering time. Proceedings of the National Academy of Sciences, 115(42), 10642–10647. https://doi.org/10.1073/pnas.1720716115

Peiffer, J. A., Spor, A., Koren, O., Jin, Z., Tringe, S. G., Dangl, J. L., Buckler, E. S., & Ley, R. E. (2013). Diversity and heritability of the maize rhizosphere microbiome under field conditions. Proceedings of the National Academy of Sciences, 110(16), 6548–6553. https://doi.org/10.1073/pnas.1302837110

Piao, S., Liu, Q., Chen, A., Janssens, I. A., Fu, Y., Dai, J., Liu, L., Lian, X., Shen, M., & Zhu, X. (2019). Plant phenology and global climate change: Current progresses and challenges. Global Change Biology, 25(6), 1922–1940. https://doi.org/10.1111/gcb.14619

Plancade, S., Marchadier, E., Huet, S., Ressayre, A., Noûs, C., & Dillmann, C. (2023). A successive time-to-event model of phyllochron dynamics for hypothesis testing: Application to the analysis of genetic and environmental effects in maize. Plant Methods, 19(1), 54. https://doi.org/10.1186/s13007-023-01029-7

Price, M. N., Dehal, P. S., & Arkin, A. P. (2010). FastTree 2 – Approximately Maximum-Likelihood Trees for Large Alignments. PLOS ONE, 5(3), e9490. https://doi.org/10.1371/journal.pone.0009490

Quast, C., Pruesse, E., Yilmaz, P., Gerken, J., Schweer, T., Yarza, P., Peplies, J., & Glöckner, F. O. (2013). The SILVA ribosomal RNA gene database project: Improved data processing and web-based tools. Nucleic Acids Research, 41(Database issue), D590-596. https://doi.org/10.1093/nar/gks1219

Rodriguez, M. N., Pioppi, A., & Kovàcs, A. T. (2025). The role of plant host genetics in shaping the composition and functionality of rhizosphere microbiomes | mSystems. https://journals.asm.org/doi/10.1128/msystems.00041-24

Rognes, T., Flouri, T., Nichols, B., Quince, C., & Mahé, F. (2016). VSEARCH: A versatile open source tool for metagenomics. PeerJ, 4, e2584. https://doi.org/10.7717/peerj.2584

Saleem, M., Hu, J., & Jousset, A. (2019). More Than the Sum of Its Parts: Microbiome Biodiversity as a Driver of Plant Growth and Soil Health. Annual Review of Ecology, Evolution, and Systematics, 50(Volume 50, 2019), 145–168. https://doi.org/10.1146/annurev-ecolsys-110617-062605

Van der Ent, S., Van Hulten, M., Pozo, M. J., Czechowski, T., Udvardi, M. K., Pieterse, C. M. J., & Ton, J. (2009). Priming of plant innate immunity by rhizobacteria and β-aminobutyric acid: Differences and similarities in regulation. New Phytologist, 183(2), 419–431. https://doi.org/10.1111/j.1469-8137.2009.02851.x

Van Nuland, M. E., Ware, I. M., Schadt, C. W., Yang, Z., Bailey, J. K., & Schweitzer, J. A. (2021). Natural soil microbiome variation affects spring foliar phenology with consequences for plant productivity and climate-driven range shifts. New Phytologist, 232(2), 762–775. https://doi.org/10.1111/nph.17599

Wagner, M. R., Lundberg, D. S., Coleman-Derr, D., Tringe, S. G., Dangl, J. L., & Mitchell-Olds, T. (2014). Natural soil microbes alter flowering phenology and the intensity of selection on flowering time in a wild Arabidopsis relative. Ecology Letters, 17(6), 717–726. https://doi.org/10.1111/ele.12276

Wagner, M. R., Lundberg, D. S., del Rio, T. G., Tringe, S. G., Dangl, J. L., & Mitchell-Olds, T. (2016). Host genotype and age shape the leaf and root microbiomes of a wild perennial plant. Nature Communications, 7(1), 12151. https://doi.org/10.1038/ncomms12151

Walters, W. A., Jin, Z., Youngblut, N., Wallace, J. G., Sutter, J., Zhang, W., González-Peña, A., Peiffer, J., Koren, O., Shi, Q., Knight, R., Glavina del Rio, T., Tringe, S. G., Buckler, E. S., Dangl, J. L., & Ley, R. E. (2018). Large-scale replicated field study of maize rhizosphere identifies heritable microbes. Proceedings of the National Academy of Sciences, 115(28), 7368–7373. https://doi.org/10.1073/pnas.1800918115

Zimmermann, A., Webber, H., Zhao, G., Ewert, F., Kros, J., Wolf, J., Britz, W., & de Vries, W. (2017). Climate change impacts on crop yields, land use and environment in response to crop sowing dates and thermal time requirements. Agricultural Systems, 157, 81–92. https://doi.org/10.1016/j.agsy.2017.07.007

3.2. Supplementary Materials

Sample ID	*Demultiplexed reads*	*DADA2 filter pass*	*% DADA2 filter pass*	*kept after DADA2 denoising*	*kept after DADA2 merging*	*% kept after DADA2 merging*
m40_s1_b1_d41	68012	67518	99.27	65375	55986	82.32
m40_s1_b1_d48	23067	22943	99.46	21062	15637	67.79
m40_s1_b1_d55	12516	12444	99.42	11983	10957	87.54
m40_s1_b1_d62	111244	110441	99.28	108417	98402	88.46
m40_s1_b1_d69	78568	78083	99.38	76439	69266	88.16
m40_s1_b1_d76	19123	18997	99.34	18604	17360	90.78
m40_s1_b1_d83	99787	99150	99.36	97504	90326	90.52
m40_s1_b2_d41	107001	106247	99.30	104394	94235	88.07
m40_s1_b2_d48	64267	63911	99.45	62564	56767	88.33
m40_s1_b2_d55	6837	6793	99.36	6404	5661	82.8
m40_s1_b2_d62	83367	82382	98.82	81003	75017	89.98
m40_s1_b2_d69	55441	54959	99.13	53906	50200	90.55
m40_s1_b2_d76	4853	4813	99.18	4499	3890	80.16
m40_s1_b2_d83	120923	119867	99.13	117898	107429	88.84
m40_s1_b3_d41	38880	38627	99.35	37314	32361	83.23
m40_s1_b3_d48	87636	87020	99.30	85071	75228	85.84
m40_s1_b3_d55	73113	72556	99.24	70903	61481	84.09
m40_s1_b3_d62	65019	64596	99.35	63396	57579	88.56
m40_s1_b3_d69	31302	31143	99.49	29885	25059	80.06
m40_s1_b3_d76	47476	47079	99.16	45771	39331	82.84
m40_s1_b3_d83	10829	10745	99.22	8636	4091	37.78
m40_s2_b1_d41	125390	124555	99.33	122205	113378	90.42
m40_s2_b1_d48	61688	61181	99.18	60063	54522	88.38
m40_s2_b1_d55	52880	52494	99.27	50908	43052	81.41
m40_s2_b1_d62	73676	73130	99.26	71685	63907	86.74
m40_s2_b1_d69	40268	39920	99.14	38924	34925	86.73
m40_s2_b1_d76	7946	7692	96.80	6505	4431	55.76
m40_s2_b1_d83	155438	153680	98.87	150915	140461	90.36
m40_s2_b2_d41	111912	111112	99.29	108895	99166	88.61
m40_s2_b2_d48	94534	93881	99.31	92045	81617	86.34
m40_s2_b2_d55	56602	56174	99.24	54942	49559	87.56
m40_s2_b2_d62	34222	33940	99.18	32563	26506	77.45
m40_s2_b2_d69	75327	74761	99.25	73082	64225	85.26
m40_s2_b2_d76	53138	52801	99.37	51752	47496	89.38
m40_s2_b2_d83	181133	179781	99.25	175753	159730	88.18
m40_s2_b3_d41	81602	81096	99.38	79446	73660	90.27
m40_s2_b3_d48	85514	84680	99.02	82708	74755	87.42
m40_s2_b3_d55	17099	16987	99.34	16496	15007	87.77

Sample ID	Demultiplexed reads	DADA2 filter pass	% DADA2 filter pass	kept after DADA2 denoising	kept after DADA2 merging	% kept after DADA2 merging
m40_s2_b3_d62	61775	61337	99.29	60163	54387	88.04
m40_s2_b3_d69	134871	133387	98.9	130940	119475	88.58
m40_s2_b3_d76	125930	124582	98.93	122626	114280	90.75
m40_s2_b3_d83	123354	122333	99.17	119751	110535	89.61
m40_s3_b1_d41	108828	108017	99.25	106217	98691	90.69
m40_s3_b1_d48	10390	10207	98.24	9302	7438	71.59
m40_s3_b1_d55	133336	132557	99.42	130619	121091	90.82
m40_s3_b1_d62	112677	111751	99.18	110149	101648	90.21
m40_s3_b1_d69	101255	100632	99.38	98386	89144	88.04
m40_s3_b1_d76	66086	65575	99.23	63915	56503	85.5
m40_s3_b1_d83	50261	49801	99.08	47492	40368	80.32
m40_s3_b2_d41	107446	106672	99.28	104866	97153	90.42
m40_s3_b2_d48	45158	44892	99.41	43897	40365	89.39
m40_s3_b2_d55	82329	81709	99.25	80185	70913	86.13
m40_s3_b2_d62	57134	56640	99.14	55629	51109	89.45
m40_s3_b2_d69	85121	84464	99.23	82963	75207	88.35
m40_s3_b2_d76	29596	29387	99.29	27259	20033	67.69
m40_s3_b2_d83	222840	221076	99.21	217305	203378	91.27
m40_s3_b3_d41	51634	51290	99.33	49409	40643	78.71
m40_s3_b3_d48	60927	60377	99.1	59298	55365	90.87
m40_s3_b3_d55	126371	125585	99.38	123396	114241	90.4
m40_s3_b3_d62	77846	77263	99.25	75669	71024	91.24
m40_s3_b3_d69	44635	44298	99.24	43387	38832	87.0
m40_s3_b3_d76	179445	178104	99.25	174927	161115	89.79
m40_s3_b3_d83	172667	171362	99.24	168738	158696	91.91
m52_s1_b1_d41	49936	49547	99.22	48128	41263	82.63
m52_s1_b1_d48	51539	51145	99.24	49637	43033	83.5
m52_s1_b1_d55	60307	59922	99.36	59003	54733	90.76
m52_s1_b1_d62	84485	83824	99.22	82306	74673	88.39
m52_s1_b1_d69	68044	67609	99.36	65869	57838	85.0
m52_s1_b1_d76	36957	36661	99.2	35820	32304	87.41
m52_s1_b1_d83	153943	152378	98.98	150207	138402	89.9
m52_s1_b2_d41	87998	87402	99.32	86222	80855	91.88
m52_s1_b2_d48	93938	93291	99.31	91685	84948	90.43
m52_s1_b2_d55	58321	57904	99.28	56370	49641	85.12
m52_s1_b2_d62	31322	31108	99.32	30037	26274	83.88
m52_s1_b2_d69	49107	48819	99.41	47530	43201	87.97
m52_s1_b2_d76	37251	36983	99.28	35789	30640	82.25
m52_s1_b2_d83	51473	51072	99.22	49933	44822	87.08
m52_s1_b3_d41	57510	57190	99.44	56207	51830	90.12
m52_s1_b3_d48	79655	79145	99.36	77677	70575	88.6

Sample ID	Demultiplexed reads	DADA2 filter pass	% DADA2 filter pass	kept after DADA2 denoising	kept after DADA2 merging	% kept after DADA2 merging
m52_s1_b3_d55	56091	55065	98.17	53645	47494	84.67
m52_s1_b3_d62	82178	81677	99.39	80052	72256	87.93
m52_s1_b3_d69	27732	27582	99.46	25844	18145	65.43
m52_s1_b3_d76	47692	46917	98.37	45782	40906	85.77
m52_s1_b3_d83	27308	27033	98.99	26331	24390	89.31
m52_s2_b1_d41	96376	95513	99.10	93690	85249	88.45
m52_s2_b1_d48	40927	40610	99.23	39336	34722	84.84
m52_s2_b1_d55	93554	92941	99.34	91053	82591	88.28
m52_s2_b1_d62	41405	41160	99.41	40032	35277	85.2
m52_s2_b1_d69	24267	24069	99.18	23087	19936	82.15
m52_s2_b1_d76	163770	162765	99.39	154147	84099	51.35
m52_s2_b1_d83	138117	136837	99.07	134817	127729	92.48
m52_s2_b2_d41	77232	76674	99.28	75283	69925	90.54
m52_s2_b2_d48	42265	41413	97.98	40137	35223	83.34
m52_s2_b2_d55	37570	37334	99.37	35662	30402	80.92
m52_s2_b2_d62	51064	50696	99.28	49338	44955	88.04
m52_s2_b2_d69	48110	47217	98.14	46065	41075	85.38
m52_s2_b2_d76	115528	114750	99.33	112340	99500	86.13
m52_s2_b2_d83	199972	198641	99.33	193964	171098	85.56
m52_s2_b3_d41	57521	57169	99.39	56096	51520	89.57
m52_s2_b3_d48	138444	112357	81.16	109910	100279	72.43
m52_s2_b3_d55	49510	49188	99.35	48317	44574	90.03
m52_s2_b3_d62	177087	175887	99.32	163561	119391	67.42
m52_s2_b3_d69	133235	116548	87.48	114300	105641	79.29
m52_s2_b3_d76	83108	82346	99.08	81195	76526	92.08
m52_s2_b3_d83	80222	79544	99.15	78138	73487	91.6
m52_s3_b1_d41	103595	102729	99.16	101336	94459	91.18
m52_s3_b1_d48	109531	108976	99.49	104481	55507	50.68
m52_s3_b1_d55	97903	97109	99.19	95675	88601	90.5
m52_s3_b1_d62	143748	142544	99.16	140578	131326	91.36
m52_s3_b1_d69	101078	100405	99.33	98314	87221	86.29
m52_s3_b1_d76	27510	27277	99.15	26472	24302	88.34
m52_s3_b1_d83	112912	111994	99.19	109660	101132	89.57
m52_s3_b2_d41	103173	102410	99.26	100669	91660	88.84
m52_s3_b2_d48	58998	58620	99.36	56316	41749	70.76
m52_s3_b2_d55	47066	46693	99.21	45780	42280	89.83
m52_s3_b2_d62	123575	122612	99.22	120658	112321	90.89
m52_s3_b2_d69	79147	78394	99.05	77461	72600	91.73
m52_s3_b2_d76	79721	79043	99.15	76898	67334	84.46
m52_s3_b2_d83	171622	170149	99.14	166825	152679	88.96
m52_s3_b3_d41	34393	34124	99.22	32997	27746	80.67

Sample ID	Demultiplexed reads	DADA2 filter pass	% DADA2 filter pass	kept after DADA2 denoising	kept after DADA2 merging	% kept after DADA2 merging
m52_s3_b3_d48	57557	57188	99.36	56039	51819	90.03
m52_s3_b3_d55	33029	32802	99.31	32002	28403	85.99
m52_s3_b3_d62	138956	137977	99.3	134163	117909	84.85
m52_s3_b3_d69	19863	19746	99.41	19157	16962	85.39
m52_s3_b3_d76	82925	82422	99.39	80609	73681	88.85
m52_s3_b3_d83	150579	149212	99.09	146386	134348	89.22
mbs_s1_b1_d41	114799	113505	98.87	111856	103694	90.33
mbs_s1_b1_d48	63895	63516	99.41	62390	58149	91.01
mbs_s1_b1_d55	32804	32467	98.97	31550	28103	85.67
mbs_s1_b1_d62	65746	65232	99.22	64269	58589	89.11
mbs_s1_b1_d69	81560	80955	99.26	79478	72740	89.19
mbs_s1_b1_d76	37785	37381	98.93	36299	31541	83.47
mbs_s1_b1_d83	257259	255237	99.21	251399	231160	89.85
mbs_s1_b2_d41	77906	77308	99.23	76160	70028	89.89
mbs_s1_b2_d48	48439	48017	99.13	46651	40623	83.86
mbs_s1_b2_d55	132762	131834	99.30	130109	120928	91.09
mbs_s1_b2_d62	43939	43656	99.36	42739	39177	89.16
mbs_s1_b2_d69	27996	27799	99.3	27057	24115	86.14
mbs_s1_b2_d76	74940	74343	99.2	72949	65231	87.04
mbs_s1_b2_d83	89564	88780	99.12	87131	79205	88.43
mbs_s1_b3_d41	146162	145220	99.36	143269	133049	91.03
mbs_s1_b3_d48	103773	102992	99.25	100865	89398	86.15
mbs_s1_b3_d55	107527	106673	99.21	104397	92408	85.94
mbs_s1_b3_d62	113091	112235	99.24	110337	102542	90.67
mbs_s1_b3_d69	55666	55241	99.24	53460	46291	83.16
mbs_s1_b3_d76	137079	135783	99.05	133228	118487	86.44
mbs_s1_b3_d83	82676	82059	99.25	80704	75168	90.92
bso_s1_b1_d41	137133	136054	99.21	133505	119192	86.92
bso_s1_b1_d48	222938	221347	99.29	216685	194684	87.33
bso_s1_b1_d55	36938	36650	99.22	35015	26359	71.36
bso_s1_b1_d62	73567	73025	99.26	71297	64739	88
bso_s1_b1_d69	48197	47835	99.25	46491	40332	83.68
bso_s1_b1_d76	43315	43012	99.3	41463	34532	79.72
bso_s1_b1_d83	81636	80990	99.21	78671	68487	83.89
bso_s1_b2_d41	102352	101036	98.71	99263	91694	89.59
bso_s1_b2_d48	59015	58527	99.17	57237	51848	87.86
bso_s1_b2_d55	81044	80394	99.20	78492	68594	84.64
bso_s1_b2_d62	92370	91679	99.25	89221	77122	83.49
bso_s1_b2_d69	14577	14478	99.32	13714	11709	80.33
bso_s1_b2_d76	92640	91991	99.3	89656	78593	84.84
bso_s1_b2_d83	80477	79957	99.35	77784	68409	85

Sample ID	Demultiplexed reads	DADA2 filter pass	% DADA2 filter pass	kept after DADA2 denoising	kept after DADA2 merging	% kept after DADA2 merging
bso_s1_b3_d41	96058	95293	99.20	93348	84605	88.08
bso_s1_b3_d48	99190	98308	99.11	95717	81510	82.18
bso_s1_b3_d55	80030	79206	98.97	77122	64648	80.78
bso_s1_b3_d62	81079	80371	99.13	78492	70638	87.12
bso_s1_b3_d69	43156	42878	99.36	41708	37394	86.65
bso_s1_b3_d76	96812	95797	98.95	93738	86538	89.39
bso_s1_b3_d83	67388	66824	99.16	65336	59250	87.92
bso_s2_b1_d41	72994	72474	99.29	70783	63381	86.83
bso_s2_b1_d48	42355	41976	99.11	41038	36534	86.26
bso_s2_b1_d55	32444	32205	99.26	31093	26684	82.25
bso_s2_b1_d62	57112	56683	99.25	55144	49506	86.68
bso_s2_b1_d69	29932	29714	99.27	28531	25027	83.61
bso_s2_b1_d76	63407	62842	99.11	61472	56200	88.63
bso_s2_b1_d83	215610	213991	99.25	209581	194762	90.33
bso_s2_b2_d41	124845	123892	99.24	120840	111039	88.94
bso_s2_b2_d48	106936	105671	98.82	103041	90247	84.39
bso_s2_b2_d55	8223	8163	99.27	6749	3128	38.04
bso_s2_b2_d62	55031	54641	99.29	53287	46665	84.8
bso_s2_b2_d69	34076	33683	98.85	32420	27197	79.81
bso_s2_b2_d76	132098	130951	99.13	128456	115509	87.44
bso_s2_b2_d83	191075	189094	98.96	185154	170190	89.07
bso_s2_b3_d41	23991	23819	99.28	22948	20083	83.71
bso_s2_b3_d48	126141	124929	99.04	122815	113129	89.68
bso_s2_b3_d55	29269	29042	99.22	28031	24783	84.67
bso_s2_b3_d62	96934	96146	99.19	94154	82447	85.05
bso_s2_b3_d69	117198	115943	98.93	113619	99201	84.64
bso_s2_b3_d76	146394	145370	99.30	142512	131546	89.86
bso_s2_b3_d83	148039	130706	88.29	126917	116887	78.96
bso_s3_b1_d41	106050	105186	99.19	103154	93513	88.18
bso_s3_b1_d48	33783	33522	99.23	32475	28678	84.89
bso_s3_b1_d55	50403	50008	99.22	48875	44066	87.43
bso_s3_b1_d62	106980	106080	99.16	103570	92656	86.61
bso_s3_b1_d69	126094	125063	99.18	122536	111041	88.06
bso_s3_b1_d76	36488	36236	99.31	34332	28551	78.25
bso_s3_b1_d83	154324	153089	99.2	148811	131218	85.03
bso_s3_b2_d41	187133	185596	99.18	181452	165543	88.46
bso_s3_b2_d48	81377	80816	99.31	78933	70651	86.82
bso_s3_b2_d55	96395	95533	99.11	93779	85145	88.33
bso_s3_b2_d62	71410	70748	99.07	69013	63221	88.53
bso_s3_b2_d69	86756	86235	99.40	84168	75465	86.99
bso_s3_b2_d76	90893	90247	99.29	88311	82640	90.92

Sample ID	Demultiplexed reads	DADA2 filter pass	% DADA2 filter pass	kept after DADA2 denoising	kept after DADA2 merging	% kept after DADA2 merging
bso_s3_b2_d83	152994	151626	99.11	147090	127075	83.06
bso_s3_b3_d41	89484	88211	98.58	86178	77378	86.47
bso_s3_b3_d48	77744	77149	99.23	75424	67587	86.94
bso_s3_b3_d55	29321	29077	99.17	28172	25020	85.33
bso_s3_b3_d62	222735	220879	99.17	215990	198853	89.28
bso_s3_b3_d69	39486	39237	99.37	37748	32359	81.95
bso_s3_b3_d76	127571	126664	99.29	123654	115102	90.23
bso_s3_b3_d83	124437	123276	99.07	120669	111521	89.62

Table S1 Summary of sequencing read processing across all samples. The first column reports the sample ID structured as a concatenation of genotype_sowing_block_days after sowing. For each sample the table reports the total number of demultiplexed reads, the number and percentage of reads passing the DADA2 quality filtering step, the number of reads retained after DADA2 denoising, and the number and percentage of reads successfully retained after paired-end merging. These metrics provide an overview of read retention and data quality throughout the bioinformatic pipeline. m40 = early-flowering plants; m52 = late-flowering; mbs = ancestral line; bso = bare soil; s1–s3 = the three sowing dates; b1–b3 = the three replicates (blocks); d41–d83 = days after sowing.

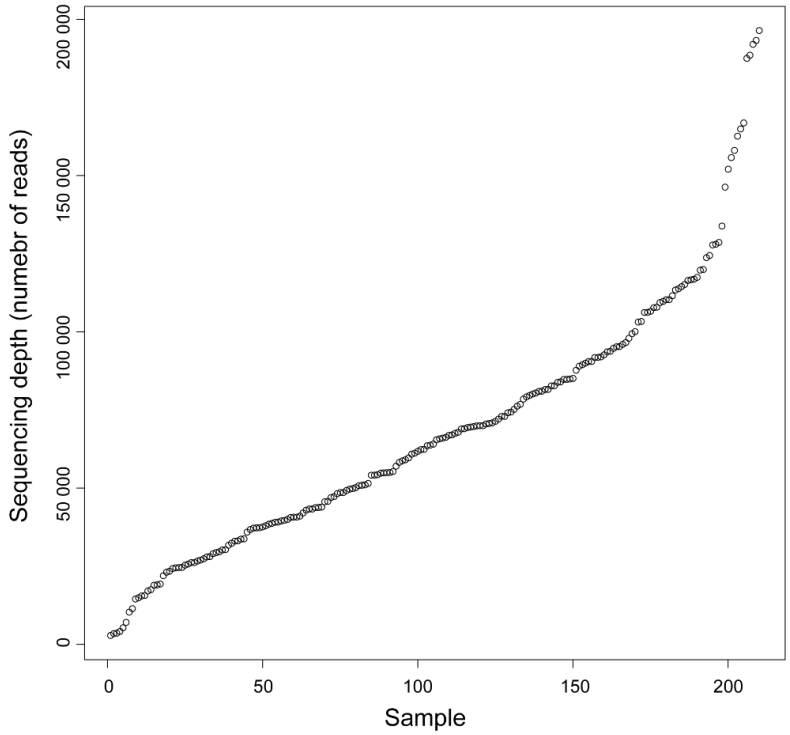


Figure S1 Plot of the 210 samples ranked in ascending order of sequencing depth. The first marked increase in sequencing depth can be observed after the first eight samples. Based on this discontinuity and on rarefaction curves, a sequencing depth threshold of 14,000 reads was decided, and the first eight samples were excluded from subsequent analyses.

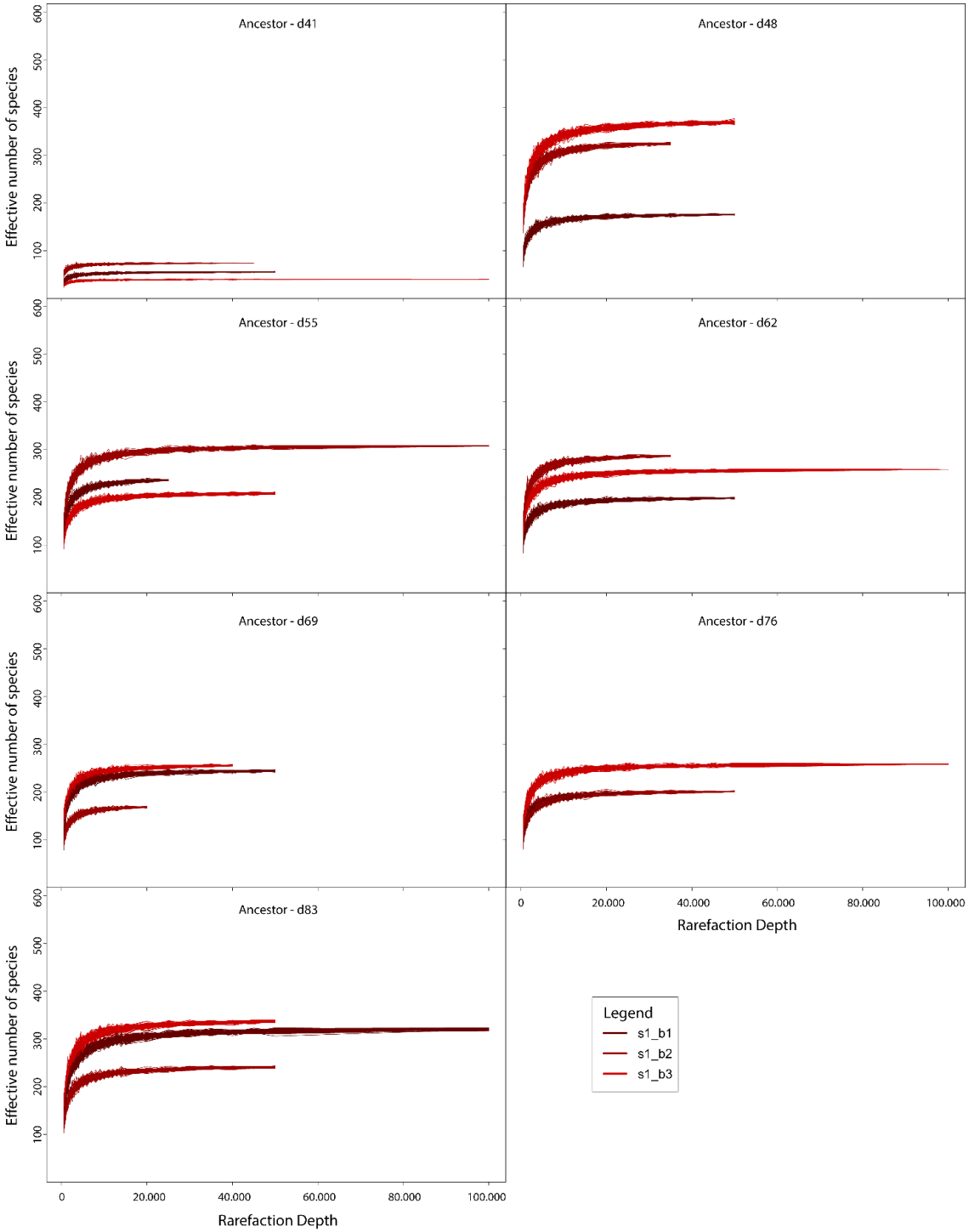


Figure S2 Multiple rarefaction curves of microbial alpha diversity from the rhizosphere of plants of the Ancestor genotype, expressed as the effective number of ASVs (ENA) across samples. Each panel represents a specific sampling time (d41–d83), and curves correspond to individual samples colored by replicates (blocks). The x-axis indicates sequencing depth (number of reads), and the y-axis shows the effective number of ASVs. All samples reached clear asymptotes, indicating sufficient sequencing depth to capture the majority of bacterial diversity present in each sample. Differences in plateau height reflect variation in alpha diversity among replicates and sampling times. Rarefaction curves were also generated for the observed ASV richness, Shannon and Simpson diversity indices, and the inverse Simpson diversity index (figures not shown).

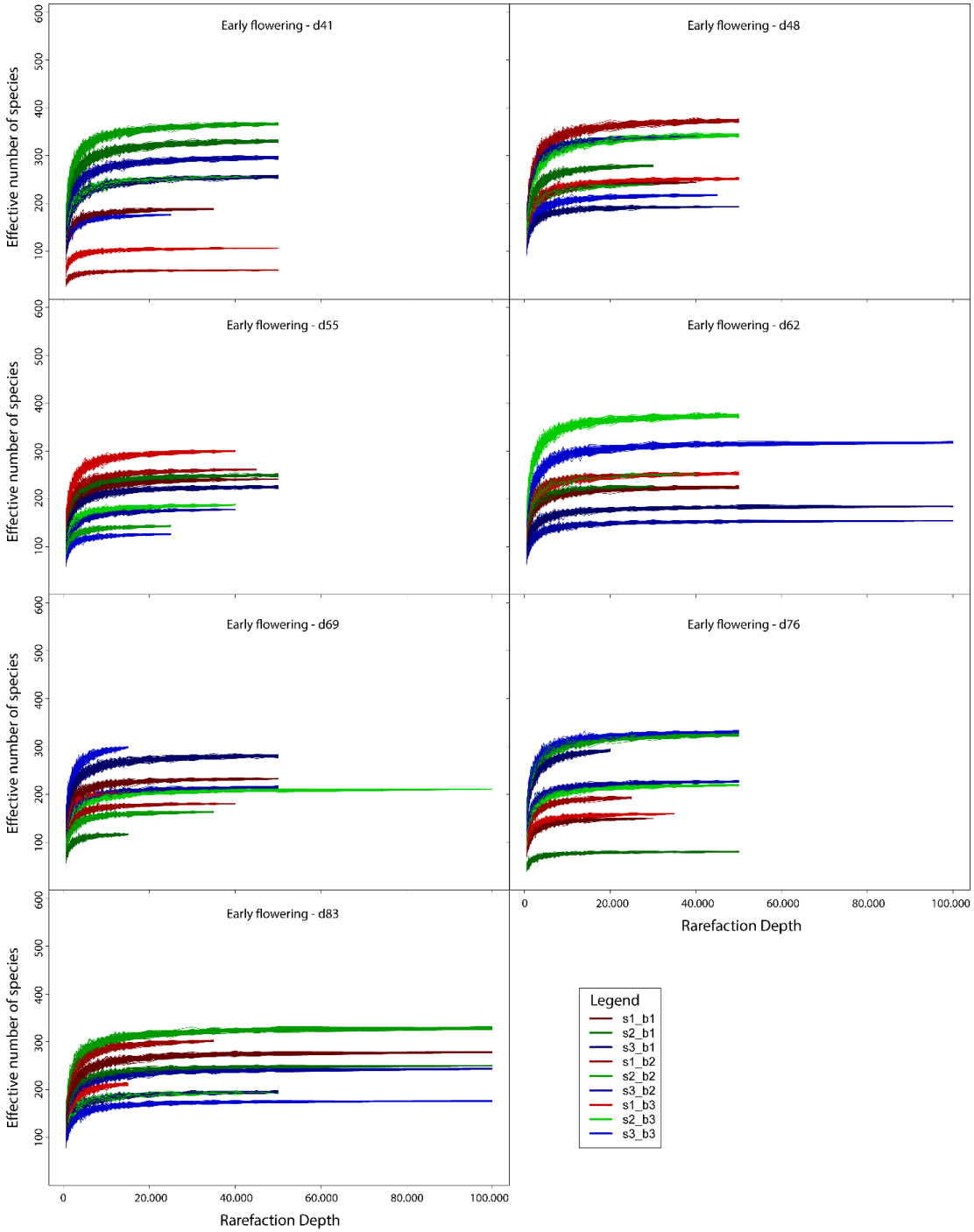


Figure S3 Multiple rarefaction curves of microbial alpha diversity from the rhizosphere of early-flowering genotype, expressed as the effective number of ASVs (ENA) across samples. Each panel represents a specific sampling time (d41–d83), and curves correspond to individual samples colored by sowing dates and replicates (blocks). The x-axis indicates sequencing depth (number of reads), and the y-axis shows the effective number of ASVs. All samples reached clear asymptotes, indicating sufficient sequencing depth to capture the majority of bacterial diversity present in each sample. Differences in plateau height reflect variation in alpha diversity among sowing dates, replicates and sampling times. Rarefaction curves were also generated for the observed ASV richness, Shannon and Simpson diversity indices, and the inverse Simpson diversity index (figures not shown).

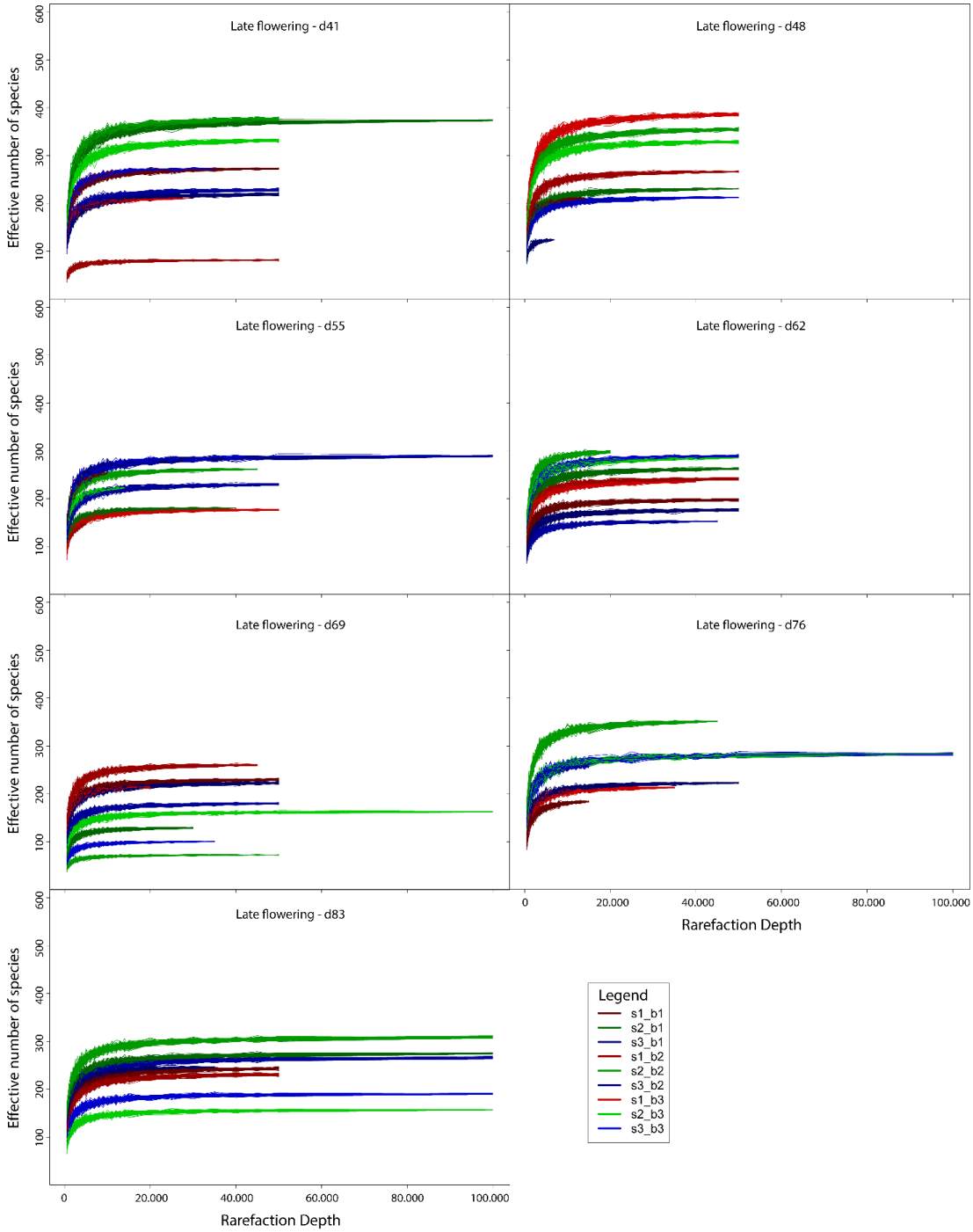


Figure S4 Multiple rarefaction curves of microbial alpha diversity from the rhizosphere of late-flowering genotype, expressed as the effective number of ASVs (ENA) across samples. Each panel represents a specific sampling time (d41–d83), and curves correspond to individual samples colored by sowing dates and replicates (blocks). The x-axis indicates sequencing depth (number of reads), and the y-axis shows the effective number of ASVs. All samples reached clear asymptotes, indicating sufficient sequencing depth to capture the majority of bacterial diversity present in each sample. Differences in plateau height reflect variation in alpha diversity among sowing dates, replicates and sampling times. Rarefaction curves were also generated for the observed ASV richness, Shannon and Simpson diversity indices, and the inverse Simpson diversity index (figures not shown).

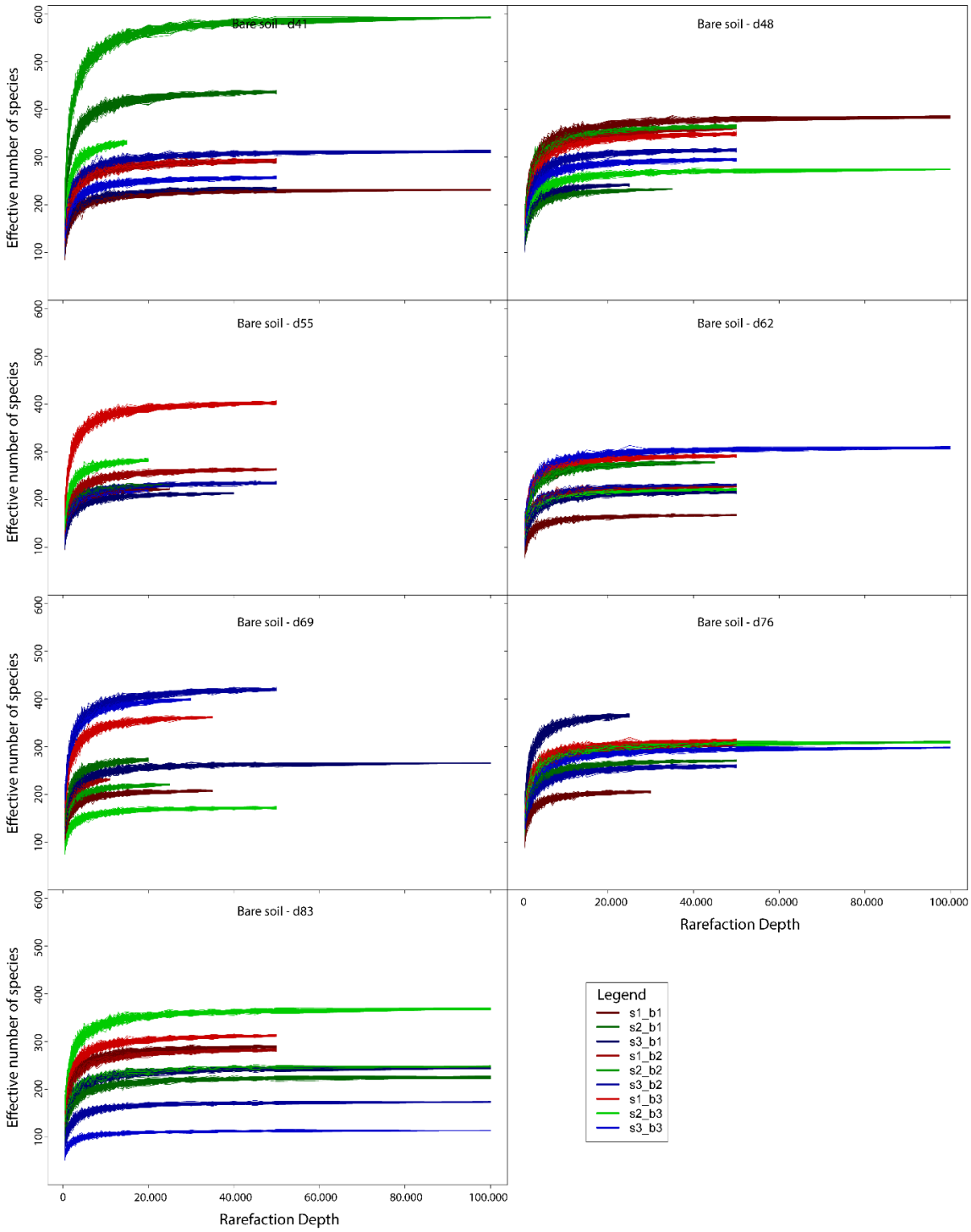


Figure S5 Multiple rarefaction curves of microbial alpha diversity from the bare soil, expressed as the effective number of ASVs (ENA) across samples. Each panel represents a specific sampling time (d41–d83), and curves correspond to individual samples colored by sowing dates and replicates (blocks). The x-axis indicates sequencing depth (number of reads), and the y-axis shows the effective number of ASVs. All samples reached clear asymptotes, indicating sufficient sequencing depth to capture the majority of bacterial diversity present in each sample. Differences in plateau height reflect variation in alpha diversity among sowing dates, replicates and sampling times. Rarefaction curves were also generated for the observed ASV richness, Shannon and Simpson diversity indices, and the inverse Simpson diversity index (figures not shown).

4. Bioextracts as Potential Environment-Friendly Anti-Mycotoxin Compounds

Increasing research attention is being directed toward preventive strategies for mycotoxin control based on sustainable crop protection approaches. In this context, bio-based extracts derived from agricultural and agro-industrial by-products are emerging as promising low-impact tools to limit fungal development and mycotoxin production. In line with the principles of circular economy, this study evaluates four plant- or seaweed-based extracts and discusses their potential to mitigate mycotoxin occurrence through sustainable and environmentally sound crop protection strategies.

4.1. Article Under Review in Scientific Reports

In vitro antifungal effect of plant-based and *Ulva* sp. extracts on *Aspergillus flavus* growth and conidia germination

Giacomo Boscarol[1], Alessandra Di Francesco[1], Enrico Braidot[1]*, Marco Vuerich[1], Francesco Boscutti[1], Valentino Volpe[2], Michele Fabro[2], Urska Vhrovsek[3], Elisa Petrussa[1]

1 Department of Agricultural, Food, Environmental and Animal Sciences (DI4A), University of Udine, Via delle Scienze 206, 33100 Udine, Italy
2 Servizio fitosanitario e chimico, ricerca, sperimentazione e assistenza tecnica, ERSA, via Sabbatini 5, 33050 Pozzuolo del Friuli (UD), Italy
3 Foundation Edmund Mach, via Edmund Mach 1, 38098 San Michele all'Adige (TN), Italy
* Corresponding Author

Abstract

Mycotoxins in cereals, particularly maize, pose a significant threat to agriculture, worsened by climate change. Therefore, developing effective mitigation strategies are urgently claimed. Plant waste and seaweed extracts offer promising sources of phytochemicals for combating fungal plant pathogens. This study investigated the *in vitro* antifungal potential and polyphenol composition of hydroalcoholic extracts from plant waste materials and seaweed (*Ailanthus altissima* (Mill.) Swingle leaves, *Humulus lupulus* L. trub, *Olea europaea* L. leaves and *Ulva* sp. thallus). With the exception of *O. europaea*, all extracts inhibited *Aspergillus flavus* growth, with *Ulva* sp. showing the highest efficacy (EC_{50} = 14.2 mg/mL). Analysis revealed enrichment in glycosylated flavonols and hydroxycinnamic acids across extracts, while *Ulva* sp. specifically contained rosmarinic acid, *p*-hydroxybenzoic acid, and uronic acid and sulfate groups, characteristics of ulvan polysaccharides. These results suggest *Ulva* biomass is a promising botanical source for *Aspergillus flavus* biocontrol, paving the way for its future application in agriculture and post-harvest systems.

Keywords

Biological control • *Aspergillus flavus* • Plant extract • Polyphenols • Ulvan polysaccharides • Waste Reuse

Highlights

Ulva, *Ailanthus* and *Humulus* trub-based hydroalcoholic extracts inhibit *in vitro A. flavus* mycelial growth at different efficacy levels

Ulva extract resulted the more promising, with a EC_{50} of 14.2 mg/mL and a 91% complete inhibition at about 20 mg/mL

Ulva extract also affected conidial germination in a dose-dependent manner, reaching a complete inhibition at 14.0 mg/mL after 16 h of incubation.

Biochemical characterization of extracts revealed Ulva to be specifically rich in rosmarinic and p-hydroxybenzoic acid and to contain ulvan polysaccharides

Ulva-derived and plant waste-based natural extracts could represent potential sustainable alternatives in maize pest management

Introduction

Aflatoxins produced by *Aspergillus* species contaminate major crops and pose severe health risks (Zingales et al., 2022). Climate-driven changes in temperature and humidity have increased contamination risks in the temperate Europe, like northern lowlands of Italy, where maize represents the predominant crop (Ferrari et al., 2023; Giorni et al., 2016; Leggieri et al., 2021). Major key factors for augmented risk of mycotoxin contamination in maize (interaction of high temperature and low water activity in kernel, European corn borer infestation and the predicted increase in global average temperature and worsening of drought stress events) are considered to be the main drivers for the emerging concerns for food and feed safety, with large economic and social impacts (Battilani et al., 2016; Medina et al., 2017; Molnár et al., 2023; Zingales et al., 2022). Extensive efforts have been made to identify natural inhibitors such as biological extracts or antagonistic microorganisms for counteracting fungal invasion and aflatoxin contamination (Ahmed et al., 2022). Among them, plant-based extracts are characterized by a high content of phenolic acids and terpenes, for which antioxidant bioactivity and antifungal properties have been widely recognized (Ahmed et al., 2022; Montibus et al., 2021), providing an environmentally friendly and safe alternative to synthetic pesticides (Giorni et al., 2023; Makhuvele et al., 2020). In particular, bio-extracts obtained from agriculture, forestry and food by-products (e.g., *Olea*, *Ailanthus*, grape canes, spent hops from brewery industry) have been shown to exert a wide range of antimicrobial actions (Bartmańska et al., 2018; Bilel et al., 2023; Y. Li et al., 2021; Taillis et al., 2023). Moreover, they are more readily available due

to the abundance of raw source biomass in nature, and the preparation processes are often less polluting than traditional chemical synthesis processes. These extracts are also believed to act synergistically with other different active compounds, and to elicit natural defence responses in plants (Filippi et al., 2019; Giorni et al., 2023; Vuerich et al., 2023). Marine seaweeds, rich in polysaccharides and polyphenols, are also emerging as valuable biostimulants or antimicrobial products for agricultural applications (El Fayoumy et al., 2022; El-Bilawy et al., 2022; Zarraonaindia et al., 2023a). In this perspective, we investigated the effectiveness of four extracts (from *Ailanthus altissima* (Mill.) Swingle as environmentally invasive organisms, *Ulva* sp. as collected environmental biomass from coastal waters, *Olea europaea* L., 1753 cv. Gargazzo and *Humulus lupulus* L., 1753 as processing wastes) against *A. flavus* mycelium growth and conidial germination. Extracts have been then characterized for their polyphenolic profile by UHPLC-MS. The results provided information on different by-products as sources for sustainable control of mycotoxigenic fungi.

Material and methods

Plant and seaweed collection and extraction

Plant materials were collected in Friuli Venezia Giulia Region during 2023 and 2024 (Table S1). *A. altissima* and *O. europaea* leaves were collected during summer, cleaned and stored at -80 °C until use. The *Ulva* biomass was handpicked during summer-mid autumn 2023-2024 from the intertidal zone in the Marano Lagoon, Northeastern Adriatic Sea coast, after natural green tide/bloom events. The collected material was visually identified and consisted predominantly of *Ulva rigida* L., 1753, with the co-occurrence of *Ulva laetevirens* Areschoug, 1854. The biomass was rigorously cleaned in the laboratory, by rinsing several times in distilled water to remove sediments and then quickly dried with blot paper and stored at -80 °C until use. *H. lupulus* trub was kindly provided by "Severino Garlatti Costa" brewery as a by-product of beer production: after whirlpool and cooling the protein-tannin-hop residue (often termed as hot trub) precipitated from the hopped wort tub is obtained, a portion of which was used for this survey. Extracts were prepared via hydroalcoholic maceration (50% ethanol, ratio 1:10) overnight in agitation and darkness at room temperature. After centrifugation at 28 000 × g for 10 min, the supernatant fraction was collected, filtered and lyophilized with Christ Epsilon 2-4 LSCplus-Del Tek. After lyophilization, all the extracts (hereafter *Ailanthus, Humulus* trub, *Olea* and *Ulva*) were suspended in 100% ethanol to a concentration of 0.25-0.3 g mL^{-1} (dry weight basis), filtered with 50 μm nylon gauze to discard solid precipitate and stored at -20 °C until use. For antifungal activity assay, two or more independently prepared batches of the extracts were used.

Antifungal assays

A. flavus (AF11999 from "Servizio fitosanitario e chimico, ricerca, sperimentazione e assistenza tecnica" of the Regional Agency for Rural Development, Friuli Venezia Giulia Region) inhibition was assessed using the agar well diffusion method (Sadallah et al., 2025). The fungal isolate was grown on potato dextrose agar (PDA, 39 g/L) (Oxoid, UK) and incubated at 25 °C for 7 days (12 h light/12 h dark photoperiod). Spores were harvested by scraping the agar plate and suspended on sterile water containing Tween80 (0.05%). To confirm the reproducibility of the antifungal activity, the assay was performed using multiple, independent batches of the extract (i.e., at least two or three separate extraction runs). Fungal pathogen suspension was infused on PDA medium (50 mL per square plate, 10 cm × 10 cm) reaching a final concentration of 1×10^5 conidia mL^{-1}. Sixteen equidistant holes per plate (8 mm, Ø) were punched aseptically with a sterile tip and 50 µL of different water-diluted concentrations of each bio-extract were added into four wells on the same line. The baseline concentration ranged from 0-170 g L^{-1}. A control plate with the same solvent:water concentration was run in parallel. Plates were incubated at 25 °C for 4 days. Inhibition was calculated as the ratio between the halo area (mm^2) devoid of fungal mycelium and the potential diffusion space (total area of imaginary circles centred on each hole) (Figure S1). Images of Petri dishes were acquired by a digital camera (Panasonic Lumix GH5) and evaluated by ImageJ Fiji software. The sample unit consisted of one plate per extract (4 holes per concentration) and the experiment was repeated at least twice. Conidial germination was monitored in malt extract broth (MEB) in multiwell microplate with *Ulva* extract doses ranging from 1.4 to 14.0 mg mL^{-1}. Each well was adjusted to the final concentration of $1x10^5$ conidia mL^{-1} and incubated in continuous agitation (150 rpm) in the dark at 28 °C for up to 24 h. Controls consisted of MEB and ethanol without extract. The onset of spore germination was monitored carefully by optical microscope by evaluating germ tube germination. Conidia were considered germinated when the germ tube was two times longer than the conidial diameter. The percentage of germination and germ tube length were determined after 16 h of incubation by acquiring photographs with a digital camera and analysing images with ImageJ Fiji software. The sample unit was composed of 6 wells for each condition. Conidia germination and germ tube elongation (µm) were determined on a number of conidia ranging from 40 to 90 per treatment (3 replicates with at least 13 conidia each). The assay was repeated twice.

Chemical analyses

Phenolic compounds were characterized by modified UHPLC-MS, adapted from Vrhovsek et al. (2012) and described in Filippi et al., (2021). LOD and LOQ values were established for each compound, with LOD calculated as one-third of LOQ. Prior to analysis, the extract was filtered using a 0.2 µm PTFE filter. Chromatography was performed on a Waters Acquity UPLC system equipped with an HSS T3 column, while mass spectrometry detection was carried out using a Waters Xevo

triple-quadrupole mass spectrometer with an ESI source. Compound identification and quantification were based on reference standards, retention times, and characteristic ion patterns. Results were expressed as $\mu g\ g^{-1}$ of dry weight of extract, and data processing was performed using Waters MassLynx software.

Uronic acids in *Ulva* extract were measured according to the colorimetric method described by Connan (2015), based on the reaction of anthrone with both neutral and uronic acid sugars with double absorbance reading at 560 and 620 nm, using glucose and glucuronic acid as standard, respectively. Total sulfate content was analysed by the turbidimetric method using the barium chloride-gelatin reagent, following the protocol described by Torres et al., (2021). The content of uronic and sulfate acids was expressed as percentage in dry mass of the extract.

Statistical analysis

All statistical analyses were performed using R (v4.2.2) and RStudio (v2024.12.0). The antifungal activity of the extracts was visualized by fitting a dose–response logistic model for each extract separately using "drda" package (R core, 2024). For each dose-response logistic model four parameters were calculated: α is the value of the function when $x \to -\infty$, δ is the height of the curve, ε is the steepness (growth rate) of the curve, φ is the x value at which 50% of the maximum δ is reached (EC_{50}). To investigate whether the extracts had different effects on fungal growth, a dose-response logistic model was fitted for each replicate separately and ANOVA analyses were performed on the four parameters describing the curves. The ANOVA assumptions were verified using the diagnostic plots of the model residuals. A Tukey's Honest Significant Difference (HSD) post hoc analysis was performed to test for significant differences among the selected parameters. A Principal Component Analysis (PCA) was performed on a centred and scaled matrix containing the concentration of polyphenolic compounds present in each extract. PCA was performed using base R function "prcomp".

To test the effect of different concentrations of *Ulva* on conidial germination and on germ tube length, ANOVA analyses were performed. The ANOVA assumptions were verified using the diagnostic plots of the model residuals. A Tukey's Honest Significant Difference (HSD) post hoc analysis was performed to identify which concentrations had significantly different effects from the others.

Results

Antifungal activity of extracts against *A. flavus*

After three days of incubation, *Ulva*, *Ailanthus*, and *Humulus* trub showed dose-dependent mycelial inhibition, showing a clear circular halo, where a larger halo area is directly proportional to greater potency of the extract (Figure S2). Conversely, in the negative control (where only the solvent/water

was applied), no such clear zone was evident, confirming that the fungal mycelium grew uniformly up to the edge of the well. To compare the *in vitro* efficacy of the three extracts, dose-response curves were built as shown in Figure 1. ANOVA analysis revealed three of the four logistic parameters of the dose-response curves were significantly different among extracts ($p < 0.001$) (Supplemental Table S2). *Ulva* and *Ailanthus* reached maximal inhibition levels above 90% ($\delta = 91.3 \pm 4\%$ and $94.8 \pm 0.9\%$, respectively), quite higher compared to that found for *Humulus* trub ($52.9 \pm 2.5\%$) (Figure 2). However, *Ulva* was 10-times more effective than *Ailanthus* and *Humulus* trub: *Ulva*'s EC_{50} was significantly lower than *Ailanthus* or *Humulus* trub ($\varphi = 14.2 \pm 0.4$ *vs.* 140.7 ± 1.1 or 113.7 ± 4.2 mg mL^{-1}, respectively). The lower limit α, explaining the minimal inhibition resulting from each dose-response curve fitting, was also significantly lower in both *Ulva* and *Humulus* trub extracts than *Ailanthus* (0.5 ± 1.9 and 2.4 ± 1.2 *vs.* 7.0 ± 0.8). The fourth parameter, the slope of the curve (η), was found to be not significantly different.

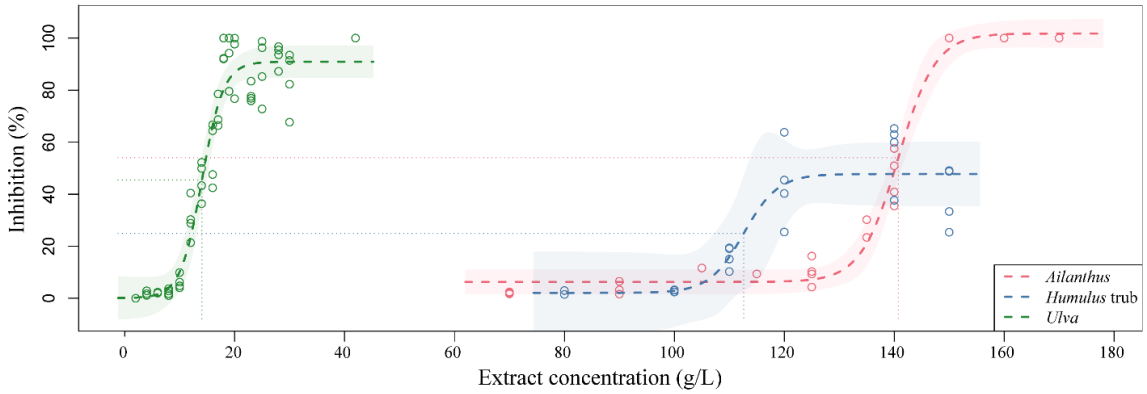


Figure 1 *In vitro* dose-response curves displaying the antifungal activity of the three most efficient extracts; each extract of *Ailanthus*, *Humulus* trub and *Ulva* was serially diluted in sterile water and evaluated by well diffusion testing and each dose-response curve was calculated using a 4-parameter logistic fit function. The full model was represented by the formula $y = \alpha + \delta / (1 + \eta * \exp(-e * (x - \varphi)))^{\wedge} (1 / \eta)$, where α = lower limit, δ = upper limit, η = slope of the curve, $\varphi = EC_{50}$, eventually simplified according to the Akaike Information Criterion. At least three different replicates of data for each concentration were used.

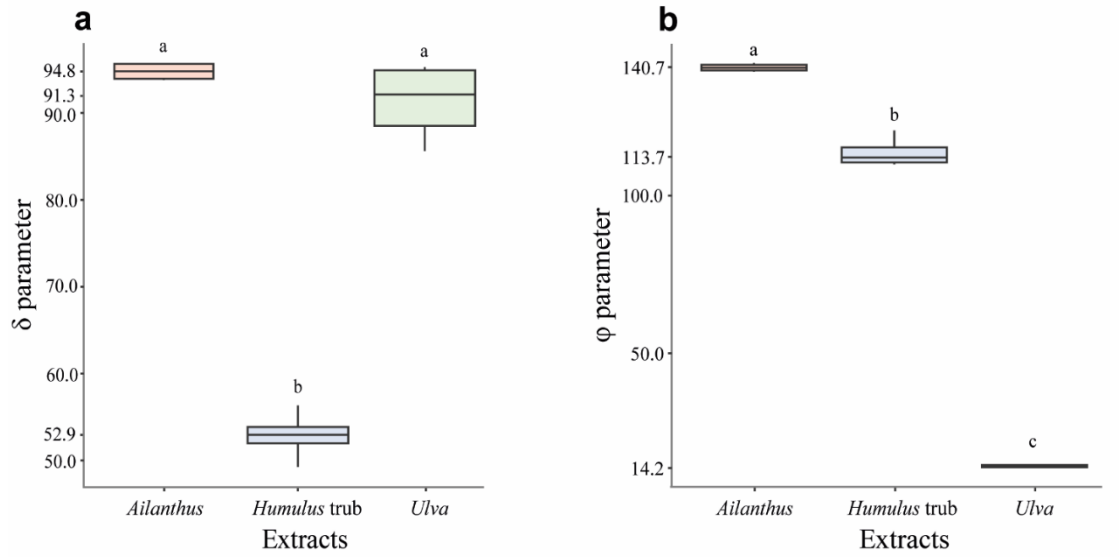


Figure 2 Boxplots of one-way ANOVA analysis for extract effect on logistic parameters of antifungal activity dose-response curve; a δ = upper limit; b φ = EC_{50}. The actual values of δ were 91.3±4 (*Ulva*), 94.8±0.9 (*Ailanthus*), and 52.9±2.5 % (*Humulus* trub), whereas for φ 14.2±0.4 (*Ulva*), 140.7±1.1 (*Ailanthus*) and 113.7±4.2 mg mL^{-1} (*Humulus* trub). Different letters denote a statistically significant difference ($p < 0.01$) between extracts. Vertical lines correspond to minimum and maximum values, coloured boxes are delimitated by first and third quartiles, horizontal line inside the boxes represents the median. The lower limit (α) and the slope of the curve (η) are not shown; η was found to be not significantly different among the three extracts.

Polyphenol profile in plant and seaweed extracts

To understand if the antifungal inhibition differences of the extracts could be associated with specific biochemical composition, we investigated their polyphenolic profile, given their well-known potential antioxidant and antimicrobial actions. Polyphenolic characterization and relative content (Table 1 and Figure S3) of the three extracts quantified 35 different phenolic compounds, the classes of glycosylated flavonoids (quercetin and kaempferol glycosides) and hydroxycinnamic acids being the most abundant. The extracts had compositions that differed in the total amount of polyphenols: *Ailanthus* yielded the highest concentration (8620±230 μg g^{-1} DW), 300 times higher than *Ulva* (26±1 μg g^{-1} DW). An intermediate value of 785±63 μg g^{-1} DW was found in *Humulus* trub. *Ailanthus* and *Humulus* trub were also characterized by a higher biochemical diversity, including at least seven different classes of polyphenols, whereas *Ulva* had only hydroxycinnamic and hydroxybenzoic acids and flavonols. In detail, *Ailanthus* is enriched in glycosylated and substituted flavonols (quercetin, kaempferol and rutin), which accounted for 55% of the total (4758 μg g^{-1} DW), with quercetin glucosides being the most abundant flavonols (2589±56 and 1443±39 μg g^{-1} DW for quercetin-3-glucoside + quercetin-3-galactoside and kaempferol-3-glucoside, respectively). *Ailanthus* was also characterized by a high amount of hydroxycinnamic acids (2498 μg g^{-1} DW in total, e.g. 29% of total

polyphenols), mostly represented by chlorogenic acids, particularly neochlorogenic acid (1861±24 μg g^{-1} DW) and hydroxybenzoic acids (851 μg g^{-1} DW in total, e.g. 10% of total polyphenols). The extract contained unique compounds, compared with *Humulus* trub and *Ulva*, such as hydrolysable tannin ellagic acid (744±52 μg g^{-1} DW, 8.63%) and lower quantities of chalcones, coumarins and hydroxyflavones like apigenin. Arbutin and sinapyl alcohol (321±5 μg g^{-1} DW, 4%) were also identified. In *Humulus* trub, two hydroxycinnamoyl alcohols (407 μg g^{-1} DW) and several proanthocyanidins (flavan-3-ols) (169 μg g^{-1} DW) represented the most abundant polyphenolic classes, accounting for 52 and 21% of the total amount, respectively. As in *Ailanthus*, flavonol glucosides were well-represented (18%), reaching quercetin and kaempferol glucosides (61±4 and 68±4 μg g^{-1} DW, respectively). Among the hydroxycinnamic acids, ferulic acid was the most represented at 21±2 μg g^{-1} DW accounting for 4.9% of the total polyphenols. In addition, the extract also contains arbutin and, to a less extent, hydroxybenzoic acids such as vanillin and vanillic acid. Interestingly, *Ulva* contained the lowest total amount of polyphenols and did not show unique classes. Indeed, flavonols, hydroxybenzoic and hydroxycinnamic acids were shared by all three extracts. However, in *Ulva* the relative contributions of these compounds were different, since hydroxycinnamic acids accounted for most of the total polyphenols (24 μg g^{-1} DW, 92% of the total) and were particularly rich in rosmarinic acid and, at a lower extent, in caffeic acid. Other well represented polyphenols were *p*-hydroxybenzoic acid and vanillin in the class of hydroxybenzoic acids (1.34 μg g^{-1} DW, 5% of the total), and flavanol glucosides (e.g., quercetin-3-substituted, kaempferol-3-glucoside and rutin), whose total amount reached 3% of the polyphenolic fraction. Notably, among hydroxybenzoic acids, the amount of *p*-hydroxybenzoic acid in *Ulva* was 6- and 14-fold higher than those of *Humulus* trub and *Ailanthus*, respectively.

Compound	***Ailanthus* (μg g^{-1} DW)**	***Humulus trub* (μg g^{-1} DW)**	***Ulva* (μg g^{-1} DW)**	***Antifungal activity***
Hydroxybenzoic acids				(El-Bilawy et al., 2022); (Huo et al., 2023)
p-hydroxybenzoic acid	0.057 ± 0.003	0.144 ± 0.034	0.795 ± 0.170	
vanillin	0.046 ± 0.004	3.934 ± 0.050	0.544 ± 0.089	(Kim et al., 2006); (Q. Li et al., 2022); (Ríos-López et al., 2024)
vanillic acid	0.099 ± 0.005	3.188 ± 0.108	n.d.	(Kim et al., 2006); (Palumbo et al., 2007)
gallic acid	107.082 ± 8.144	n.d.	n.d.	(Palumbo et al., 2007)
ellagic acid	744.156 ± 52.386	n.d.	n.d.	
Coumarins				
daphnetin	6.099 ± 0.506	n.d.	n.d.	

esculin	17.186 ± 0.405	n.d.	n.d.	
Hydroxycinnamic acids				
p-coumaric acid	1.244 ± 0.323	6.940 ± 0.772	n.d.	(Kim et al., 2006)
caffeic acid	4.750 ± 0.214	0.376 ± 0.036	0.113 ± 0.027	(Palumbo et al., 2007); (Y. Guo et al., 2024)
ferulic acid	n.d.	20.511 ± 1. 815	n.d.	(H. Yan et al., 2023)
neochlorogenic acid	1860.807 ± 24.497	4.192 ± 1.199	n.d.	
cryptochlorogenic acid	32.293 ± 2.997	2.413 ± 0.647	n.d.	
chlorogenic acid	598.738 ± 18.701	4.104 ± 0.079	n.d.	(Palumbo et al., 2007)
rosmarinic acid	n.d.	n.d.	24.022 ± 0.255	(Chernapalli et al., 2024); (Y. Xu et al., 2023)
Hydroxycinnamyl alcohols				
coniferyl alcohol	n.d.	6.436 ± 0.789	n.d.	(Ninkuu et al., 2023)
sinapyl alcohol	321.645 ± 4.867	400.606 ± 23.360	n.d.	
Chalcones				
phlorizin	35.729 ± 2.664	n.d.	n.d.	
Flavones				
apigenin	0.148 ± 0.054	n.d.	n.d.	(Castano-Duque et al., 2024)
luteolin	0.803 ± 0.140	n.d.	n.d.	(Castano-Duque et al., 2024)
luteolin-7-O-Glc	0.270 ± 0.088	n.d.	n.d.	
apigenin-7-glc	3.699 ± 0.233	n.d.	n.d.	
Flavan-3-ols				
catechin	n.d.	12.121 ± 0.892	n.d.	(Palumbo et al., 2007); (Cadenillas et al., 2024)
epicatechin	n.d.	4.231 ± 1.159	n.d.	(Cadenillas et al., 2024)
procyanidin B1	n.d.	77.187 ± 14.573	n.d.	
procyanidin B2 + B4	n.d.	7.311 ± 0.233	n.d.	
procyanidin B3	n.d.	67.763 ± 14.891	n.d.	
Flavonols				
kaempferol	40.068 ± 0.394	1.230 ± 0.391	n.d.	(Sadeghi et al., 2024)
quercetin	89.590 ± 3.222	1.786 ± 0.313	n.d.	(X.-M. Li et al., 2019); (Castano-Duque et al., 2024)
quercetin-3-Rha	80.484 ± 1.947	n.d.	n.d.	
kaempferol-3-Glc	1442.518 ± 38.694	61.174 ± 3.844	0.371 ± 0.049	
quercetin-3-Glc+ quercetin-3-Gal	2588.968 ± 55.716	68.452 ± 4.318	0.316 ± 0.111	
quercetin-3-Glc acetyl	1.323 ± 0.301	0.230 ± 0.226	n.d.	
kaempferol-3-rutinoside	90.314 ± 3.598	3.642 ± 0.392	n.d.	
rutin	425.061 ± 11.807	7.820 ± 0.859	0.178 ± 0.038	(Oliveira et al., 2016); (Sadeghi et al., 2024)

Hydroquinone glycosides			
arbutin	127.147 ± 26.187	19.539 ± 2.699	n.d.

Table 1 Polyphenolic profile and relative content of *Ailanthus*, *Humulus* trub and *Ulva* hydroalcoholic extracts by HPLC-MS analysis. Values are means ± SD of triplicate analysis. n.d., not detectable.

Polyphenol PCA analysis

The PCA of the polyphenolic composition (Figure 3) effectively distinguished across the three extracts (*Ailanthus*, *Humulus* trub and *Ulva*). PC1 described 71.9% of the total variance, and PC2 accounted for the remaining 26.6%. PC1 strongly separated the 3 replicates of *Ailanthus* from the others, mainly driven by quercetin-3-Glc, neochlorogenic acid, rutin, arbutin, ellagic acid and kaempferol, which are highly correlated among them and account for most of the total variance. PC2 distinguished between *Humulus* trub and *Ulva*, with the latter characterized only by rosmarinic acid and *p*- hydroxybenzoic acid. For this reason, *Ulva* being the most effective one as demonstrated in the previous paragraph, we further investigated the antifungal capacity of those 2 polyphenols.

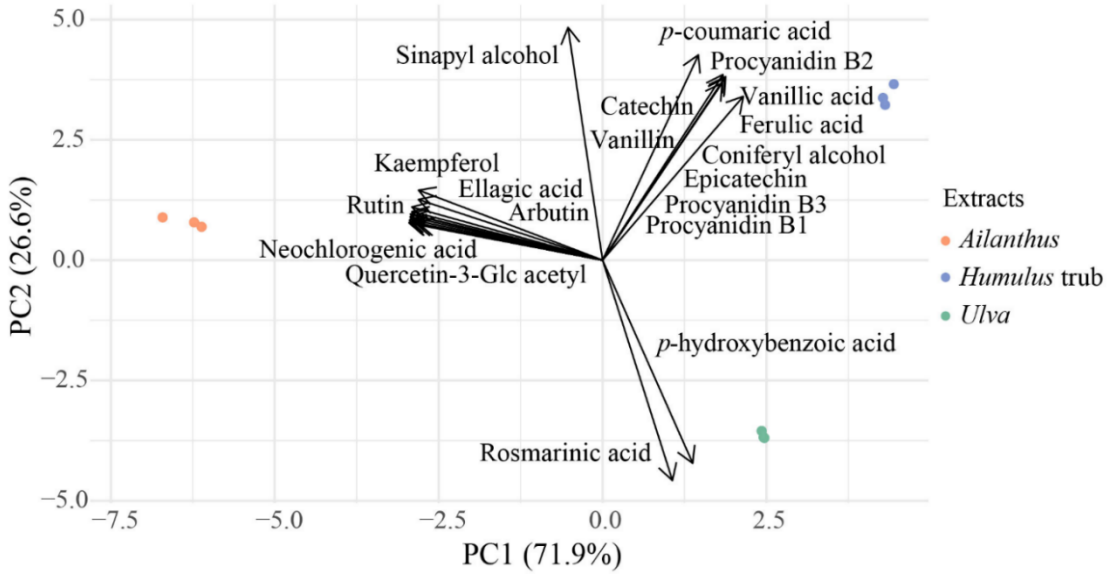


Figure 3 Principal Component Analysis (PCA) of the polyphenolic composition in *Ailanthus*, *Humulus* trub and *Ulva*.

Uronic and sulfate acid content in *Ulva* extract

The *Ulva* extract was further characterized by its relative content of uronic and sulfate acids through spectrophotometric assays. These assays revealed that the extract contained 24±16% to 35±23% of uronic acids (based on dry mass) across autumn to spring samples, and 32±1% of total sulfate (data not shown).

Antifungal activity of *Ulva* extract on *A. flavus* conidial germination

Ulva was the only extract tested in the conidial germination assay because it showed the best efficacy against fungal growth in the antifungal activity assay. We examined the germination rate of *A. flavus* under bright-field microscope in the presence of three different aqueous dilutions of Ulva extract, corresponding respectively to EC_{50}, 1/2 EC_{50}, and 1/10 EC_{50} concentrations (14.0, 7.0 and 1.4 mg mL^{-1}). Conidial germination of *A. flavus* initiated after 10 h, reaching 97.0±2.3% germination at 16 h in control samples. *Ulva* significantly reduced the percentage of germinated spores in a concentration-dependent manner ($p < 0.001$) (Supplemental Table S3 and Figure 4). Lower doses of 1.4 and 7 mg mL^{-1} of *Ulva* decreased conidial germination rate to 66 and 19%, respectively. Where germ tubes were measurable, tube length was significantly decreased (50% and 66% compared to the control for 1.4 and 7.0 mg mL^{-1}, respectively). Incubation with 14.0 mg mL^{-1} extract caused a complete inhibition of conidial germination.

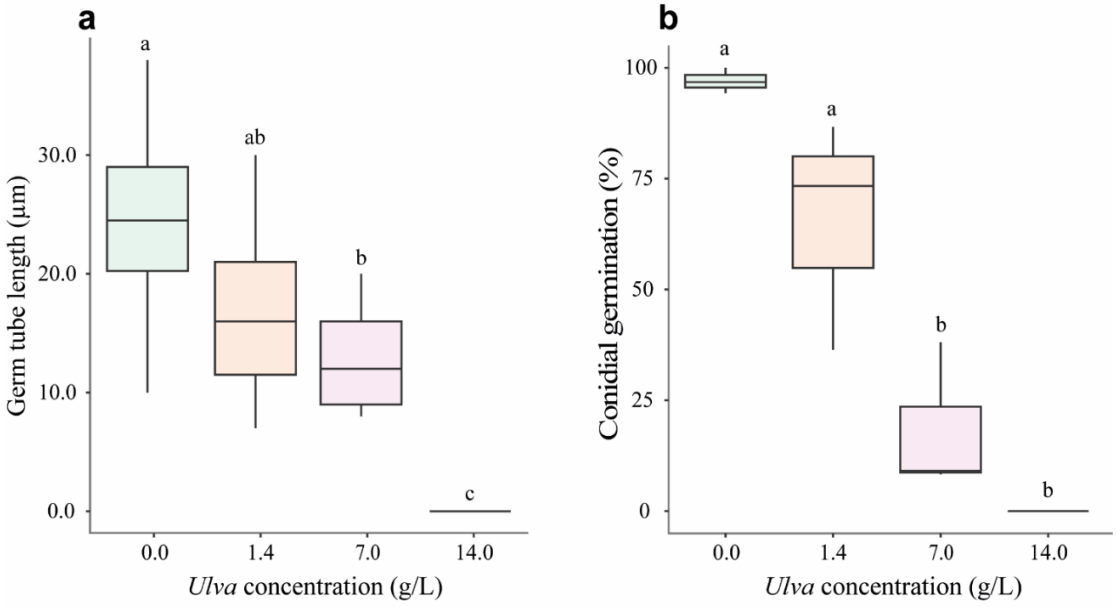


Figure 4 Effect of *Ulva* extract on *A. flavus* conidial germination. Inhibition effect of different concentrations of *Ulva* (a) on germ tube length (µm) and (b) on conidial germination (%) of *A. flavus* after 16 h of incubation at 28 °C. Values are mean ± SD. Different letters denote a statistically significant difference ($p < 0.01$) between concentrations.

Discussion

The contamination of maize by toxigenic fungi remains a critical threat to food safety, necessitating sustainable alternatives to synthetic pesticides (Giorni et al., 2023; Scaglioni et al., 2018). While many plant-based extracts demonstrate antifungal potential (Lagogianni & Tsitsigiannis, 2019; Matrose et

al., 2021; Montibus et al., 2021; Tian et al., 2023), this study specifically highlights the comparative value of spent biomass and seaweed as promising sources of polyphenols. All the extracts used, preliminarily screened for their inhibitory effect against *A. flavus*, were previously reported in literature as active against different fungal species (Bartmańska et al., 2018; Bilel et al., 2023; Kozuharova et al., 2022; Y. Li et al., 2021; Taillis et al., 2023). However, *Olea* extract was found to be ineffective against *A. flavus* at all the investigated doses. The lack of efficacy in *Olea* extract likely stems from the extraction method and solvent polarity, which may not have captured the bioactive compounds typically associated with its antifungal properties (Bilel et al., 2023). *Humulus* trub was the least effective against *A. flavus,* even though abundant in polyphenolic compounds. Nonetheless, the extract affected – though at high concentrations – the fungal growth, similarly to what reported by others (Bartmańska et al., 2018; Giorni et al., 2023). The use of spent biomasses, such as *Humulus* trub (a brewing industry by-product), is strategically important as these materials are recognized sources for developing high-added-value ingredients and products, with polyphenols and bitter acids standing out among their bioactive compounds (Silva et al., 2023). In this context, although *Humulus* trub showed a moderate effect in our screening, its polyphenolic profile was notable, containing compounds with known antifungal potential (H. Yan et al., 2023), specifically, ferulic acid, hydroxycinnamyl alcohols, *p*-hydroxybenzoic acid, and vanillin. Furthermore, the presence of flavonoids, particularly catechins and quercetin derivatives, contributes to the extract's chemical complexity. These compounds, especially the flavonoid derivatives, are well-documented for their broad biological activities, including membrane disruption and enzyme inhibition in fungal species, which provides a plausible explanation for the observed, albeit moderate, fungistatic activity at higher concentrations (Cadenillas et al., 2024; Castano-Duque et al., 2024; X.-M. Li et al., 2019; Palumbo et al., 2007; Ponts et al., 2011; H. Yan et al., 2023). *Ailanthus altissima* demonstrated higher chemical diversity than other extracts, featuring a wide array of flavonols and hydroxycinnamic acids. Recently, methanolic extracts from *Ailanthus* leaves were found to be rich in flavones and flavonols, and caffeic and chlorogenic acids (Cocîrlea et al., 2024; Poljuha et al., 2017). While these polyphenols are known to complex with microbial proteins, disrupt cell membranes, and interfere with enzyme function, the extract's bioactivity likely results from a synergistic effect between phenolics and other metabolites such as lipophilic triterpenoids or saponins (S.-S. Guo et al., 2023). *A. altissima* has turned to be one of the most aggressive alien species in Europe for which its harvesting as a low-cost raw material for natural pesticide production could also be a rewarding strategy in reducing its populations and impacts on local biodiversity (Kozuharova et al., 2022). However, in our study, *Ailanthus* extract exerted some fungistatic activity at higher concentrations compared to *Ulva*.

The *Ulva* extract demonstrated the highest efficacy, characterized by the unique presence of rosmarinic acid and a high concentration of *p*-hydroxybenzoic acid. Rosmarinic acid is a natural caffeic acid ester known as a defence molecule against pathogens and herbivores and a UV protectant

in diverse terrestrial plant (Coiai et al., 2021). Interestingly, Chernapalli et al., (2024) stated that purified rosmarinic acid significantly affected mycotoxigenic fungi, in addition to airborne filamentous fungi (Y. Xu et al., 2023). Further *in silico* investigations of antifungal activity of rosmarinic acid by molecular docking studies evidenced that it inhibited different fungal target proteins involved in fungal carbon metabolism and infection process (Althobaiti, 2024; Chernapalli et al., 2024; Moin et al., 2024; Y. Xu et al., 2023). These reports proved this phenolic acid to be a promising candidate in inhibiting fungal growth and suggested some plausible mechanisms involved. Nonetheless, besides our study, only a few chemical profiling studies identified rosmarinic acid in marine algal extracts and green alga *Ulva fasciata* (Ghallab et al., 2022) or its possible involvement in *in vitro* inhibition of pathogenic fungi (Pourakbar et al., 2021). On the contrary, *p*-hydroxybenzoic acid in algal extracts has been recently documented as the highest phenolic compound in *U. fasciata* extract with antifungal effects (El-Bilawy et al., 2022). Interestingly, this phenolic acid has recently been shown to exhibit *in vivo* preventive and curative action at millimolar concentration as elicitor against kiwifruit rot caused by *A. flavus* (Huo et al., 2023). According to literature, cinnamic- and benzoic-derived phenolic compounds could act as natural host defences against *Fusarium* and *Aspergillus* spp., since their content was found to be higher in resistant maize genotypes reacting to silk infection than their non-resistant counterparts (Lorán et al., 2022; Thompson & Raizada, 2018). Accordingly, the lower amount of *p*-hydroxybenzoic acid per dry weight found in *Ailanthus* and *Humulus* trub extracts with respect to *Ulva* (being 6 and 14 times lower, respectively) could be consistent with the lower EC_{50} values. Moreover, even though not specifically present only in *Ulva* extract, also vanillin, caffeic acid, flavonols derivatives and rutin may have acted synergistically with the dominant polyphenols contributing to the high efficacy of the extract, by interfering with cell wall and membrane structure or ergosterol biosynthesis (Castano-Duque et al., 2024; Y. Guo et al., 2024; Kim et al., 2006; Q. Li et al., 2022; X.-M. Li et al., 2019; Ríos-López et al., 2024). Besides that, it is noteworthy that other studies emphasized that bioactive compounds are generally more effective in whole extract, acting synergistically or additively, rather than as single compounds, and that minor components are critical for their maximal antifungal activities (Ljunggren et al., 2020; Loi et al., 2020; Pinto et al., 2013). In addition, Scaglioni et al., (2019) demonstrated that antioxidants, such as carotenoids, present in the complex mixture of a natural extract, can interact with polyphenols, thereby influencing the overall antifungal effects that cannot be definitively determined from data on individual compounds alone. The exceptional efficacy of the *Ulva* extract, however, suggests the involvement of other potent non-phenolic metabolites in addition to the polyphenols. Accordingly, using a green and safe extraction method (hydroalcoholic solvent and room temperature during maceration) optimized for polyphenols, we also specifically tested for the presence of uronic and sulfated acid groups, characteristic of ulvan polysaccharides, given the potential of these sulfated biopolymers to contribute significantly to the overall antifungal action. Ulvans have gained great attention recently as emerging biopolymers easily

extractable from algal biomass using hot water and subsequent ethanol precipitation (Coiai et al., 2021), exhibiting a broad spectrum of biological and antioxidant activities (Kraithong et al., 2024). Recent scientific studies in agriculture have explored the potential of seaweed ulvans as active substances for their well-known ability to induce plant resistance against fungal diseases (Bahmani et al., 2023; Poveda & Díez-Méndez, 2023) and *in vivo* protection in wheat (de Borba et al., 2021) and grapevine (Shomron et al., 2022; Zarraonaindia et al., 2023b). Indeed, treatments with ulvans extracted from *U. lactuca* showed several antifungal actions against pathogenic fungi (Ben Salah et al., 2018; El Fayoumy et al., 2022; Salim et al., 2020). However, other studies did not confirm the direct involvement of ulvans in the antifungal processes (Araújo et al., 2008; de Borba et al., 2021; Paulert et al., 2009; Reis et al., 2018). The presence of the sulfate group is an essential factor for the antimicrobial and antifungal activities of algal polysaccharides, as it is correlated with antioxidant action (Massocato et al., 2024). Discussions on biological activity of these compounds relate their antifungal action to the sulfated polysaccharides' interaction with the mycelium surface, leading to binding with membrane receptors and alterations in plasmalemma permeability (Sruthy & Baiju, 2024). The protective action *in vivo* is instead attributed to the stimulation of the plant defences (pathogen-related, scavenger proteins, and the oxylipin pathway) rather than a direct antifungal effect (Paulert et al., 2009). The explanation for this duality of effects *in vivo* and *in vitro* may lie in the multitude of structures and compositions that sulfated polymers of algal origin exhibit (M. Li et al., 2023). Given the superior antifungal efficacy of the *Ulva* treatment, this bio-extract demonstrates significant potential for future *in vivo* and field-scale applications directed at the biocontrol of maize and the mitigation of mycotoxin contamination. Consequently, further research is still necessary to fully understand ulvans and *Ulva* bioextract mechanisms and effectiveness.

Conclusions

In conclusion, we have proven that *Ulva* natural bio-extract exhibited a significantly higher *in vitro* antifungal efficacy against *A. flavus* compared to other polyphenol-rich extracts from processing waste or environmental collected biomass. The unique composition of *Ulva* extract, including specific polyphenols and ulvan polysaccharides, could synergistically contribute to its higher effectiveness. Additionally, the well-established role of these compounds in stimulating plant defence responses or regulating hormonal pathways, also highlights their potential as bio-stimulants. This dual functionality could contribute to reducing fungal pathogens' growth by enhancing the plant defences. These findings pave the way for a deeper understanding of the underlying mechanisms and further investigation into their possible application for alternative management of fungal diseases in open-field conditions. Future work could therefore prioritize the controlled cultivation of these *Ulva* species to ensure a uniform biomass or establish a quality control metric based on key marker compounds to guarantee batch-to-batch consistency for the eventual standardization process.

In conclusion, the final observed antifungal efficacy across all three extracts (*Humulus* trub, *Ailanthus* and *Ulva*) should be considered not solely a function of the quantified phenolic compounds, but rather a composite result stemming from the synergistic action of diverse specialized metabolites. Future work is crucial to move beyond correlation and implement bioassay-guided fractionation to precisely dissect the quantitative contribution of these non-phenolic principles. Researchers must, however, consider that the isolation of pure active compounds is often challenging due to the potential chemical degradation during purification or the loss of synergistic effects from other minor components present in the original crude extract (Caesar & Cech, 2019; Méndez et al., 2021).

References

Ahmed, O. S., Tardif, C., Rouger, C., Atanasova, V., Richard-Forget, F., & Waffo-Téguo, P. (2022). Naturally occurring phenolic compounds as promising antimycotoxin agents: Where are we now? *Comprehensive Reviews in Food Science and Food Safety*, *21*(2), 1161–1197. https://doi.org/10.1111/1541-4337.12891

Althobaiti, F. (2024). *Fungicidal activity of rosmarinic acid against* Aspergillus fumigatus *and Aspergillus brevipes isolated from raw cow milk in western Saudi Arabia in sight of* in vitro *and* in silico *studies*. https://doi.org/10.5281/ZENODO.10634379

Araújo, L., Stadnik, M. J., Borsato, L. C., & Valdebenito-Sanhueza, R. M. (2008). Fosfito de potássio e ulvana no controle da mancha foliar da gala em macieira. *Tropical Plant Pathology*, *33*, 148–152. https://doi.org/10.1590/s1982-56762008000200009

Bahmani, R., More, P., Babarinde, S., Zhou, M., & Prithiviraj, B. (2023). Seaweeds for plant disease management: Current research advances and future perspectives. *Phytoparasitica*, *51*(4), 783–802. https://doi.org/10.1007/s12600-023-01074-x

Bartmańska, A., Walecka-Zacharska, E., Tronina, T., Popłoński, J., Sordon, S., Brzezowska, E., Bania, J., & Huszcza, E. (2018). Antimicrobial properties of spent hops extracts, flavonoids isolated therefrom, and their derivatives. *Molecules*, *23*(8), Article 8. https://doi.org/10.3390/molecules23082059

Battilani, P., Toscano, P., Van der Fels-Klerx, H. J., Moretti, A., Camardo Leggieri, M., Brera, C., Rortais, A., Goumperis, T., & Robinson, T. (2016). Aflatoxin B_1 contamination in maize in Europe increases due to climate change. *Scientific Reports*, *6*(1), 24328. https://doi.org/10.1038/srep24328

Ben Salah, I., Aghrouss, S., Douira, A., Aissam, S., El Alaoui-Talibi, Z., Filali-Maltouf, A., & El Modafar, C. (2018). Seaweed polysaccharides as bio-elicitors of natural defenses in olive trees against *Verticillium* wilt of olive. *Journal of Plant Interactions*, *13*(1), 248–255. https://doi.org/10.1080/17429145.2018.1471528

Bilel, H., Yahia, M., & Moustafa, S. M. N. (2023). An overview of chemical composition and fungicidal activity of Olive (*Olea Europea* L.) Leaf Extract. *Egyptian Journal of Chemistry*, *66*(1), 303–311. https://doi.org/10.21608/ejchem.2022.120206.5397

Cadenillas, L. F., Billerach, G., Hernandez, C., Durrieu, V., & Bailly, J.-D. (2024). Inhibition of aflatoxin B_1 production by procyanidins present in *Annona muricata* and *Uncaria tomentosa* aqueous extracts. *Toxins*, *16*(11), 454. https://doi.org/10.3390/toxins16110454

Caesar, L. K., & Cech, N. B. (2019). Synergy and antagonism in natural product extracts: When 1 + 1 does not equal 2. *Natural Product Reports*, *36*(6), 869–888. https://doi.org/10.1039/C9NP00011A

Castano-Duque, L., Lebar, M. D., Mack, B. M., Lohmar, J. M., & Carter-Wientjes, C. (2024). Investigating the impact of flavonoids on *Aspergillus flavus*: Insights into cell wall damage and biofilms. *Journal of Fungi*, *10*(9), 665. https://doi.org/10.3390/jof10090665

Chernapalli, V., Zahoor Gul, M., Anwar, H. M., Susmitha Kuruganti, N. S., & Rupula, K. (2024). Antifungal effects of rosmarinic acid, α-tocopherol and α-tocopherol acetate on /*Aspergillus parasiticus* (NRRL 2999) and *Candida albicans* (MTCC 183) and assessment of chitin and ergosterol biomarkers. *Advances in Biotechnology & Microbiology*, *18*(03). https://doi.org/10.19080/AIBM.2024.18.555987

Cocîrlea, M. D., Soare, A., Petrovici, A. R., Silion, M., Călin, T., & Oancea, S. (2024). Phenolic composition and bioactivities of invasive *Ailanthus altissima* (Mill.) swingle leaf extracts obtained by two-step sequential extraction. *Antioxidants*, *13*(7), 824. https://doi.org/10.3390/antiox13070824

Coiai, S., Campanella, B., Paulert, R., Cicogna, F., Bramanti, E., Lazzeri, A., Pistelli, L., & Coltelli, M.-B. (2021). Rosmarinic acid and ulvan from terrestrial and marine sources in anti-microbial bionanosystems and biomaterials. *Applied Sciences*, *11*(19), Article 19. https://doi.org/10.3390/app11199249

Connan, S. (2015). Spectrophotometric assays of major compounds extracted from algae. In D. B. Stengel & S. Connan (Eds.), *Natural Products From Marine Algae* (Vol. 1308, pp. 75–101). Springer New York. https://doi.org/10.1007/978-1-4939-2684-8_3

de Borba, M. C., Velho, A. C., Maia-Grondard, A., Baltenweck, R., Magnin-Robert, M., Randoux, B., Holvoet, M., Hilbert, J.-L., Flahaut, C., Reignault, P., Hugueney, P., Stadnik, M. J., & Siah, A. (2021). The algal polysaccharide ulvan induces resistance in wheat against *Zymoseptoria tritici* without major alteration of leaf metabolome. *Frontiers in Plant Science*, *12*, 1–14. https://doi.org/10.3389/fpls.2021.703712

El Fayoumy, R. A., El-Sheekh, M. M., & Abu Ahmed, S. E. (2022). Potential of ulvan polysaccharide from *Ulva lactuca* as antifungal against some foodborne fungi isolated from spoiled tomato

sauce cans. *Journal of Aquatic Food Product Technology*, *31*(7), 658–671. https://doi.org/10.1080/10498850.2022.2093149

El-Bilawy, E. H., Al-Mansori, A.-N. A., Alotibi, F. O., Al-Askar, A. A., Arishi, A. A., Teiba, I. I., Sabry, A. E.-N., Elsharkawy, M. M., Heflish, A. A., Behiry, S. I., & Abdelkhalek, A. (2022). Antiviral and antifungal of *Ulva fasciata* extract: HPLC analysis of polyphenolic compounds. *Sustainability*, *14*(19), 12799. https://doi.org/10.3390/su141912799

Ferrari, L., Rizzi, N., Grandi, E., Clerici, E., Tirloni, E., Stella, S., Bernardi, C. E. M., & Pinotti, L. (2023). Compliance between food and feed safety: Eight-year survey (2013–2021) of Aflatoxin M1 in raw milk and Aflatoxin B1 in feed in Northern Italy. *Toxins*, *15*(3), Article 3. https://doi.org/10.3390/toxins15030168

Filippi, A., Braidot, E., Petrussa, E., Fabro, M., Vuerich, M., & Boscutti, F. (2021). Plant growth shapes the effects of elevation on the content and variability of flavonoids in subalpine bilberry stands. *Plant Biology*, *23*(2), 241–249. https://doi.org/10.1111/plb.13194

Filippi, A., Petrussa, E., Boscutti, F., Vuerich, M., Vrhovsek, U., Rabiei, Z., & Braidot, E. (2019). Bioactive polyphenols modulate enzymes involved in grapevine pathogenesis and chitinase activity at increasing complexity levels. *International Journal of Molecular Sciences*, *20*(24). Scopus. https://doi.org/10.3390/ijms20246357

Ghallab, D. S., Shawky, E., Ibrahim, R. S., & Mohyeldin, M. M. (2022). Comprehensive metabolomics unveil the discriminatory metabolites of some Mediterranean Sea marine algae in relation to their cytotoxic activities. *Scientific Reports*, *12*(1), 8094. https://doi.org/10.1038/s41598-022-12265-7

Giorni, P., Bertuzzi, T., & Battilani, P. (2016). Aflatoxin in maize, a multifaceted answer of *Aspergillus flavus* governed by weather, host-plant and competitor fungi. *Journal of Cereal Science*, *70*, 256–262. https://doi.org/10.1016/j.jcs.2016.07.004

Giorni, P., Bulla, G., Leni, G., Soldano, M., Tacchini, M., Guerrini, A., Sacchetti, G., & Bertuzzi, T. (2023). Enhancement of agri-food by-products: Green extractions of bioactive molecules with fungicidal action against mycotoxigenic fungi and their mycotoxins. *Frontiers in Nutrition*, *10*. https://doi.org/10.3389/fnut.2023.1196812

Guo, S.-S., Duan, Z.-K., Huang, X.-X., & Song, S.-J. (2023). Phytochemical investigation on the leaves of *Ailanthus altissima* (Mill.) Swingle. *Biochemical Systematics and Ecology*, *110*, 104668. https://doi.org/10.1016/j.bse.2023.104668

Guo, Y., Li, C., Wang, M., Xu, H., Zhang, S., Liu, J., Jin, Y., & Ge, Y. (2024). Postharvest caffeic acid dipping enhances disease resistance and storage capacity of 'Zaosu' pear fruit via regulating phenylpropane metabolism. *Postharvest Biology and Technology*, *209*, 112716. https://doi.org/10.1016/j.postharvbio.2023.112716

Huo, Z.-Y., Shi, X.-C., Wang, Y.-X., Jiang, Y.-H., Zhu, G.-Y., Herrera-Balandrano, D. D., Wang, S.-Y., & Laborda, P. (2023). Antifungal and elicitor activities of *p*-hydroxybenzoic acid for the control of aflatoxigenic *Aspergillus flavus* in kiwifruit. *Food Research International*, *173*, 113331. https://doi.org/10.1016/j.foodres.2023.113331

Kim, J. H., Campbell, B. C., Mahoney, N., Chan, K. L., & May, G. S. (2006). Targeting antioxidative signal transduction and stress response system: Control of pathogenic *Aspergillus* with phenolics that inhibit mitochondrial function. *Journal of Applied Microbiology*, *101*(1), 181–189. https://doi.org/10.1111/j.1365-2672.2006.02882.x

Kozuharova, E., Pasdaran, A., Al Tawaha, A. R., Todorova, T., Naychov, Z., & Ionkova, I. (2022). Assessment of the potential of the invasive arboreal plant *Ailanthus altissima* (Simaroubaceae) as an economically prospective source of natural pesticides. *Diversity*, *14*(8), Article 8. https://doi.org/10.3390/d14080680

Kraithong, S., Bunyameen, N., Theppawong, A., Ke, X., Lee, S., Zhang, X., & Huang, R. (2024). Potentials of *Ulva* spp.-derived sulfated polysaccharides as gelling agents with promising therapeutic effects. *International Journal of Biological Macromolecules*, *273*, 132882. https://doi.org/10.1016/j.ijbiomac.2024.132882

Lagogianni, C. S., & Tsitsigiannis, D. I. (2019). Effective biopesticides and biostimulants to reduce aflatoxins in maize fields. *Frontiers in Microbiology*, *10*. https://doi.org/10.3389/fmicb.2019.02645

Leggieri, M. C., Toscano, P., & Battilani, P. (2021). Predicted Aflatoxin B_1 increase in Europe due to climate change: Actions and reactions at global level. *Toxins*, *13*(4), Article 4. https://doi.org/10.3390/toxins13040292

Li, M., Wang, M., Chen, J., Wu, J., & Xia, Z. (2023). Sulfur dioxide improves the thermotolerance of maize seedlings by regulating salicylic acid biosynthesis. *Ecotoxicology and Environmental Safety*, *254*, 114746. https://doi.org/10.1016/j.ecoenv.2023.114746

Li, Q., Zhao, Y., Zhu, X., & Xie, Y. (2022). Antifungal effect of *o*-vanillin on mitochondria of *Aspergillus flavus*: Ultrastructure and TCA cycle are destroyed. *International Journal of Food Science and Technology*, *57*(5), 3142–3149. https://doi.org/10.1111/ijfs.15647

Li, X.-M., Li, Z.-Y., Wang, Y.-D., Wang, J.-Q., & Yang, P.-L. (2019). Quercetin inhibits the proliferation and aflatoxins biosynthesis of *Aspergillus flavus*. *Toxins*, *11*(3), 154. https://doi.org/10.3390/toxins11030154

Li, Y., Zhao, M., & Zhang, Z. (2021). Quantitative proteomics reveals the antifungal effect of canthin-6-one isolated from *Ailanthus altissima* against *Fusarium oxysporum* f. Sp. *Cucumerinum in vitro*. *PLOS ONE*, *16*(4), e0250712. https://doi.org/10.1371/journal.pone.0250712

Ljunggren, J., Bylund, D., Jonsson, B. G., Edman, M., & Hedenström, E. (2020). Antifungal efficiency of individual compounds and evaluation of non-linear effects by recombining fractionated turpentine. *Microchemical Journal*, *153*, 104325. https://doi.org/10.1016/j.microc.2019.104325

Loi, M., Paciolla, C., Logrieco, A. F., & Mulè, G. (2020). Plant bioactive compounds in pre- and postharvest management for aflatoxins reduction. *Frontiers in Microbiology*, *11*, 1–16. https://doi.org/10.3389/fmicb.2020.00243

Lorán, S., Carramiñana, J. J., Juan, T., Ariño, A., & Herrera, M. (2022). Inhibition of *Aspergillus parasiticus* growth and aflatoxins production by natural essential oils and phenolic acids. *Toxins*, *14*(6), Article 6. https://doi.org/10.3390/toxins14060384

Makhuvele, R., Naidu, K., Gbashi, S., Thipe, V. C., Adebo, O. A., & Njobeh, P. B. (2020). The use of plant extracts and their phytochemicals for control of toxigenic fungi and mycotoxins. *Heliyon*, *6*(10), e05291. https://doi.org/10.1016/j.heliyon.2020.e05291

Massocato, T. F., Robles-Carnero, V., Rodrigues Moreira, B., Castro-Varela, P., Bonomi-Barufi, J., Abdala-Díaz, R., Rubi Rörig, L., & López Figueroa, F. D. (2024). Characterization and biological activities of the ulvan polysaccharide-rich fraction obtained from *Ulva rigida* and *Ulva pseudorotundata* and their potential for pharmaceutical application. *Marine Biotechnology*, *26*(2), 324–337. https://doi.org/10.1007/s10126-024-10299-8

Matrose, N. A., Obikeze, K., Belay, Z. A., & Caleb, O. J. (2021). Plant extracts and other natural compounds as alternatives for post-harvest management of fruit fungal pathogens: A review. *Food Bioscience*, *41*, 100840. https://doi.org/10.1016/j.fbio.2020.100840

Medina, Á., González-Jartín, J. M., & Sainz, M. J. (2017). Impact of global warming on mycotoxins. *Current Opinion in Food Science*, *18*, 76–81. https://doi.org/10.1016/j.cofs.2017.11.009

Méndez, D., Escalona-Arranz, J. C., Pérez, E. M., Foubert, K., Matheeussen, A., Tuenter, E., Cuypers, A., Cos, P., & Pieters, L. (2021). Antifungal activity of extracts, fractions, and constituents from *Coccoloba cowellii* leaves. *Pharmaceuticals*, *14*(9), 917. https://doi.org/10.3390/ph14090917

Moin, A. T., Robin, T. B., Patil, R. B., Rani, N. A., Prome, A. A., Sakif, T. I., Hossain, M., Chowdhury, D. U. S., Rashid, S. S., Mollah, A. K. M. M., Islam, S., Uddin, M. H., Khalequzzaman, M., Islam, T., & Islam, N. N. (2024). Antifungal plant flavonoids identified *in silico* with potential to control rice blast disease caused by *Magnaporthe oryzae*. *PLOS ONE*, *19*(4), e0301519. https://doi.org/10.1371/journal.pone.0301519

Molnár, K., Rácz, C., Dövényi-Nagy, T., Bakó, K., Pusztahelyi, T., Kovács, S., Adácsi, C., Pócsi, I., & Dobos, A. (2023). The effect of environmental factors on mould counts and afb1 toxin production by *Aspergillus flavus* in maize. *Toxins*, *15*(3), Article 3. https://doi.org/10.3390/toxins15030227

Montibus, M., Vitrac, X., Coma, V., Loron, A., Pinson-Gadais, L., Ferrer, N., Verdal-Bonnin, M.-N., Gabaston, J., Waffo-Téguo, P., Richard-Forget, F., & Atanasova, V. (2021). Screening of wood/forest and vine by-products as sources of new drugs for sustainable strategies to control *Fusarium graminearum* and the production of mycotoxins. *Molecules*, *26*(2), Article 2. https://doi.org/10.3390/molecules26020405

Ninkuu, V., Yan, J., Fu, Z., Yang, T., Ziemah, J., Ullrich, M. S., Kuhnert, N., & Zeng, H. (2023). Lignin and its pathway-associated phytoalexins modulate plant defense against fungi. *Journal of Fungi*, *9*(1), 52. https://doi.org/10.3390/jof9010052

Oliveira, V. M., Carraro, E., Auler, M. E., & Khalil, N. M. (2016). Quercetin and rutin as potential agents antifungal against *Cryptococcus* spp. *Brazilian Journal of Biology*, *76*, 1029–1034. https://doi.org/10.1590/1519-6984.07415

Palumbo, J. D., O'Keeffe, T. L., & Mahoney, N. E. (2007). Inhibition of ochratoxin A production and growth of *Aspergillus* species by phenolic antioxidant compounds. *Mycopathologia*, *164*(5), 241–248. https://doi.org/10.1007/s11046-007-9057-0

Paulert, R., Talamini, V., Cassolato, J. E. F., Duarte, M. E. R., Noseda, M. D., Smania, A., & Stadnik, M. J. (2009). Effects of sulfated polysaccharide and alcoholic extracts from green seaweed *Ulva fasciata* on anthracnose severity and growth of common bean (*Phaseolus vulgaris* L.). *Journal of Plant Diseases and Protection*, *116*(6), 263–270. https://doi.org/10.1007/BF03356321

Pinto, E., Hrimpeng, K., Lopes, G., Vaz, S., Gonçalves, M. J., Cavaleiro, C., & Salgueiro, L. (2013). Antifungal activity of *Ferulago capillaris* essential oil against *Candida*, *Cryptococcus*, *Aspergillus* and dermatophyte species. *European Journal of Clinical Microbiology & Infectious Diseases*, *32*(10), 1311–1320. https://doi.org/10.1007/s10096-013-1881-1

Poljuha, D., Sladonja, B., Šola, I., Dudaš, S., Bilić, J., Rusak, G., Motlhatlego, K. E., & Eloff, J. N. (2017). Phenolic composition of leaf extracts of *Ailanthus altissima* (Simaroubaceae) with antibacterial and antifungal activity equivalent to standard antibiotics. *Natural Product Communications*, *12*(10), 1934578X1701201021. https://doi.org/10.1177/1934578X1701201021

Ponts, N., Pinson-Gadais, L., Boutigny, A.-L., Barreau, C., & Richard-Forget, F. (2011). Cinnamic-derived acids significantly affect *Fusarium graminearum* growth and *in vitro* synthesis of type B trichothecenes. *Phytopathology®*, *101*(8), 929–934. https://doi.org/10.1094/PHYTO-09-10-0230

Pourakbar, L., Moghaddam, S. S., Enshasy, H. A. E., & Sayyed, R. Z. (2021). Antifungal activity of the extract of a macroalgae, *Gracilariopsis persica*, against four plant pathogenic fungi. *Plants*, *10*(9), Article 9. https://doi.org/10.3390/plants10091781

Poveda, J., & Díez-Méndez, A. (2023). Use of elicitors from macroalgae and microalgae in the management of pests and diseases in agriculture. *Phytoparasitica*, *51*(4), 667–701. https://doi.org/10.1007/s12600-022-01009-y

R core, T. (2024, June 14). *R: The R Project for Statistical Computing*. Https://Www.r-Project.Org/. https://www.r-project.org/

Reis, R. P., Carvalho Junior, A. A. de, Facchinei, A. P., Calheiros, A. C. dos S., & Castelar, B. (2018). Direct effects of ulvan and a flour produced from the green alga *Ulva fasciata* Delile on the fungus *Stemphylium solani* Weber. *Algal Research*, *30*, 23–27. https://doi.org/10.1016/j.algal.2017.12.007

Reverberi, M., Beccaccioli, M., & Zaccaria, M. (2021). The Role of Aflatoxins in Aspergillus flavus Resistance to Stress. *The Genus Aspergillus - Pathogenicity, Mycotoxin Production and Industrial Applications*. https://www.academia.edu/es/77039366/The_Role_of_Aflatoxins_in_Aspergillus_flavus_Resistance_to_Stress

Ríos-López, A. L., Dávila-Aviña, J., González, G. M., & Flores-Maldonado, O. (2024). Antifungal and antivirulence activity of vanillin and tannic acid against *Aspergillus fumigatus* and *Fusarium solani*. *Current Microbiology*, *81*(6), 156. https://doi.org/10.1007/s00284-024-03678-w

Sadallah, A., Aprea, E., Cignola, R., Caratti, A., Cordero, C., Angeli, A., Martens, S., & Di Francesco, A. (2025). Propolis hydroalcoholic extracts: Biochemical characterization and antifungal efficacy. *Horticulturae*, *11*(2), Article 2. https://doi.org/10.3390/horticulturae11020122

Sadeghi, A., Rajabiyan, A., Nabizade, N., Meygoli Nezhad, N., & Zarei-Ahmady, A. (2024). Seaweed-derived phenolic compounds as diverse bioactive molecules: A review on identification, application, extraction and purification strategies. *International Journal of Biological Macromolecules*, *266*, 131147. https://doi.org/10.1016/j.ijbiomac.2024.131147

Salim, D., Caro, P. D., Laboratoire de Chimie Agro-industrielle (LCA), Universite de Toulouse, INRA, Toulouse INP, ENSIACET, 4 allee Emile Monso, Toulouse (310 30), France, Merah, O., Universite Paul Sabatier, IUTA, Departement Genie Biologique, 24 rue d'Embaques 32000 Auch, France, Chbani, A., & Faculte de la Sante publique III, Universite Libanaise, Bohsas, Tripoli, Liban. (2020). Control of post-harvest citrus green mold using *Ulva lactuca* extracts as a source of active substances. *International Journal of Bio-Resource and Stress Management*, *11*(3), 287–296. https://doi.org/10.23910/1.2020.2107

Scaglioni, P. T., Blandino, M., Scarpino, V., Giordano, D., Testa, G., & Badiale-Furlong, E. (2018). Application of fungicides and microalgal phenolic extracts for the direct control of fumonisin contamination in maize. *Journal of Agricultural and Food Chemistry*, *66*(19), 4835–4841. https://doi.org/10.1021/acs.jafc.8b00540

Scaglioni, P. T., Pagnussatt, F. A., Lemos, A. C., Nicolli, C. P., Del Ponte, E. M., & Badiale-Furlong, E. (2019). Nannochloropsis sp. And *Spirulina* sp. As a source of antifungal compounds to mitigate contamination by *Fusarium graminearum* species complex. *Current Microbiology*, *76*(8), 930–938. https://doi.org/10.1007/s00284-019-01663-2

Shomron, A., Duanis-Assaf, D., Galsurker, O., Golberg, A., & Alkan, N. (2022). Extract from the macroalgae *Ulva rigida* induces table grapes resistance to *Botrytis cinerea*. *Foods*, *11*(5), Article 5. https://doi.org/10.3390/foods11050723

Silva, K. F. C. e, Strieder, M. M., Pinto, M. B. C., Rostagno, M. A., & Hubinger, M. D. (2023). Processing strategies for extraction and concentration of bitter acids and polyphenols from brewing by-products: A comprehensive review. *Processes*, *11*(3), 921. https://doi.org/10.3390/pr11030921

Sruthy, E. S., & Baiju, E. C. K. (2024). Exploration of secondary metabolites from green algae as antimicrobial agents: A comprehensive review. *Botanica Serbica*, *48*(2), 127–140. https://doi.org/10.2298/BOTSERB2402127S

Taillis, D., Becissa, O., Pébarthé-Courrouilh, A., Renouf, E., Palos-Pinto, A., Richard, T., & Cluzet, S. (2023). Antifungal activities of a grapevine byproduct extract enriched in complex stilbenes and stilbenes metabolization by *Botrytis cinerea*. *Journal of Agricultural and Food Chemistry*, *71*(11), 4488–4497. https://doi.org/10.1021/acs.jafc.2c07843

Thompson, M. E. H., & Raizada, M. N. (2018). Fungal pathogens of maize gaining free passage along the silk road. *Pathogens (Basel, Switzerland)*, *7*(4), 81. https://doi.org/10.3390/pathogens7040081

Tian, F., Woo, S. Y., Lee, S. Y., Park, S. B., Im, J. H., & Chun, H. S. (2023). Plant-based natural flavonoids show strong inhibition of aflatoxin production and related gene expressions correlated with chemical structure. *Food Microbiology*, *109*, 104141. https://doi.org/10.1016/j.fm.2022.104141

Torres, P. B., Nagai, A., Jara, C. E. P., Santos, J. P., Chow, F., & Santos, D. Y. A. C. D. (2021). Determination of sulfate in algal polysaccharide samples: A step-by-step protocol using microplate reader. *Ocean and Coastal Research*, *69*, e21021. https://doi.org/10.1590/2675-2824069.21-010pbt

Vrhovsek, U., Masuero, D., Gasperotti, M., Franceschi, P., Caputi, L., Viola, R., & Mattivi, F. (2012). A versatile targeted metabolomics method for the rapid quantification of multiple classes of phenolics in fruits and beverages. *Journal of Agricultural and Food Chemistry*, *60*(36), 8831–8840. https://doi.org/10.1021/jf2051569

Vuerich, M., Petrussa, E., Filippi, A., Cluzet, S., Fonayet, J. V., Sepulcri, A., Piani, B., Ermacora, P., & Braidot, E. (2023). Antifungal activity of chili pepper extract with potential for the control

of some major pathogens in grapevine. *Pest Management Science*, *79*(7), 2503–2516. https://doi.org/10.1002/ps.7435

Xu, Y., Guo, Y., Mao, H., Xiong, Z., Luo, M., Luo, R., Lu, S., Huang, L., & Hong, Y. (2023). Integration of transcriptomics and proteomics to elucidate inhibitory effect and mechanism of rosmarinic acid from *Perilla frutescens* (L.) Britt. In treating *Trichophyton mentagrophytes*. *Chinese Medicine*, *18*(1), 67. https://doi.org/10.1186/s13020-023-00772-2

Yan, H., Meng, X., Lin, X., Duan, N., Wang, Z., & Wu, S. (2023). Antifungal activity and inhibitory mechanisms of ferulic acid against the growth of *Fusarium graminearum*. *Food Bioscience*, *52*, 102414. https://doi.org/10.1016/j.fbio.2023.102414

Zarraonaindia, I., Cretazzo, E., Mena-Petite, A., Díez-Navajas, A. M., Pérez-López, U., Lacuesta, M., Pérez-Álvarez, E. P., Puertas, B., Fernandez-Diaz, C., Bertazzon, N., & Cantos-Villar, E. (2023a). Holistic understanding of the response of grapevines to foliar application of seaweed extracts. *Frontiers in Plant Science*, *14*. https://doi.org/10.3389/fpls.2023.1119854

Zarraonaindia, I., Cantos-Villar, E., Diez, A., Mena-Petite, A., Pérez-Álvarez, E., Cretazzo, E., Pébarthé-Courrouilh, A., Bertazzon, N., Lacuesta, M., Puertas, B., Pérez-López, U., Cluzet, S., Hachero-Cruzado, I., & Córdoba-Granados, J. (2023b). Seawines: Use of macroalgae as biostimulants against fungal diseases in grapevines. *BIO Web of Conferences*, *68*. https://doi.org/10.1051/bioconf/20236801005

Zingales, V., Taroncher, M., Martino, P. A., Ruiz, M.-J., & Caloni, F. (2022). Climate change and effects on molds and mycotoxins. *Toxins*, *14*(7), Article 7. https://doi.org/10.3390/toxins14070445

4.2. Supplementary Materials

Species	*Organ*	*Site*
Ailanthus altissima (Mill.) Swingle	Leaf	Lowland rural site Pagnacco (Udine) 46° 7' 30.63"N; 13° 11' 44.01"E
Humulus lupulus L.	Flowers (hops)	"Severino Garlatti Costa" brewery Flagogna (Udine) 46° 12' 18.890"N; 12° 57' 6.141"E
Olea europaea L., cv. Gargazzo	Leaf	Experimental farm "A. Servadei" University of Udine 46° 2' 3.79"N; 13° 13' 38.34"E
Ulva sp.	Thallus	Marano lagoon (Udine) 45° 42' 1.84"N; 13° 9' 3.35"E

Table S1 Collected material for hydroalcoholic extraction and Friuli Venezia Giulia Region site location.

Parameter	*Df*	*Sum Sq*	*F value*	*Pr(>F)*
a	2	88.153	18.92	**<0.001 *****
δ	2	4327.90	211.53	**<0.001 *****
φ	2	35533.00	2061.01	**<0.001 *****

Table S2 One-way ANOVA analysis of the effect of extract on logistic parameters of the antifungal activity dose-response curves. α = lower limit, δ = upper limit, φ = EC_{50}.

Parameter	*Df*	*Sum Sq*	*F value*	*Pr(>F)*
Germ tube length (µm)	3	2141	23.19	**<0.001 *****
Conidia germination (%)	3	17553	24.00	**<0.001 *****

Table S3 One-way ANOVA analysis of effect of concentration of *Ulva* extract on germ tube length and conidia germination percentage of *A. flavus* after 16 h of incubation at 28°C.

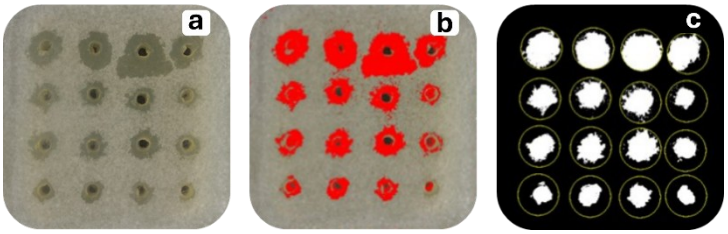


Figure S1 Process to determine the inhibition; (a) representative images of Petri dishes used in agar-well diffusion test showing inhibition of *A. flavus* mycelium growth; the percentage of inhibition was calculated as the ratio between the halo area (red in b) and the total area of imaginary circles centred on each hole (yellow circles in c), designed so that the circles area was maximum.

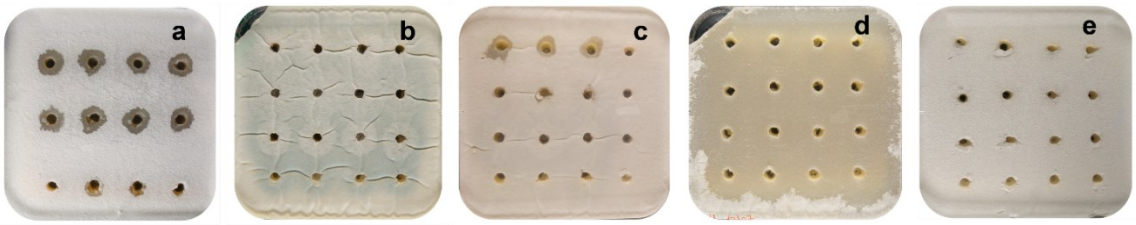


Figure S2 Representative images of Petri dishes used in agar-well diffusion test showing inhibition of *A. flavus* incubated with several dilutions of the four different extracts; upper to lower lanes of wells are incubated with decreasing concentrations of each extract corresponding to range of (a) 135-90 g L^{-1} *Ailanthus*; (b) 80-20 g L^{-1} *Olea*; (c) 110-80 g L^{-1} *Humulus* trub; (d) 50-30 g L^{-1} *Ulva*, (e) similar aliquots of hydroalcoholic solutions without extract were used as negative control.

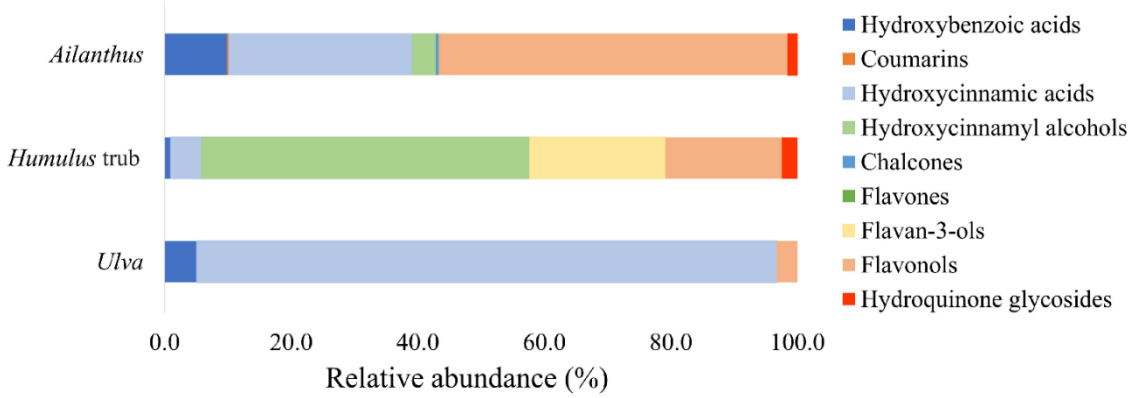


Figure S3 Relative abundance (%) of phenolic compounds per chemical classes identified in *Ailanthus*, *Humulus* trub and *Ulva* extracts.

5. General Conclusions

This PhD Thesis set out to elucidate how environmental conditions shape maize morphophysiological traits in the field and how these plant responses, in case of fungal infection, influence in turn the occurrence of mycotoxins in the grain. By integrating ecophysiological measurements, mycotoxin analyses, statistical modelling, and multispectral images, the work aimed to improve predictive understanding of contamination risk under field conditions. In parallel, this Thesis explored the potential of sustainable, low-impact bio-extracts derived from agricultural or agro-industrial by-products as preventive tools against mycotoxigenic pathogens, within a circular economy framework.

Overall, the results highlight the central role of timing and biological interactions in determining mycotoxin risk. Both plant–environment interactions and mycotoxin contamination emerged as highly stage-dependent processes, reinforcing the need to move beyond static assessments and toward integrative, phenology-based approaches.

From the perspective of prevention and sustainable management, the *in vitro* experiments demonstrated that natural bio-extracts can exhibit strong antifungal activity against *Aspergillus flavus*, with marked differences among sources. In particular, the *Ulva*-derived extract showed a significantly higher antifungal efficacy than other polyphenol-rich extracts obtained from different biological sources. *Ulva* extract inhibited *A. flavus* radial growth by approximately one order of magnitude (10×) compared with the other extracts and reduced conidial germination in a clear dose-dependent manner, achieving complete (100%) inhibition already at relatively low concentrations.

This enhanced activity cannot be attributed solely to total phenolic content but rather appears to arise from the synergistic action of diverse specialized metabolites, including specific polyphenols and ulvan polysaccharides. Beyond their direct antifungal effects, these compounds are also known to modulate plant defence responses and hormonal pathways, suggesting a dual role as antifungal agents and bio-stimulants, with the potential for enhanced efficacy under *in vivo* conditions through the activation of plant-mediated defence mechanisms.

Such multifunctionality is especially attractive in the context of sustainable agriculture, as it may reduce pathogen pressure both directly and indirectly by enhancing host resilience. At the same time, the results underline the complexity of natural extracts: future research should prioritize bioassay-guided fractionation to better disentangle the contribution of individual compounds, while carefully considering the risk of losing synergistic effects during purification. For practical application, the controlled cultivation of *Ulva* biomass or the definition of quality control markers will be essential steps toward standardization and reproducibility.

Regarding the regional-scale experiment on the multitemporal relationships between environmental conditions, plant morphophysiological traits, and mycotoxin accumulation, the analyses provided

clear evidence that aflatoxin and fumonisin contamination are governed by different, though partially overlapping, drivers. Plant morphophysiological traits responded to environmental factors in a highly dynamic manner across phenological stages. Some traits, such as chlorophyll content, appeared to be largely genetically determined and relatively insensitive to environmental variability, whereas others, including plant height and specific leaf area, showed strong but time-dependent responses to temperature, rainfall, and soil properties.

Interestingly, some traits resulted well described by statistical models already at early phenological stages, underlying the importance of early-stage conditions in shaping plant traits throughout the entire season. These early and mid-season plant responses were not only relevant for biomass accumulation and yield formation but played also a role in shaping mycotoxin outcomes. Grain yield components, such as kernel dry weight and $\delta^{13}C$, were influenced by early vigour and functional traits, confirming the importance of early crop establishment and mid-season growth for final productivity. Importantly, aflatoxin contamination emerged as a process partially mediated by plant physiology: high temperatures and low rainfall early in the season increased risk, but plant traits such as height and kernel $\delta^{13}C$, particularly at the beginning of stem elongation, also contributed to explaining variability. This suggests that the plant's capacity to cope with stress can modulate susceptibility to aflatoxin accumulation.

In contrast, fumonisin contamination was more directly and consistently linked to environmental conditions, with temperature during vegetative growth and rainfall patterns playing a dominant role. The strong association with cumulative precipitation close to harvest indicates that warm and wet conditions in later phenological stages are especially conducive to fumonisin production, highlighting the importance of end-of-season climate in determining risk.

Complementary to field-based measurements, preliminary analyses from an ongoing study demonstrate the potential of drone-acquired multispectral imagery for remotely monitoring maize health and physiological status. When integrated with machine-learning approaches, particularly random forest models, multispectral data were able to effectively describe spatial and temporal variability in plant condition, capturing key signals related to crop vigour and stress responses. These results suggest that remote sensing can provide a scalable, non-destructive tool to support field monitoring, improve early detection of stress conditions associated with mycotoxin risk, and strengthen predictive frameworks by linking plant spectral responses with environmental drivers and contamination outcomes.

Taken together, these findings support a multi-stage and integrative framework for mycotoxin risk assessment in maize. Rather than relying on single environmental indicators or end-of-season observations, effective prediction and mitigation require tracking crop development, plant functional responses, and environmental conditions across the entire growing cycle. This approach allows the identification of critical windows of vulnerability (i.e., early stem elongation for aflatoxins and late

grain filling to harvest for fumonisins) where targeted interventions may be most effective. In this context, the dent stage emerges as a particularly strategic phase for management, where agronomic decisions such as correct irrigation practices could help limit fungal growth and toxin accumulation.

Finally, the experiment regarding rhizosphere microbiome in maize demonstrated that rhizosphere bacterial diversity was primarily structured by seasonal environmental variation rather than flowering-time divergence, with phenological effects emerging only in interaction with sowing date. These findings indicate that, in agroecosystems, environmental seasonality seems to override host developmental timing as the main driver of rhizobiome assembly. In practical terms, this points to the conclusion that climatic modifications may directly alter rhizobiome communities rather than through modifications in plant developmental timing. Consequently, predictions of plant-microbiome responses to climate change should account not only for shifts in host phenology but also for the direct effects of changing environmental conditions on microbial community assembly and dynamics.

Overall, the results of this Thesis highlight phenology as a key integrative component of plant–environment interactions.

In conclusion, this Thesis contributes to a deeper systemic understanding of maize–environment–pathogen interactions by linking climate drivers, plant ecophysiology and mycotoxin dynamics across phenological stages. It also highlights the promise of sustainable bio-based solutions as complementary tools for mycotoxin prevention. Together, these results provide a foundation for developing predictive models and integrated management strategies that are better suited to the challenges posed by climate variability and the need for more sustainable agricultural systems.

6. Future Perspectives

The results presented in this Thesis open several promising avenues for the development of integrated strategies aimed at mitigating pathogen pressure in maize systems.

In particular, this work highlights the potential of advanced statistical modelling to investigate environmental and morphophysiological legacies across different phenological stages. The use of multi-temporal models offers promising opportunities to disentangle delayed or cumulative effects of climatic and soil-related drivers on crop performance and contamination risk, thereby improving our understanding of time-dependent plant-environment interactions.

In addition, the integration of UAV-based multispectral remote sensing with machine learning approaches such as random forest models further represents a key avenue for future developments. These methods proved valuable for capturing complex, non-linear relationships between spectral traits and plant responses, and their extension across both temporal and spatial scales, through the integration of multi-year and large-area multispectral satellite imagery, represents a key direction for future research.

Finally, this work lays a solid foundation for further investigation into the potential of plant- and seaweed-derived bioextracts as antifungal agents, with the potential to reduce pathogen establishment and proliferation in a more sustainable manner compared to conventional chemical control. In this perspective, a key next step is the validation of laboratory findings under realistic field conditions.

In particular, Chapter 2 (Multispectral Imagery as a Tool to Remotely Investigate Maize Health) and Chapter 4 (Bioextracts as Potential Environment-Friendly Anti-Mycotoxin Compounds) present interesting open questions, some of which we have already started to investigate through the experiments presented in the following sections.

6.1. Multispectral Imagery as a Tool to Remotely Investigate Maize Health – Upscaling to Satellites

Regarding multispectral remote sensing and statistical modelling, future work will focus on fully exploiting the information content of the random forest models developed using drone-acquired multispectral imagery. Ongoing analyses aim to interpret variable importance and model structure to better understand which spectral features and temporal windows are most informative for describing plant health, stress responses, and conditions associated with mycotoxin risk. Building on this foundation, a major subsequent step will be the spatial upscaling of these approaches using satellite-based multispectral data, such as Sentinel-2 and other comparable platforms. This will enable the extension of plot-scale insights to the regional scale, allowing the generation of spatially explicit risk maps across all maize-growing areas of the region. Crucially, these satellite-derived risk maps will be

validated using ground truth data from the fields analysed in this Thesis, where detailed drone-based, morphophysiological, and mycotoxin measurements are available.

This multi-scale validation strategy will strengthen the reliability of the models and support, in the longer term, their integration into operational decision-support tools. Embedding plant stress and mycotoxin risk prediction layers within existing agricultural platforms, such as the AgriCS (Agricoltura, Conoscenza, Sviluppo) Project (https://agrics.regione.fvg.it/agricsweb/), developed by ERSA (Regional Agency for Rural Development of Friuli Venezia Giulia, Italy) and funded under the EAFRD (European Agricultural Fund for Rural Development), would allow the direct translation of scientific outputs into actionable information for farmers, technicians, and policymakers. Such integration would enhance early-warning capabilities and support informed decision-making under increasingly variable climatic conditions. Enriching AgriCS with mycotoxin risk prediction layers would represent a concrete step toward providing farmers, technicians, and policymakers with actionable, science-based information.

Finally, in collaboration with ERSA, there is strong interest in replicating the same experimental design over multiple years. Establishing a long-term monitoring network based on consistent protocols would allow the construction of a multi-year time series, capturing interannual variability in climate, crop responses, and mycotoxin contamination. Such a dataset would be valuable for improving model robustness, assessing climate-driven trends, and refining early-warning systems under future climatic scenarios. Ultimately, this long-term perspective would strengthen the capacity to anticipate mycotoxin risks and design adaptive, sustainable management strategies for maize production systems.

6.2. Bioextracts as Potential Environment-Friendly Anti-Mycotoxin Compounds – An Open-Field Experiment

Aim of the Study

Based on the results of our previous experiments, which demonstrated that *Ulva* extract has great potential in reducing *Aspergillus flavus* mycelial growth and conidial germination *in vitro*, we decided to evaluate it under more realistic conditions. The aim of this study is to evaluate the efficacy of *Ulva* extract in reducing the occurrence of the pathogen and, possibly, the accumulation of mycotoxins on maize kernels under different water regimes in a realistic scenario. To this end, an open-field experiment was established in summer 2024 at the "Azienda Agraria Sperimentale A. Servadei" (Udine, NE Italy), focusing on *Ulva* extract application during silk emergence, which is a critical stage for fungal infection.

Importantly, this experiment goes beyond toxin quantification alone, as fungal DNA was also collected to characterize changes in fungal abundance and community composition. This integrated approach will allow disentangling whether observed reductions in mycotoxin contamination are driven by direct effects on toxigenic fungi or shifts in the broader fungal community. Such evidence will be crucial to evaluate the robustness, consistency, and ecological implications of using *Ulva*-based products as preventive tools in open-field agriculture.

Experimental Design

On 13 May 2024, 600 maize plants of the FAO class 500 were sown and arranged in four rows with an inter-row spacing of 70 cm and an intra-row spacing of 20 cm (Figure 1A). The same day, diammonium phosphate and potassium chloride were applied at a rate of 200 kg ha^{-1} each. Irrigation was supplied through a drip irrigation system, uniformly delivering 7 mm day^{-1} of water to maintain soil moisture at field capacity. To accurately control the amount of water available to the plants, the field was covered with a transparent plastic sheet, leaving a 1.5 m gap between the lower edge of the cover and the soil surface, while keeping the ends of the tunnel open, to ensure air circulation and prevent excessive greenhouse effect (Figure 1D).

The field experiment was arranged in a design with two factors: irrigation regime and bio-extract treatment. Each experimental plot consisted of eight plants, and plots were randomized as shown in Figure 1A. A total of five replicates were established. Border plants were excluded from measurements to minimize edge effects (Figure 1A).

The application of differential irrigation regimes across the experimental plots started on 11 July. Irrigation consisted of three levels: drought stress (D, 0 mm day^{-1}), optimal irrigation (O, 7 mm day-

^{1}) and excessive irrigation (E, 14 mm day^{-1}). The differential irrigation regime ended on 30 July, after which all plots received 14 mm day^{-1}.

On 22 July we treated 120 ears, one per plant, with 20 mL of *Ulva* extract at 2 g L^{-1} (*Ulva* treatment). Another 120 ears, one per plant, were treated with an hydroalcoholic solution (EtOH) at a concentration of 2 g L^{-1} (Control).

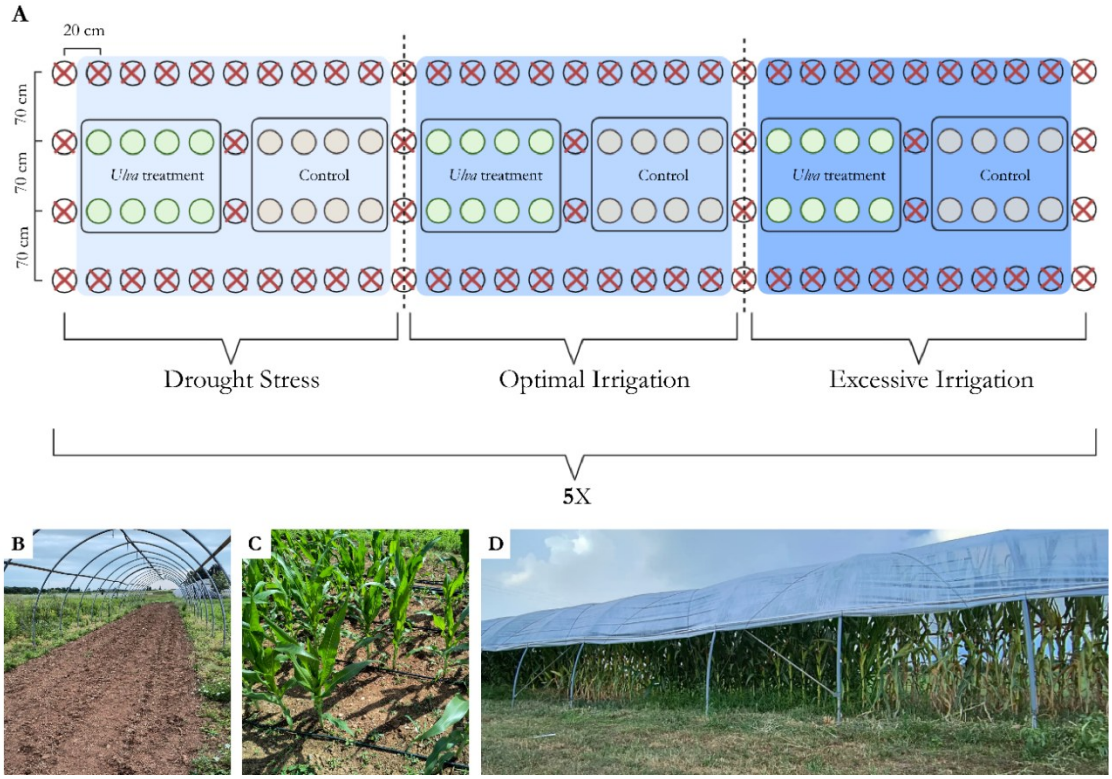


Figure 1 Experimental Design. (A) Each circle represents a maize plant; plants with a red cross were excluded from measurements to minimize edge effects. The experiment was a 2 × 3 factorial design: bio-extract treatment (two levels: *Ulva* treatment, in green, and Control, in grey) and irrigation regime (three levels: Drought Stress, Optimal Irrigation and Excessive Irrigation, represented by progressively darker shades of blue). Number of replicates: 5. (B) A detail of the 30 m field shortly after sowing. (C) A detail of the drip irrigation system. (D) Side view of the 30 m field covered with a transparent plastic sheet, leaving a 1.5 m gap between the lower edge of the cover and the soil surface to ensure air circulation and prevent excessive greenhouse effect.

Data Collection

Pre-treatment data were collected on 18 July (T0), while post-treatment data were collected on 29 July (T1), according to the protocol described below. Harvest was conducted on 16 September.

Soil moisture and temperature

At the beginning of the season, two temperature sensors and eight soil water potential sensors were installed a few centimetres below ground and recorded data on an hourly basis.

Plant morphophysiological traits

At T0 and T1 stomatal conductance was measured between 11.00 am and 12.00 am on 90 fully expanded leaves (three per plot) using a portable porometer (LI-600 Porometer/Fluorometer, LI-COR Biosciences, USA).

Plant height was measured for 90 plants (three per plot), and 90 leaves (three per plot) were collected. Leaves were placed in moistened plastic bags and transported to the laboratory, where they were photographed for specific leaf area (SLA) determination. Three 1-cm-diameter leaf discs were sampled from each leaf for pigment analysis and stored at -80 °C until use. Leaves were then weighed, oven-dried at 70 °C for 48 h and reweighed to obtain fresh and dry mass to calculate dry matter content (DMC). Dry leaves were then ground into a fine powder under liquid nitrogen using a mortar and pestle. The resulting powder was analysed for carbon and nitrogen contents and isotopic signatures using a CHNS Elemental Analyser (Vario Microcube, © Elementar) coupled to a stable isotope ratio mass spectrometer (IRMS; Isoprime 100, © Elementar).

Genetic data

At T0 and T1 we also collected silks from 90 plants (three per plot) using gloves continuously disinfected with ethanol. Samples from the same plot were pooled into a single 50 mL RNase-free Falcon tube, resulting in 30 tubes in total, and immediately frozen in liquid nitrogen. Upon transfer to the laboratory, samples were stored at -80 °C for subsequent DNA extraction.

Productivity and mycotoxin accumulation data

On 16 September, 90 fully ripe ears (three per plot), corresponding to stage 99 of the BBCH scale for cereals (Lancashire et al., 1991; Meier, 2018), were harvested. Once transferred to the laboratory, ears were weighed, shelled, oven-dried at 70 °C for 48 h and reweighed to obtain fresh and dry mass of cobs and kernels. Kernels were mill-ground and the resulting powder was divided into two subsamples. One subsample was sent to the Regional Agency for Rural Development (ERSA) for mycotoxin quantification, while the other was analysed for carbon and nitrogen contents and isotopic signatures using a CHNS Elemental Analyser (Vario Microcube, © Elementar) coupled to a stable isotope ratio mass spectrometer (IRMS; Isoprime 100, © Elementar).

Analyses

Analyses are currently ongoing.

References

Lancashire, P. D., Bleiholder, H., Boom, T. V. D., Langelüddeke, P., Stauss, R., Weber, E., & Witzenberger, A. (1991). A uniform decimal code for growth stages of crops and weeds. *Annals of Applied Biology*, *119*(3), 561–601. https://doi.org/10.1111/j.1744-7348.1991.tb04895.x

Meier, U. (2018). Growth stages of mono- and dicotyledonous plants: BBCH Monograph. https://doi.org/10.5073/20180906-074619

7. Side Projects and Activities

During the development of this PhD project, opportunities arose to collaborate on additional research projects not directly related to the present Thesis, but nevertheless closely connected through shared research themes, including remote sensing, agroecology and landscape ecology. Moreover, I attended and actively participated in national and international scientific congresses.

7.1. Side projects

7.1.1. Alkaline Wetlands Ecology

Multitrophic assessment of restoration actions in alkaline wetlands

Edoardo Asquini[1,2,3], Giacomo Boscarol[3], Francesco Boscutti[3,2]

1 University of Palermo, 90133 Palermo, Italy
2 NBFC, National Biodiversity Future Centre, 90133 Palermo, Italy
3 University of Udine, 33100 Udine, Italy

Abstract

The project seeks to gain a deeper insight into the impacts of climate change on ecosystems, with particular attention to its effects on trophic networks. By linking plant and insect responses with remote sensing techniques, we will be able to upscale these interactions and extend our findings across multiple ecological levels.

The main pressures imposed by global changes are rising temperatures and altered rainfall regimes, which can affect ecosystems both directly and indirectly at every level. Another major driver of habitat degradation is landscape anthropization, expressed through land-use change, soil and water pollution, and habitat fragmentation.

To address these threats, we have selected two target ecosystems: dry mountain grasslands and restored alkaline wetlands. Both represent biodiversity hotspots of great importance, yet they remain at risk of degradation.

A central component of our research will be the analysis of vegetation responses. We will conduct vegetation surveys within permanent plots along ecological gradients (elevation and waterlogging), used as proxies for climate change–driven effects. In addition, we will apply functional trait analyses at both individual and community scales to capture a higher degree of ecological complexity.

The second core of our work focuses on insect communities. We will concentrate primarily on pollinators and predators (Odonata). These surveys will allow us to explore interactions between

trophic levels and habitat features. To this end, we plan to employ bipartite networks, landscape analyses, and linear regression models.

To strengthen the upscaling potential, field data will be complemented by multispectral surveys and multi-year orthophotos. These tools will be applied for time-series analyses, the construction of orthomosaics, and the spectral characterization of habitat patches.

7.1.2. Alpine Grasslands Ecology

Physiological responses of plants to abiotic stress in Alpine environments

Marco Vuerich[1], Arianna Del Pino[1], Giacomo Boscarol[1], Francesco Boscutti[1,2]

1 University of Udine, 33100 Udine, Italy
2 NBFC, National Biodiversity Future Centre, 90133 Palermo, Italy

Abstract

Climate change is rapidly shifting ecological thresholds in many terrestrial ecosystems, altering environmental stress gradients and moving species ecological and physiological response, often exceeding their phenotypic plasticity. Among the terrestrial plant communities, the alpine habitats are among the most sensitive to the abiotic stress shifts, prompting urgent studies on the alpine plant and ecosystems.

Extreme drought events in the Alps have increased significantly in recent decades; nevertheless, few studies are conducted to understand the possible impacts on the ecosystem.

The project aims to understand how the increase of temperature and the reduction of precipitation may affect alpine species. Additionally, it is crucial to study the consequences on communities and the entire ecosystem.

Three different treatments have been hypothesized; coverage in the first part of the season, coverage in the second part of the season, coverage during the entire season. Sampling will be carried out during the four main phases of the study: beginning, middle, end, recovery.

The chosen functional traits focus on species, community, ecosystem, and remote sensing. The treatments are expected to lead to increased stress and transpiration in plants, decrease in biodiversity, and reduction in photosynthetic capacity levels.

The study is of fundamental importance to deepen the understanding of the consequences of extreme events and to be able to mitigate their effects.

Introduction

In recent decades, there has been a progressive change in climatic conditions, with significant environmental and socio-economic repercussions. The main greenhouse gases (GHGs) responsible for the greenhouse effect are CO_2 (410 ppm), CH_4 (1866 ppb), and N_2O (332 ppb) (Calvin et al. 2023).

The increase in temperature leads to variations in the chemical, physical, and biological processes on Earth, resulting in more frequent extreme events such as prolonged droughts, violent precipitation,

and heat waves (Calvin et al. 2023). There is also a significant alteration of the biosphere, with changes in ecosystem functions, species distribution, and biodiversity loss (Bellard et al. 2012, Pearson et al. 2013).

In alpine areas, climate change is having a more pronounced impact compared to other regions of the Earth. This is due to a phenomenon known as "Arctic amplification," which causes rapid warming of these areas. Various studies show that the growing season tends to lengthen, becoming drier and advancing spring melt (Farrer et al. 2015). Plants will therefore be increasingly subject to decreased production, increased nutrient loss, and changes in biological interactions (Ernakovich et al. 2014).

Alpine systems are biodiversity hotspots (Vitasse et al. 2021), but there is an observed increase in the growth limits of various plant communities, causing a contraction of areas at higher elevations (Theurillat and Guisan 2001). Climate change can cause three different adaptive responses in the species involved: migration to more suitable habitats, persistence despite the altered climate, and extinction of communities that are no longer suitable (Theurillat and Guisan 2001). A clear example of the phenomenon just described is the advance of forests and the spread of shrubs, which lead to a reduction in alpine grasslands (Tocco et al. 2013).

Aim of the study

The abiotic stresses that plant species are subjected to are numerous. This study aims to delve into the biological responses of plant alpine species to extreme drought events.

Specifically, it seeks to investigate how species, communities, and ecosystems respond to prolonged periods of water scarcity and increased temperature. The study will examine the direct effects on species, the ecological thresholds beyond which community stability is affected, the system's resistance/resilience capacity, and the potential use of remote sensing to expand the scale of the study.

Material and methods

The suitable areas for the project are the alpine grasslands in the Friuli Venezia Giulia region. The reference species must be representative of the studied habitat; an example is *Sesleria caerulea*, a characteristic herbaceous plant of basophilic alpine grasslands.

To simulate drought conditions, transparent plastic covers will be used, placed over the selected sampling areas. This way, the water supply is limited, sunlight can penetrate the cover, and the temperature inside increases due to the greenhouse effect. Besides the control without coverage, the treatments conducted will be three:

- Coverage during the first half of the vegetative growth
- Coverage during the second half of the vegetative growth

- Coverage throughout the entire vegetative growth

All cases, temperature and humidity will be measured and taken at the beginning, middle, and end of the study. Additionally, it will be crucial to repeat the analyses in subsequent years to verify the physiological and adaptive responses of different species.

Functional traits of species:

- Plant height: competition
- Leaf area: photosynthesis, growth, transpiration
- SLA (Specific Leaf Area): leaf area/dry weight
- Dry matter: tissue density, nutrient use
- Stomatal density and size: transpiration, gas and nutrient flow
- NSC (Non-Structural Carbohydrates): quantity and location of reserves
- Leaf iron: stress level and antioxidant capacity
- Antioxidants and phenolic compounds: evaluation of abiotic stress level
- Vegetative phenology: stages of the vegetative cycle, which vary based on competition and available resources

Functional traits of communities:

- Biodiversity
- Species abundance

Functional traits of the ecosystem:

- CO_2 fluxes
- NPP (Net Primary Productivity)

Functional traits of remote sensing:

- NDVI (Normalized Difference Vegetation Index): areas with chlorophyll (green) show higher values compared to yellowed areas
- Classification: understanding if some species have replaced others

Expected results

Species

The increase in temperatures and the absence of precipitation could lead to increase in transpiration and competition for nutrients. If temperature values rise significantly, plants will close their stomata to prevent water loss. Increased stress causes imbalances in the production of antioxidants and phenolic compounds, and often the leaf iron content can also be altered. The vegetative cycle tends to be advanced (Vitasse et al. 2021), causing a decrease in non-structural carbohydrates used as reserves.

Community and Ecosystem

A decrease in biodiversity is expected due to the limitation of water resources. Species more vulnerable to increased temperatures and decreased precipitation will tend to decline, while more resilient species may increase. Overall, species diversity decreases, but the number of individuals of a single species might increase.

Remote Sensing

The lack of water and high temperatures could lead to early senescence, in which case NDVI values will decrease due to yellowing. Additionally, drone photos allow for understanding if some species have supplanted others.

Conclusions

The increase in temperatures in alpine areas has recently reached around 2 °C, compared to the global average of 0.8 °C increase since the pre-industrial era. Therefore, it is crucial to deepen research to understand the consequences and mitigation methods of extreme events.

The study will allow for a deeper understanding of the functioning of alpine ecosystems, investigate the effects of extreme events at different ecological levels, and lay the groundwork for a more detailed understanding of how ecology may be altered due to climate change.

References

Bellard, Celine, Cleo Bertelsmeier, Paul Leadley, Wilfried Thuiller, e Franck Courchamp. 2012. «Impacts of Climate Change on the Future of Biodiversity». ECOLOGY LETTERS 15 (4): 365–77.

Calvin, Katherine, Dipak Dasgupta, Gerhard Krinner, Aditi Mukherji, Peter W. Thorne, Christopher Trisos, José Romero, et al. 2023. «IPCC, 2023: Climate Change 2023: Synthesis Report. Contribution of Working Groups I, II and III to the Sixth Assessment Report of the Intergovernmental Panel on Climate Change [Core Writing Team, H. Lee and J. Romero (Eds.)]. IPCC, Geneva, Switzerland.» First. Intergovernmental Panel on Climate Change (IPCC).

Ernakovich, Jessica G., Kelly A. Hopping, Aaron B. Berdanier, Rodney T. Simpson, Emily J. Kachergis, Heidi Steltzer, e Matthew D. Wallenstein. 2014. «Predicted Responses of Arctic and Alpine Ecosystems to Altered Seasonality under Climate Change». GLOBAL CHANGE BIOLOGY 20 (10): 3256–69.

Farrer, Emily C., Isabel W. Ashton, Marko J. Spasojevic, Shiyang Fu, David J. X. Gonzalez, e Katharine N. Suding. 2015. «Indirect Effects of Global Change Accumulate to Alter Plant Diversity but Not Ecosystem Function in Alpine Tundra». JOURNAL OF ECOLOGY 103 (2): 351–60.

Pearson, Richard G., Steven J. Phillips, Michael M. Loranty, Pieter S. A. Beck, Theodoros Damoulas, Sarah J. Knight, e Scott J. Goetz. 2013. «Shifts in Arctic Vegetation and Associated Feedbacks under Climate Change». NATURE CLIMATE CHANGE 3 (7): 673–77.

Theurillat, J. P., e A. Guisan. 2001. «Potential Impact of Climate Change on Vegetation in the European Alps: A Review». CLIMATIC CHANGE 50 (1–2): 77–109.

Tocco, Claudia, Massimiliano Probo, Michele Lonati, Giampiero Lombardi, Matteo Negro, Beatrice Nervo, Antonio Rolando, e Claudia Palestrini. 2013. «Pastoral Practices to Reverse Shrub Encroachment of Sub-Alpine Grasslands: Dung Beetles (Coleoptera, Scarabaeoidea) Respond More Quickly Than Vegetation». A cura di Bazartseren Boldgiv. PLoS ONE 8 (12): e83344.

Vitasse, Yann, Sylvain Ursenbacher, Geoffrey Klein, Thierry Bohnenstengel, Yannick Chittaro, Anne Delestrade, Christian Monnerat, et al. 2021. «Phenological and Elevational Shifts of Plants, Animals and Fungi under Climate Change in the European Alps». BIOLOGICAL REVIEWS 96 (5): 1816–35.

7.1.3. Fire Ecology – Article Published in Fire Ecology

Interpreting the shifts in forest structure, plant community composition, diversity, and functional identity by using remote sensing-derived wildfire severity

Giacomo Trotta[1,2*], Luca Cadez[1,2*], Francesco Boscutti[2,3], Marco Vuerich[2,3], Edoardo Asquini[2,3,4], Giacomo Boscarol[2], Paolo Cingano[1,2], Giacomo Azzani[2], Sara Pischedda[2], Antonio Tomao[2] and Giorgio Alberti[2,3]

1 University of Trieste, 34127 Trieste, Italy
2 University of Udine, 33100 Udine, Italy
3 NBFC, National Biodiversity Future Centre, 90133 Palermo, Italy
4 University of Palermo, 90133 Palermo, Italy
* Corresponding Authors

DOI: doi.org/10.1186/s42408-024-00330-7

Abstract

Background

Wildfires are increasingly impacting ecosystems worldwide especially in temperate dry habitats, often interplaying with other global changes (e.g., alien plant invasions). Understanding the ecological consequences of wildfires is crucial for effective conservation and management strategies. The aim of this study was to investigate the impacts of wildfire severity on plant community (both the canopy trees and herbaceous layer) and alien plant invasion, combining field observations and remotely sensed data. We conducted an observational study in the Karst forests (North-East Italy) 1 year after the large wildfire which affected the area in 2022. We assessed the impact through 35 field plots (200 m2 each) distributed among different fire severity (i.e., the loss of organic matter) classes assessed using the differenced normalized burn ratio (dNBR) calculated from satellite images. In each plot, tree species, diameter, vitality, resprouting capacity, and seedling density were measured. In addition, herb species richness (taxonomical diversity) was quantified, and plant cover was visually estimated. Functional diversity was also assessed considering six functional traits retrieved from databases.

Results

Some woody species (e.g., *Quercus pubescens*) showed a higher resistance to the fire (i.e., lower mortality rate), while others showed a higher resilience (i.e., recovery after fire through resprouting or seedlings, e.g., *Cotinus coggygria*). The transition to a shrub-dominated community (i.e., *Cotinus coggygria*) where fire severity was the highest underlines the dynamic nature of the post-fire succession. We detected a significant variation in the herbaceous plant community composition, diversity, and functional

identity (i.e., community-weighted mean of trait) along the fire severity gradient. In particular, high-fire severity areas exhibited higher species richness compared to low-severity or unburned areas. Total alien plant cover increased with fire severity, while native cover remained constant. We also found shifts in species that enhance traits related to germination potential and growth strategy.

Conclusions

Our results highlight the vulnerability of the forest stands to an increase in wildfire severity, resulting in significant mortality and changes in tree community structure. This study contributes to the understanding of ecological processes after wildfires using a novel remote sensing approach in a temperate forest, emphasizing the need for conservation strategies aimed at mitigating high severity wildfires.

Keywords

Biological invasion • Forest community • Functional traits • Herbaceous community • Karst landscape • Remote sensing approach • Vegetation dynamics

Introduction

Wildfires represent one of the most influential ecological disturbance agents affecting ecosystem distribution, properties, and functions over geological periods (Bowman et al., 2009). Fires trigger changes in primary productivity of the ecosystems and shape local plant communities by altering the ecological succession, nutrient cycle, and light availability of the sub-canopy layer, resulting in new available niches (Sousa, 1984; Glenn-Lewin et al., 1992).

Plant species differ in their fitness (i.e., survival and/or reproductive success) as a consequence of adaptation to varying fire regimes (Cavender-Bares et al., 2004). Tree species can be classified into five groups according to their response strategy to fire (Moris et al., 2022):

(i) resisters, which survive frequent surface fires thanks to their thick and insulating bark; (ii) embracers, which recover quickly from the canopy seed bank; (iii) avoiders, which are easily killed but live where fires are infrequent; (iv) resilient (i.e., used as synonyms of endurers), which are able to resprout after the event; (v) colonizers, which establish on burned areas following the long-distance seed dispersal.

Anthropogenic climate change is causing an increase in the frequency and severity of extreme fire events due to changes in local, regional, and global weather parameters that drive fire behavior (Clarke et al., 2013; North et al., 2015; Sharples et al., 2016; Bowman et al., 2017; Tedim et al., 2018). This trend is expected to increase in the future (Liu et al., 2010; Jolly et al., 2015) because of climate change projection. In recent years, for example, there have been increasing media reports of major fires

disasters: the wildfires in Chile in 2017, Portugal in 2018, California in 2021, Brazil in 2019, Australia in 2019–2020, and Siberia in 2022–2023.

Prior to 2012, around 65,000 fires occurred in Europe every year, burning around half a million hectares of wild and forested land (San-Miguel-Ayanz et al., 2012), mainly in the Southern Mediterranean countries. In the Mediterranean basin, there is evidence that fires were common during the late Quaternary (Carrión et al., 2003), and fire was likely common prior to the Quaternary as most plant species evolved adaptive mechanisms to persist and regenerate after disturbance events such as recurrent fires (Pausas et al., 2004; Pausas and Verdú 2005). Although for fire adapted habitat wildfire can benefit from these events, the main concern of recent years regards the increasing frequency of this phenomenon. Fire frequency in Europe has been increasing in the last decades due to climate change (Senf and Seidl 2021; Patacca et al., 2023), socio-economic factors, and especially rural abandonment (Mancini et al., 2018; Colonico et al., 2022), in which the interplay causes an increase in biomass resulting in an increase in available fuel in the environment (i.e., higher severity). Indeed, these processes caused an increased flammability at the landscape scale due to an accumulation of fuel (e.g., dead biomass in forests) and its continuity (Moreira et al., 2011; Pausas and Fernández-Muñoz 2012; Badeau et al., 2024), thus calling for an active monitoring and prevention effort (Corona et al., 2015; Spadoni et al., 2023).

An increase in wildfire frequency and/or severity, defined as the loss of organic matter (Keeley 2009), will have major economic impacts, will increase plant and seed mortality, and may drive changes in species composition, dominance, and spatial distribution towards species adapted to more frequent and intense fires (Segura et al., 1998; Morrison 2002; Penman and Towerton 2008). Changes in soil properties are expected to strongly interplay with the plant community assemble, as observed in other ecosystems (Trotta et al., 2024). Besides habitat disruption, another adverse consequence of wildfire on vegetation is the potential to promote the ingression of new species into landscapes (Keeley 2006). A common consequence of wildfire in the northern hemisphere is the regression of ecosystems to more juvenile seral stages with an evident simplification of their structural complexity (Poldini et al., 2018), while in the southern hemisphere, the response depends on the various vegetation across regions (see Lehmann et al., 2014). This leads to a rapid establishment of herbaceous species shifting from forest specialist towards plants with a ruderal adaptive strategy, the majority of which can be alien (Ivanova et al., 2014; Trotta et al., 2023b). Alien species are a topic of global concern in terms of ecosystem preservation as they have shown their potential to alter ecosystem processes (Root et al., 2003; Raizada et al., 2008); decrease native species abundance and richness via competition, predation, hybridization, and indirect effects (Blackburn et al., 2004; Gaertner et al., 2009; Boscutti et al., 2020; Vitti et al., 2020; Trotta et al., 2023c); change native community structure (Hejda et al., 2009); alter nutrient cycling (Pellegrini et al., 2021); impact landscape perception (Pejchar and Mooney

2009); and alter the fire regimes of the ecosystem invaded (D'Antonio and Vitousek 1992; Brooks et al., 2004).

Remote sensing (RS) has been largely used to assess landscape change (Sellers et al., 1995; Vuerich et al., 2024; Cingano et al., 2024). Over the last decades, new satellite sensors (e.g., Sentinel-2 MSI, Landsat-8 OLI/TIRS) have been providing valuable data at increasingly higher temporal, spatial, and spectral resolutions. This growing variety and quality of remotely sensed data enables a wide range of fire-related applications, from detecting fire occurrence (Wooster et al., 2021) and severity (Keeley 2009; Veraverbeke et al., 2011) to monitoring post-fire recovery (Frazier et al., 2013). Satellite-derived spectral vegetation indices based on the ratio between short-wave infrared (SWIR) and near infrared (NIR) wavelengths have demonstrated a good capability in characterizing post-fire forest severity and dynamics, with strong correlations with field-based measurement (Keeley 2009; Cardil et al., 2019; Gibson et al., 2022). In particular, the normalized burn ratio (NBR) has become one of the most widely accepted spectral indices to assess burn severity (Lutes et al., 2006; Eidenshink et al., 2007; Escuin et al., 2008; French et al., 2008; Avetisyan et al., 2023; Jodhani et al., 2024). The difference between NBR of the vegetation pre-fire and post-fire is expressed as delta NBR (i.e., hereafter dNBR), but its potential use as a tool to assess the functional response of the vegetation community to fire has not been widely explored.

The functional response of a plant community to a wildfire can be used to study the response to the new environment and to the disturbance across taxa (Donato et al., 2009). Traits related to regeneration strategies (i.e., seed longevity, germination, growth form) and competition (i.e., growth rate, shade tolerance) are a well-known proxy to determine the functional response of the community (Noble and Slatyer 1980). Wildfire is a well-recognized ecological disturbance able to alter the structure and composition of vegetation communities, whose magnitude (i.e., fire severity) can greatly shape the impacts on both the herbaceous and tree forest layer (Bond et al., 2005; Bowman et al., 2009). Thus, determining the functional response of the plant community by combining field and remote sensing approaches appears crucial, especially in areas prone to repeated fire events where not all the species are adapted.

Our research hypothesis posits that varying fire severities (i.e., expressed as varying dNBR values) elicit differential responses in plant vegetation (i.e., both understory and tree layer), leading to a potential shift in community composition, functional response, and the potential for alien plant invasion in the Karst region. We expect that traits typical of ruderal and alien species will be advantageous for species colonizing ecosystems severely affected by wildfire. We also expect different tree species to respond differently to wildfire severity, especially in terms of resilience and resistance, but without knowing the specific species response. We also suppose a higher invasion of alien species with increasing levels of disturbance (i.e., high wildfire severity). Through our findings, we aim to provide valuable insights for biodiversity conservation, ecosystem management, and planning in the

Karst landscapes. Indeed, the Karst region in Italy and Slovenia, as it is happening in other habitat, is becoming more and more prone to wildfires (Šturm and Podobnikar 2017). However, despite this higher susceptibility, the potential impact of such disturbances on vegetation dynamics as well as on the resistance and resilience of Karst ecosystems has not been completely understood.

Material and methods

Study area and 2022 fire

The Karst region is a limestone plateau with an average elevation of 334 m above sea level located in between Italy and Slovenia, world famous for its peculiar topography and geological phenomena (Cucchi et al., 2015). Being at the boundary between Mediterranean Sea, the Alps, and the Dinaric mountains, the area is characterized by a high level of biodiversity, hosting a large number of protected animal and plant species under the protection of the European Habitat directive 92/43/EEC. For these reasons, most of the Italian Karst area is included in the Natura 2000 protected sites network. The most representative forest stands are composed by mixedbroad leaves species of temperate areas such as downy oak (*Quercus pubescens* Willd.), hophornbeam (*Ostrya carpinifolia* Scop.), and manna ash (*Fraxinus ornus* L.) with the occurrence of European smoketree (*Cotinus coggygria* Scop.). Artificial black pine stands (*Pinus nigra* J.F. Arnold) are also present as remnants of the large reforestation program launched by the Austro-Hungarian Empire at the beginning of the last century. These stands are characterized by the presence of senescent pines in the upper layer and mixed broadleaf species in the understory layer. Most of the areas are not subjected to forestry management since the forest establishment. Alien species such as black locust (*Robinia pseudoacacia* L.) and tree of heaven (*Ailanthus altissima* (Mill.) Swingle) are widespread especially in disturbed areas (i.e., both natural or human induced disturbance) and close to settlements. Karstic dry grasslands, characterized by *Centaurea rupestris* L. and *Carex humilis* L., are also common in the area even though they have been disappearing in the last decades due to agricultural abandonment and natural forest expansion.

The climate is Pannonian continental with average temperatures in January and July of 4.0 °C and 22.9 °C respectively, with an annual average of 13.1 °C. However, temperatures are milder at lower altitude, along the sea. Rainfall ranges between 900 and 2000 mm per year depending on the altitude. The soil is extremely drained and classified in the family of red Mediterranean soils.

The 2022 wildfire broke out following an extremely dry and hot summer. It started on July 15 and was extinguished on July 29 with a total burnt area of around 4000 ha between Italy and Slovenia (Čahojová et al., 2024) (Fig. 1). Even though wildfires are common in the area (190 fires occurred within the Italian Karst since 1970 most of which were less than 1 ha in area (Autonomous Friuli Venezia Giulia Region 2023), the 2022 wildfire can be considered an extreme event for the area due

to its extent. For the purposes of the current research, we limited our study area to the burnt patch in the municipality of Doberdò del Lago (Italy, 500 ha), the municipality that was the most effected in Italy.

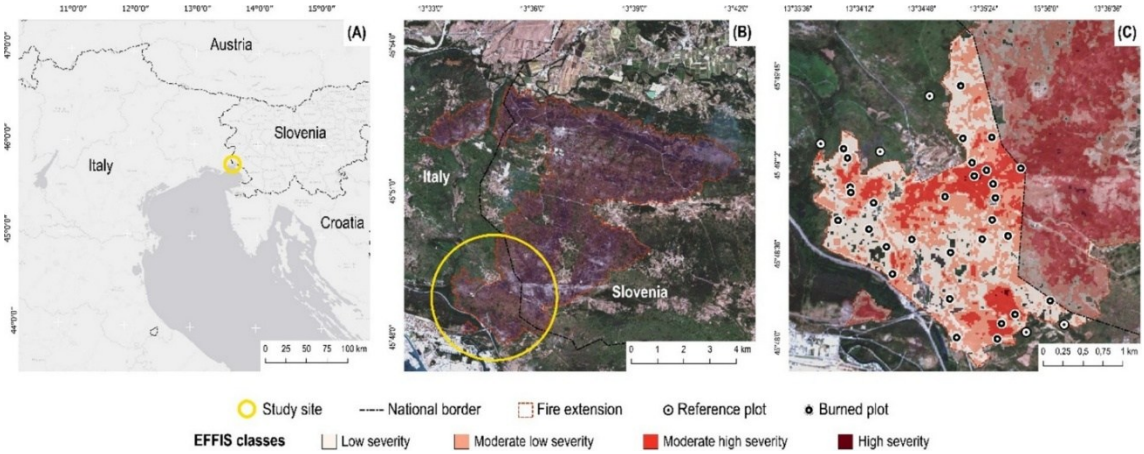


Figure 1 Study area and sampling design. Localization of the Karst (A), the 2022 wildfire area (B), and the study area and sampling plots classified according to EFFIS severity classes (C) are represented.

Fire severity calculation and sampling design

The severity of the 2022 wildfire was assessed using the dNBR index (Fig. 1). Such an index was calculated using Sentinel-2 images (Level-2A, tile T33TUL), taken on July 2 (pre fire) and August 16 (post fire) respectively, through the Semi-Automatic Classification Plugin (SCP) in the QGis software using the NIR band (8A) and the SWIR (12) (EFFIS 2020), both with a resolution of 20 × 20 m. The severity map was then classified according to the European Forest Fire Information System (EFFIS) fire severity classes (Lutes et al., 2006). Non-burned vegetation shows very high reflectance in the NIR, and low reflectance in the SWIR portion of the spectrum, while recently burned areas show low reflectance in the NIR and high reflectance in the SWIR. Applying the difference between the before and after wildfire RS data allow to calculate the difference NBR (dNBR or ΔNBR; Lutes et al., 2006; Miller and Thode 2007; Miller and Quayle 2015).

Using EFFIS map of fire severity, we randomly selected 30 points distributed proportionally to the area of each EFFIS class (class 1: 15 plots; class 2: 10 plots; class 3: 5 plots). In addition, 5 reference plots were selected in the surrounding forest stands not subjected to any fire in the last decades (i.e., since 1965) and representing the vegetation before the fire events.

In each of the 35 selected points, we established a permanent circular plot of 200 m2 (8 m of radius; Maringer et al., 2020), where the tree and understory data were collected. A permanent sampling network was developed, through a picket located in the center of each plot with the GPS position recorded.

Tree and understory data collection

In all plots, diameter at breast height (1.30 m; DBH) of all tree and shrub stems larger than 2 cm was recorded in the summer of 2023 and the species identified. Each stem was also classified as alive or dead. Aboveground mortality was then calculated as the ratio between dead and total stems (alive + dead). Resprouting stems from each stump were counted and their average height measured. The number of tree seedlings divided for species and their average height were measured within a subplot of 2 m radius centered in each plot.

For the herbaceous layer (i.e., all herbaceous species and only woody species with less than 50 cm of height), the cover of each plant species was visually estimated as cover percentage for the whole 200 m2 plot (Rapson 2018). Taxonomy and nomenclature followed Bartolucci et al., (2018) and Galasso et al., (2018) for native and alien species, respectively. Taxonomic diversity of the herbaceous layer was assessed using species richness (i.e., number of species). Functional identity of each community was quantified using six functional traits per species expected to be ecologically relevant and to respond to major environmental changes due to fire disturbance (Cornelissen et al., 2003), namely light demand, nutrient demand, life-span, specific leaf area (SLA), seed mass (i.e., for individual seed), and seed number (i.e., number of seed for each individual plant). According to literature, those are the traits which are expected to be affected by fire severity (Cornelissen et al., 2003; Müller et al., 2007). These traits were derived from "Flora Indicativa" (Landolt et al., 2010) and the "LEDA Traitbase" (Kleyer et al., 2008). The functional identity of the community was assessed calculating the community-weighted mean (CWM) of each trait, relying on the occurrence and abundance (i.e., cover value) of each species.

Statistical analyses

All the statistical analyses were performed in R environment (R Core Team 2022). Differences in mortality (i.e., percentage of dead trees) of the four most common species (i.e., *F. ornus*, *C. coggygria*, *Q. pubescens*, and *O. carpinifolia*) with dNBR were tested using generalized linear mixed-effects models (GLMM) with binomial distribution with the "glmer" function (p-value ≤ 0.05) of the "lme4" R package (Bates et al., 2015). Model included stem mortality as dependent variable and fire severity (dNBR), species, and their interaction as fixed effects, using the plot id as a random factor to adjust the model degree of freedom. We first tested the full model, and, where not significant, we manually backward simplified the model (summary of the full model reported in Table S2).

Differences in resprouting and recruitment were tested using linear mixed models (LMM), using the plot id as a random factor to adjust the model degree of freedom. For these variables (i.e., resprouting percentage and new seedlings), we considered the interaction significant between species and dNBR, given the proximity to 0.05 of the p-value (respectively 0.056 and 0.081). The number of recruitments was linear-transformed using square root to improve the model. Pairwise comparisons were

performed using the function "emtrends" of the "emmeans" R package (Lenth 2022) to test the different response between species.

The effects of fire severity (dNBR) on the species richness and abundance (i.e., species cover) of native and alien species (i.e., alien status) were tested using linear mixed-effects models (LMM; $p < 0.05$), with the plot id included as random factor (Zuur et al., 2009). Significance was assessed using the ANOVA test and the R^2 using the "rsq.lmm" function of the "rsq" package (Zhang 2023). Both species richness and abundance were transformed with a Z-transformation, to better compare the trend between alien and native species. Both linear and non-linear trend (i.e., log-transformed fire severity) were tested. Non-linear relationships were kept when model diagnostics were better.

Changes in the understory species composition across all plots were inspected by Kruskal's non-metric multidimensional scaling (NMDS) unconstrained ordination (Wildi 2017). To highlight the relationships between species composition, forest parameters, and functional traits, a further fitting of environmental variables was performed. All the multivariate analyses were performed in the "vegan" package (Oksanen et al., 2024).

To test the effects of fire severity on the community functional identity of the selected traits (i.e., CWM of each trait), we used linear models (p-value ≤ 0.05). Significance was assessed using the ANOVA test and the R^2 in the summary function. Data normality was tested with the Shapiro–Wilk's test, and the homoscedasticity was visually tested with the residuals of the model. Given that most of the results exhibit a logistic trend, the dNBR index was used as log-transformed index. All graph visualization was performed using "visreg" (Breheny and Burchett 2017) or "ggplot2" package (Wickham 2016).

Results

A total of 21 species (19 native and 2 alien species) were recorded in the tree layer (i.e., both canopy and subcanopy). The most common native trees were *Fraxinus ornus* (found in 100% of the surveyed plots, 24 individuals on average per plot), *Cotinus coggygria* (91%, 24 individuals on average per plot), *Quercus pubescens* (77%, 5 individuals on average per plot), and *Ostrya carpinifolia* (63%, 4 individuals on average per plot). Two alien tree species were recorded: *Robinia pseudoacacia* (3% of the surveyed plot) and *Hesperocyparis arizonica* (3% of the surveyed plot). The analysis of dendrometric data showed that stem density, basal area, and mean diameter of dead stems increased with fire severity (Table 1). On the other hand, the average diameter of living trees did not differ between EFFIS classes, except for the high-severity class, where almost no living stems were measured.

We counted 202 species in the understory, 183 of which were native and 19 alien. The most common native species were *Asparagus acutifolius* (94%), *Sesleria autumnalis* (91%), *Brachypodium rupestre* (77%), *Rubus ulmifolius* (74%), and *Sonchus oleraceus* (69%). The most occurrent alien species were *Erigeron canadensis* (63%), *Senecio inaequidens* (37%), and *Phytolacca americana* (26%). A complete list of all the

species and their frequencies in the sampling plots is reported in the tab Supplementary Materials (Table S1).

The percentage of stem mortality of all sizes showed a positive and significant relationship (p-value < 0.001) with fire severity (expressed as increasing values of dNBR) (Fig. 2a), regardless of the species (i.e., p-value of the interaction between dNBR and species = 0.75; Table 2a). Among the four most frequent tree species, *Quercus pubescens* exhibited the lowest mean overall stem mortality, while the other three species (*Fraxinus ornus*, *Cotinus coggygria* and *Ostrya carpinifolia*) did not show any significant difference (Fig. 2b).

The percentage of resprouting stumps across species in each plot was positively correlated with wildfire severity, showing a logistic increase of resprouting as dNBR increased ($R^2 = 0.21$, p-value = 0.056; Table 2b; Fig. 2c) with different responses among the four most common tree species. *Cotinus coggygria* showed the highest resprouting capacity as the fire severity increases, while *Ostrya carpinifolia* had almost no increase (p-value = 0.055). *Quercus pubescens* was characterized by the lowest value of resprouting percentage (p-value = 0.021), while the other 3 species had no difference.

On the contrary, the number of new seedlings (i.e., species recruitment) decreased with increasing the fire severity ($R^2 = 0.37$, p-value = 0.081; Fig. 2d; Table 2c) with *Quercus pubescens* characterized by a greater decrease when compared with *Ostrya carpinifolia* (p-value = 0.064). *Cotinus coggygria* was the species with the highest mean value of new seedling (p-value < 0.001), while the other 3 species showed no differences. We found 13 new woody alien trees of *Ailanthus altissima* across all plots, with a mean height of 18 cm and a mean cover of 0.15%.

EFFIS class	n. plots	Alive stems			Dead stems		
		N ha-1	m2 ha-1	davg (cm)	N ha-1	m2 ha-1	davg (cm)
Control	5	4846 ± 3030	25.11 ± 7.53	10 ± 6	458 ± 370	1.16 ± 0.86	5 ± 3
Low and moderate severity	15	1668 ± 1283	12.89 ± 8.63	9 ± 5	3638 ± 1703	7.52 ± 3.01	6 ± 2
Moderate high severity	10	358 ± 399	5.04 ± 6.24	10 ± 8	3502 ± 1059	13.55 ± 8.84	7 ± 3
High severity	5	30 ± 67	0.01 ± 0.02	0 ± 1	3323 ± 1281	15.53 ± 8.03	8 ± 2

Table 1 Main dendrometry parameters in the surveyed plots by EFFIS class and control (mean ± s.d.).

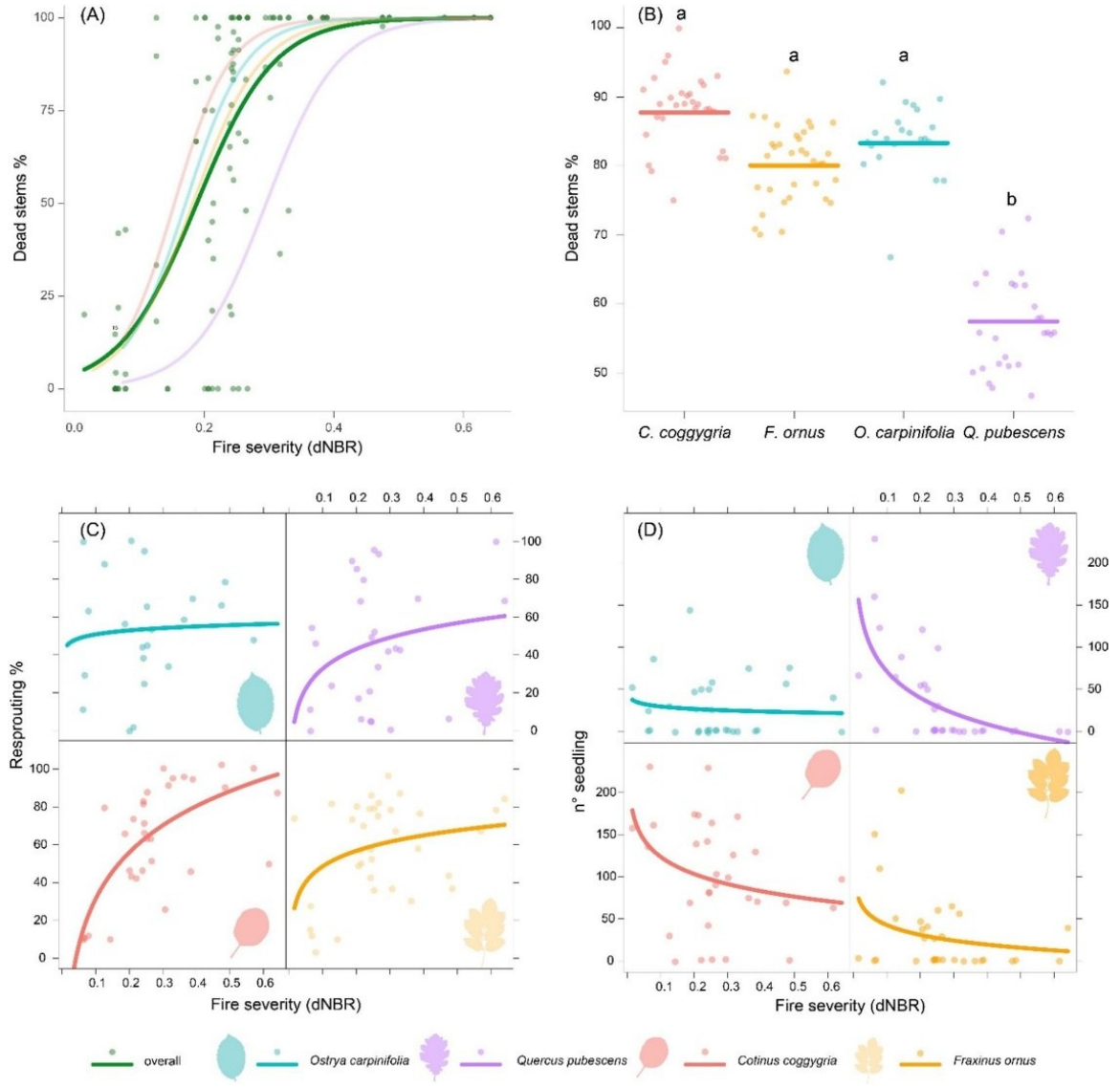


Figure 2 Effect plots of the tested models. A Percentage of dead stems of the 4 most common tree species. In the graphs are displayed the 4 curves, one for each species considered (i.e., F. *ornus*, *C. coggygria*, *O. carpinifolia*, *Q. pubescens*) with colored line, while the solid green line represents the overall mortality. B The difference in mortality percentage between species. C Relationship between percentage of plants with resprouting and logarithm of dNBR of the 4 species considered. D Relationship between square root of number of seedling (i.e., recruitment potential) and dNBR of the four most frequent species.

		numDF	Deviance	Resid. Dev	*p*-value
Tree mortality	(Intercept)	113		990.4	**0.004**
(a)	dNBR	112	48.03	51.00	**< 0.001**
	Species	109	17.54	33.46	**< 0.001**
		numDF	**denDF**	***F*-value**	***p*-value**
Resprouting	(Intercept)	1	75	315.15	**< 0.001**
(b)	log(dNBR)	1	33	12.45	**0.001**
	Species	3	75	1.87	0.143
	log(dNBR):species	3	75	2.64	**0.056**
N° of seedlings	(Intercept)	1	88	113.12	**< 0.001**
(c)	log(dNBR)	1	31	14.45	**< 0.001**
	Species	3	88	16.23	**< 0.001**
	log(dNBR):species	3	88	2.32	**0.081**

Table 2 ANOVA of the "GLMM" and of "LMM" models. The p-value is highlighted in bold when p-value < 0.05. We considered as significant also the p-value obtained in the (b) and (c) model with the interaction of dNBR and the species, given the proximity with 0.05.

		umDF	denDF	*F*-value	*p*-value
Species richness (*Z* transformed)	(Intercept)	1	33	< 0.001	1.000
(a)	log(dNBR)	1	33	23.951	**< 0.001**
	Status	1	33	< 0.001	1.000
Plant abundance (*Z* transformed)	(Intercept)	1	33	0.611	0.440
(b)	log(dNBR)	1	33	4.247	**0.047**
	Status	1	29	0.464	0.501
	log(dNBR):Status	1	29	6.573	**0.016**

Table 3 ANOVA of the linear mixed models. The p-value is highlighted in bold when p-value < 0.05.

Fire severity also affected plant diversity independently of species status (i.e., native vs alien species showed no statistically significant difference, Table 2a). Species richness significantly increased with fire severity ($R^2 = 0.43$; p-value < 0.001; Table 3a; Fig. 3a).

Plant cover was affected by the interaction between fire severity and plant exotic status (Table 3b): alien cover was increased by high value of dNBR reaching a plateau at the highest severity values,

while native cover remained stable (Fig. 3b). A summary for each full model is reported in the Supplementary Materials (Table S2).

Species composition analysis revealed the presence of one major species turnover gradient indicated principally by the axis of the NMDS1, mainly related to the wildfire severity (Fig. 4). Along this gradient, the species composition showed a shift from species usually present in (i) mature forest habitats (i.e., *Ruscus aculeatus*, *Polygonatum odoratum*), to (ii) a transitional stage dominated by species typical of open forests and ecotones between forests and the karst dry grasslands (i.e., *Sesleria autumnalis*, *Dictamnus albus*), to (iii) species typically belonging to karst dry grasslands (i.e., *Centaurea jacea*, *Allium carinatum*, *Pentanema spiraeifolium*), and, finally, when the severity reached its maximum, (iv) to ruderal stage, often dominated by alien species (i.e. *Erigeron canadensis*, *Erigeron sumatrensis*). The environmental variables fitted to the two NMDS axes also showed a significant relationship between the understory species composition and main forest structure. More specifically, where tree stem mortality and resprouting were higher, the understory showed a high species richness as well as alien and annual species frequency. Along the NMDS2, it was also possible to note a gradient of nutrient availability, favoring more acquisitive species (i.e., high values of SLA).

Given the low frequency and data availability about the alien plant functional traits, the functional identity of the community (i.e., community-weighted mean of each trait CWM) was assessed without considering the status of the species.

We found a significant effect of fire severity on the selected traits of the understory community (Table 4). In particular, the community exhibited a higher nutrient indicator value where severity of wildfire was higher ($R^2 = 0.36$; Fig. 5a). The same trend was observed for light indicator value ($R^2 = 0.49$; Fig. 5b). High values of fire severity induced a decrease in plant community life span, as shown by the rapid increase in the percentage of annuals species ($R^2 = 0.54$; Fig. 5c). Similar trends were found for the community mean of SLA, which logistically increases with increasing fire severity ($R^2 = 0.19$; Fig. 5d). In addition, the community mean of reproductive traits (i.e., seed number and seed mass) were affected by fire severity that selected communities producing more seeds ($R^2 = 0.47$; Fig. 5e) and with a lower mass ($R^2 = 0.15$; Fig. 5f).

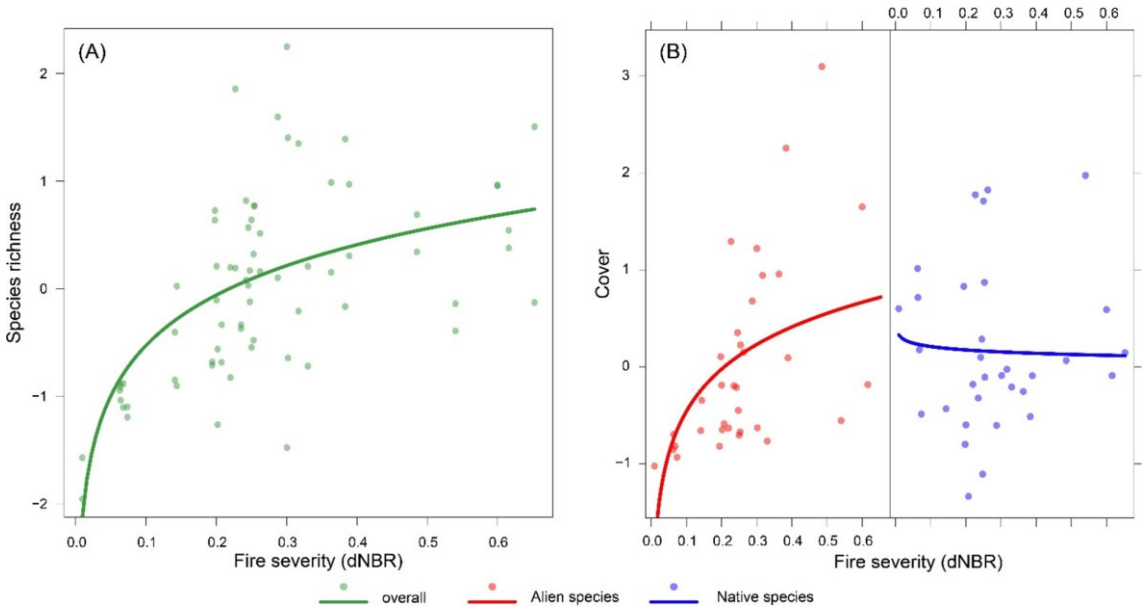


Figure 3 A Relationship between species richness (Z transformed) and the logarithm of dNBR. B Relationship between plant cover (Z transformed) and logarithm of dNBR divided for species status (i.e., alien or native).

Discussion

Remote sensing-derived fire severity was able to predict the gradual changes that occurred in a Karst forest ecosystem, shedding light on the complex ecological processes triggered by fire. We showed that wildfire severity increases the mortality and decreases resprouting of the tree layer. Our findings also suggested that fire is able to create new available niches, triggered by changes in light availability and soil nutrients, favoring the spread of annual, acquisitive species such as native ruderal and invasive alien species.

The species surveyed in the forest layer were consistent with previous research in the Karst, highlighting that the study area well-represents the forest association Ostryo-Quercetum pubescentis, previously described as the zonal vegetation (climax) of the supra-Mediterranean Karst (Favretto and Poldini 1985). The low frequency of alien trees (i.e., alien woody species above 1.3 m height) recorded in our sample plots (i.e., both burned and the external reference plots) can be linked to the ecological integrity and maturity of the selected forest stands and to the absence of previous large-scale disturbance events (Langmaier and Lapin 2020; Trotta et al., 2023a). In contrast, although native species dominate the herbaceous layer, the occurrence of several alien species in the burned areas highlighted the ongoing pressure of biological invasions in the area (Motard et al., 2015; Čahojová et al., 2024).

Our results showed that the response to fire severity by the tree layer is species-dependent. As expected, wildfire severity directly impacts the mortality of tree and shrub stems (Woolley et al., 2011). Overall, the studied stands seem to be resistant at low severity, but, once the severity is too high, the

stem mortality raises logistically to the 100% (Fig. 2a). Among the four most frequent and abundant tree species, *Quercus pubescens* appeared to be the most resistant species (Fig. 2b), consistently to previous studies (Falk et al., 2022). This species reaches higher heights, and the crown is therefore protected from surface fires; moreover, thicker bark insulates better the cambium (Pellegrini et al., 2017; Nemens et al., 2019; Cansler et al., 2020). In the burned area, the tree resprouting ability was promoted by fire, but species response was specific and contrasting (Fig. 2c). *Fraxinus ornus* and *Quercus pubescens* increase their resprouting ability with fire severity; the resprouting of *Ostrya carpinifolia* was not stimulated by increasing severity. The shrub species *Cotinus coggygria*, on the other hand, showed the highest stem mortality but concurrently the highest resilience, thanks to its high resprouting ability, an adaptation to the frequent surface fires occurring in its range. *Cotinus coggygria* ability to cope with fire events was already demonstrated (Pilon et al., 2021). Postfire seeding in our study was affected by increasing value of severity consistent with other studies (Crotteau et al., 2013).

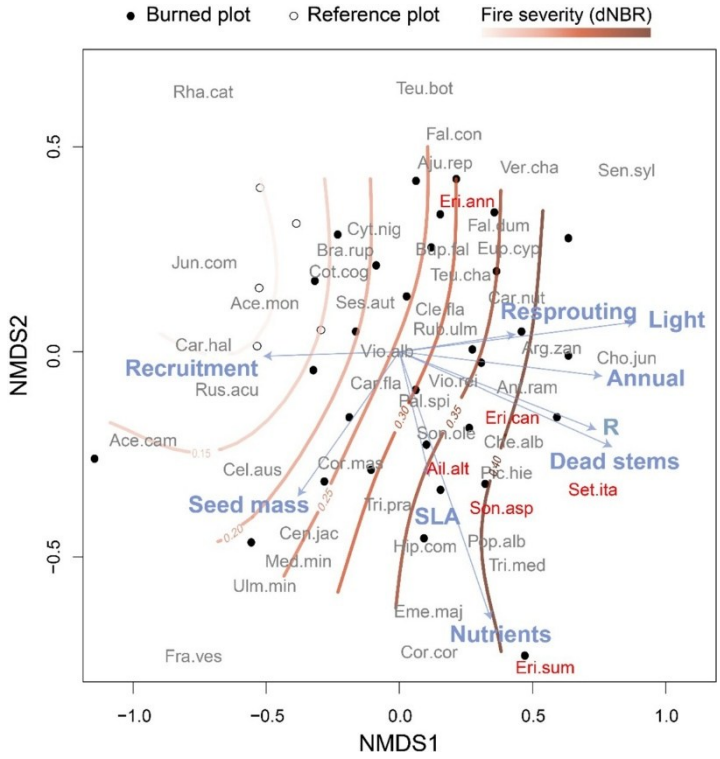


Figure 4 Non-metric multidimensional scaling (NMDS) ordination of the study. The red line represents the isoline of dNBR values. A selection of species was plotted according to species scores. Alien species are reported in red and native species in gray. The dots represent the site location (i.e., green unburned areas while orange burned areas). Significant correlation of Landolt's indicator values (Nutrients, Light), functional traits (SLA = specific leaf area, seed mass, annual = annual species), and collected parameters (R = species richness, resprouting, recruitment, trees' death). The reference for the species code is reported in Table S1.

		Df	Sum.sq	Mean.sq	*F*-value	*p*-value
Nutrients	Residuals	33	0.56158	0.017018		
(a)	log(dNBR)	1	0.31360	0.313602	18.428	**< 0.001**
Light	Residuals	33	1.0498	0.03181		
(b)	log(dNBR)	1	1.0201	1.02012	32.068	**< 0.001**
Percentage annuals species	Residuals	33	867.43	26.29		
(c)	log(dNBR)	1	1011.78	1011.78	38.491	**< 0.001**
SLA	Residuals	33	137.01	4.152		
(d)	log(dNBR)	1	31.82	31.820	7.6642	**0.0092**
Seed mass (mg)	Residuals	32	19,878.9	621.2		
(e)	dNBR	1	3359.9	3359.9	5.4086	**0.027**
Seed number (per plant)	Residuals	29	107,990,777	3,723,820		
(f)	log(dNBR)	1	93,672,314	93,672,314	25.155	**< 0.001**

Table 4 ANOVA of the linear models. The p-value is highlighted in bold when p-value < 0.05.

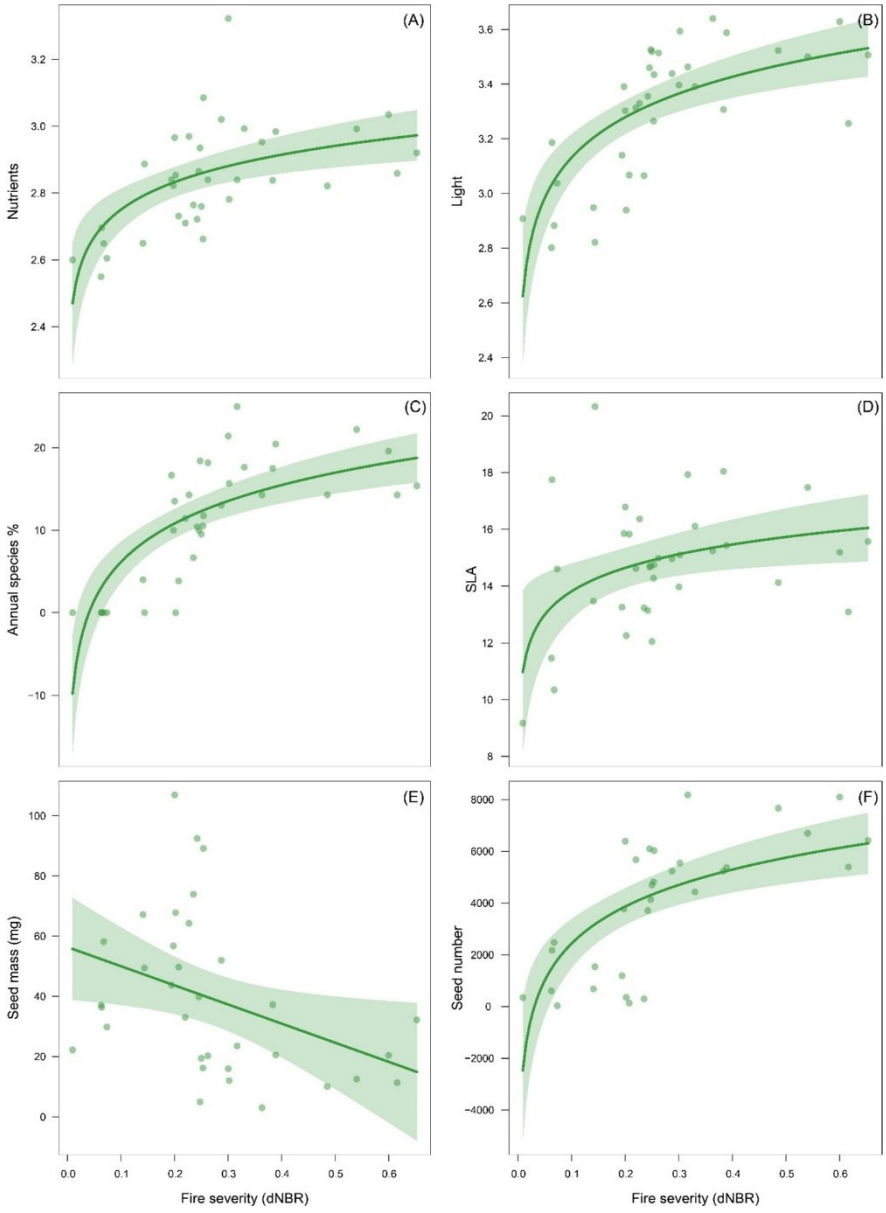


Figure 5 Relationship between functional identity indices and dNBR. In particular, (A) relationship with Landolt's indicator values of nutrients, (B) Landolt's indicator values of light request, (C) percentage of annual species, (D) specific leaf area, (E) seed mass, and (F) seed number. All the parameters are the community-weighted mean values.

Interestingly, the species with the lowest number of seedling recruitment was *Quercus pubescens*, while *Ostrya carpinifolia* was not affected by fire severity showing a constant low number of seedlings in the sample areas. This can suggest a life history tradeoff for the species *Quercus pubescens*, investing more in resistance of the single tree instead of promoting resilience capability. Altogether, our data showed that the higher was the fire severity, the higher was the possibility to move the forest community towards initial development stages dominated by the shrub *Cotinus coggygria* and some scattered *Quercus*

pubescens surviving the disturbance event. This novel community might slow down the succession of the Karst forest, limiting the growth of new Quercus sp. seedlings (Gavinet et al., 2019) mainly due to allelopathic substances released in the soil which affect the germination. The interplay between species in the tree germination is still a poorly understood mechanism, but our result, together with other findings in the literature, seems to confirm that *Cotinus coggygria* may take advantage in the germination process (Rey Benayas et al., 2005; Gavinet et al., 2016). Once the shrub layer is established, all the vegetation succession is delayed by the high amount of stem density created by the shrub layer. This layer limits the resources for the Quercus sp. seedlings to establish; therefore, more time is needed for the fully recover (Vesk et al., 2008). This appears a crucial aspect for ecosystem restoration after fire disturbance, especially in the face of an increasing number of extreme wildfire events in the Karst area following the ongoing climate change, which could favor an intermediate succession dominated by *Cotinus coggygria*.

As far as the herbaceous layer is concerned, fire severity increased the overall species richness, independent to their exotic status (i.e., not significant interaction). Indeed, high fire severity promote habitat heterogeneity when compared with the initial forest stage (Agee 1993; Perry et al., 2011), by increasing the number of available niches (Burkle et al., 2015). In particular, environmental heterogeneity promotes a scattered distributions of clustered populations of species that colonized the new available niches across habitats (Myers et al., 2015; Dawe et al., 2022; Trotta et al., 2023a). Among the colonizers, increasing fire severity appears to create the perfect condition for pioneer and ruderal species, most of them alien (e.g., *Erigeron canadensis*, *Erigeron sumatrensis*). Consistently with other studies, our results suggest that alien cover is enhanced by fire severity (Reilly et al., 2020; Trotta et al., 2023b), significantly shifting their relative abundance contribution to the whole understory community. This potential shift in abundance was also associated to a gradual species turnover induced by fire severity. In particular, we showed fire severity is a significant gradient mimicking the departure from climax vegetation along a vegetation succession. Here, the disturbance intensity (fire severity) well represents the floristic distance of burned vegetation to the unburned forest, potentially triggering different pathways to the restoration of the original understory vegetation cover (Dawe et al., 2022). A mid-severity is partially replacing the original understory, favoring some characteristic species of open forest and Karst dry grassland. This intermediate disturbance level seems hence to promote biodiversity by creating new opportunities for light demanding species, consistently to what observed in other forests due to intensive coppice management (Della Longa et al., 2020). A more severe fire is, instead, able to trigger a dramatic change in the forest understory with a main forest species replacement in favor to ruderal and alien species. This is probably due to the higher light availability but also to the great availability of bare soil to colonize as well as to the immediate increase of nutrient supply generated by burned organic matter in the first year after the fire event (Fuentes-Ramirez et al., 2018). These speculations are indirectly supported by the CWM indicator values

calculated for nutrients and light request. In particular, our analysis showed that plant community had a higher demand for nutrients and light in areas subjected to the most intense fire, probably due to the low canopy cover and the soil nutrient enrichment after the fire (Hobbs and Huenneke 1992). This confirms what found in literature where it was observed that nutrients increase during the early stage of forest recovery (i.e., 1 year after the fire) according to fire severity, while total nitrogen, total carbon, and soil organic matter exhibited a long-term nutrient depletion, especially in areas affected by high severity burning (Francos et al., 2018; Fuentes-Ramirez et al., 2018).

Consistently to previous studies, we found fire severity to affect changes in recovery and succession in plant communities via changes not only on species composition but also on functional trait community identity (Anderson-Teixeira et al., 2013; Poulos et al., 2020; Liang and Hurteau 2023). Our results on the functional identity of the newly formed herbaceous community (i.e., CWM of each considered trait) have given new insight on the traits that are promoted by wildfire severity. The new community was dominated by annual plants and by plants with higher SLA. Both these traits are generally associated with fast-growing species as they confer an advantage in environment with high supply of resources, allowing the plant to rapidly occupy the new niches available (Montesinos 2022). The functional trait filter induced by fire contributes to explain the high abundance (i.e., cover value) of alien and ruderal plants; plant guilds generally well adapted species to resource-rich environments (D'Antonio 1999). The reproductive strategy selected by fire severity underlines the changes in the functional identity of the understory. The new community exhibits plants that produce light seeds (small) but in large quantity. These two characteristics are often associated with a disturbed environment where, although seed mass is an important parameter in determining the establishment of seedlings (Howe et al., 1985; Kidson and Westoby 2000), the spread velocity (and then the colonization success) is higher by increasing the propagule pressure (Martínez-Ghersa and Ghersa 2006). We expect that the normal evolution of a forest affected by wildfire will be a gradual recolonization by forest specialist and at the end the full recovery of the forest community, with the disappearance of the ruderal and alien species given the right amount of time (Trotta et al., 2023a). In the future, we are planning to conduct a study aiming at elucidating the process through a chronosequence of wildfires in the Karst landscape.

Our study uniquely demonstrates how fire severity can strongly alter the initial response, diversity, and functional identity of the Karst ecosystems, therefore highlighting the need for conservation strategies aimed at limiting fire damages through prevention measures. Wildfires are common in the area: more than 190 fires have occurred within the Italian Karst since 1970. Fortunately, most of them were less than 1 ha in area probably thanks to an active land governance (Spadoni et al., 2023). A well-managed land use mosaic, where pastoral and forestry activities are supported and maintained, can reduce fuel load and continuity, thus helping to decrease the spread, intensity, and severity of fires (Moreira et al., 2011, 2020; Corona et al., 2015; Colonico et al., 2022). However, local or

fragmented initiatives might result ineffective, especially in a scenario of increasing frequency of extreme fire events (Ascoli et al., 2023). In fact, integrated solutions which involve different sectoral policies (e.g., forestry, agriculture, nature conservation, energy, tourism) within a unified strategy for managing wildfire risk can mitigate more efficiently the effects of wildfires at landscape scale (Ascoli et al., 2023). Our results suggest that, from a management perspective, policies need to promote more resilient species in fire-prone areas, as these species can help improve ecosystem resilience. In addition, to limit the spread of alien species, it is essential to reduce the spread of fast-growing annual species, which tend to increase in the seed bank when there is fragmentation due to agricultural and urban environments or forest tracks (Boscutti et al., 2022).

Conclusions

We evidenced that remote sensing-derived fire severity was an effective tool to depict a fine-tuned picture of the gradual changes occurring in broadleaf forest after a fire event. Our results highlighted the vulnerability of temperate Karst forest to a high level of fire severity, as that forecasted following the ongoing change in climate, resulting in significant tree stem mortality and potential long-term changes in tree community structure and composition. The fire might promote a rapid transition to a shrub-dominated community (i.e., *Cotinus coggygria*) promoting a long-lasting shrub stand potentially affecting the future dynamic nature of postfire succession. Furthermore, our study highlights the role of fire severity in shaping herbaceous community dynamics: high severity fires promote habitat heterogeneity and niche availability, leading to an increase in species richness and a change in functional identity. Such an increase is accompanied by a shift towards pioneer and ruderal species, many of which are alien, potentially threatening native biodiversity. Overall, our study highlights the complex interactions between wildfire severity, vegetation dynamics, and functional traits and emphasizes the need for conservation and management practices considering the effects of high severity fire on ecosystem resilience and biodiversity.

References

Autonomous Friuli Venezia Giulia Region. 2023. Forest fire perimeter of Friuli Venezia Giulia.

Avetisyan, D., N. Stankova, and Z. Dimitrov. 2023. Assessment of spectral vegetation indices performance for post-fire monitoring of different forest environments. Fire 6:290. https://doi.org/10.3390/fire6080290.

Badeau, J., F. Guibal, P.Z. Fulé, S. Chauchard, P. Moneglia, and C. Carcaillet. 2024. 202 years of changes in Mediterranean fire regime in Pinus nigra forest. Corsica. Forest Ecology and Management 554:121658. https://doi.org/10. 1016/j.foreco.2023.121658.

Bartolucci, F., L. Peruzzi, G. Galasso, A. Albano, A. Alessandrini, N. M. G. Ardenghi, et al., 2018. An updated checklist of the vascular flora native to Italy. Plant Biosystems an International Journal Dealing with All Aspects of Plant Biology 152: 179–303. https://doi.org/10.1080/11263 504.2017.1419996.

Bates D, Mächler M, Bolker B, Walker S. 2015. Fitting linear mixed-effects models using lme4. Journal of Statistical Software 67:1–48. https://doi.org/10. 18637/jss.v067.i01.

Blackburn, T. M., P. Cassey, R. P. Duncan, K. L. Evans, and K. J. Gaston. 2004. Avian extinction and mammalian introductions on oceanic islands. Science 305:1955–1958. https://doi.org/10.1126/science.1101617.

Bond, W. J., F. I. Woodward, and G. F. Midgley. 2005. The global distribution of ecosystems in a world without fire. New Phytologist 165:525–538. https://doi.org/10.1111/j.1469-8137.2004.01252.x.

Boscutti, F., E. Pellegrini, V. Casolo, M. de Nobili, M. Buccheri, and G. Alberti. 2020. Cascading effects from plant to soil elucidate how the invasive Amorpha fruticosa L. impacts dry grasslands. Journal of Vegetation Science 31:667–677.

Boscutti, F., F. Lami, E. Pellegrini, M. Buccheri, F. Busato, F. Martini, et al., 2022. Urban sprawl facilitates invasions of exotic plants across multiple spatial scales. Biological Invasions 24: 1497–1510. https://doi.org/10.1007/ s10530-022-02733-6.

Bowman, D. M. J. S., J. K. Balch, P. Artaxo, W. J. Bond, J. M. Carlson, M. A. Cochrane, et al., 2009. Fire in the Earth System. Science 324: 481–484. https://doi.org/10.1126/science.1163886.

Bowman, D. M., G. J. Williamson, J. T. Abatzoglou, C. A. Kolden, M. A. Cochrane, and A. M. Smith. 2017. Human exposure and sensitivity to globally extreme wildfire events. Nature Ecology & Evolution 1:0058.

Breheny, P., and W. Burchett. 2017. Visualization of regression models using visreg. R J 9:56.

Brooks, M. L., C. M. D'Antonio, D. M. Richardson, J. B. Grace, J. E. Keeley, J. M. DiTomaso, et al., 2004. Effects of invasive alien plants on fire regimes. BioScience 54:677–688. https://doi.org/10.1641/0006-3568(2004) 054[0677:EOIAPO]2.0.CO;2.

Burkle L. A, Myers J. A, Belote R. T. 2015. Wildfire disturbance and productivty as drivers of plant species diversity across spatial scales. Ecosphere 6:art202. https://doi.org/10.1890/ES15-00438.1.

Čahojová L, Jakob A, Breg Valjavec M, Čarni A. 2024. Response of vulnerable karst forest ecosystems under different fire severities in the Northern Dinaric Karst mountains (Slovenia). Fire Ecology 20:38. https://doi.org/10. 1186/s42408-024-00267-x.

Cansler, C. A., S. M. Hood, J. M. Varner, P. J. van Mantgem, M. C. Agne, R. A. Andrus, et al., 2020. The Fire and Tree Mortality Database, for empirical modeling of individual tree mortality after fire. Science Data 7: 194. https://doi.org/10.1038/s41597-020-0522-7.

Cardil, A., B. Mola-Yudego, Á. Blázquez-Casado, and J. R. González-Olabarria. 2019. Fire and burn severity assessment: Calibration of relative differenced normalized burn ratio (RdNBR) with field data. Journal of Environmental Management 235:342–349. https://doi.org/10.1016/j. jenvman.2019.01.077.

Carrión, J. S., P. Sánchez-Gómez, J. F. Mota, R. Yll, and C. Chaín. 2003. Holocene vegetation dynamics, fire and grazing in the Sierra de Gádor, southern Spain. The Holocene 13:839–849. https://doi.org/10.1191/0959683603 hl662rp.

Cavender-Bares, J., K. Kitajima, and F. A. Bazzaz. 2004. Multiple trait associations in relation to habitat differentiation among 17 Floridian oak species. Ecological Monographs 74:635–662. https://doi.org/10.1890/03-4007.

Cingano, P., M. Vuerich, F. Petruzzellis, L. Orzan, G. Trotta, V. Casolo, et al., 2024. Seagrasses on the move: Tracing the multi-decadal species distribution trends in lagoon meadows using Landsat imagery. Ecological Informatics 82: 102685. https://doi.org/10.1016/j.ecoinf.2024.102685.

Clarke, H., C. Lucas, and P. Smith. 2013. Changes in Australian fire weather between 1973 and 2010. International Journal of Climatology 33:931–

944. https://doi.org/10.1002/joc.3480.

Colonico, M., A. Tomao, D. Ascoli, P. Corona, F. Giannino, J.V. Moris, et al., 2022. Rural development funding and wildfire prevention: Evidences of spatial mismatches with fire activity. Land Use Policy 117:106079. https:// doi.org/10.1016/j.landusepol.2022.106079.

Cornelissen, J. H., S. Lavorel, E. Garnier, S. Díaz, N. Buchmann, D. E. Gurvich, et al., 2003. A handbook of protocols for standardised and easy measurement of plant functional traits worldwide. Australian Journal of Botany 51:335–380.

Corona, P., D. Ascoli, A. Barbati, G. Bovio, G. Colangelo, M. Elia, V. Garfì, F. Iovino, R. Lafortezza, and V. Leone. 2015. Integrated forest management to prevent wildfires under Mediterranean environments. Annals of Silvicultural Research 39:1–22.

Crotteau, J. S., J. Morgan Varner, and M. W. Ritchie. 2013. Post-fire regeneration across a fire severity gradient in the southern Cascades. Forest Ecology and Management 287:103–112. https://doi.org/10.1016/j.foreco.2012. 09.022.

Cucchi, F., L. Zini, and C. Calligaris, eds. 2015. Le acque del Carso Classico: Progetto Hydrokarst = Vodonosnik klasičnega Krasa: Projekt Hydrokarst. Trieste: EUT Edizioni Università di Trieste.

D'Antonio, C. M., and P. M. Vitousek. 1992. Biological invasions by exotic grasses, the grass/fire cycle, and global change. Annual Review of Ecology and Systematics 23:63–87.

D'Antonio C. M. 1999. Disturbance and biological invasions: direct effects and feedbacks. Á In: Walker, L. R (ed.), Ecosystems of disturbed ground. Elsevier, pp. 413Á.

Dawe, D. A., M.-A. Parisien, A. Van Dongen, and E. Whitman. 2022. Initial succession after wildfire in dry boreal forests of northwestern North America. Plant Ecology 223:789–809. https://doi.org/10.1007/ s11258-022-01237-6.

Della Longa, G., F. Boscutti, L. Marini, and G. Alberti. 2020. Coppicing and plant diversity in a lowland wood remnant in North-East Italy. Plant Biosystems-an International Journal Dealing with All Aspects of Plant Biology 154:173–180.

Donato, D. C., J. B. Fontaine, W. D. Robinson, J. B. Kauffman, and B. E. Law. 2009. Vegetation response to a short interval between high-severity wildfires in a mixed-evergreen forest. Journal of Ecology 97:142–154. https://doi. org/10.1111/j.1365-2745.2008.01456.x.

EFFIS Fire Severity. 2020. In: European Forest Fire Information System EFFIS. https://effis.jrc.ec.europa.eu/about-effis/technical-background/fire-severity. Accessed 27 Jul 2022.

Eidenshink J, Schwind B, Brewer K, Zhu Z. L, Quayle B, Howard S. 2007. A project for monitoring trends in burn severity. Fire Ecology 3:3–21. https:// doi.org/10.4996/fireecology.0301003

Escuin, S., R. Navarro, and P. Fernández. 2008. Fire severity assessment by using NBR (Normalized Burn Ratio) and NDVI (Normalized Difference

Vegetation Index) derived from LANDSAT TM/ETM images. International Journal of Remote Sensing 29:1053–1073. https://doi.org/10.1080/01431 160701281072.

Falk, D. A., P. J. van Mantgem, J. E. Keeley, R. M. Gregg, C. H. Guiterman, A. J. Tepley, et al., 2022. Mechanisms of forest resilience. Forest Ecology and Management 512:120129. https://doi.org/10.1016/j.foreco.2022.120129.

Favretto, D., and L. Poldini. 1985. The vegetation in the dolinas of the Karst region near Trieste (Italy). Studia Geobotanica 5:5–18.

Francos, M., X. Úbeda, P. Pereira, and M. Alcañiz. 2018. Long-term impact of wildfire on soils exposed to different fire severities. A case study in Cadiretes Massif (NE Iberian Peninsula). Science of the Total Environment 615: 664–671. https://doi.org/10.1016/j.scitotenv.2017.09.311.

Frazier, A. E., C. S. Renschler, and S. B. Miles. 2013. Evaluating post-disaster ecosystem resilience using MODIS GPP data. International Journal of Applied Earth Observation and Geoinformation 21:43–52. https://doi.org/ 10.1016/j.jag.2012.07.019.

French, N. H. F., E. S. Kasischke, R. J. Hall, K. A. Murphy, D. L. Verbyla, E. E. Hoy, and J. L. Allen. 2008. Using Landsat data to assess fire and burn severity in the North American boreal forest region: An overview and summary of results. International Journal of Wildland Fire 17:443–462. https://doi. org/10.1071/WF08007.

Fuentes-Ramirez, A., M. Barrientos, L. Almonacid, C. Arriagada-Escamilla, and

C. Salas-Eljatib. 2018. Short-term response of soil microorganisms, nutrients and plant recovery in fire-affected Araucaria araucana forests. Applied Soil Ecology 131:99–106. https://doi.org/10.1016/j.apsoil.2018. 08.010.

Gaertner, M., A. Den Breeyen, C. Hui, and D.M. Richardson. 2009. Impacts of alien plant invasions on species richness in Mediterranean-type

ecosystems: A meta-analysis. Progress in Physical Geography 33:319–338. https://doi.org/10.1177/0309133309341607.

Galasso, G., F. Conti, L. Peruzzi, N. M. G. Ardenghi, E. Banfi, L. Celesti-Grapow, et al., 2018. An updated checklist of the vascular flora alien to Italy. Plant Biosystems an International Journal Dealing with All Aspects of Plant Biology 152:556–592. https://doi.org/10.1080/11263504.2018.1441197.

Gavinet, J., B. Prévosto, and C. Fernandez. 2016. Do shrubs facilitate oak seedling establishment in Mediterranean pine forest understory? Forest Ecology and Management 381:289–296. https://doi.org/10.1016/j.foreco. 2016.09.045.

Gavinet, J., M. Santonja, V. Baldy, H. Hashoum, S. Peano, T. Tchong, et al., 2019. Phenolics of the understory shrub Cotinus coggygria influence Mediterranean oak forests diversity and dynamics. Forest Ecology and Management 441:262–270. https://doi.org/10.1016/j.foreco.2019.03.049.

Gibson, R. K., L. A. White, S. Hislop, R. H. Nolan, and J. Dorrough. 2022. The post-fire stability index; a new approach to monitoring post-fire recovery by satellite imagery. Remote Sensing of Environment 280:113151. https:// doi.org/10.1016/j.rse.2022.113151.

Glenn-Lewin D. C., Peet R. K., Veblen T. T. 1992. Plant succession: theory and prediction. Springer Science & Business Media.

Hejda, M., P. Pyšek, and V. Jarošík. 2009. Impact of invasive plants on the species richness, diversity and composition of invaded communities. Journal of Ecology 97:393–403. https://doi.org/10.1111/j.1365-2745. 2009.01480.x.

Hobbs, R. J., and L. F. Huenneke. 1992. Disturbance, diversity, and invasion: Implications for conservation. Conservation Biology 6:324–337.

Howe, H. F., E. W. Schupp, and L. C. Westley. 1985. Early consequences of seed dispersal for a neotropical tree (Virola surinamensis). Ecology 66:781–791.

Ivanova, A. A., E. O. Kopylova-Guskova, A. B. Shipunov, and P. A. Volkova. 2014. Post-fire succession in the northern pine forest in Russia: A case study. Wulfenia 21:119–128.

Jodhani, K. H., H. Patel, U. Soni, R. Patel, B. Valodara, N. Gupta, A. Patel, and P. J. Omar. 2024. Assessment of forest fire severity and land surface temperature using Google Earth Engine: A case study of Gujarat State, India. Fire Ecology 20: 23. https://doi.org/10.1186/s42408-024-00254-2.

Jolly, W. M., M. A. Cochrane, P. H. Freeborn, Z. A. Holden, T.J . Brown, G. J. Williamson, and D. M. J. S. Bowman. 2015. Climate-induced variations in global wildfire danger from 1979 to 2013. Nature Communications 6:7537. https://doi.org/10.1038/ncomms8537.

Keeley, J. E. 2006. Fire management impacts on invasive plants in the western United States. Conservation Biology 20:375–384. https://doi.org/10.1111/j.1523-1739.2006.00339.x.

Keeley, J. E. 2009. Fire intensity, fire severity and burn severity: A brief review and suggested usage. International Journal of Wildland Fire 18:116. https://doi.org/10.1071/WF07049.

Kidson, R., and M. Westoby. 2000. Seed mass and seedling dimensions in relation to seedling establishment. Oecologia 125:11–17. https://doi.org/10. 1007/PL00008882.

Kleyer, M., R.M. Bekker, I.C. Knevel, J.P. Bakker, K. Thompson, M. Sonnenschein, et al., 2008. The LEDA Traitbase: A database of life-history traits of the Northwest European flora. Journal of Ecology 96:1266–1274.

Landolt, E., B. Bäumler, A. Ehrhardt, O. Hegg, F. Klötzli, W. Lämmler, et al., 2010. Flora indicativa: Okologische Zeigerwerte und biologischeKennzeichen zur Flora der Schweiz und der Alpen. Haupt, Bern. 378 pp.

Langmaier M, Lapin K. 2020. A systematic review of the impact of invasive alien plants on forest regeneration in European temperate forests. Frontiers Plant Science 11. https://doi.org/10.3389/fpls.2020.524969.

Lehmann, C. E. R., T. M. Anderson, M. Sankaran, S. I. Higgins, S. Archibald, W. A. Hoffmann, et al., 2014. Savanna vegetation-fire-climate relationships differ among continents. Science 343:548–552. https://doi.org/10.1126/ science.1247355.

Lenth, R. 2022. emmeans: Estimated marginal means, aka least-squares means. R Package Version 1 (7): 2.

Liang, S., and M. D. Hurteau. 2023. Novel climate–fire–vegetation interactions and their influence on forest ecosystems in the western USA. Functional Ecology 37:2126–2142.

Liu, Y., J. Stanturf, and S. Goodrick. 2010. Trends in global wildfire potential in a changing climate. Forest Ecology and Management 259:685–697. https:// doi.org/10.1016/j.foreco.2009.09.002.

Lutes D. C., Keane R. E., Caratti J. F., Key C. H., Benson N. C., Sutherland S, Gangi L. J. 2006. FIREMON: Fire effects monitoring and inventory system. U.S. Department of Agriculture, Forest Service, Rocky Mountain Research Station, Ft. Collins, CO.

Mancini, L. D., P. Corona, and L. Salvati. 2018. Ranking the importance of wildfires' human drivers through a multi-model regression approach. Environmental Impact Assessment Review 72:177–186. https://doi.org/10. 1016/j.eiar.2018.06.003.

Maringer, J., T. Wohlgemuth, A. Hacket-Pain, D. Ascoli, R. Berretti, and M. Conedera. 2020. Drivers of persistent post-fire recruitment in European beech forests. Sci Total Environ 699:134006. https://doi.org/10.1016/j.scitotenv. 2019.134006.

Martínez-Ghersa, M. A., and C. M. Ghersa. 2006. The relationship of propagule pressure to invasion potential in plants. Euphytica 148:87–96. https:// doi.org/10.1007/s10681-006-5943-7.

Miller J. D., Quayle B. 2015. Calibration and validation of immediate post-fire satellite-derived data to three severity metrics. Fire Ecology 11:12–30. https://doi.org/10.4996/fireecology.1102012.

Miller, J. D., and A. E. Thode. 2007. Quantifying burn severity in a heterogeneous landscape with a relative version of the delta normalized burn ratio (dNBR). Remote Sensing of Environment 109:66–80. https://doi.org/10. 1016/j.rse.2006.12.006.

Montesinos, D. 2022. Fast invasives fastly become faster: Invasive plants align largely with the fast side of the plant economics spectrum. Journal of Ecology 110:1010–1014. https://doi.org/10.1111/1365-2745.13616.

Moreira, F., O. Viedma, M. Arianoutsou, T. Curt, N. Koutsias, E. Rigolot, et al., 2011. Landscape – wildfire interactions in southern Europe: Implications for landscape management. Journal of Environmental Management 92:2389–2402. https://doi.org/10.1016/j.jenvman.2011.06.028.

Moreira, F., D. Ascoli, H. Safford, M. A. Adams, J. M. Moreno, J. M. C. Pereira, et al., 2020. Wildfire management in Mediterranean-type regions: Paradigm change needed. Environmental Research Letters 15:011001. https://doi. org/10.1088/1748-9326/ab541e.

Moris, J. V., M. J. Reilly, Z. Yang, W. B. Cohen, R. Motta, and D. Ascoli. 2022. Using a trait-based approach to asses fire resistance in forest landscapes of the Inland Northwest, USA. Landscape Ecology 37:2149–2164. https:// doi.org/10.1007/s10980-022-01478-w.

Morrison, D. A. 2002. Effects of fire intensity on plant species composition of sandstone communities in the Sydney region. Austral Ecology 27:433–441. https://doi.org/10.1046/j.1442-9993.2002.01197.x.

Motard, E., S. Dusz, B. Geslin, M. Akpa-Vinceslas, C. Hignard, O. Babiar, et al., 2015. How invasion by Ailanthus altissima transforms soil and litter communities in a temperate forest ecosystem. Biological Invasions 17:1817–1832. https://doi.org/10.1007/s10530-014-0838-3.

Müller, S. C., G. E. Overbeck, J. Pfadenhauer, and V. D. Pillar. 2007. Plant functional types of woody species related to fire disturbance in forest– grassland ecotones. Plant Ecology 189:1–14. https://doi.org/10.1007/ s11258-006-9162-z.

Myers, J.A., J.M. Chase, R.M. Crandall, and I. Jiménez. 2015. Disturbance alters beta-diversity but not the relative importance of community assembly mechanisms. Journal of Ecology 103:1291–1299. https://doi.org/10.1111/1365-2745.12436.

Nemens, D. G., J. M. Varner, and P. W. Dunwiddie. 2019. Resilience of Oregon white oak to reintroduction of fire. Fire Ecology 15:29. https://doi.org/10. 1186/s42408-019-0045-9.

Noble, I. R., and R. O. Slatyer. 1980. The use of vital attributes to predict successional changes in plant communities subject to recurrent disturbances. Vegetatio 43:5–21.

North, M. P., S. L. Stephens, B. M. Collins, J. K. Agee, G. Aplet, J. F. Franklin, and P. Z. Fulé. 2015. Reform forest fire management. Science 349:1280–1281. https://doi.org/10.1126/science.aab2356.

Oksanen, J., G. Simpson, F. Blanchet, R. Kindt, P. Legendre, P. Minchin, R. O'Hara, P. Solymos, M. Stevens, E. Szoecs, H. Wagner, M. Barbour, M. Bedward, B. Bolker, D. Borcard, G. Carvalho, M. Chirico, M. De Caceres, S. Durand, H. Evangelista, R. FitzJohn, M. Friendly, B. Furneaux, G. Hannigan, M. Hill, L. Lahti, D. McGlinn, M. Ouellette, E. Ribeiro Cunha, T. Smith, A. Stier, C. Ter Braak, and J. Weedon. 2024. vegan: Community Ecology Package. R package version 2.7-0. https://github.com/vegandevs/vegan, https:// vegandevs.github.io/vegan/.

Patacca, M., M. Lindner, M. E. Lucas-Borja, T. Cordonnier, G. Fidej, B. Gardiner, et al., 2023. Significant increase in natural disturbance impacts on European forests since 1950. Global Change Biology 29:1359–1376. https:// doi.org/10.1111/gcb.16531.

Pausas, J. G., and S. Fernández-Muñoz. 2012. Fire regime changes in the Western Mediterranean Basin: From fuel-limited to drought-driven fire regime. Climatic Change 110:215–226. https://doi.org/10.1007/ s10584-011-0060-6.

Pausas, J. G., and M. Verdú. 2005. Plant persistence traits in fire-prone ecosystems of the Mediterranean basin: A phylogenetic approach. Oikos 109:196–202.

Pausas, J. G., R. A. Bradstock, D. A. Keith, and J. E. Keeley. 2004. Plant functional traits in relation to fire in crown-fire ecosystems. Ecology 85:1085–1100.

Pejchar, L., and H.A. Mooney. 2009. Invasive species, ecosystem services and human well-being. Trends in Ecology & Evolution 24:497–504.

Pellegrini, A. F. A., W. R. L. Anderegg, C. E. T. Paine, W. A. Hoffmann, T. Kartzinel, S. S. Rabin, et al., 2017. Convergence of bark investment according to fire and climate structures ecosystem vulnerability to future change. Ecology Letters 20:307–316. https://doi.org/10.1111/ele.12725.

Pellegrini, E., F. Boscutti, G. Alberti, V. Casolo, M. Contin, and M. De Nobili. 2021. Stand age, degree of encroachment and soil characteristics modulate changes of C and N cycles in dry grassland soils invaded by the N2-fixing shrub Amorpha fruticosa. Science of the Total Environment 792:148295. https://doi.org/10.1016/j.scitotenv.2021.148295.

Penman, T.D., and A.L. Towerton. 2008. Soil temperatures during autumn prescribed burning: Implications for the germination of fire responsive species? International Journal of Wildland Fire 17:572–578. https://doi. org/10.1071/WF07092.

Perry, D.A., P.F. Hessburg, C.N. Skinner, T.A. Spies, S.L. Stephens, A.H. Taylor, et al., 2011. The ecology of mixed severity fire regimes in Washington, Oregon, and Northern California. Forest Ecology and Management 262:703–717. https://doi.org/10.1016/j.foreco.2011.05.004.

Pilon, N. A. L., M. G. B. Cava, W. A. Hoffmann, R. C. R. Abreu, A. Fidelis, and G. Durigan. 2021. The diversity of post-fire regeneration strategies in the cerrado ground layer. Journal of Ecology 109:154–166. https://doi.org/ 10.1111/1365-2745.13456.

Poldini, L., P. Ganis, M. Vidali, A. Altobelli, F. Bader, and S. Cantele. 2018. Inclusion of phytosociological data in an index of vegetation fire danger: Application and mapping on the Karst area around Trieste (Italy). Plant Biosystems an International Journal Dealing with All Aspects of Plant Biology 152:810–817. https://doi.org/10.1080/11263504.2017.1347110.

Poulos, H. M., A. M. Barton, G. P. Berlyn, D. W. Schwilk, C. E. Faires, and W. C. McCurdy. 2020. Differences in leaf physiology among juvenile pines and oaks following high-severity wildfire in an Arizona Sky Island Mountain range. Forest Ecology and Management 457:117704.

R Core Team. 2022. R: a language and environment for statistical computing. Vienna, Austria: R Foundation for Statistical Computing.

Raizada, P., A. S. Raghubanshi, and J. S. Singh. 2008. Impact of invasive alien plant species on soil processes: A review. Proceedings of the National Academy of Sciences India Section B–Biological Sciences 78:288–298.

Rapson, G. L. 2018. Changing methodology results in operational drift in the meaning of leaf area index, necessitating implementation of foliage layer index. Ecology and Evolution 8:638–644. https://doi.org/10.1002/ ece3.3662.

Reilly, M. J., M. G. McCord, S. M. Brandt, K. P. Linowksi, R. J. Butz, and E. S. Jules. 2020. Repeated, high-severity wildfire catalyzes invasion of non-native plant species in forests of the Klamath Mountains, northern California, USA. Biological Invasions 22:1821–1828. https://doi.org/10.1007/ s10530-020-02227-3.

Rey Benayas, J. M., J. Navarro, T. Espigares, J. M. Nicolau, and M. A. Zavala. 2005. Effects of artificial shading and weed mowing in reforestation of Mediterranean abandoned cropland with contrasting Quercus species. Forest Ecology and Management 212:302–314. https://doi.org/10.1016/j. foreco.2005.03.032.

Root, T. L., J. T. Price, K. R. Hall, S. H. Schneider, C. Rosenzweig, and J.A. Pounds. 2003. Fingerprints of global warming on wild animals and plants. Nature 421:57–60. https://doi.org/10.1038/nature01333.

San-Miguel-Ayanz, J., E. Schulte, G. Schmuck, et al., 2012. Comprehensive Monitoring of Wildfires in Europe: The European Forest Fire Information System (EFFIS). Approaches to Managing Disaster Assessing Hazards, Emergencies and Disaster Impacts. InTech. Available at: http://dx.doi.org/ 10.5772/28441.

Segura, A .M., M. Holmgren, J. J. Anabalón, and E. R. Fuentes. 1998. The significance of fire intensity in creating local patchiness in the Chilean matorral. Plant Ecology 139:259–264. https://doi.org/10.1023/A:10097 15328868.

Sellers, P. J., B. W. Meeson, F. G. Hall, G. Asrar, R. E. Murphy, R. A. Schiffer, et al., Try. 1995. Remote sensing of the land surface for studies of global change: Models — algorithms — experiments. Remote Sensing of Environment 51:3–26. https://doi.org/10.1016/0034-4257(94)00061-Q.

Senf, C., and R. Seidl. 2021. Mapping the forest disturbance regimes of Europe. Nat Sustain 4:63–70. https://doi.org/10.1038/s41893-020-00609-y.

Sharples, J. J., G. J. Cary, P. Fox-Hughes, S. Mooney, J. P. Evans, M. S. Fletcher, M. Fromm, P. F. Grierson, R. McRae, and P. Baker. 2016. Natural hazards in Australia: Extreme bushfire. Climatic Change 139:85–99.

Sousa, W. P. 1984. The role of disturbance in natural communities. Annual Review of Ecology and Systematics 15:353–391.

Spadoni, G. L., J. V. Moris, G. Vacchiano, M. Elia, M. Garbarino, E. Sibona, et al., Ascoli. 2023. Active governance of agro-pastoral, forest and protected areas mitigates wildfire impacts in Italy. Science of the Total Environment 890:164281. https://doi.org/10.1016/j.scitotenv.2023.164281.

Šturm, T., and T. Podobnikar. 2017. A probability model for long-term forest fire occurrence in the Karst forest management area of Slovenia. International Journal of Wildland Fire 26:399–412. https://doi.org/10.1071/ WF15192.

Tedim, F., V. Leone, M. Amraoui, C. Bouillon, M. R. Coughlan, G. M. Delogu, P. M. Fernandes, C. Ferreira, S. McCaffrey, and T.K. McGee. 2018. Defining extreme wildfire events: Difficulties, challenges, and impacts. Fire 1:9.

Trotta, G., F. Boscutti, A. Jamoneau, G. Decocq, and A. Chiarucci. 2023a. There is room for everyone: Invasion credit cannot be inferred from the species–area relationship in fragmented forests. Applied Vegetation Science 26:e12745. https://doi.org/10.1111/avsc.12745.

Trotta, G., M. Vuerich, E. Petrussa, F. R. Hay, S. Assolari, and F. Boscutti., 2023c. Germination performance of alien and native species could shape community assembly of temperate grasslands under different temperature scenarios. Plant Ecology. https://doi.org/10.1007/ s11258-023-01365-7.

Trotta, G., M. Vuerich, E. Pellegrini, M. Vilà, E. Asquini, P. Cingano, and F. Boscutti. 2024. Containing alien plants in coastal dunes: Evidence from a soil manipulation experiment. Journal of Environmental Management 366:121780. https://doi.org/10.1016/j.jenvman.2024.121780.

Trotta G., Castello M., Petruzzellis F., Pischedda S., Boscutti F. 2023b. First record of naturalization of Erechtites hieraciifolius (L.) Raf. ex DC. (Asteraceae) in Italy. Natural History Sciences 10. https://doi.org/10.4081/nhs.2023.716.

Veraverbeke, S., S. Lhermitte, W. W. Verstraeten, and R. Goossens. 2011. A time-integrated MODIS burn severity assessment using the multi-temporal differenced normalized burn ratio (dNBRMT). International Journal of Applied Earth Observation and Geoinformation 13:52–58. https://doi.org/ 10.1016/j.jag.2010.06.006.

Vesk, P. A., R. Nolan, J. R. Thomson, J. W. Dorrough, and R. M. Nally. 2008. Time lags in provision of habitat resources through revegetation. Biological Conservation 141: 174–186. https://doi.org/10.1016/j.biocon.2007.09.010.

Vitti, S., E. Pellegrini, V. Casolo, G. Trotta, and F. Boscutti. 2020. Contrasting responses of native and alien plant species to soil properties shed new light on the invasion of dune systems. Journal of Plant Ecology 13:667–675. https://doi.org/10.1093/jpe/rtaa052.

Vuerich, M., P. Cingano, G. Trotta, E. Petrussa, E. Braidot, D. Scarpin, A. Bezzi, M. Mestroni, E. Pellegrini, and F. Boscutti. 2024. New perspective for the upscaling of plant functional response to flooding stress in salt marshes using remote sensing. Science and Reports 14:5472. https://doi.org/10. 1038/s41598-024-56165-4

Wickham, H. 2016. ggplot2: Elegant graphics for data abalysis. New York: Springer-Verlag.

Wildi, O. 2017. Data analysis in vegetation ecology. Wiley Blackwell. 236 pp. ISBN 978-0-470-66102-4.

Woolley, T., D. C. Shaw, L. M. Ganio, and S. Fitzgerald. 2011. A review of logistic regression model used to predict post-fire tree mortality of western North American conifers. International Journal of Wildfire 21:1-35. https://doi.org/10.1071/WF09039

Wooster, M. J., G. J. Roberts, L. Giglio, D. P. Roy, P. H. Freeborn, L. Boschetti, et al., 2021. Satellite remote sensing of active fires: History and current status, applications and future requirements. Remote Sensing of Environment 267:112694. https://doi.org/10.1016/j.rse.2021.112694

Zhang, D. 2023. rsq: R-Squared and Related Measures. R package version 2.6 https://CRAN.R-project

Zuur, A. F., E. N. Ieno, N. J. Walker, A. A. Saveliev, and G. M. Smith. 2009. Mixed effects models and extensions in ecology with R. Springer.

7.1.4. Lagoon Ecology

Functional traits and plant-soil feedback mechanisms in *Cymodocea nodosa* meadows

Paolo Cingano[1,2], Giacomo Boscarol[1], Francesco Boscutti[1]

1 University of Udine, 33100 Udine, Italy
2 University of Trieste, 34127 Trieste, Italy

Abstract

Seagrasses play a vital role in coastal ecosystems by providing essential ecosystem services, including oxygen production, carbon sequestration, shoreline stabilization, and the creation of habitats for diverse marine organisms (Duarte et al., 2013). At the seascape scale, in sheltered environments and in areas of recent colonization, seagrass meadows often display striking spatial patterns, such as circular vegetated patches, unvegetated gaps, or so-called fairy circles (Ruiz-Reynés et al., 2017). These patterns reflect the clonal growth dynamics of seagrass populations and can undergo rapid regime shifts, including sudden collapses that lead to bare patch centres. These mechanisms can be drastically influenced by the shifting regimes of seawater intrusions as the aftermaths of sea level rise.

The emergence and configuration of self-organized spatial patterns are closely linked to the ecological condition of seagrass communities, as they respond sensitively to environmental changes. Strong plant–plant and plant–soil feedback mechanisms have been identified as key drivers of these dynamics, indicating the presence of nonlinear responses to external environmental pressures (Maxwell et al., 2017). However, further experimental evidence are required for identifying the drivers behind sudden pattern shifts and the consequent rapid loss of entire meadows. Disentangling these processes is crucial for assessing the resilience and vulnerability of seagrass ecosystems under changing water regime and other environmental conditions.

To investigate these dynamics, 52 meadows of *Cymodocea nodosa* (Ucria) Asch. were sampled across a vast lagoon system in the Northern Adriatic Sea. Sampling was conducted at the patch scale along a gradient of patch age, targeting the edge and the centre of each patch, respectively. To characterize the age and clonal growth of the patches, patch diameter was measured and compared with historical orthophotos of the study area. At each location, above and belowground biomass, growth and functional traits (i.e, shoot density, leaf dry matter content, leaf area, leaf length, specific leaf area) of the species and sediment properties were collected. Statistical analyses were conducted using linear mixed-effects models to assess the effects of patch position and age on plant and soil variables. In addition, trait correlation networks were used to explore patterns of phenotypic integration across patch locations. Preliminary results indicated that, in the early stages of clonal growth, seagrass

patches tend to expand in terms of size, increasing total biomass and shoot density. However, over the long term, a progressive loss of above-ground biomass occurs in the central location of the patches, a phenomenon that, in some cases, leads to the formation of fairy circles. In contrast, we observed a consistent maintenance of below-ground biomass in the meadows over time, regardless of patch location, highlighting the ecological resilience associated with spatial pattern modification. Finally, correlation networks among plant traits at different patch locations reveal marked changes in phenotypic integration, emphasizing the need to further investigate plant–soil feedback mechanisms through a functional approach to gain a more comprehensive understanding of the ecological dynamics driving the formation of such spatial patterns.

References

Duarte CM, Losada IJ, Hendriks IE, Mazarrasa I, Marbà N. The role of coastal plant communities for climate change mitigation and adaptation. Nature Clim Change. 2013;3(11):961–8. .

Ruiz-Reynés D, Gomila D, Sintes T, Hernández-García E, Marbà N, Duarte CM. Fairy circle landscapes under the sea. Science Advances. 2017;3(8):e1603262.

Maxwell PS, Eklöf JS, Van Katwijk MM, O'Brien KR, De La Torre-Castro M, Boström C, et al. The fundamental role of ecological feedback mechanisms for the adaptive management of seagrass ecosystems - a review: Review of feedbacks in seagrass. Biol Rev. 2017;92(3):1521–38.

7.1.5. River Ecology

Monitoring Tagliamento river dynamics from a biodiversity and landscape perspective

Giacomo Boscarol[1], Giacomo Trotta[2,1], Maurizia Sigura[1], Valentino Casolo[1,3], Elisa Pellegrini[1], Giorgio Alberti[1,3], Marco Vuerich[1,3], Daniel Moro[2,1], Sara Gargiulo[2,1], Edoardo Asquini[4,3,1], Paolo Cingano[2,1], Daniéle Lagnaz[5], Florent Jouy[6], Jana Chmieleski[7], Michał Habel[8], Dawid Szatten[8], Marta Brzezińska[8], Francesco Boscutti[1,3]

1 University of Udine, Udine, Italy
2 University of Trieste, Trieste, Italy
3 National Biodiversity Future Centre, Palermo, Italy
4 University of Palermo, Palermo, Italy
5 Zurich University of Applied Science, Zurich, Switzerland
6 Eberswalde University for Sustainable Development, Eberswalde, Germany
7 Nationalpark Unteres Odertal, Germany
8 Kazimierz Wielki University, Bydgoszcz, Poland

Abstract

Rivers play a critical role in biodiversity conservation and ecological connectivity. Understanding how plant communities vary in these dynamic systems and how their changes are visible using remote sensing is crucial for implementing effective conservation strategies. The Tagliamento river (N-E Italy) is characterized by flood events and a wide pristine gravel-bed where river bars are characterized by complex habitats corresponding to different successional stages. It is therefore subjected to nature conservation initiatives.

In this area, 51 plots of 100 m² area have been sampled during 2022 and 2023 seasons, within an Erasmus+ program involving four European countries. In each plot we performed vegetation surveys and collected soil data. Moreover, we analysed satellite images back to the 1980s to calculate principal multispectral indices and the age of the river bars. We found satellite-derived indices very effective in tracing changes of vegetation over time. NDVI was strongly positively related to the river bars age. Moreover, the plant functional diversity of the community appears to be driven by the river bars age and linked to the NDVI.

Our results provide new insights into the dynamics of riverbed vegetation and the application of satellite imagery for remote sensing and conservation of these valuable habitats.

7.2. Conferences – Oral Communications

Asquini E., **Boscarol G.**, Cingano P., Trotta G., Paniccia D., Vuerich M., Zandigiacomo P., Boscutti F. When fens flower again: assessing restoration outcomes through plant–pollinator networks. In: II International Symposium on Biodiversity and Ecosystem Functions under Global Change, 12-14 November 2025, Alghero (Sassari), Italy.

Boscarol G., Vuerich M., Di Francesco A., Boscutti F., Volpe V., Fabro M., Braidot E., Petrussa E. Ecophysiological response of maize (*Zea mays* L.) to water stress: remote sensing and upscaling techniques for a more efficient management of water resources in agriculture. In: 7th Joint Workshop of the agriculture-oriented PhD Programs, 29 September – 03 October 2025, Udine, Italy.

Vuerich M., Asquini E., **Boscarol G.**, Braidot E., Carbognani M., Chiari G., Cingano P., Del Pino A., Forte T.G.W., Grillo F., Petraglia A., Trotta G., Zancani M., Boscutti F. The role of duration and timing of induced heat waves in shaping plant community of alpine grasslands: an upscaling approach. In: 120th annual congress of the Italian Botanical Society (SBI) – XI International Plant Science Conference, 03-06 September 2025, Gorizia, Italy.

Asquini E., **Boscarol G.**, Cingano P., Trotta G., Paniccia D., Vuerich M., Zandigiacomo P., Boscutti F. Assessing restoration success through plant–pollinator networks in lowland wetlands. In: 120th annual congress of the Italian Botanical Society (SBI) – XI International Plant Science Conference, 03-06 September 2025, Gorizia, Italy.

Boscarol G., Petrussa E., Trotta G., Boscutti F., Scarpin D., Braidot E., Volpe V., Barbieri S., Fabro M., Vuerich M. Novel approach to link the physiological response of maize (*Zea mays* L.) to drought and the occurrence of mycotoxins. In: XX International Botanical Congress (IBC), 21-27 July 2024, Madrid, Spain.

Boscarol G., Trotta G., Sigura M., Casolo V., Pellegrini E., Alberti G., Vuerich M., Moro D., Gargiulo S., Asquini E., Cingano P., Lagnaz D., Jouy F., Chmieleski J., Habel M., Szatten D., Brzezińska M., Boscutti F. Depicting vegetation dynamics along the Tagliamento river bars: a remote sensing approach to monitor biodiversity in alpine rivers. In: 7th European Congress of Conservation Biology (ECCB), 17-21 June 2024, Bologna, Italy.

Boscarol G., Braidot E., Petrussa E. Ecophysiological response of maize (*Zea mays* L.) to water stress: remote sensing and upscaling techniques for a more efficient management of water resources in agriculture. In: 5th Joint Workshop of the agriculture-oriented PhD Programs, 25-28 September 2023, Catania, Italy.

7.3. Conferences – Poster Communications

Vuerich M., Asquini E., **Boscarol G.**, Braidot E., Carbognani M., Chiari G., Cingano P., Del Pino A., Forte T.G.W., Grillo F., Petraglia A., Trotta G., Zancani M., Boscutti F. Influence of heat wave duration and timing on alpine grassland plant communities: an upscaling perspective. In: II International Symposium on Biodiversity and Ecosystem Functions under Global Change, 12-14 November 2025, Alghero (Sassari), Italy.

Boscarol G., Petrussa E., Trotta G., Boscutti F., Braidot E., Volpe V., Barbieri S., Fabro M., Vuerich M. Mycotoxin contamination in maize can be predicted by analyzing morphophysiological traits at different phenological stages. In: XIV Congress of the Italian Society of Plant Biology (SIBV), 16-19 September 2025, Palermo, Italy.

Boscarol G., Di Francesco A., Braidot E., Vuerich M., Boscutti F., Volpe V., Fabro M., Vrhovsek U., Petrussa E. *In vitro* antifungal effect of plant-based and Ulva sp. extracts on Aspergillus flavus growth and conidia germination. In: 120th annual congress of the Italian Botanical Society (SBI) – XI International Plant Science Conference, 03-06 September 2025, Gorizia, Italy.

Cingano P., Pellegrini E., Tomat S., Asquini E., **Boscarol G.**, Trotta G., Vuerich M., Boscutti F. Functional traits and plant-soil feedback mechanisms contribute to the understanding of spatial pattern formation of *Cymodocea nodosa* meadows. In: 120th annual congress of the Italian Botanical Society (SBI) – XI International Plant Science Conference, 03-06 September 2025, Gorizia, Italy.

Vuerich M., Asquini E., **Boscarol G.**, Braidot E., Carbognani M., Chiari G., Cingano P., Del Pino A., Forte T. G. W., Grillo F., Petraglia A., Trotta G., Zancani M., Boscutti F. The role of duration and timing of induced heat waves in shaping plant community of alpine grasslands: an upscaling approach. In: 120th annual congress of the Italian Botanical Society (SBI) – XI International Plant Science Conference, 03-06 September 2025, Gorizia, Italy.

Boscutti F., Sigura M., Casolo V., Pellegrini E., Alberti G., Vuerich M.,Moro D., Gardossi A.L., Gargiulo S., Asquini E., Cingano P., **Boscarol G.**, Lagnaz D., Jouy F., Chmieleski J., Habel M., Szatten D., Brzezińska M., Trotta G. Tracing vegetation dynamics on river islands by remote sensing. In: 66th International Association for Vegetation Science (IAVS) Annual Symposium, 16-20 September 2024, Funchal (Madeira), Portugal.

Vuerich M., Trotta G., Cadez L., Boscutti F., Asquini E., **Boscarol G.**, Cingano P., Azzani G., Pischedda S., Tomao A., Alberti G. Remote sensing-derived wildfire severity predicts the shifts in forest structure, plant community composition, diversity, and functional identity. In: Forum Nazionale della Biodiversità, 20-21 May 2024, Palermo, Italy.

Scarpin D., Nerva L., Chitarra W., Moffa L., D'Este F., Vuerich M., Filippi A., **Boscarol G.**, Braidot E., Petrussa E. Sustainable agriculture by chitosan nanoparticles: characterisation and functionalisation with double-stranded RNA molecules able to limit *Botrytis cinerea* mycelium growth. In: Nano Innovation Conference & Exhibition, 09-13 September 2023, Rome, Italy.

Boscarol G., Boscutti F., Di Francesco A., Firrao G., Vuerich M., Scarpin D., Trotta G., Braidot E., Volpe V., Lazzarin T., Martinuzzi M., Fabro M., Petrussa E. Interactions between plant response to environment and fungal microbiome in developing maize silks in relation to mycotoxin risk. In: 118th annual congress of the Italian Botanical Society (SBI) – IX International Plant Science Conference, 13-16 September 2023, Pisa, Italy.

Vuerich M., **Boscarol G.**, Trotta G., Petrussa E., Scarpin D., Braidot E., Barbieri S., Boscutti F. Novel approach to link the physiological response of maize to drought and the occurrence of mycotoxins. In: 118th annual congress of the Italian Botanical Society (SBI) – IX International Plant Science Conference, 13-16 September 2023, Pisa, Italy.

Boscarol G., Braidot E., Petrussa E. Ecophysiological response of maize (*Zea mays* L.) to water stress: remote sensing and upscaling techniques for a more efficient management of water resources in agriculture. In: 5th Joint Workshop of the agriculture-oriented PhD Programs. 25-28 September 2023, Catania, Italy.

8. Acknowledgments

First dutiful and sincere thanks go to my supervisor Dr. Elisa Petrussa and my co-supervisor Prof. Enrico Braidot, for their constant support, wise guidance and inexhaustible willingness.
Heartfelt thanks go to the entire Plant Biology group for their meaningful friendship and constant support. Among them, Prof. Francesco Boscutti, Ari, Edo, Giacomino, Lore, Marcus and Paul.
I also thank the colleagues from other research groups, both within the University of Udine and externally, including the team at ERSA, without whom I could not have achieved these results.
I would also like to express my gratitude to Prof. Maud Tenaillon, Prof. Judith Legrand and Prof. Philippe Deschamps for their guidance, and to all the members of the Génétique Quantitative et Évolution group of the Institut Diversité, Écologie et Évolution du Vivant (IDEEV) of Gif-sur-Yvette for their hospitality during my period abroad.
Finally, I thank my family and Alice for wholeheartedly supporting me and for patiently helping me work through my doubts about what lies ahead.